

**Some pages of this thesis may have been removed for copyright restrictions.**

If you have discovered material in Aston Research Explorer which is unlawful e.g. breaches copyright, (either yours or that of a third party) or any other law, including but not limited to those relating to patent, trademark, confidentiality, data protection, obscenity, defamation, libel, then please read our [Takedown policy](#) and contact the service immediately (openaccess@aston.ac.uk)

# **The Role of Metastasis-Associated Proteins in Trophoblast Motility and Invasion**

**Maral Ebrahimzadeh Asl Tabrizi**

**Doctor of Philosophy**

**Aston University**

October 2020

© Maral Ebrahimzadeh Asl Tabrizi, 2020

Maral Ebrahimzadeh Asl Tabrizi asserts her moral right to be identified as the author of this thesis.

This copy of the thesis has been supplied on condition that anyone who consults it is understood to recognise that its copyright rests with its author and that no quotation from the thesis and no information derived from it may be published without proper acknowledgement.

# **The Role of Metastasis-Associated Proteins in Trophoblast Motility and Invasion**

**Maral Ebrahimzadeh Asl Tabrizi**

**For the degree of Doctor of Philosophy, 2020**

## **Thesis Summary**

During placental development, the pathways that regulate the invasion of trophoblasts into the decidua will lead to remodelling the uterine vasculature and will eventually give rise to placenta formation. The same pathways get reactivated during cancer development and can lead to tumour cell invasion and the metastatic process. As a consequence, there are striking similarities between the behaviour of tumour cells and the trophoblasts, due to their similar gene expression pattern and protein profile and we set about to determine whether factors which have been shown to play important roles in cancer biology are also expressed and regulate trophoblast function.

In this study we have focused on three different metastasis-associated proteins with well-defined roles in cancer progression, which have been closely linked with poor prognosis for cancer patients but have not been greatly studied in the context of placental development. The proteins are a small calcium-binding protein S100P, the ERM protein ezrin and the cytoskeleton-membrane linking protein, IQGAP1. After showing their expression and localisation pattern in human placental villi, we showed that these proteins are highly expressed during the earlier stages of the gestation, suggesting a potential role in early placenta development and implantation. We then studied their expression and localisation in trophoblast cell lines and primary trophoblasts. Using the trophoblast cell lines, through loss-of-function, and where relevant, gain of function studies, we showed that these three metastasis-associated proteins promote trophoblast motility and invasion.

We also investigated some of the possible mechanisms that might have been involved in the mentioned pathways including changes in focal adhesions, protein localisation and phosphorylation. We have yet to investigate the underlying mechanisms that link these three proteins to trophoblast motility and invasion, and whether all or two of them work together to make these processes possible.

[Keywords: placenta, S100P, ezrin, IQGAP1, focal adhesion]

## **Acknowledgements**

First of all, I would like to express my sincere gratitude to my first supervisor Dr Stephane Gross for letting me be a part of his lab as well as his continuous support during my research project and writing of this thesis, for his immense patience and motivation, as well as the invaluable knowledge he has impacted on me. I am also genuinely grateful for the insightful comments and encouragements of my second supervisor Prof. Asif Ahmed.

I wish to express my gratitude to Dr Thamir Ismail from the University of Liverpool for making the S100P-expressing clones. I offer my appreciation to Prof. Melissa Westwood from the University of Manchester for supplying wax-embedded human placenta sections and for letting me work in their labs at Royal Manchester Children's Hospital. My gratitude goes as well to Prof. Janesh Gupta from the University of Birmingham, for providing us with human placenta samples.

I also wish to thank the School of Life and Health Sciences at Aston University for awarding me with a scholarship, Charlotte Bland for kindly helping in microscopy, and Orienne Gru for helping me with my viability data, during her short stay at our lab.

I thank my colleague Tara Lancaster and all past and present members of Lab MB331, who not only made my lab work time utterly pleasant but never hesitated to share their expertise generously.

A big thank you to my beloved Mum and Dad for all their support, both emotionally and financially, and for making me believe in myself. To my lovely sisters Mahsa and Bitu, and my dear Grandma who have always been there for me despite the distance between us, thanks a lot.

Last (but certainly not least) I want to thank my best friend, soulmate and husband Mo, for putting up with me through the hard times and for sharing the happy times.

# Contents

List of publications.....	8
Abbreviations .....	9
List of Tables .....	13
List of Figures .....	15
Chapter 1. Introduction.....	19
1.1. Placenta implantation.....	20
1.1.1. Placenta types.....	20
1.1.2. Implantation .....	21
1.1.3. Blastocyst formation .....	21
1.1.4. Placenta development.....	23
1.2. Cellular migration and invasion .....	26
1.2.1. Migration.....	26
1.2.2. Invasion.....	29
1.3. Metastasis-associated proteins and implantation .....	30
1.3.1. Metastasis-associated proteins .....	30
1.3.2. Tumour metastasis and implantation similarities.....	32
1.3.3. Why study metastasis-associated proteins in implantation? .....	34
1.4. S100 family of proteins.....	35
1.4.1. Genetics.....	35
1.4.2. Structure .....	35
1.4.3. Function .....	37
1.4.4. S100P .....	38
1.5. ERM family of proteins .....	40
1.5.1. Genetics.....	41
1.5.2. Structure .....	41
1.5.3. Function .....	43

1.5.4.	Ezrin.....	45
1.6.	IQGAP family of proteins.....	49
1.6.1.	Genetics.....	49
1.6.2.	Structure.....	49
1.6.3.	Function.....	52
1.6.4.	IQGAP1.....	54
1.7.	Hypothesis.....	58
1.7.1.	Aims.....	58
1.7.2.	Objectives.....	58
Chapter 2.	Materials and Methods.....	59
2.1.	Materials.....	60
2.2.	Methods.....	66
2.2.1.	Immunohistochemistry (IHC).....	66
2.2.2.	Cell culture.....	69
2.2.3.	Trypan blue exclusion viability assay.....	72
2.2.4.	MTT viability assay.....	73
2.2.5.	Primary EVT isolation and culture.....	73
2.2.6.	Protein expression measurement by western blot analysis.....	74
2.2.7.	Protein knock-down.....	79
2.2.8.	Boyden chamber assays.....	79
2.2.9.	Immunofluorescence staining.....	82
2.2.10.	Statistical analysis.....	83
Chapter 3.	S100P regulates trophoblast motility and invasion.....	85
3.1.	Introduction.....	86
Aim	.....	86
Objectives.....		87
3.2.	Results.....	87

3.2.1.	Immunohistochemical staining optimisation .....	87
3.2.2.	Placental S100P expression gradually decreases during gestation.....	89
3.2.3.	S100P is expressed in human trophoblasts and EVTs .....	91
3.2.4.	S100P expression in human trophoblast cell lines .....	94
3.2.5.	S100P expression in different microenvironments mimicking physiological conditions .....	96
3.2.6.	S100P expression knockdown.....	98
3.2.7.	Boyden chamber assay optimisation.....	100
3.2.8.	Knocking down S100P reduces trophoblast motility .....	104
3.2.9.	Knocking down S100P reduces trophoblast invasion .....	106
3.2.10.	Stable S100P transfection .....	108
3.2.11.	Moderate levels of S100P expression enhance trophoblast motility.....	110
3.2.12.	Moderate levels of S100P expression enhances trophoblast invasion .....	112
3.2.13.	S100P expression reduced the size and the number of focal adhesions.....	114
3.2.14.	S100P expression does not affect the viability of HTR8/SVneo .....	116
3.2.15.	Reversing the motile/invasive phenotype in HTR8/SVneo clones .....	118
3.2.16.	Regression analysis .....	124
3.2.17.	Extracellular S100P promotes trophoblast migration and invasion .....	126
3.2.18.	Primary EVT isolation .....	134
3.3.	Discussion .....	140
Chapter 4.	Ezrin regulates trophoblast motility and invasion.....	146
4.1.	Introduction.....	147
	Aim .....	148
	Objectives.....	148
4.2.	Results.....	149
4.2.1.	Immunohistochemical staining optimisation .....	149
4.2.2.	Placental ezrin expression decreases gradually during gestation.....	151
4.2.3.	Ezrin is expressed in human trophoblasts and EVTs .....	152

4.2.4.	Ezrin is expressed in human trophoblast cell lines .....	155
4.2.5.	Ezrin localisation in trophoblast cell lines .....	157
4.2.6.	Ezrin expression knockdown .....	159
4.2.7.	Ezrin knockdown does not affect trophoblast viability.....	161
4.2.8.	Ezrin knockdown reduces trophoblast motility.....	163
4.2.9.	Ezrin knockdown reduces trophoblast invasion.....	165
4.2.10	Regression analysis .....	167
4.2.11.	Ezrin knockdown does not affect FAs .....	169
4.2.12.	Ezrin phosphorylation inhibition.....	172
4.2.13.	Ezrin inhibition modifies the localisation of ezrin and phospho-ezrin in HTR8/SVneo.....	174
4.2.14.	Ezrin inhibition does not affect trophoblast viability.....	176
4.2.15.	The effect of ezrin inhibition on trophoblast motility .....	178
4.2.16.	The effect of ezrin inhibition on trophoblast invasion .....	180
4.2.17.	Ezrin inhibition affects FA number and size in HTR8/SVneo.....	182
4.2.18.	Ezrin expression and localisation in primary EVT.....	184
4.2.19.	Phospho-ezrin localisation in first and second trimester EVTs .....	186
4.2.20.	Ezrin inhibition in primary EVTs.....	188
4.2.21.	The effect of ezrin inhibition on the motility of primary EVTs.....	190
4.2.22.	The effect of ezrin inhibition on the invasion of primary EVTs.....	192
4.2.23.	Ezrin inhibition does not affect FAs in primary first trimester EVTs.....	194
4.3.	Discussion .....	196
Chapter 5.	IQGAP1 regulates trophoblast motility and invasion .....	202
5.1.	Introduction.....	203
	Aim .....	203
	Objectives.....	203
5.2.	Results.....	204
5.2.1.	Immunohistochemical staining optimisation .....	204

5.2.2.	Placental IQGAP1 expression decreases gradually during gestation.....	207
5.2.3.	IQGAP1 is expressed in human trophoblasts and EVT.....	209
5.2.4.	IQGAP1 is expressed in human trophoblast cell lines .....	211
5.2.5.	IQGAP1 localisation in human trophoblast cell lines .....	213
5.2.6.	IQGAP1 expression knockdown.....	215
5.2.7.	IQGAP1 knockdown does not affect trophoblast viability .....	217
5.2.8.	IQGAP1 knockdown reduces trophoblast motility .....	219
5.2.9.	IQGAP1 knockdown reduces trophoblast invasion .....	221
5.2.10	Regression analysis .....	223
5.2.11.	The effect of IQGAP1 knockdown on trophoblast FAs.....	225
5.2.12.	IQGAP1 is expressed in primary EVTs .....	228
5.3.	Discussion .....	230
Chapter 6.	Conclusions .....	233
6.1.	General discussion .....	234
6.2.	Future work .....	238
References.....		240
Appendix.....		267

# List of publications

Tabrizi, M.E.A., Lancaster, T.L., Ismail, T. M., Georgiadou A., Ganguly, A., Mistry, J., J., Wang, K., Rudland, P.S., Ahmad, S., and Gross, S.R. 2018. ‘S100P Enhances the Motility and Invasion of Human Trophoblast Cell Lines’. *Scientific Reports*, 8(1):11488.

Tabrizi M.E.A, Westwood, M., Gupta, J., Gross S.R. (in preparation). ‘Ezrin Enhances Motility and Invasion in Human Trophoblast Cell lines and Primary Cells’.

Lancaster, T.L., Tabrizi M.E.A., Westwood, M., Gupta, J., and Gross, S.R. (in preparation). ‘An Extracellular Membrane-Bound S100P Pool Regulates Motility and Invasion of Human Trophoblast Cell lines and Primary Cells’.

Parkes, C., Kamal, A., Tabrizi, M.E.A., Gross, S.R., Barraclough, R., Moss, D., and Hapangama, D. (in preparation). ‘S100P in Endometrial Cancer’.

# Abbreviations

ACA	Epsilon-aminocaproic acid
ANOVA	Analysis of variance
APC	Adenomatous polyposis coli
APS	Ammonium persulphate
B7HI	Integrin $\beta$ 7hi
BSA	Bovine serum albumen
Ca <sup>2+</sup>	Calcium ion
cAMP	Cyclic adenosine monophosphate
CB	Cytoskeleton buffer
CD	Cluster of differentiation
CD200	Cluster of differentiation 200
CEACAM1	Carcinoembryonic antigen-related cell adhesion molecule 1
CLIP-170	Cytoplasmic linker protein
CO <sub>2</sub>	Carbon dioxide
Ctrl	Control
DAB	3,3'-Diaminobenzidine
DAPI	4',6-diamidino-2-phenylindole
diH <sub>2</sub> O	Deionised water
DMEM	Dulbecco's Modified Eagle's Medium
DMSO	Dimethyl sulphoxide
DNA	Deoxyribonucleic acid
ECM	Extracellular matrix
EGF	Epidermal growth factor
EGTA	Ethylene glycol tetraacetic acid
EMT	Epithelial–mesenchymal transition

ERK1/2	Extracellular signal–regulated kinases 1 and 2
ERM	Ezrin, radixin and moesin
ERMAD	Ezrin-radixin-moesin association domain
EVT	Extravillous trophoblast
F-actin	Filamentous actin
FA	Focal adhesion
FASL	Fas ligand
FCS	Foetal calf serum
FERM	Four-point one, ezrin, radixin, moesin
FITC	Fluorescein isothiocyanate
g/L	Gram/litre
GRO- $\alpha$	Growth-regulated oncogene- $\alpha$
HER2	Human epidermal growth factor receptor 2
HLA-G	Major histocompatibility complex, class I, G
HRP	Horseradish peroxidase
ICAM	Intercellular adhesion molecule
IDO	Indoleamine 2,3-dioxygenase
IgG	Immunoglobulin G
IHC	Immunohistochemistry
IL-8	Interleukin 8
IL-10	Interleukin 10
IQGAP1	IQ motif-containing GTPase activating protein 1
kDa	Kilodalton
mA	Milliampere
MAPK	Mitogen-activated protein kinase
McpI	Methyl-accepting chemotaxis protein
MEM	Minimum Essential Medium

MET	Mesenchymal–epithelial transition
mg/ml	Milligram/millilitre
MIF	Macrophage migration inhibitory factor
mM	Millimolar
MMP	Matrix metalloproteinase
mRNA	Messenger ribonucleic acid
MTT	3-(4,5-Dimethylthiazol-2-yl)-2,5-diphenyltetrazolium bromide
NC	Negative control
NEAA	Non-essential amino acids
nM	Nanomolar
NMIIA	Non-muscle myosin IIA
n.s.	Non-significant
PA	Plasminogen activator
PBS	Phosphate-buffered saline
PFA	Paraformaldehyde
PGE2	Prostaglandin E2
PIGF	Placental growth factor
PIP <sub>2</sub>	Phosphatidylinositol 4,5-bisphosphate
PKA	Protein kinase A
PKC	Protein kinase C
PSG	Pregnancy-Specific Glycoprotein
PVDF	Polyvinylidene fluoride or polyvinylidene difluoride
RAGE	Receptor for advanced glycation endproducts
RANTES	Regulated on activation, normal T cell expressed and secreted
SD	Standard deviation
SDS	Sodium dodecyl sulphate
SDS-PAGE	Sodium dodecyl sulphate–polyacrylamide gel electrophoresis

SEM	Standard error of the mean
SGHPL-4 and -5	Saint George's Hospital Placental Cell lines 4 and 5
siRNA	Small interfering RNA
TCM	Trophoblast complete medium
TEMED	N,N,N',N'-Tetramethylethylenediamine
TGF- $\beta$	Transforming growth factor- $\beta$
tPA	Tissue-type plasminogen activator
TRAIL	Tumour-necrosis-factor related apoptosis inducing ligand
TRITC	Tetramethylrhodamine-isothiocyanate
uPA	Urokinase-type plasminogen activator
V	Volt
v/v	Volume/volume
VASP	Vasodilator-stimulated phosphoprotein
VCAM	Vascular cell adhesion protein
VEGF	Vascular endothelial growth factor
VEGFR	Vascular Endothelial Growth Factor Receptors
w/v	Weight/volume
WASP	Wiskott–Aldrich syndrome protein
Zn <sup>2+</sup>	Zinc ion
$\mu\text{g/mL}$	Microgram/millilitre
$\mu\text{M}$	Micromolar

# List of Tables

Table 1.1 Proteins that interact with S100P and their effect on cancer.....	39
Table 1.2 The association between S100P expression and poor prognosis in cancer.....	40
Table 1.3 Proteins that interact with ezrin and their effect on cells. ....	46
Table 1.4 The association of ezrin expression with poor prognosis in many cancers. ....	48
Table 1.5 Proteins that interact with IQGAP1 and their effect on cells.....	55
Table 1.6 The association of IQGAP1 expression with poor prognosis in many cancers. ....	57
Table 2.1 Equipment and software.....	62
Table 2.2 Reagents.....	66
Table 2.3 The buffers used for IHC, and their ingredients. ....	68
Table 2.4 Antibody dilutions for IHC.....	69
Table 2.5 Cell lines. ....	70
Table 2.6 Cell lines and their culture media.....	71
Table 2.7 The solutions used for EVT isolation and their ingredients.....	74
Table 2.8 SDS-PAGE buffers used for 16% tricine gel and their ingredients. ....	76
Table 2.9 SDS-PAGE buffers used for 10% polyacrylamide gel and their ingredients. ....	76
Table 2.10 The solutions used for western blot transfer and detection.....	78
Table 2.11 Primary and secondary antibody dilutions used in western blot.....	78
Table 2.12 The solutions needed for preparing the cells for immunofluorescence staining.....	83
Table 2.13 Antibody dilutions used in immunofluorescence staining.....	83
Table 3.1 The average number of focal adhesions per cell in HTR8/SVneo clones, represented as percentages .....	114
Table 3.2 The average number of focal adhesions per cell in Jeg-3 cells, represented as percentages.....	132
Table 4.1 Average FA count per cell in HTR8/SVneo and SW71 cells.....	169
Table 4.2 Average FA count per cell in HTR8/SVneo cells, following ezrin inhibition.....	182

Table 4.3 Average membrane projection count per cell in primary first and second trimester EVTs. ....	186
Table 4.4 Average membrane projection count per cell in primary EVTs. ....	188
Table 4.5 Average FA count per cell in primary EVTs. ....	194
Table 5.1 Average FA count per cell in HTR8/SVneo and SW71 cells. ....	225

# List of Figures

Figure 1.1 Six layers separate the foetal and the maternal blood during early pregnancy.....	20
Figure 1.2 Blastocyst formation.....	22
Figure 1.3 Trophoblasts at the foeto-maternal interface. ....	24
Figure 1.4 Trophoblast differentiation. ....	25
Figure 1.5 Cell migration steps. ....	28
Figure 1.6 Metastasis steps. ....	31
Figure 1.7 Strong similarity between tumour invasion and trophoblast invasion.....	33
Figure 1.8 Schematic diagram of the secondary structure of a monomeric S100 protein.....	36
Figure 1.9 Primary structure of ERM family of proteins. ....	41
Figure 1.10 Conformational forms of ERM proteins. ....	42
Figure 1.11 Conformational change in an ERM protein (moesin) upon activation. ....	43
Figure 1.12 Schematic diagram of IQGAP1 structure with its multiple domains and binding partners.....	50
Figure 1.13 IQGAP1 exists in three conformations.....	51
Figure 3.1 Primary antibody concentration optimisation for IHC. ....	88
Figure 3.2 S100P expression in human placenta is the highest during first trimester of gestation. ....	90
Figure 3.3 S100P expression in human trophoblasts and EVTs. ....	92
Figure 3.4 Endogenous S100P expression in different trophoblast cell lines. ....	95
Figure 3.5 S100P expression in physiological-like conditions enhances S100P expression. ....	97
Figure 3.6 Knocking down S100P expression by siRNA transfection in Jeg-3 and BeWo cells. ....	99
Figure 3.7 Transwell migration assay optimisation results.....	101
Figure 3.8 Transwell invasion assay optimisation results.....	103
Figure 3.9 S100P knockdown reduces trophoblast migration.....	105
Figure 3.10 The effect of S100P knockdown on trophoblast invasion. ....	107

Figure 3.11 S100P expression in HTR8/SVneo SGB217 clones and their levels compared with Jeg-3 .....	109
Figure 3.12 S100P expression and trophoblast migration.....	111
Figure 3.13 S100P expression and trophoblast invasion.....	113
Figure 3.14 The effect of exogenous S100P expression on focal adhesions in HTR8/SVneo EVT cells.....	115
Figure 3.15 S100P expression does do not affect the viability of HTR8/SVneo clones.....	117
Figure 3.16 Knocking down S100P expression in S100P-expressing HTR8/SVneo clones. ...	119
Figure 3.17 S100P expression and S100P knockdown do not affect the viability of HTR8/SVneo clones. ....	121
Figure 3.18 S100P knockdown in S100P-expressing HTR8/SVneo clones brings migration and invasion down to same levels as the control clone.....	123
Figure 3.19 Positive correlation between trophoblast migration/invasion and S100P expression. ....	125
Figure 3.20 S100P antibody and ACA do not affect the viability of trophoblast cell lines Jeg-3 and HTR8/SVneo clones 3, 5 and 7. ....	127
Figure 3.21 The effect of S100P antibody and ACA on the migration of Jeg-3 and HTR8/SVneo clones .....	129
Figure 3.22 The effect of S100P antibody and ACA on the invasion of Jeg-3 and HTR8/SVneo clones. ....	131
Figure 3.23 Extracellular S100P inhibition does not affect focal adhesions in Jeg-3 cells.....	133
Figure 3.24 Primary EVT culture.....	135
Figure 3.25 HLA-G staining in primary EVTs. ....	137
Figure 3.26 S100P expression was detected in primary EVTs. ....	139
Figure 4.1 Primary ezrin antibody concentration optimisation for IHC. ....	150
Figure 4.2 Ezrin expression in human placenta is the highest during the first and second trimesters of gestation. ....	152
Figure 4.3 Ezrin expression in human trophoblasts and EVTs. ....	154
Figure 4.4 Ezrin and phospho-ezrin expression in human trophoblast cell lines.....	156
Figure 4.5 Ezrin expression and localisation in trophoblast cell lines. ....	158

Figure 4.6 Ezrin siRNA treatment knocks down ezrin expression in trophoblast cell lines. ....	160
Figure 4.7 Trophoblast viability with ezrin knockdown. ....	162
Figure 4.8 The effect of ezrin knockdown on trophoblast migration. ....	164
Figure 4.9 The effect of ezrin knockdown on trophoblast invasion. ....	166
Figure 4.10 Positive correlation between trophoblast migration/invasion and ezrin expression. .....	168
Figure 4.11 Knocking down ezrin does not affect the FAs. ....	171
Figure 4.12 The effect of ezrin inhibition on phospho-ezrin levels. ....	173
Figure 4.13 The effect of ezrin inhibition on ezrin and phospho-ezrin localisation in EVT cell lines. ....	175
Figure 4.14 Trophoblast viability with ezrin inhibition. ....	177
Figure 4.15 Ezrin phosphorylation inhibition reduces trophoblast motility. ....	179
Figure 4.16 Ezrin phosphorylation inhibition reduces trophoblast invasion. ....	181
Figure 4.17 Ezrin inhibition affects the FAs in HTR8/SVneo. ....	183
Figure 4.18 Ezrin expression and localisation in primary EVTs. ....	185
Figure 4.19 Phospho-ezrin localisation in EVTs from first and second trimester. ....	187
Figure 4.20 The effect of ezrin inhibition on primary EVT morphology. ....	189
Figure 4.21 Ezrin inhibition leads to motility reduction in primary EVT. ....	191
Figure 4.22 Ezrin inhibition leads to invasion reduction in primary EVT. ....	193
Figure 4.23 Ezrin inhibition does not affect the FAs in HTR8/SVneo. ....	195
Figure 5.1 IQGAP1 antibody concentration optimisation for IHC. ....	205
Figure 5.2 IQGAP1 expression in human placenta is the highest during the first trimester of gestation. ....	208
Figure 5.3 IQGAP1 expression in human trophoblasts and EVTs. ....	210
Figure 5.4 IQGAP1 expression in human trophoblast cell lines. ....	212
Figure 5.5 IQGAP1 expression and localisation in trophoblast cell lines. ....	214
Figure 5.6 IQGAP1 siRNA treatment knocks down IQGAP1 expression in trophoblast cell lines. ....	216

Figure 5.7 Trophoblast viability with IQGAP1 knockdown.....	218
Figure 5.8 The effect of IQGAP1 knockdown on trophoblast motility. ....	220
Figure 5.9 The effect of IQGAP1 knockdown on trophoblast invasion. ....	222
Figure 5.10 Positive correlation between trophoblast migration/invasion and IQGAP1 expression.....	224
Figure 5.11 The effect of IQGAP1 knockdown on FAs. ....	227
Figure 5.12 IQGAP1 expression and localisation in primary EVT.....	229

# Chapter 1.

## Introduction

## 1.1. Placenta implantation

### 1.1.1. Placenta types

The placenta is a temporary organ that physically attaches the growing embryo/foetus to its mother, and facilitates the metabolic interchange between them, while forming a barrier against the transmission of many bacteria (Gude et al. 2004). In the beginning of placenta formation, six layers separate maternal and foetal blood, three of which are foetal membranes: the endothelium of the foetal capillaries, connective tissue, and epithelium of the chorion (the outermost layer of foetal membranes). The other three are of maternal origin: the endothelium lining of the endometrial blood vessels, connective tissue and the endometrial epithelial cells (Figure 1.1). Depending on the species, some of the maternal layers are destroyed in the process of placentation (Bowen 2011).

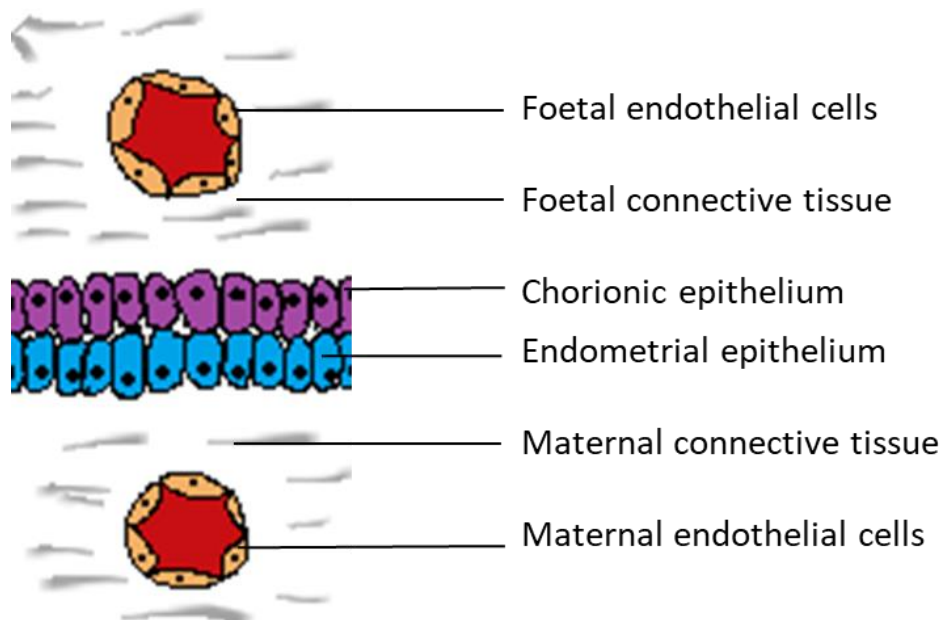


**Figure 1.1 Six layers separate the foetal and the maternal blood during early pregnancy.** (Adapted with modification from Bowen 2011).

Placenta types in placental mammals (eutherians) can be classified based on the number of layers between foetal and maternal blood: 1. Epitheliochorial, the least invasive type, in which three layers of maternal tissue separate the foetal and maternal blood from each other, found in horses, pigs, and ruminants. 2. Endotheliochorial, which is partially invasive as it has lost the maternal epithelial layer, found in cats and dogs. 3. Haemochorial, the most invasive type, in which all

three maternal layers are destroyed, letting the foetal tissues to come in direct contact with the maternal blood, found in humans and rodents (Furukawa, Kuroda & Sugiyama 2014).

Another categorisation of the placenta is based on its morphology and the contact points between the maternal and the foetal side: 1. Diffuse, in which the placenta covers the entire surface of the endometrium, found in horses and pigs. 2. Cotyledonary, in which there are numerous contact points between the maternal and foetal vascular system, instead of a single placenta, found in ruminants. 3. Zonary, in which the placenta forms a complete or incomplete band surrounding the foetus, found in carnivores. 4. Discoid, in which the placenta forms a discoid form, found in primates and rodents (Furukawa, Kuroda & Sugiyama 2014).

In this work, we will be focusing on the haemochorial discoid placenta found in humans.

### **1.1.2. Implantation**

Implantation, a critical step in viviparous birth in mammals, is the process of invasion and attachment of the conceptus into the inner surface of the uterus, which later brings the growing vessels of the embryo into functional contact with the maternal circulation, via the placenta; if successful, this can result in the growth and development of a new offspring (Dey et al. 2004). For successful implantation, effective cross-talk between the blastocyst and the endometrium needs to take place (Hantak, Bagchi & Bagchi 2014). The stages of implantation are described as follows.

### **1.1.3. Blastocyst formation**

Before moving down the Fallopian tube, the fertilised ovum (zygote) stays in the tube for 3-4 days, during which a number of ordinary mitotic divisions make it into a mulberry-like mass of cells, called the morula (Alberts et al. 2014). In humans, around 5 days after fertilisation, a hollow sphere of 16-32 cells known as the early blastocyst is formed, which has a cavity, known as the blastocoel, as well as two distinct layers of cells. The trophoblast forms the outermost layer of the blastocyst and is made out of trophoblasts (Greek *trophein*: to feed, and *blastos*: germinator) that later will form the placenta. The inner compact mass of cells will eventually give rise to the definitive structures of the foetus (Alberts et al. 2014). After another two days, the zona pellucida membrane degrades (known as zona hatching), forming the late-stage blastocyst, and trophoblast cells form two distinct layers of cells: the relatively undifferentiated cytotrophoblast, with distinct boundaries that later form the villi, to physically attach the placenta to the uterus, and

differentiated syncytiotrophoblasts, the external layer of cells with no distinct boundaries, formed by the fusion of mononuclear cytotrophoblasts (Hill 2019) (Figure 1.2).



**Figure 1.2 Blastocyst formation.** Panel A shows blastocyst formation from the ovary to the uterus; Upon release from the follicle into the Fallopian tube, the ovum will move along the tube, where fertilisation occurs, and the zygote will be formed. The first divisions will also happen within the tube, while the first differentiation will happen soon after the multicellular morula enters the uterus, giving rise to the blastocyst, which has invading capabilities (Adapted from Hill 2019). Panel B shows blastocyst implantation at 8-9 days following fertilisation.

#### **1.1.4. Placenta development**

The implantation of the blastocyst (summarised from Hill 2019) happens during the receptive window of implantation. This process starts with loose adherence of the newly hatched blastocyst to the endometrium (adplantation); the blastocyst then moves to the final site of implantation (rolling), and finally firmly adheres to the endometrium, which will result in hormonal feedback, mainly human chorionic gonadotropin (hCG), secreted from the syncytiotrophoblast, to the corpus luteum in the ovary (Jarvela, Ruokonen & Tekay 2008).

In early gestational age, the embryo is fully covered with chorionic villi (villi which are formed from the chorion, the outermost membrane around the embryo). During the first two weeks, the villi are made solely out of trophoblasts, are small in size and do not contain any vasculature (known as primary villi). In a few days, however, the villi grow in size and mesoderm starts growing in them (known as secondary villi); in a day or two, they become vascularised (known as tertiary villi). The tertiary villi (made out of trophoblasts, mesoderm and vasculature) either remain floating (known as free villi) and disappear after the first trimester from all around the embryo, or anchor themselves to the basal plate, the region that is in contact with the uterine wall (known as anchoring villi or stem villi).

Around weeks 2-4 of gestation, the cells located at the maternal side of the trophoblast columns, which are clusters of cytotrophoblasts at the tip of the anchoring villi, start to further differentiate into another subtype of trophoblasts known as the extravillous trophoblasts (EVTs) (Aplin 1991; Pollheimer et al. 2018) (Figure 1.3).

**Foetal Side**

**Maternal Side**

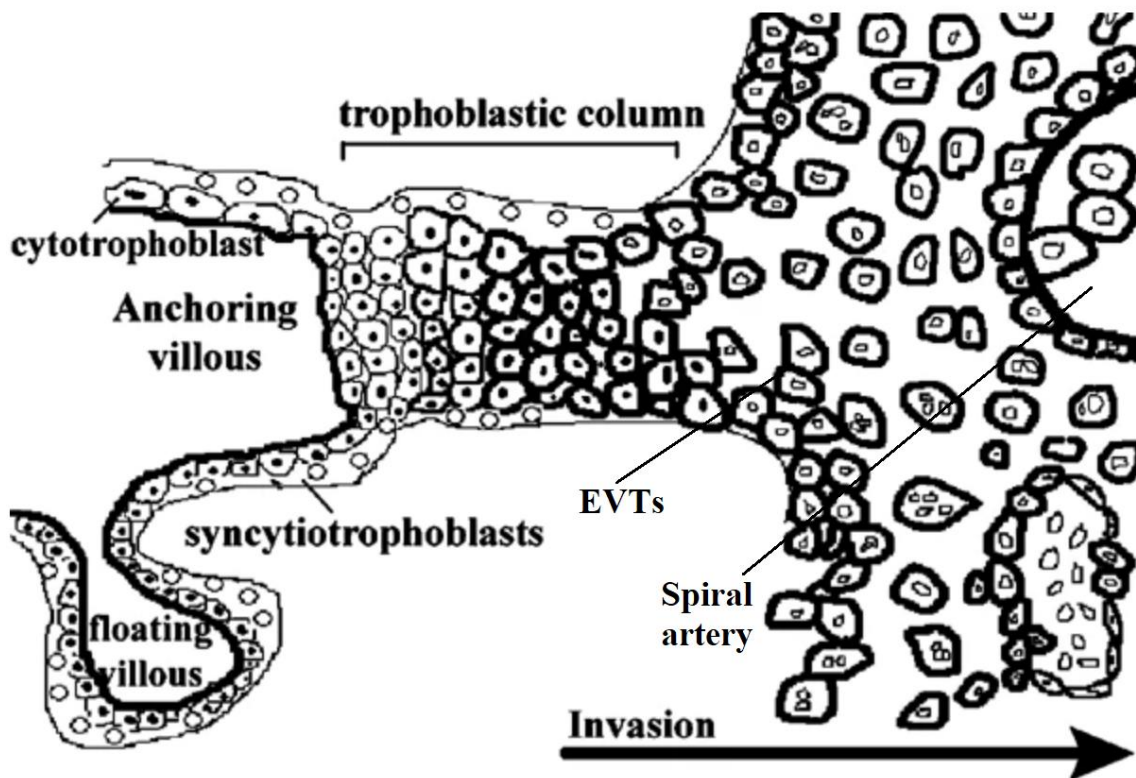


**Figure 1.3 Trophoblasts at the foeto-maternal interface.** The EVT's are an invasive subpopulation of cytotrophoblasts, that leave trophoblastic columns and invade the endometrium (Hill 2019) (Figure adapted with modification from (Liu et al. 2004).

The EVT's are characterised by high proliferative and invasive properties, which gives them the ability to leave the basement membrane of the villi, penetrate into the endometrium by digesting the uterine epithelial cells and then the stroma through phagocytic capabilities and the expression of matrix metalloproteinases (MMPs) 2, 9, 14 (Isaka et al. 2003; H. Wang et al. 2014; Welsh & Enders 1987) and membrane-type matrix metalloproteinase 1 (MT1-MMP) (Hiden et al. 2013). Soon after appearing, EVT's will give rise to two distinct subpopulations: the interstitial EVT's that invade the decidua and the inner third of the myometrium and anchor the placenta to the uterus, and the endovascular EVT's with phagocytic capabilities that remodel the maternal spiral arteries, allowing maternal blood flow through the intra-villus space inside the placenta bed. Interstitial EVT may also differentiate into endovascular EVT's or into giant cells, with endocrine capabilities (Fu et al. 2013; Red-Horse et al. 2004; Wang & Zhao 2010) (Figure 1.4).

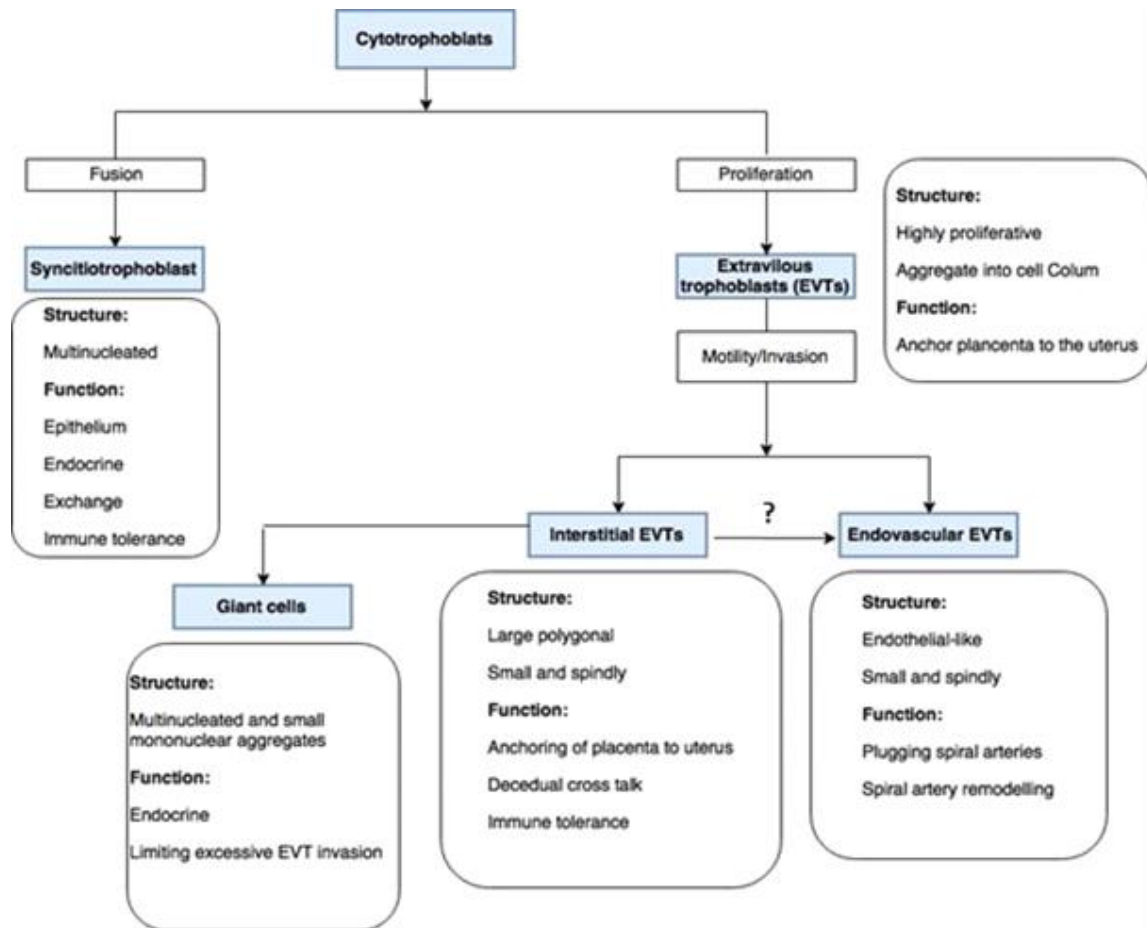


**Figure 1.4 Trophoblast differentiation.** (Adapted from Fu et al. 2013).

Towards the end of the second trimester, stem villi and terminal villi along with three other less differentiated villi types make up the villous “tree”, the main structure of the placenta. Stem villi give stability to the villus tree and terminal villi (which are attached to the stem villi by intermediate structures) are covered with the syncytiotrophoblast layer that further erodes the uterine wall and capillaries, by the secretion of lytic enzymes and pro-apoptotic factors, and comes into direct contact with maternal blood, making the terminal villi a place for diffusive exchange. This provides the growing foetus with nutrition, waste elimination, and thermoregulation (Hill 2019).

## 1.2. Cellular migration and invasion

### 1.2.1. Migration

Cell migration is a multi-step process that requires the dissociation of cell-cell contacts, changes in the dynamic of cell adhesion to the matrix and extension of membrane protrusions. From single cell organisms like amoeba to complex multi-cellular organisms, movement capabilities, in response to chemical and mechanical signals, are crucial for survival (Manahan et al. 2004). Any motility-related process in cells, such as cell migration, invasion, adhesion, division, endocytosis or morphologic changes, cannot take place without spatially and temporally controlled cytoskeletal actin dynamics (assembly and disassembly) (Dormann & Weijer 2006; Kaksonen, Toret & Drubin 2006; Pollard & Borisy 2003; Rafelski & Theriot 2004). Any abnormal activation or deactivation caused to the steps of this highly regulated process can have disastrous effects, such as cancer, inflammation, vascular diseases and viral and bacterial infections (Vicente-Manzanares, Webb & Horwitz 2005).

Directional migration requires cell adhesion and cell polarity to collaborate in response to a complex network of signalling cascades (Carmona-Fontaine, Matthews & Mayor 2008). This type of migration (known as adhesive crawling) is generally composed of two major steps: 1. The displacement of cytoplasm at leading edge 2. The removal of debris accumulated at the trailing edge (Petrie, Doyle & Yamada 2009).

Cell adhesion attaches cells to neighbouring cells and/or to the extracellular matrix (ECM), a gel-like network of proteoglycans and fibrous proteins produced intracellularly by cells and secreted into the spaces surrounding them, with the help of single-pass transmembrane proteins located on the cell surface, known as cell adhesion molecules (CAMs) (Alberts et al. 2014; Frantz, Stewart & Weaver 2010). CAMs are divided into four major groups: immunoglobulin superfamily cell adhesion molecules (IgCAMs), cadherins, integrins and selectins (Gonzalez-Amaro & Sanchez-Madrid 1999; Joseph-Silverstein & Silverstein 1998).

Cellular motility and sub-cellular force generation are regulated by a highly conserved chemo-mechanical process that requires the inherently contractile cytoskeletal actin-myosin complexes (actomyosin), in which the ATP-dependent myosin motor proteins pull on actin filaments (which polymerise with the help of actin regulator families Wiskott–Aldrich syndrome protein (WASP) and formin, along with actin nucleator Arp2/3 complex) in both the skeletal muscle, and non-muscle cells (Breitsprecher & Goode 2013; Cooper 2000; Zigmond 2000). Actomyosin provides protrusive forces at the leading edge of the cell by ruffling fan-like lamellipodium and filopodial

spikes that spread beyond the lamellipodium border (Pollard & Borisy 2003). Actomyosin also forms stress fibres, i.e. bundles of 10–30 actin filaments, linked together by  $\alpha$ -actinin, anchored to focal adhesion (FA) complexes, which connect the actin cytoskeleton to the ECM (Tojkander, Gateva & Lappalainen 2012). Another type of stress fibre that does not directly bind to FAs forms arc-shaped actin bundles that run parallel to the leading edge of the cell in lamellipodium (known as the transverse arc network), and contribute to cell migration (Hotulainen & Lappalainen 2006). When the cell body has moved forward, rear retraction fibres anchored to the front adhesions pull the trailing end of the cell along (Ridley et al. 2003).

Microtubules, on the other hand, regulate the polarity of the actin cytoskeleton and help organelles and proteins move throughout the cell by providing a polarised network (Omelchenko et al. 2002). To make cell protrusions, actin filaments need to cooperate with microtubules to induce a polarised morphology in the cell by asymmetrically distributing the cytoskeleton and the signalling molecules within the cell (Krause & Gautreau 2014; Watanabe, Noritake & Kaibuchi 2005). This cooperation is regulated by Rho family GTPases (G proteins subfamily of the Ras superfamily, which cycle between the inactive GDP-bound state and the active GTP-bound state) including Ras homolog gene family, member A (RhoA), Ras-related C3 botulinum toxin substrate 1 (Rac1) and cell division control protein 42 homolog (Cdc42) (Boureux et al. 2007; Bustelo, Sauzeau & Berenjeno 2007), along with several downstream members of the protein kinase family (Kiley et al. 1999; Tang et al. 2008). The affected pathways result in the capture and stabilisation of microtubules, through their effectors such as cytoplasmic linker protein (CLIP-170) and adenomatous polyposis coli (APC), at the cell cortex, leading to the formation of a polarised microtubule array (Heasman & Ridley 2008; Watanabe, Noritake & Kaibuchi 2005). The cell migration steps have been visualised in a simplified diagram in Figure 1.5.

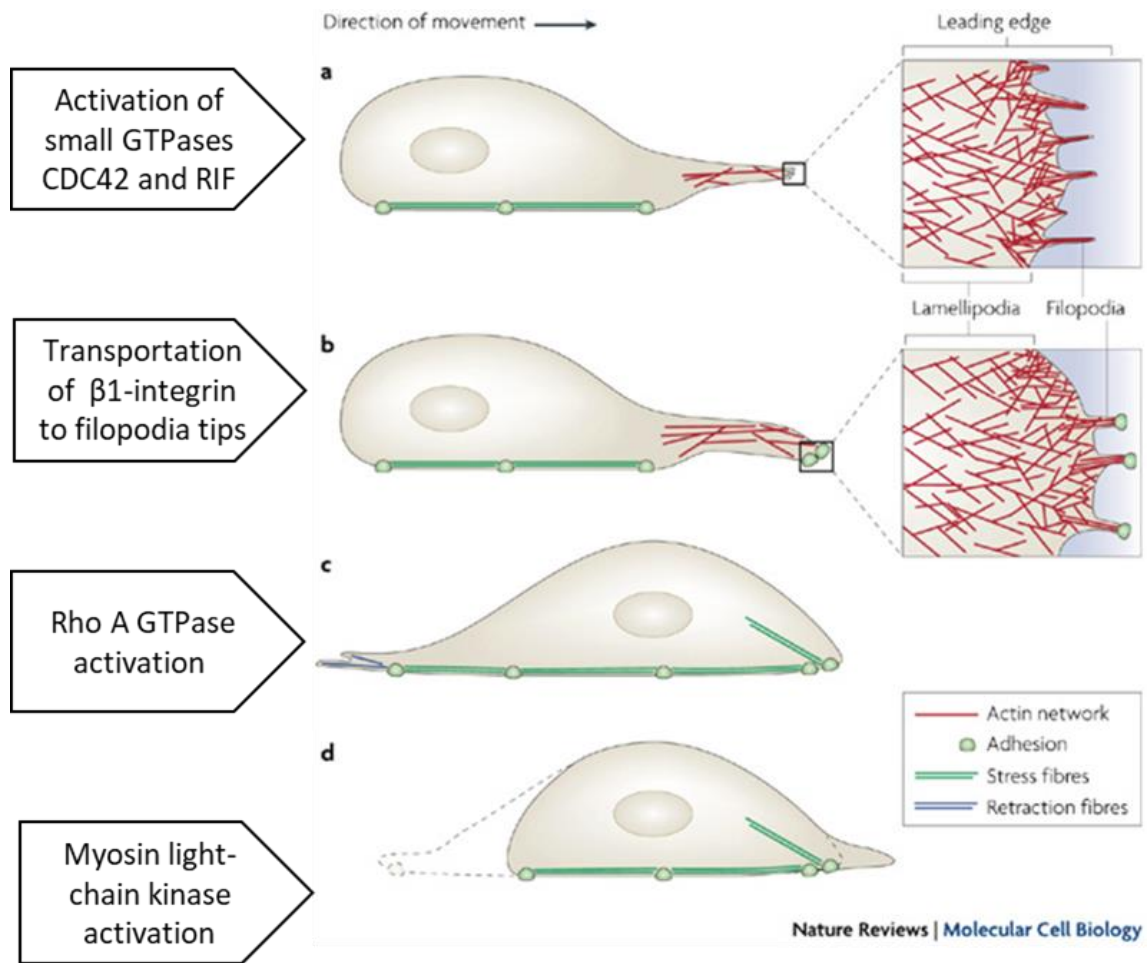


**Figure 1.5 Cell migration steps.** The migration starts with the formation of actin containing protrusion at the leading edge of the cell known as lamellipodia, which contain spike-like filopodia (a). Then, the plasma membrane of the protrusion needs to adhere the surface (b). Stress fibres will then push the cell body and the nucleus forward (c). Lastly, the rear of the cell is pulled along by retraction fibres (d) (Arjonen, Kaukonen & Ivaska 2011; Kumar et al. 2006). (Adapted with modification from Mattila and Lappalainen 2008).

Despite being the most common and the best-characterised type, adhesive crawling (which includes sheet-like, 2D lamellipodium) is not the only type of migration in advanced eukaryotic cells. Macrophages, neutrophils and metastatic tumour cells exhibit an adhesion-independent amoeboid type of migration, in which the cytoplasm slides, forming a 3D actin-filled structure, called pseudopodium, which pulls the cell forward (Allen & Allen 1978; Titus & Goodson 2017) and spermatozoa show flagellar locomotion (Ishijima, Oshio & Mohri 1986).

### **1.2.2. Invasion**

Cellular invasion is a multi-step process that includes cytoskeletal alterations (including formation of feet-like invadopodia), which cause changes in ECM by the secretion of proteases including matrix metalloproteinases (MMPs) and cytokines such as interleukins and growth factors, which eventually make cell migration to a nearby tissue possible (Friedl & Alexander 2011). It should be noted that migration and invasion of cancer cells follow similar mechanisms to those of normal cells, which take place during embryo development and leucocyte migration, and it is the tumour cells' lack of physiological "stop signals" that leads to problems (Friedl & Alexander 2011; Krakhmal et al. 2015).

Tumour invasion is seen as the first and the foremost step of metastasis, a very complex process during which the cancer cells extend and penetrate into the neighbouring tissues, breaching the barriers between the tissue, and travel into a new site via the circulation (Cancer Australia 2019). The invasive movement of cells takes place in either or both of the patterns explained below (Cavallaro & Christofori 2004; Friedl, Zanker & Brocker 1998; Giampieri et al. 2009; Palecek et al. 1997; Sahai & Marshall 2003):

1. Collectively: In this pattern, a group of cells, located at the leading edge, detach from the primary tumour. These include elongated fibroblast-like mesenchymal leading cells, that have gone through epithelial-mesenchymal transition (EMT), forming pseudopodia at their leading front and a lagging cell body at their rear end. These mesenchymal leading cells can digest and remodel the ECM, creating a path for migrating cells and are accompanied by tightly interconnected (by cadherin- $\beta$ -catenin- $\alpha$ -catenin complex) following cells. In this pattern, migration takes place slowly.
2. Individually: In this pattern, individual cells acquire round shape and amoeboid migration capability, which enable them to migrate through the ECM, faster than mesenchymal cells.

These two types of invasive/migratory (mesenchymal and amoeboid) cells show high degrees of plasticity and are able to transition into one another, as a result of their interaction with their surrounding environment (Krakhmal et al. 2015; Pankova et al. 2010).

### **1.3. Metastasis-associated proteins and implantation**

#### **1.3.1. Metastasis-associated proteins**

Metastatic lesions and colonisation of the organs with tumour cells can lead to organ failure and death (van Zijl, Krupitza & Mikulits 2011), making metastasis accountable for 90% of cancer-related deaths (Le, Denko & Giaccia 2004). The occurrence of metastasis, into an ectopic microenvironment (host tissue), is a multi-step process regulated by numerous genetic and epigenetic changes (Langley & Fidler 2011). These steps include: 1. aberrant cell growth and proliferation, due to enhanced survival and angiogenesis of tumour cells, 2. detachment of tumour cells from their microenvironment, due to disrupted adhesion, 3. degradation of the ECM and the basement membrane, due to acquired invasiveness, 4. entering the blood or lymphatic vessels (intravasation), due to acquired motility, 5. traveling to a new site, while sustaining their viability, 6. leaving the circulation (extravasation), due to vascular permeability, 7. settling and proliferating in the host tissue, and 8. eventually giving rise to secondary tumours in distant organs and tissues (Hanahan & Weinberg 2011) (Figure 1.6).

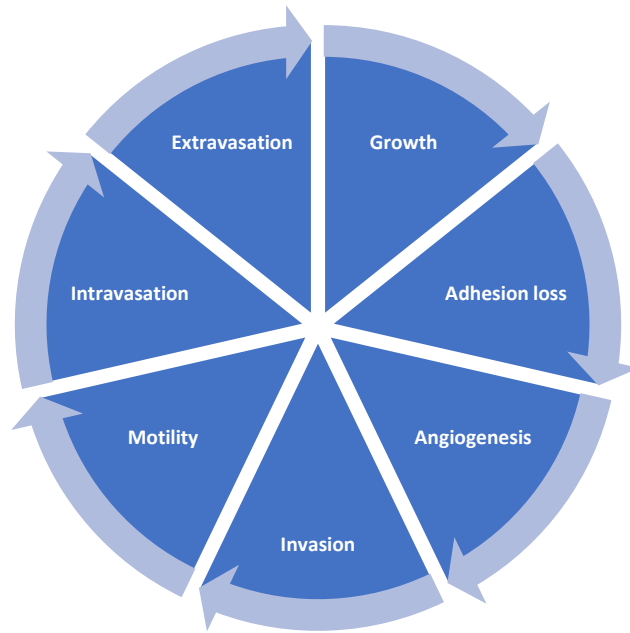


**Figure 1.6 Metastasis steps.** The main steps in tumour metastasis along with some of their main effectors have been summarised in this chart. (Based on data reported in Hanahan and Weinberg 2011).

The factors involved in metastasis also can be categorised according to the seed and soil hypothesis, which states that cancer cells (seeds) can give rise to metastasis, wherever the microenvironment (soil) allows them to (Langley & Fidler 2011):

1. The pro-metastatic factors of tumours include:
  - Cancer stem cells, which can provide the tumour with a heterogeneous population of cells
  - Circulating tumour cells, which have shed into the vasculature
  - EMT and its reverse, mesenchymal to epithelial transition (MET)
  - Metastatic dormancy, in which tumour cells disseminate to secondary sites and become dormant for long periods before giving rise to metastasis, tumour-secreted factors such as cytokines
  - Chemokines and extracellular vesicles
  - Autophagy
2. The pro-metastatic factors in the primary host include:
  - Hypoxia
  - Proteins expressed by tumour-associated macrophages, mesenchymal cells, endothelial cells and adipocytes, which enhance tumour invasion

- Tumour perfusion
  - Physical properties of the ECM, which usually is stiffer than normal tissues, due to excess activities of lysyl oxidase, which cross-links collagen fibres and elevated levels of fibronectin and collagen (Lu, Weaver & Werb 2012)
3. The pro-metastatic factors in the distant organ or the secondary host tissue microenvironment, which make the tumour growth within the lung, liver, bone, and brain more likely compared to other organs.

The over-expression of a certain group of proteins have been related to clinical manifestation of tumour metastasis, aggressive phenotype and poor prognosis for cancer patients. These proteins are known as “Metastasis-associated proteins” (Ho et al. 2009). These proteins can be involved in any of the steps of metastasis, such as the proto-oncogene tyrosine-protein kinase Src (Summy & Gallick 2003), small integrin-binding ligand N-linked glycoprotein family (Bellahcene et al. 2008), SPARC protein family (Bradshaw 2012), integrins (Desgrosellier & Cheresh 2010), thrombospondins (Lawler & Lawler 2012), T-lymphoma invasion and metastasis-inducing protein-1 (Izumi et al. 2019), vimentin, and tropomyosin (Sun et al. 2008). The injection of mice with benign tumour cells that have been induced to express of some of these proteins such as S100A4 (Davies et al. 1993), S100P (Wang et al. 2006) and anterior gradient homologue 2 (Liu et al. 2005) (these three proteins are also known as metastasis-inducing proteins) lead to metastasis in mice.

In the existing literature the term “metastasis-associated proteins” (abbreviated as MTA proteins), other than the way described in this work, may also refer, specifically, to a protein family, that has been shown to have a role in cancer progression by regulating chromatin remodelling (Sen, Gui & Kumar 2014).

### **1.3.2. Tumour metastasis and implantation similarities**

The resemblance between the development of solid tumours and the placenta was reported for the first time in the early 20<sup>th</sup> century (Beard 1905). “Cancer, a developmental biology” was a theory proposed in late 20<sup>th</sup> century suggesting that tumorigenesis and embryology have a lot in common, assuming that tumour cells are in fact embryonic cells that continue their proliferation into the body (Pierce 1983). Later in the 21<sup>st</sup> century, the progress in molecular biology showed similarities between embryonic and tumour cells (Figure 1.7), in terms of gene expression and the protein profile, which makes both cell types immortal, undifferentiated and invasive, features that are known to attribute to the ‘pseudo-malignant’ phenotype of trophoblasts (Monk & Holding 2001; Rousseaux et al. 2013).

Developing cytotrophoblasts and metastatic tumour cells both go through EMT. During this process they obtain mesenchymal phenotype, separate from the epithelium and migrate away from their originating epithelial layer (the tips of the villous columns for trophoblasts) and invade into a new tissue (uterine lining for trophoblasts) (DaSilva-Arnold et al. 2018). Cells that go through EMT show loss of cell junctions and epithelial markers (i.e. E-cadherin) and elevated matrix degradation and expression of mesenchymal markers including N-cadherin, fibronectin and laminin (Vergara et al. 2016). EMT “switch” is mediated by transcription factors such as Snail, zinc-finger E-box-binding and basic helix-loop-helix transcription factors (Lamouille, Xu & Derynck 2014). Additionally, transforming growth factor- $\beta$  (TGF $\beta$ ) family signalling plays a prominent role in initiating and controlling EMT (Lamouille, Xu & Derynck 2014).

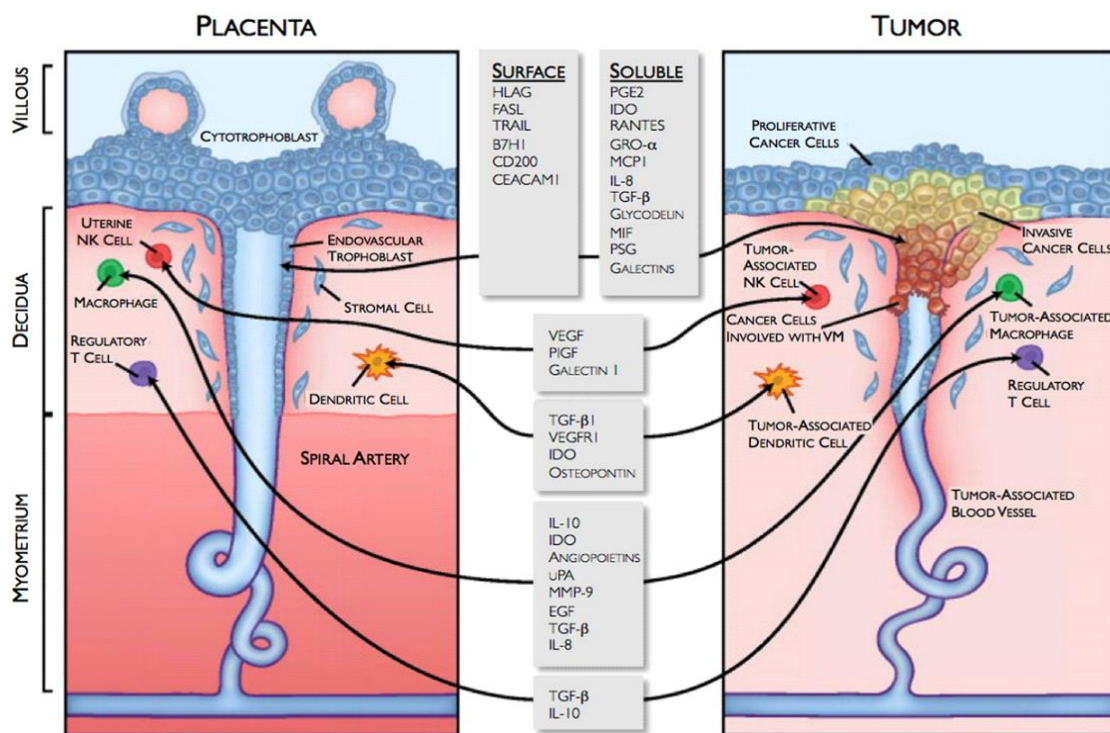


**Figure 1.7 Strong similarity between tumour invasion and trophoblast invasion.** The placenta and tumour cells express proteins that will give them the ability to invade, maintain adequate blood and nutrient supply and grow in a new environment (adapted from Holtan et al. 2009).

Moreover, placental mammals (eutherial), especially those with highly invasive haemochorial placentas, have higher rates of malignancies compared with other animals. Conversely, metastatic carcinomas and sarcomas are rarely reported in non-mammalian organisms, and the incidence of solid tumours seems to be mostly locally invasive (Albuquerque et al. 2018). These striking

similarities between placental cell invasion and tumour invasion provide a rationale for the hypothesis that many metastasis-associated proteins could possibly play crucial roles in placental implantation.

### **1.3.3. Why study metastasis-associated proteins in implantation?**

Successful embryo implantation, consisting of three steps, i.e. apposition, attachment and invasion of the blastocyst, as a result of the cross-talk of a receptive endometrium and a healthy embryo; however, it only occurs in only 50% of all human implantations (Achache & Revel 2006; Dekel et al. 2010). While approximately 5-10% of otherwise successful pregnancies can be affected by preeclampsia, a pregnancy-related disorder caused by a maternal inflammatory response to placentation, characterised by hypertension and proteinuria. It is known as the main cause maternal/foetal morbidity and mortality; 1% can be affected by an even more serious variant of the disease known as HELLP syndrome, which stands for haemolysis (H), elevated liver enzymes (EL) and low platelet count (LP), both of which are mainly accompanied by reduced placental perfusion due to abnormal implantation (Haram, Mortensen & Nagy 2014; Roberts & Lain 2002).

Preeclampsia and its accompanying disorders, which can include intrauterine growth restriction (IUGR), preterm birth (PTB) and miscarriages, have been linked with oxidative stress and a reduction in angiogenic factors (Ahmed, Rezai & Broadway-Stringer 2017). These disorders are associated with inadequate invasion of EVT's into the decidua and abnormal artery remodelling (Ball et al. 2006; Brosens, Robertson & Dixon 1972; Khong et al. 1986; Reister et al. 2006). When compared with other mammal species, humans have about a 50% lower chance of successful pregnancy in a menstrual cycle, making it rather inefficient (Edwards 2007). Therefore, in spite of all the advances in knowledge and technology related to pregnancy-related issues, it is fair to say that implantation is still in need of more thorough research in terms of the relevant cellular pathways.

This work aims to study the effect of three different metastasis-associated proteins that have been closely linked with tumour cell motility and invasion, S100P (a member of the S100 family), ezrin (a member of the ERM family) and IQGAP1 (a member of the IQGAP family), on the physiological process of implantation and how their expression affects trophoblast motility and invasion, processes that are crucial for successful remodelling of maternal arteries in order to provide an adequate blood supply to the foetus (Sato, Fujiwara & Konishi 2011). To achieve our aim, the expression of these proteins was studied in human placenta tissue sections from different

gestational ages to learn more about their levels and cytological differences. Further work was carried out using human trophoblast cell lines to study the changes in their motile and invasive capabilities and some of the molecular mechanisms involved during the above mentioned processes.

## **1.4. S100 family of proteins**

S100 proteins are members of a large super-family of  $\text{Ca}^{2+}$ -binding proteins with EF-hands ( $\text{Ca}^{2+}$ -binding domains with two alpha helices linked by a loop region, found in  $\text{Ca}^{2+}$ -binding protein such as calmodulin, parvalbumin and troponin C), in which “S100” refers to their solubility in 100% ammonium sulphate at neutral pH (Moore 1965).

### **1.4.1. Genetics**

About 25 members of this family of proteins have been identified exclusively in all vertebrates (Zimmer et al. 2013), which include 16 S100A proteins (S100A1–S100A16) and others (such as S100B, S100G, S100P and S100Z). S100 genes have been divided into four major subgroups based on their phylogenetic relationships, the oldest of which (A1/A10/A11/B/P/Z subgroup) appeared around the same time as the vertebrates (about 500 million years ago). The other three subgroups (A13/A14/A16, A2/A3/A4/A5/A6, and A7/A8/A9/A12/G) emerged later around the same time as the appearance of the common ancestor of reptiles, birds and mammals, by a series of tandem gene duplication; Therefore, they are believed to be paralogues (Gross et al. 2014; Zimmer et al. 2013). S100A1-A16 are located on chromosome 1 (1q21), while S100B, S100G, S100P, S100Z, S100G. S100Z and S100P are located on chromosomes 21, X, 5 and 4, respectively (Shang, Cheng & Zhou 2008).

### **1.4.2. Structure**

S100 proteins are small (10-12 KDa) acidic proteins with no enzymatic activities (in most cases) that have remarkably diverse functions due to their ability to form homo- and (less commonly) heterodimers (S100A1-S100B, S100A8-S100A9 S100A1-S100A4, S100A1-S100P, and S100A11-S100B ) as well as multimeric forms (S100B multimer and S100A4 multimer) along with being expressed in a highly cell- and tissue-specific manner (Marenholz, Heizmann & Fritz 2004; Oslejskova et al. 2009; Ostendorp et al. 2007; Rambotti et al. 1999; Schafer & Heizmann 1996; Spratt et al. 2019). Most S100 proteins contain two EF-hands (Figure 1.8): a C-terminal canonical EF-hand with a typical sequence of 12 amino acids loop (which is similar to EF-hands in other  $\text{Ca}^{2+}$ -binding proteins) and a higher affinity ( $K_d = 20\text{-}50 \mu\text{M}$ ) for  $\text{Ca}^{2+}$  along with an N-

terminal unconventional or pseudo EF-hand with a 14 amino acid loop and a lower affinity ( $K_d = 200\text{-}500\ \mu\text{M}$ ) for  $\text{Ca}^{2+}$  (which is unique to S100 proteins) (Donato 1986; Kawasaki, Nakayama & Kretsinger 1998).  $K_d$  or the equilibrium dissociation constant refers to the ratio of dissociation reaction ( $K_{\text{off}}$ )/association reaction ( $K_{\text{on}}$ ), where  $K_{\text{off}}$  shows the rate at which the two molecules separate and  $K_{\text{on}}$  shows the rate at which the two molecules bind to each other. The constant indicates the strength of the interaction a between a molecule to its ligand and the lower the  $K_d$ , the greater the affinity (Eaton, Gold & Zichi 1995).

Despite structural similarities between the family members, they differ in function, post-translational modification, spatial/temporal expression patterns and binding orientations for target proteins (Ikura & Ames 2006). Other than binding to  $\text{Ca}^{2+}$ , some S100 proteins can bind to  $\text{Zn}^{2+}$  (Schafer & Heizmann 1996; Zimmer et al. 1995) and  $\text{Cu}^{2+}$  (Nishikawa et al. 1997; Schafer et al. 2000), while at least one member of the family (S100A10) can function independently of  $\text{Ca}^{2+}$ , due to a mutation in its EF-hands, which makes them permanently active and unable to bind to  $\text{Ca}^{2+}$  (Rety et al. 1999).

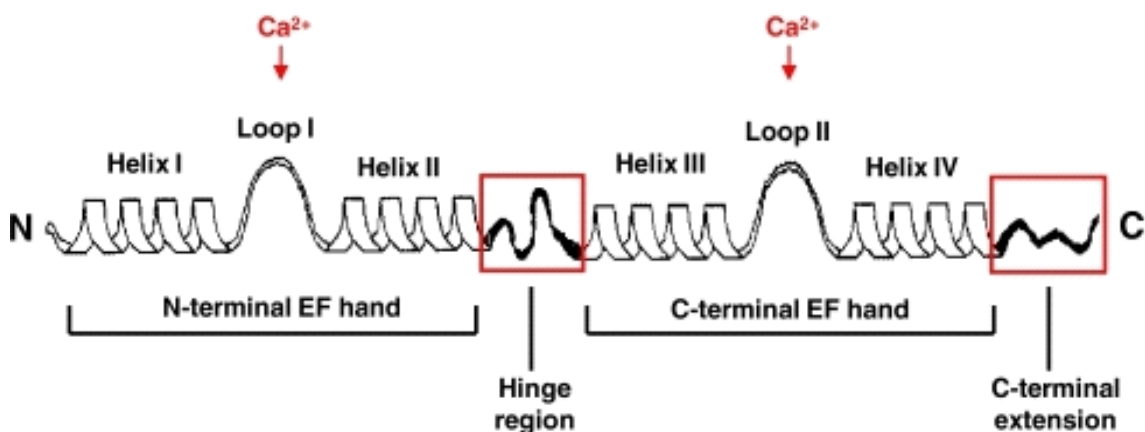


**Figure 1.8 Schematic diagram of the secondary structure of a monomeric S100 protein.** S100 proteins consist of an N-terminal (non-canonical) and a C-terminal (canonical) EF hand that are attached together by an intermediate hinge region. The regions marked in red boxes show the most variability among the members of the S100 protein family (Image adapted from Rohde et al. 2010).

Similar to other  $\text{Ca}^{2+}$ -binding proteins, such as calmodulin and troponin C, S100 proteins undergo a conformational change upon binding to  $\text{Ca}^{2+}$ , which acts as a switch that exposes their hydrophobic target-binding region, allowing binding to target proteins, and subsequent exertion of their biological effects (Drohat et al. 1998; Sastry et al. 1998; Smith & Shaw 1998).

### **1.4.3. Function**

S100 proteins have been linked to diseases such as diabetes, cardiomyopathy, neurodegenerative disorders and different types of cancers ( reviewed by Marenholz et al. 2004). Several, intra- and extracellular, target proteins (including nucleic acids, enzymes, cytoskeletal elements, receptors and transcription factors) have been identified for S100 proteins, involved in controlling different cellular functions. Some proteins might interact with more than one of the family members and result in similar activities. The main cellular functions that have been linked to S100 proteins have been summarised as follows:

#### **1.4.3.1. S100 proteins and cellular proliferation and differentiation**

S100A1 and S100B interact with microtubules using their C-terminal domain and control their disassembly at the onset of mitosis in a pH- and  $\text{Ca}^{2+}$ -dependent manner in glial cells, and therefore might be potential regulators of proliferation (Sorci et al. 1998; Sorci, Agneletti & Donato 2000). S100A2 and S100A4 interact with tumour suppressor P53 and lead to the regulation of cell proliferation by stimulating its transcriptional activity and enhancing its expression (Mueller et al. 2005; Orre et al. 2013; Pan et al. 2018). Moreover, S100A1, S100A6, S100A12, S100B, and S100P interact with calcyclin-binding protein/Siah-1-interacting protein and can potentially enhance survival and tumorigenesis by inhibiting  $\beta$ -catenin degradation (Filipek et al. 2002). S100A3 has a role in the differentiation of hair follicular cells and the formation of the mature hair shaft, through regulating transglutaminase type 1 (an enzyme with the ability to form proteolysis-resistant protein crosslinking bonds) (Kizawa et al. 1998). S100A9 induces apoptosis upon P53 activation (Li et al. 2009) and, by making a heterocomplex with S100A8, can regulate proliferation and differentiation (Voss et al. 2011). S100A9 can also induce survival upon interacting with nuclear factors, via the stimulation of NADPH oxidase and down-regulation of p38 mitogen-activated protein kinase (MAPK) (Kuwayama et al. 1993; Nemeth et al. 2009). S100A16 induces adipocyte differentiation and proliferation as well as insulin resistance (Liu et al. 2011). S100A12 has a role in vascular remodelling by increasing MMP2 expression as well as phosphorylation and nuclear translocation of Smad2 (a member of SMAD protein family that are signal transducers and transcriptional modulators) (Hofmann Bowman et al. 2010).

#### **1.4.3.2. S100 proteins and $\text{Ca}^{2+}$ homeostasis**

S100A1 and S100B control intercellular  $\text{Ca}^{2+}$  homeostasis; this is important as  $\text{Ca}^{2+}$  plays a critical role in the stability of voltage-gated ion channels, preventing them from opening/closing spontaneously and leading to hyper-/hypo-activity of muscle and nerve cells. S100A1 and S100B

can also have enzyme activities (Boden & Kaplan 1990; Rambotti et al. 1999). A deficiency in S100A1 in the myocardium and skeletal myofibres impedes  $\text{Ca}^{2+}$  cycling in the sarcoplasmic reticulum, and can lead to impaired contractile performance (Prosser et al. 2008; Rohde et al. 2010).

#### **1.4.3.3. S100 proteins and cellular migration/invasion**

The majority of S100 proteins (S100A1, S100A2, S100A4, S100A6, S100A7, S100A8, S100A9, S100A8-S100A9 heterodimer, S100A10, S100A11 S100A12, S100B, and S100P) have been associated with cellular motility and invasion under both normal and pathological conditions, by either directly binding to actin filaments or to actin binding proteins as well as enzymes and transcription factors (reviewed by Donato et al. 2013; Gross et al. 2014). The identified cellular mechanisms involved in S100 protein-mediated migration include the dynamics of filamentous actin (F-actin) polymerisation (Nagy et al. 2001; Yang et al. 2001), actin cross-linking (Bowers et al. 2012; Du et al. 2012; Ford & Zain 1995; Goh Then Sin et al. 2011), as well as the activation of the receptor for advanced glycation endproducts (RAGE) (Fuentes et al. 2007; Kataoka et al. 2012; Lawrie et al. 2005). S100A4, A10 and A14 are involved in invasion via the activation of plasmin pathway and MMPs (Chen et al. 2012; Sapkota et al. 2011; Semov et al. 2005; L. Wang et al. 2012; Zhang, Fogg & Waisman 2004).

#### **1.4.4. S100P**

S100 calcium-binding protein P (S100P), also known as migration-inducing gene 9 protein (MIG9), is a member of the S100 protein family (Donato 2001). The protein consists of 95 amino acid residues, weighs 10.4KDa, and was isolated from human placenta for the first time in 1992 (Becker et al. 1992). It functions as a homodimer or a heterodimer with S100A10 and S100A6 (Wang et al. 2004; Whiteman et al. 2007).

##### **1.4.4.1. S100P Expression**

The S100P gene is located on chromosome 4 (4p16) (Shang et al. 2008) and is expressed in many human tissues, such as the placenta, where it shows high expression levels, as well as the lung, skeletal muscle, and heart (Jin et al. 2003). Most of the studies related to this protein have, however, focused primarily on cancer.

Despite the high expression levels of this protein both physiological states or cancer tissues, little is known about how its expression is regulated. At the transcriptional level, three cis-

regulatory elements (CREs), with binding sites for STAT/CREB, SMAD and SP/KLF have been identified in the promoter region of the S100P gene (Gibadulinova et al. 2008).

#### 1.4.4.2. S100P-interacting proteins

A series of proteins interacting with S100P in cancer cells have been identified (Table 1.1). While ezrin, NMII and IQGAP1 cacyBP/SIP are localised inside the cell, RAGE, integrin  $\alpha 7$  and cathepsin-D are present at the cell surface, suggesting that S100P can function both intra and extracellularly. Most of these interactions suggest that S100P has a role in the regulation of cancer cell migration and invasion, whilst data reporting the interaction of S100P with any of these factors in the context of non-pathological conditions is not clear (Du et al. 2012; Filipek et al. 2002; Heil et al. 2011; Hsu et al. 2015; Kikuchi et al. 2019; Koltzschler et al. 2003; Mercado-Pimentel et al. 2015).

S100P binding partners	Possible effect on the cell
NMIIA	Enhanced motility
Ezrin	Enhanced motility
Integrin $\alpha 7$	Enhanced motility and invasion
Cathepsin-D	Enhanced invasion
RAGE	Enhanced proliferation
IQGAP1	Reduced proliferation
CacyBP/SIP	Unknown

**Table 1.1 Proteins that interact with S100P and their effect on cancer.** The interaction between S100P with NMII and ezrin up-regulates cellular motility (Du et al. 2012; Kikuchi et al. 2019; Koltzschler et al. 2003), while its interaction with integrin  $\alpha 7$  promotes both motility and invasion (Hsu et al. 2015). S100P might enhance cell proliferation through interacting with RAGE (Mercado-Pimentel et al. 2015) or reduce it though interacting with IQGAP1 (Heil et al. 2011). S100P also binds to CacyBP/SIP, but the effects are not yet known (Filipek et al. 2002).

#### 1.4.4.3. S100P in cancer

S100P over-expression has been reported in many cancers (Table 1.2). Ectopic expression of this protein in cancers is mainly due to hypomethylation (Sato et al. 2004), and it has been associated with sex hormones in cancers of the prostate (Averboukh et al. 1996; Basu et al. 2008) and

(possibly) breast (Schor et al. 2006). S100P has been suggested to be used as a marker for early diagnosis in pancreas (Downen et al. 2005; Ohuchida et al. 2006) and prostate cancer (Hu et al. 2014). Since its elevated levels of expression have been associated with a poor prognosis, it has been recommended to be used as a prognosis marker for cancers of colon (Q. Wang et al. 2012), breast (Peng et al. 2016; Wang et al. 2006), liver (Yuan et al. 2013) and ovaries (Wang et al. 2015). Moreover, S100P knockdown was not only shown to reduce tumour growth and metastasis, but seems to enhance the response to chemotherapeutic drugs as well (Arumugam et al. 2005; Arumugam, Ramachandran & Logsdon 2006).

### **Cancer types associated with S100P expression**

Breast cancer (Peng et al. 2016; Wang et al. 2006)
Colorectal cancer (Fuentes et al. 2007; Q. Wang et al. 2012)
Hepatocellular carcinoma (Yuan et al. 2013)
Invasive ductal carcinoma (Guerreiro Da Silva et al. 2000)
Non-small cell lung carcinoma (Diederichs et al. 2004)
Oral squamous cell carcinoma (Raffat et al. 2018)
Ovarian cancer (Wang et al. 2015)
Pancreatic carcinoma (Downen et al. 2005; Ohuchida et al. 2006)
Prostate cancer (Hu et al. 2014; Mousses et al. 2002)

**Table 1.2 The association between S100P expression and poor prognosis in cancer.**

## **1.5. ERM family of proteins**

The ERM family consists of three members including ezrin, radixin and moesin. These proteins are found at adhesion sites, lamellipodia, filopodia, ruffling membranes, the cleavage furrow of mitotic cells, apical microvilli as filopodia, lamellipodia, apical microvilli and contractile cell rear (known as the uropod or trailing edge), linking the cell membrane via transmembrane proteins, phospholipids and membrane-associated cytoplasmic proteins to the underlying cytoskeleton via interactions with F-actin. ERM proteins also play roles in cAMP and Rho GTPase signalling pathways (Fehon, McClatchey & Bretscher 2010; Tsukita & Yonemura 1999; Tsukita, Yonemura & Tsukita 1997; Wakayama et al. 2009).

In adult mammals, the expression of ERM members show tissue specificity: ezrin is predominant in epithelial cells, moesin in endothelial and radixin in hepatocytes (Fouassier et al. 2001; Hanzel et al. 1991).

### 1.5.1. Genetics

The three paralogue members of the ERM family likely arose by gene duplication. They are found in all vertebrates, while other species only contain a single ERM gene, and yeast have no ERM gene at all (Bretscher, Edwards & Fehon 2002; Turunen, Wahlstrom & Vaheri 1994). The primary structure of ERM proteins are highly conserved in different species; N-ERMAD (also known as FERM) and C-ERMAD domains of different ERM proteins in vertebrates and moesin and ERM-1, their homologues in *Drosophila* and *C. elegans*, respectively, share about 75% identity (Arpin et al. 2011). In humans, the genes encoding ezrin, radixin and meosin are located on chromosome 6, 11 and X, respectively (Fehon, McClatchey & Bretscher 2010).

### 1.5.2. Structure

Ezrin, radixin, and moesin have an amino acid length of 585, 582, and 576 and 70-75 kDa in molecular weight, and are very similar to one another (Maresso, Baldwin & Barbieri 2004). They closely related to neurofibromatosis type 2 (NF2) tumour suppressor merlin (McClatchey & Fehon 2009) and regulate cortical organisation by binding to the cytoplasmic tails of membrane proteins, such CD43, CD44 and intracellular adhesion molecule 2 (ICAM-2), via their globular amino-terminus; this contains three lobes: F1, F2 and F3, which are also known as the four-point one, ezrin, radixin, moesin (FERM) domain. FERM is followed by an extended  $\alpha$ -helical domain and a linker section, bound to a positively charged actin-binding carboxy-terminus domain, also known as the C-ERMAD tail (Tsukita, Yonemura & Tsukita 1997) (Figure 1.9).

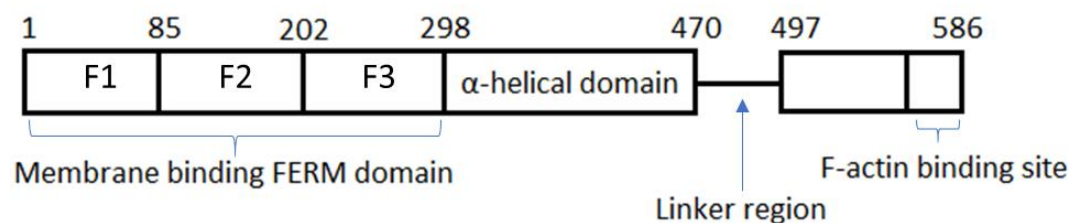


**Figure 1.9 Primary structure of ERM family of proteins.** ERM proteins are composed of an N-terminal FERM domain linked to a C-terminal ERMAD by an  $\alpha$ -helical and a linker region. (Adapted with modification from Ponuwei 2016).

The ERM proteins are found in two forms (Figure 1.10): 1. An inactive structure in which the C-ERMAD domain binds to the FERM domain with a high affinity ( $K_d=176$  nM), covering the F2 and F3 domains and masking the F-actin-binding as well as the membrane-binding regions, forming a closed monomers (intramolecular binding), homo/hetero-dimers and oligomers (head-to-tail intermolecular binding). 2. An open-active structure, where the head-to-tail interaction is disrupted (also can be found in the form of dimers, and oligomers) (Berryman, Gary & Bretscher 1995; Bretscher, Gary & Berryman 1995; Fehon, McClatchey & Bretscher 2010; Gary & Bretscher 1993; Zhu, Liu & Forte 2005). This activation occurs upon binding of membrane phosphatidylinositol 4,5-bisphosphate (PIP<sub>2</sub>) to the FERM domain and phosphorylation of the conserved threonine residues Thr558, Thr564, Thr567 of C-ERMAD domain in human moesin, radixin and ezrin, respectively, resulting in a reduction in the affinity of the N-terminal FERM domain for C-ERMAD (Fehon, McClatchey & Bretscher 2010; Fievet et al. 2004).

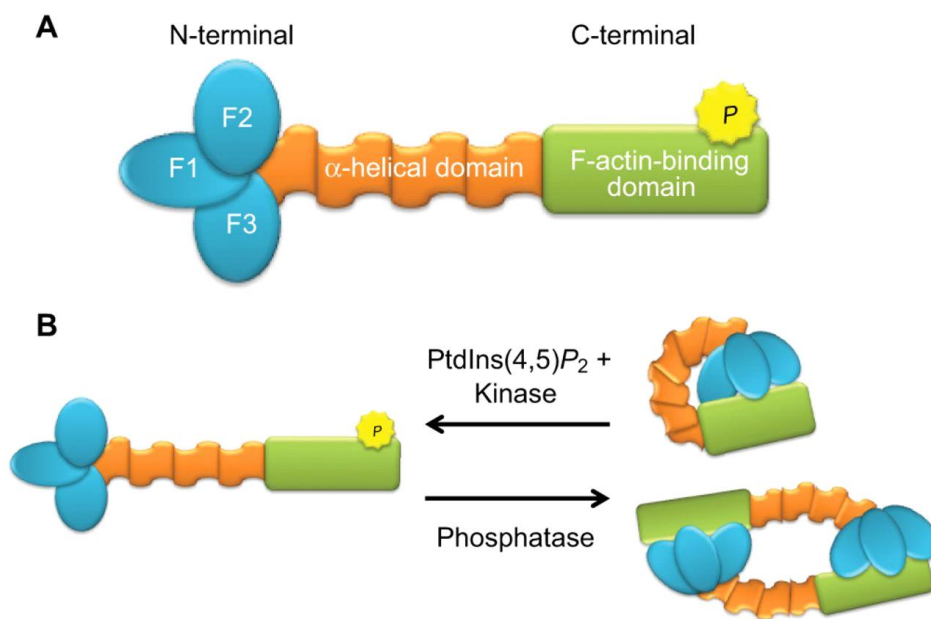


**Figure 1.10 Conformational forms of ERM proteins.** Panel A shows different regions of the protein and panel B show the two conformations: and open (active) and two forms of closed (inactive). (Adapted from Clucas and Valderrama 2014).

Protein kinase A (PKA) (Zhou et al. 2003), PKB (Akt2) (Shiue et al. 2005), PKC $\alpha$  (Ng et al. 2001), PKC $\theta$  (Pietromonaco et al. 1998), and atypical PKC $\zeta$  (Wald et al. 2008), G protein-coupled receptor kinase 2 (GRK2) (Penela et al. 2008), mammalian STE20-like protein kinase 4 Mst4 (Fidalgo et al. 2012; ten Klooster et al. 2009), mammalian Ste20-like Nck-interacting kinase

(NIK) (Baumgartner et al. 2006), mouse STE20-like protein kinase LOK (Belkina et al. 2009), sterile20-like kinase (Slik) (Cybulsky et al. 2017; Hipfner, Keller & Cohen 2004), and Rho-kinase phosphorylate the C-terminal threonine region of ERM proteins and result in their activation. (Matsui et al. 1998). Moreover, the  $\alpha$ -helical region has also been shown to play a role in this conformational change through an interaction with ERM-binding proteins (Arpin et al. 2011). The active form of the protein can then establish membrane-cortex connections by binding to F-actin on one side and to the membrane from the other (Bosk et al. 2011) (Figure 1.11).

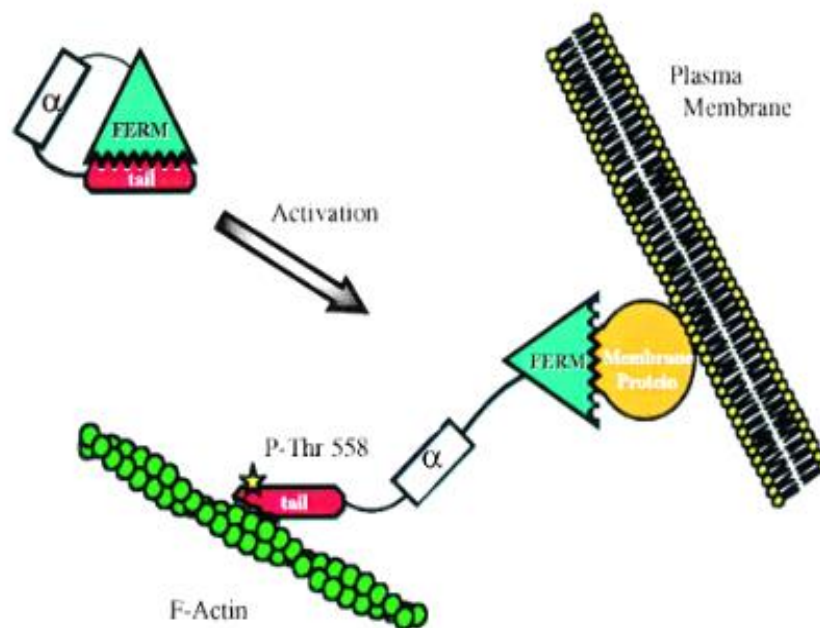


**Figure 1.11 Conformational change in an ERM protein (moesin) upon activation.** ERM proteins consist of three domains. In their inactive form, the N-terminal and the C-terminal regions are bound together, preventing them from interacting with the membrane and F-actin. (Adapted from Pearson et al. 2000).

### 1.5.3. Function

#### 1.5.3.1. ERM proteins and cellular proliferation and differentiation

ERM proteins have also been linked to EMT and increased proliferation through phosphoinositide 3-kinase/Akt pathway (Kong et al. 2016), and upon p38 and Rho kinase

activation (Huang et al. 2011). Ezrin inhibition has been associated with PKC $\alpha$ -mediated internalization and degradation of HER2 and apoptosis promotion (Jeong et al. 2019).

### **1.5.3.2. ERM proteins and cell morphology**

ERM protein activation by Rho and Rac promotes stress fibre and FA complex formation as well as actin polymerisation (Mackay et al. 1997). Ezrin degradation due to oxidative stress affects cell morphology (rounding up and blebbing) (Grune et al. 2002). During mitosis, moesin promotes roundness by enhancing cortical stiffness due to stress fibre loss (Kunda et al. 2008) and has been shown to promote epithelial integrity by regulating actin organization and polarity by the inhibition of the Rho pathway (Speck et al. 2003).

### **1.5.3.3. ERM proteins and cell adhesion**

ERM proteins are usually localised at cell cortex, connecting the membrane to actin, while a smaller proportion of them can be seen in cell-cell as well as cell-ECM contacts though interacting with ICAM-1, ICAM-2 and CD44 (Heiska et al. 1998; Legg et al. 2002; Naba et al. 2008; Tsukita et al. 1994). As expected, ERM downregulation leads defective and cell-cell and cell-ECM adhesion (Takeuchi et al. 1994). Likewise, moesin has been shown to promote E-cadherin stabilisation in adherens junctions in primary embryonic epithelia (Pilot et al. 2006) and ezrin in mouse and ERM-1 in *C. elegans* embryos have been shown to play important roles in adherence junction formation on the apical surface of the differentiating epithelium (Dard et al. 2001; Van Furden et al. 2004).

### **1.5.3.4. ERM proteins and cellular migration/invasion**

ERM proteins have been shown to play a significant role in the metastasis by enhancing the migration and invasion of tumour cells (Ghaffari et al. 2019; Ou-Yang et al. 2011; Park et al. 2017; Tang et al. 2019; Zhang & Wang 2019). Ezrin promotes cell migration through phosphorylation of the transmembrane receptor CD44 and subsequently interacting with it upon activation by PKC (Legg et al. 2002; Ng et al. 2001), as well as through colocalising Fes kinase at the leading edge of the cells and upon activation by hepatocyte growth factor (HGF) (Naba et al. 2008). GRK2 has been reported to phosphorylate radixin and enhance migration though rac1 activation (Kahsai, Zhu & Fenteany 2010). However, consistently phosphorylated and active ezrin in T-lymphocytes reduces migration, though interruption of lamellipodia formation as well as increasing membrane tension (resistance to shape change) (Liu et al. 2012). ERM proteins also enhance invasion by promoting MMP-2 (Tang et al. 2019) and MMP-7 (Jiang, Wang & Chen 2014) expression.

#### **1.5.4. Ezrin**

Ezrin (also known as cytovillin or villin-2), a member of ERM protein family, was first identified as a component of the microvillus cytoskeleton of intestinal epithelial cells (Bretscher 1983) and gastric parietal cells (Yao, Thibodeau & Forte 1993). Other cell lines also express ezrin as a component of microvilli (Bretscher 1989; Goslin et al. 1989; Gould et al. 1986). Other than threonine 567 (Fehon, McClatchey & Bretscher 2010), ezrin also can be phosphorylated by different kinases on tyrosine residues Tyr81 (Bretscher 1989), Tyr353, Tyr145 (Errasfa & Stern 1994), Tyr477 (Heiska & Carpen 2005), and serine 66 (Zhou et al. 2003). Changes in ezrin phosphorylation have been associated with changes in cellular function; for example, in gastric parietal cells, ezrin phosphorylation promotes changes its sub-cellular localisation (from apical vacuoles to microvillar membrane projections) and acid production through regulation of cell polarity and redistribution of cell membrane and cargo proteins (Urushidani, Hanzel & Forte 1989; Zhou et al. 2005). In fibroblast-like synoviocytes of rheumatoid arthritis patients, ezrin leads to enhanced migration and invasion (Xiao et al. 2014).

##### **1.5.4.1. Ezrin expression**

Human ezrin gene, EZR or VIL2, is located on chromosome 6 (q25.3) (Bethesda (MD): National Library of Medicine (US) 2019). Ezrin protein is highly expressed in thyroid, adrenal glands, lymph nodes, lung, kidneys, urinary bladder, oesophagus, stomach, small intestine, colon and placenta (Bethesda (MD): National Library of Medicine (US) 2019). Within cells, it is localised mainly at the membrane, the cytoskeleton (Neisch & Fehon 2011) as well as the nucleus (Batchelor, Woodward & Crouch 2004). Ezrin plays an essential role in embryo development by regulating microvilli formation by having a role in the formation of the apical/terminal web, a structure at the surface of epithelial cells, which is located at the base of the apical microvilli. Ezrin is also important in cell polarisation (critical to morphogenesis in multicellular tissues); ezrin knockout mice die soon after birth, due to extensive structural malformations (Saotome, Curto & McClatchey 2004).

##### **1.5.4.2. Ezrin-interacting proteins**

Ezrin has multiple binding partners that promote different cellular behaviours (Table 1.3).

<b>Ezrin binding partners</b>	<b>Possible effect on the cell</b>
EBP50	Membrane localisation of ezrin
CD49	Enhanced cell-cell adhesion and motility
CD49	Apoptosis
Merlin	Genome instability and tumorigenesis
PI 3-kinase	Enhanced survival
PKA	Proliferation
NHERF1	Enhanced survival
VCAM	Enhanced survival
ICAM1/ICAM2	Enhanced cell-cell adhesion
S100P	Enhanced motility
IQGAP1	Recruits IQGAP1 to cell cortex

**Table 1.3 Proteins that interact with ezrin and their effect on cells.** Ezrin–radixin–moesin (ERM)-binding phosphoprotein 50 (EBP50) has been shown to have a role in the localisation of ezrin in the apical membrane of polarised epithelial (Morales et al. 2004). The interaction of ezrin with CD43 enhances cell-cell contacts and motility through regulating cell morphology (Serrador et al. 1998), while its interaction with CD95 (FAS) promotes apoptosis (Fais, De Milito & Lozupone 2005; Parlato et al. 2000). When interacting with moesin-ezrin-radixin-like protein (merlin), ezrin can disrupt cell polarity and cause potential genome instability and tumorigenesis (Hebert et al. 2012). The interaction of ezrin with phosphatidylinositol 3-kinase (PI 3-kinase), vascular cell adhesion molecule 1 (VCAM-1) and sodium-hydrogen antiporter 3 regulator 1 (NHERF1) can enhance cell survival via the AKT pathway (Barreiro et al. 2002; Chen, Zhang, and Massague 2011; Gautreau et al. 1999; Jeong et al. 2019). Ezrin anchoring to protein kinase A (PKA) induces cAMP-mediated T-cell activation and proliferation (Ruppelt et al. 2007). The interaction between ezrin and intercellular adhesion molecule 1 and 2 (ICAM-1/ICAM-2) regulates cytoskeletal rearrangement and might lead to cell-cell adhesion (Heiska et al. 1998). The interaction of S100P with ezrin might promote cell motility (Austermann et al. 2008). Ezrin can bind to and recruit IQGAP1 to the cell cortex (Nammalwar, Heil & Gerke 2015).

### **1.5.4.3. Ezrin in cancer**

Ezrin has been linked with poor prognosis and aggressiveness in a wide variety of cancers (listed in Table 1.4), and it has been suggested to be used as a tumour marker of significant clinical value (Bruce et al. 2007). Increases in ezrin expression (Bruce et al. 2007; Geiger et al. 2000; Huang et

al. 2010; Khanna et al. 2004; Yu et al. 2004; Zhou et al. 2014) and phosphorylation (Mak et al. 2012; Sikorska et al. 2019; Zhou et al. 2014) are linked with metastasis and poor survival. Moreover, changes in the subcellular localisation of ezrin (Arslan et al. 2012; Elzagheid et al. 2008; Jin et al. 2014; Sarrio et al. 2006; Schlecht et al. 2012) have been linked to metastasis and tumour progression in carcinomas, sarcomas and astrocytic cancers (Antelmi et al. 2013; Horwitz et al. 2016; Liang et al. 2017). For example, in breast tissue, the highest level of ezrin expression is at the apical membrane, the cytosol and the membrane in normal, low-grade and high-grade tumours, respectively, while levels of phospho-ezrin seem to positively correlate with the tumour grade and negatively with prognosis (Antelmi et al. 2013). Moreover, metastatic breast cancer cells show increased nuclear localisation (Halon et al. 2013), while highly metastatic hepatocellular carcinoma cells show less nuclear localisation when compared with less-metastatic tumours (Hago et al. 2017).

### **Cancer types associated with ezrin expression**

Astrocytic cancer (Geiger et al. 2000)
Breast carcinoma (Sarrío et al. 2006)
Cervical cancer (Kong et al. 2013)
Colorectal cancer (Elzagheid et al. 2008; Patara et al. 2011)
Cutaneous basal and squamous cell carcinoma (Abdou et al. 2011)
Endometrioid carcinoma (Kobel et al. 2006)
Endometrial hyperplasia and uterine adenocarcinoma (Ohtani et al. 2002)
Gastric carcinoma (Zhao, Zhang & Xin 2011)
Gastrointestinal stromal cancer (Wei et al. 2009)
Head and neck squamous cell carcinoma (Madan et al. 2006)
Hepatocellular carcinoma (Kang et al. 2010)
Laryngeal squamous cell carcinoma (Wang, Liu & Zhao 2014)
Lung cancer (Li et al. 2012; Suzuki et al. 2015)
Nasopharyngeal carcinoma (Wang et al. 2011)
Oesophageal squamous cell carcinoma (Xie et al. 2011)
Oral potentially malignant disorders (Mohanraj et al. 2017)
Osteosarcoma (Salas et al. 2007)
Ovarian cancer (Song et al. 2005)
Pancreatic adenocarcinoma (Akisawa et al. 1999)
Rectal cancer (Korkeila et al. 2011)
Soft tissue sarcomas (Carneiro et al. 2011)
Uveal malignant melanoma (Makitie et al. 2001)

**Table 1.4 The association of ezrin expression with poor prognosis in many cancers.**

## 1.6. IQGAP family of proteins

IQ motif-containing GTPase-activating protein (IQGAP) proteins are scaffolding proteins (also known as scaffoldins) that control signalling pathways, from cell surface receptors to the nucleus, by binding to the components of the pathway, assembling them into a specific part of the cell, and therefore enhancing the efficacy of the pathway through regulating the integration, crosstalk and feedback between the components (Abel et al. 2016; Pan et al. 2012). Although it regulates a wide range of fundamental cellular processes, yeast IQGAP1 was originally introduced as a crucial regulator of actin-ring formation and cytokinesis (Epp & Chant 1997; Lippincott & Li 1998).

### 1.6.1. Genetics

IQGAPs are evolutionary conserved in eukaryotes. They are found with a single structure in fungi, known as IQGAP-related protein or Iqg1 in *Candida albicans* (Li, Wang & Wang 2008), Iqg1p or Cyk1p in *Saccharomyces cerevisiae* (Epp & Chant 1997; Osman & Cerione 1998; Shannon & Li 1999) and Rng2p in *Chizosaccharomyces pombe* (Chang, Woollard & Nurse 1996; Eng et al. 1998). IQGAPs are also found in four types in amoeba *Dictyostelium discoideum* (ddIQGAP1, ddIQGAP2 ddIQGAP3 and a putative ddIQGAP4) (Vlahou & Rivero 2006), and three isotypes with a high degree of homology (IQGAP1, 2 and 3) in vertebrates, including humans (Hedman, Smith & Sacks 2015).

IQGAP1, the most abundant and the best characterised isotype, appears to be ubiquitously expressed in all tissues (Choi & Anderson 2016; Weissbach et al. 1994), while IQGAP2 is highly expressed in the liver and platelets (Cupit et al. 2004). IQGAP3 has been mainly found in brain, lung and testis (Wang et al. 2007). In humans, IQGAP1 is encoded by the *Iqgap1* gene, located on chromosome 15 (Abel et al. 2016).

### 1.6.2. Structure

IQGAP1, 2 and 3 are composed of 1657, 1575 and 1631 amino acids, respectively (Watanabe, Wang & Kaibuchi 2015), forming five distinct domains (Figure 1.12):

- Calponin homology (CH) domain, which facilitates cytoskeletal remodelling by binding to polymerised F-actin and has a role in protein dimerisation (Mateer et al. 2002, 2004).

- Six coiled-coil domains, also known as heptad domains, which show homology to the myosin family, and bind to the FERM region of ezrin (Ho et al. 1999; Liu, Guidry & Worthylake 2014).
- WW or proline-rich motif-binding domain, with two conserved tryptophan residues (W), that associate with Erk (Macias, Wiesner & Sudol 2002) and the proline-rich parts of other proteins (Macias, Wiesner & Sudol 2002).
- Four isoleucine/glutamine-containing (IQ) domains, containing 20-25 amino acids, that bind to receptors including epidermal growth factor receptor (EGFR) (McNulty et al. 2011) and human epidermal growth factor receptor 2 (HER2) (White et al. 2011), as well as cytoskeletal components such as myosin (Weissbach, Bernards & Herion 1998) and calmodulin (Ho et al. 1999; Joyal et al. 1997). These domains also interact with signalling pathways, i.e. MAPK signalling (Roy, Li & Sacks 2005) and phosphoinositide signalling (PIPKI $\gamma$ ) (Choi & Anderson 2016), as well as S100B (Mbele et al. 2002) and S100P (Heil et al. 2011).
- Ras-GAP domain (GRD) that binds to GTPases such as Cdc42 (Hart et al. 1996; Joyal et al. 1997), Rac1 (Hart et al. 1996; Noritake et al. 2005) and TC10 (Neudauer et al. 1998) in their GTP-bound form, and has homology with Ras-GTPase activating proteins (Ras-GAPs). However this domains lacks GAP function, as it contains a conserved threonine instead of the arginine finger, which is essential for GTP hydrolysis (Briggs & Sacks 2003; Kurella et al. 2009).
- Ras-GAP C-terminus (RGCT) which interacts with cell adhesion proteins such as E-cadherin (Kuroda et al. 1998) and  $\beta$ -catenin (Briggs, Li & Sacks 2002) and cytoskeleton regulators such as neural Wiskott-Aldrich syndrome protein (N-WAS), Arp2/3 (Le Clainche et al. 2007), CLIP-170 (Fukata et al. 2002) and APC (Watanabe et al. 2004).

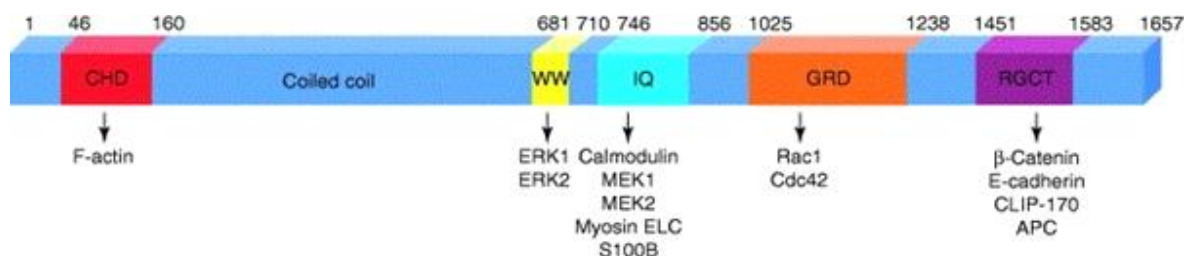


**Figure 1.12 Schematic diagram of IQGAP1 structure with its multiple domains and binding partners.** (Adapted from Brown and Sacks 2006).

IQGAP1 exists in three proposed conformational forms (Figure 1.13): a closed inactive form, where there is an intramolecular interaction between the N- and C- termini that can be relieved by phosphorylation of conserved serine residue 1443 located between the GRD and RGCT domains, by PKC $\epsilon$ , allowing for binding of type I $\gamma$  phosphatidylinositol 4-phosphate 5-kinase (PIPKI $\gamma$ ) to the IQ domain (Choi et al. 2013; Grohmanova et al. 2004; Li et al. 2005). This generates the partially open form, and a fully open form, in which Rho GTPases Rac1 and Cdc42 are bound to the GRD domain or PIP $_2$  is bound to the RGCT domain (Brandt & Grosse 2007; Choi & Anderson 2016; Fukata et al. 2002; Watanabe et al. 2004). The RGCT domain in the fully open form of IQGAP1 can then interact with the actin polymerisation regulators neural Wiskott-Aldrich syndrome protein (N-WAS) and Arp2/3 complex (Le Clainche et al. 2007) as well as regulators of microtubule dynamics, i.e. APC and CLIP-170 (Choi & Anderson 2016; Fukata et al. 2002; Watanabe et al. 2004).

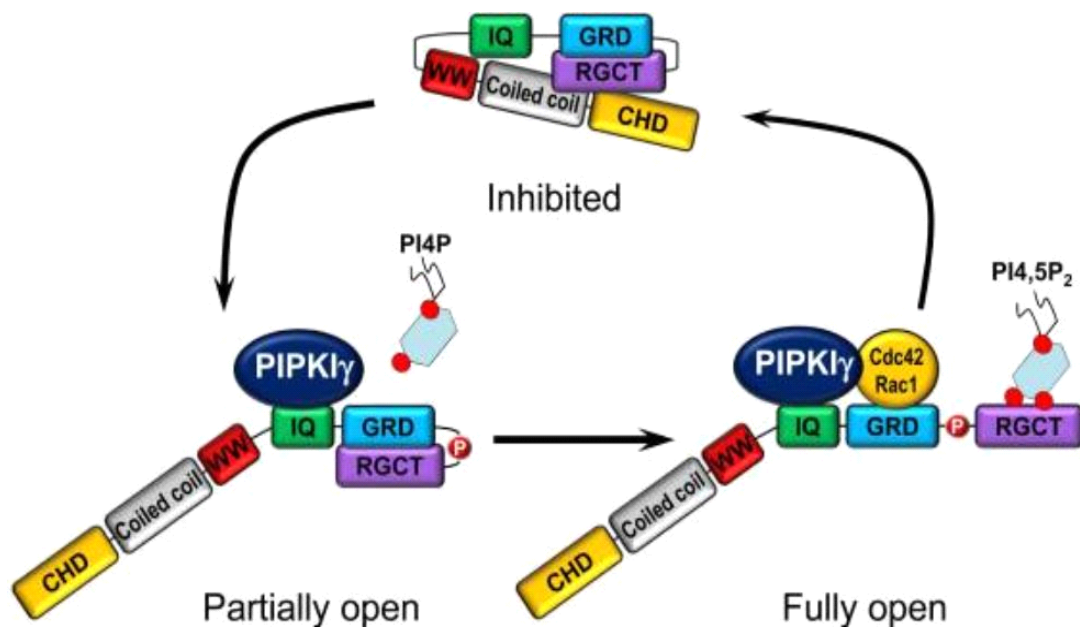


**Figure 1.13 IQGAP1 exists in three conformations.** In the autoinhibited closed structure, GRD and RGCT are bound together and there is a second fold that binds the N and C termini together. Opening of the latter fold by phosphorylation partially opens the protein, allowing for PIPKI $\gamma$  binding and the subsequent binding of PIP $_2$  and Rho GTPases, making the fully open form (Adapted from Choi and Anderson 2016).

Similar to many proteins, including receptors, transcription factors, ion channels and enzymes that need to form dimers and oligomers to function normally (Marianayagam, Sunde & Matthews 2004), IQGAP1 also forms parallel (head to head) dimers and oligomers through intermolecular

interactions between an area localised between amino acids 763-63, enabling it to bind to cofactors such as Cdc42, Rac and calmodulin, also giving it the ability to crosslink actin (Bashour et al. 1997; Liu et al. 2016; Mateer et al. 2002; Ren et al. 2005).

### **1.6.3. Function**

IQGAPs play crucial roles in several physiological process including:

- Lung function: IQGAP1 has a role in airway smooth muscle contractility and is significantly downregulated in samples from asthma patients compared with healthy controls (Bhattacharya et al. 2014).
- Insulin secretion: IQGAP1 plays a role in insulin secretion by facilitating vesicle trafficking in response to glucose stimulation (Kimura et al. 2013; Rittmeyer et al. 2008).
- Neuronal function: IQGAP1 expression is associated with neurite outgrowth by facilitating alterations in the actin cytoskeleton (Li et al. 2005) and has a role neuronal proliferation and migration (Kholmanskikh et al. 2006). IQGAP1 also plays a role in neurogenesis (generation of neurons from progenitor cells) (Balenci et al. 2007).
- Kidney function: IQGAP1 is involved in cell adhesion in kidney tubules and glomeruli (Lehtonen et al. 2005), as well as the slit diaphragm, which are the junctions between the foot processes of podocytes, i.e. the cells that wrap around glomerular capillaries (Grahammer, Schell & Huber 2013; Rigotherier et al. 2012).
- Cardiovascular system: IQGAP1 plays a role in cardiac remodelling and morphology (Sbroggiò et al. 2011) and promotes angiogenesis by enhancing endothelial cell migration and proliferation (Kohno et al. 2013; Yamaoka-Tojo et al. 2004).

IQGAP1 is also associated with carcinogenesis by enhancing tumour proliferation, invasion, and angiogenesis (Jadeski et al. 2008; Jameson et al. 2013).

The main cellular functions that have been linked to IQGAPs have been summarised as follows.

#### **1.6.3.1. IQGAPs and scaffolding diverse pathways**

IQGAPs acts as a scaffold protein for the RAS-RAF-MEK-ERK signalling pathway by directly binding to ERK1, ERK2, MEK1, MEK2 and B-RAF (Bardwell et al. 2017; Ren, Li & Sacks 2007; Roy, Li & Sacks 2005). IQGAPs are also involved in Wnt signalling. They regulate the canonical Wnt pathway by binding to leucine-rich repeat-containing G-protein coupled receptor 4 (LGR4) and its ligands R-spondins (RSPOs) as well as the non-canonical pathway by binding Ca<sup>2+</sup>/calmodulin and Cdc42 (Briggs & Sacks 2003; Carmon et al. 2014; Osman & Cerione 1998)..

### **1.6.3.2. IQGAPs and cytoskeletal dynamics**

IQGAP1 is highly concentrated at the cell cortex, where it colocalises with cortical actin filaments, directly binds (using its CH domain) to and cross-links actin filaments (by linking Cdc42 to F-actin), and stimulates the branched nucleation of actin filaments (Bashour et al. 1997; Le Clainche et al. 2007; Erickson, Cerione & Hart 1997; Hart et al. 1996; Mateer et al. 2002). Its participation in F-actin organisation can be affected by the  $\text{Ca}^{2+}$  concentration. Calmodulin, an important mediator of  $\text{Ca}^{2+}$  signalling, binds to the IQ motif of IQGAP proteins (Hart et al. 1996) and, with a lower affinity, to the CHD domain (Ho et al. 1999). Higher concentrations of  $\text{Ca}^{2+}$  enhance IQGAP1 and calmodulin association, while decreasing the association between IQGAP1 and Cdc42 and F-actin (Ho et al. 1999; Joyal et al. 1997; Mateer et al. 2002).

### **1.6.3.3. IQGAPs and cytokinesis**

IQGAPs in fungi, amoeba, *C. elegans*, and mammals have been shown to play a crucial role the formation of contractile ring between parent and daughter cells during cytokinesis (Adachi et al. 1997; Bielak-Zmijewska et al. 2008; Epp & Chant 1997; Faix & Dittrich 1996; Skop et al. 2004).

### **1.6.3.4. IQGAPs and proliferation and differentiation**

IQGAP1 promotes proliferation through interactions with Cdc42 and mTOR kinase (Wang et al. 2009), while its interaction with  $\beta$ -catenin also promotes both proliferation and differentiation (Jin et al. 2015; Su, Liu & Song 2017). IQGAP1 phosphorylation at serine residues 1441 and 1443, by PKC, promotes the appearance of new projection from neurons (neurite outgrowth) (Li et al. 2005). IQGAP1 and IQGAP3 promote epidermal growth and differentiation by activating EGFR and regulating MAPK (Monteleon et al. 2015).

### **1.6.3.5. IQGAPs and cellular migration/ invasion**

IQGAP1 has been shown to regulate motility by interacting with actin cytoskeleton and actin modulating proteins. For example, it links the fibroblast growth factor to Arp2/3 complex-dependent actin assembly (Bensenor et al. 2007), binds to Cdc42 and/or Rac1 and subsequently increases their levels at the leading edge of cells (Mataraza et al. 2003), regulates adhesion site dynamics by interacting with calmodulin,  $\beta$ -catenin, E-cadherin and (Foroutannejad et al. 2014; Fukata et al. 1999; Noritake et al. 2005), and affects cell polarity by interacting with microtubule plus-end scaffold proteins CLIP170 and APC (Fukata et al. 2002; Watanabe et al. 2004).

IQGAP1 has been shown to regulate invasion by acting as a downstream effector of endothelin-1 receptor signalling and recruitment of membrane-type 1 MMP, MMP2 and MMP9 to invadopodia (Chellini et al. 2019; Sakurai-Yageta et al. 2008).

#### **1.6.4. IQGAP1**

IQGAP1 (also known as p195), a 190 kDa protein, is the most-studied member of the IQGAP family (Weissbach et al. 1994). Like other scaffold proteins, IQGAP1 binds to many proteins and regulates many essential cellular processes such as cell adhesion, cell migration and cytokinesis (Brown & Sacks 2006). Similar to other members of the IQGAP family, IQGAP1 is a key mediator of multiple signalling pathways such as MAPK,  $\beta$ -catenin and Rac1, by integrating the signals from receptors such as EGFR (Erickson, Cerione & Hart 1997), M3 muscarinic acetylcholine receptor (Ruiz-Velasco, Lanning & Williams 2002), vascular endothelial growth factor receptor type 2 (VEGFR2) (Yamaoka-Tojo et al. 2004), CD44 (Bourguignon et al. 2005), and glutamate receptor 4 (GluR4) (Nuriya, Oh & Haganir 2005) directly or through second messengers such as PKC,  $Ca^{2+}$ , Ras GTPase, and PKA. This results in response outputs such as cell migration, adhesion and differentiation (Brown & Sacks 2006). Moreover, IQGAP1 has a role in actin polymerisation at the leading edge of the cells (Le Clainche et al. 2007) as well as actin ring formation (Lippincott & Li 1998). The activity of IQGAP1 can be regulated by changes in its sub-cellular localisation, binding to other proteins, dimerisation, post-translational localisation and phosphorylation (Brown & Sacks 2006).

Other than having a role in physiological functions such as in the kidney (Rigothier et al. 2012), neurons (Li et al. 2005), cardiovascular system (Kohno et al. 2013; Yamaoka-Tojo et al. 2004), lung (Bhattacharya et al. 2014) and insulin secretion (Kimura et al. 2013; Rittmeyer et al. 2008), IQGAP1 also is a potential therapeutic target in cancer (Jadeski et al. 2008) as well as bacterial (Brown et al. 2008; Karlsson et al. 2012) and viral infections (Morita et al. 2007).

##### **1.6.4.1. IQGAP1 expression**

IQGAP1 is ubiquitously expressed at high levels in animals, protists and fungi (Schwanhauser et al. 2011; Weissbach et al. 1994). The IQGAP1 gene is located on chromosome 15 (q26) (Bessède et al. 2016). The protein is localised in the plasma membrane, apical membrane, cytoplasm, nuclear envelope and cell junctions, colocalising with actin; its altered expression and localisation have been reported in metastatic tumours (Rotoli et al. 2017).

IQGAP1 knockout mice are viable and develop normally, but have been shown to be prone to late-onset gastric hyperplasia (Li et al. 2000) and heart malfunctions when they were subject to chronic conditions of pressure overload (Sbroggio et al. 2011).

#### 1.6.4.2. IQGAP1-interacting proteins

Being a large multi-domain protein, IQGAP1 binds to more than 50 proteins in malignant as well as normal cells (Brown & Sacks 2006), some of which have been listed in Table 1.5. None of these protein interactions have been reported in trophoblasts.

<b>IQGAP1 Binding partner</b>	<b>Potential effect on the cell</b>
Calmodulin	Enhanced cell proliferation, motility and adhesion
Cdc42	Enhanced cell proliferation, motility and adhesion
$\beta$ -Catenin	Enhanced cell proliferation and cell-cell adhesion
B-Raf	Enhanced cell proliferation and angiogenesis
Protein 4.1R	Enhanced migration
Rac1	Regulation of cell-cell adhesion
Arf6	Enhanced cell migration and invasion
ERK1/2	Enhanced cell invasion
MEK1/2	Enhanced cell invasion
Sec3/8	Enhanced cell invasion
Rap1	Regulation of cell-cell adhesion
CXCR2	Regulation of endosome trafficking
S100B	Rearrangement of cell membrane morphology
S100P	Reduced Proliferation
Ezrin	Promotes cortical localisation of IQGAP1

**Table 1.5 Proteins that interact with IQGAP1 and their effect on cells.** IQGAP1 interacts with a large number of proteins, some of which have been summarised in this table: calmodulin and Cdc42 have compete with one another in biding to IQGAP1 and their interaction subsequently regulate cell proliferation, migration and adhesion (Hart et al. 1996; Ho et al. 1999; Joyal et al. 1997; Kuroda et al. 1996; Wang et al. 2009). Moreover, calmodulin can modulate the

binding of IQGAP1 to  $\beta$ -catenin, which enhances cell-cell adhesion and proliferation (Briggs, Li & Sacks 2002). IQGAP1 interaction with B-Raf increases B-Raf activity and therefore enhances proliferation and angiogenesis (Meyer, Sacks & Rahimi 2008; Ren, Li & Sacks 2007). IQGAP1 can form a complex with APC and CLIP-170 and regulate morphology, cell polarisation and directional migration (Swiech et al. 2011; Watanabe et al. 2004). Protein 4.1R (a cytoskeletal protein) enhances cell migration by binding to and recruiting IQGAP1 into the leading edge of the cell (Ruiz-Saenz et al. 2011). IQGAP1 can regulate cell adhesion by interacting with GTPases Rac1 (Hart et al. 1996; Noritake et al. 2004) and Rap1 (Jeong et al. 2007). ADP-ribosylation factor 6 (ARF6) forms a complex with IQGAP1 and Rac1, and enhances cell migration and invasion (Hu et al. 2009). IQGAP1 regulates MAPK signalling pathway by binding to ERK1/2 and MEK1/2, and therefore enhances invasion (Jadeski et al. 2008; Roy, Li & Sacks 2005). IQGAP1 also promotes invasion by interacting with Sec3 and Sec8 subunits of exocyst (a protein involved in vesicle trafficking), leading to MMP accumulation in the invadopodium, by enhancing the transportation of the MMP-containing exosomes towards the leading edge of the cell (Sakurai-Yageta et al. 2008). IQGAP1 binds to C-X-C motif chemokine receptor 2 (CXCR2) and enhances endosome trafficking and signal transduction (Bamidele et al. 2015; Neel et al. 2011). S100 family members S100B (Mbele et al. 2002) and S100P (Heil et al. 2011) bind to IQGAP1 in the membrane, regulating cell morphology and proliferation, respectively. Ezrin can promote the membrane localisation of IQGAP1 (Nammalwar, Heil & Gerke 2015).

#### **1.6.4.3. IQGAP1 in cancer**

Unlike IQGAP2, which seems to be a tumour suppressor, IQGAP1 expression has been widely associated with carcinogenesis (White, Brown & Sacks 2009) and its over-expression has been linked with many cancers (Table 1.6). Moreover, invasive cancer cell lines of different origins express high levels of the protein, mainly localised within the membrane, especially in the invasive front of cells (Johnson, Sharma & Henderson 2009). IQGAP1 over-expression been indicated as a marker for poor prognosis in cancers of glial cells, head and neck, sinonasal squamous cells, laryngeal squamous cells, thyroid, liver, stomach, breast, pancreas, endometrium and colorectal cells (P. Dong et al. 2016; Hu et al. 2019; Jin et al. 2012; Li et al. 2017; Liu et al. 2010; McDonald et al. 2007; Nabeshima et al. 2002; Walch et al. 2008; X.-X. Wang et al. 2014; Wang et al. 2018; C.-C. Wu et al. 2018; Zeng et al. 2018).

### **Cancer types associated with IQGAP1 expression**

Breast cancer (Zeng et al. 2018)
Colorectal carcinomas (Nabeshima et al. 2002)
Endometrial cancer (P. Dong et al. 2016)
Gastric cancer (Walch et al. 2008)
Glioma (McDonald et al. 2007)
Head and neck squamous cell carcinoma (C.-C. Wu et al. 2018)
Hepatocellular carcinoma (Jin et al. 2015; Li et al. 2017)
Laryngeal squamous cell carcinoma (Wang et al. 2018)
Ovarian carcinomas (Dong et al. 2006)
Pancreatic cancer (Hu et al. 2019; Wang et al. 2013)
Sinonasal squamous cell carcinomas (Jin et al. 2012)
Squamous cell carcinoma of the oesophagus (X.-X. Wang et al. 2014)
Thyroid cancer (Liu et al. 2010)

**Table 1.6 The association of IQGAP1 expression with poor prognosis in many cancers.**

## **1.7. Hypothesis**

Our hypothesis for this work was that S100P, ezrin and IQGAP1, which are associated with tumour metastasis, are equally important in trophoblast motility and invasion and therefore placenta development.

### **1.7.1. Aims**

To study the role of S100P, ezrin and IQGAP1 in trophoblast motility and invasion.

### **1.7.2. Objectives**

- Establish the expression of S100P, ezrin and IQGAP1 in human placenta samples at different stages of gestation
- Establish the expression of S100P, ezrin and IQGAP1 in trophoblast cell lines.
- To test whether modulating the expression of S100P, ezrin and IQGAP1 affects trophoblast motility.

## Chapter 2.

# Materials and Methods

## 2.1. Materials

All equipment (Table 2.1), reagents (Table 2.2) and cell lines (Table 2.5 Cell lines.) used throughout this work were obtained from either Dr Stephane Gross's laboratory at Aston University or Prof. Melissa Westwood's laboratory at the University of Manchester. Where required, the solutions and utensils were sterilised by either autoclaving at 121°C or filtering through Millex PES syringe filters (Thermo Fisher Scientific, UK).

<b>Company</b>	<b>Equipment (and software)</b>
Acculabs Diagnostics UK Ltd, Billingham, UK	ATILON Portable Digital Scale
Appleton Woods, Birmingham, UK	24- and 96-well plates 35- and 150-mm petri dishes 200 µl pipette tips AppJET pipette controller Autoclave tapes Gyro Rocker SSL3 Nitrile gloves T25 and T75 tissue culture flasks
BANDELIN electronic GmbH & Co. KG, Berlin, Germany	SONOPLUS ultrasonic homogenizer
Bio-Rad, Hemel Hempstead, UK	1.0 mm and 0.75 mm 10-well combs Bio-Rad mini-Protean II electrophoresis system Casting stand Extra Thick Blot Filter Paper Mini Trans-Blot Cell PowerPac™ Basic Power Supply Mini cell buffer dam Polyvinylidene difluoride (PVDF) membrane short plates and spacer plates Trans-Blot SD Semi-Dry Transfer Cell
BioTek Potton, Bedfordshire, UK	Plate Reader EL800
Bioquell, Andover, UK	Microflow Class II advanced biological safety cabinet

Carl Zeiss Microscopy GmbH, Oberkochen, Germany	Cell Observer system with CCD camera (AxioCam MRm)
Cole-Parmer Instrument Co Ltd, St Neots, UK	Advanced Jenway pH Meter 3510
Corning Limited, Flintshire, UK	Matrix Matrigel
DJB Labcare Ltd, Buckinghamshire, UK	Eppendorf Centrifuge 5810R
ELGA LabWater, High Wycombe, UK	Purelab Option DV35 Water Purification System
GraphPad Software Inc., San Diego, USA	Prism 7.04
Greiner Bio-one, Stonehouse, UK	Cell scraper Sterile cryovial (2.0 ml) ThinCert™ Cell Culture Inserts (Transwells) for 24 well plate, 8µm pore size
Hamamatsu Photonics, Japan	NanoZoomer-XR Whole Slide Scanner
Keison Products, Chelmsford, UK	Stuart Gyro-Rocker (SSL3)
Lab Unlimited UK - Carl Stuart Group, Camberley, UK	Stuart Hotplate Stirrer SB 162-3
Leica Microsystems Ltd, Milton Keynes, UK	Inverted epifluorescence microscope (DM14000B) AxioVision Version 4.7 software Leica HI1210 water bath Leica RM2245 microtome
LI-COR Environmental - UK Ltd, Cambridge, UK	C-DiGit Blot Scanner Image Studio Lite Ver 5.2
Microsoft, Redmond, UK	Microsoft Office 365
National Institutes of Health, Maryland, USA	Fiji-ImageJ
Nikon Ltd, London, UK	Nikon ECLIPSE TS100 Microscope
Sigma-Aldrich, Poole, UK	1 ml Plastic Pasteur pipettes 1-14 Microfuge PAP pen for immunostaining Protease Inhibitor Cocktail Sigma 2-6 Benchtop Centrifuge Trypsin Solution (2.5%)

Thermo Fisher Scientific, Loughborough, UK	Aluminium foil Bottle Borosilicate Screw cap (250 ml, 500 ml, 1000 ml) Cling Film EVOS XL Core Cell Imaging System Falcon 15 ml and 50 ml Conical Centrifuge Tubes Fujifilm Corporation RX NIF Sheet X-ray Films Microscope glass slides Microcentrifuge tubes (0.5 ml, 1.5 ml, 2.0 ml) Millex Syringe Filter PES (0.22 µm pore) MINI LAB ROLLER ROTATOR W/36X1 Mr. Frosty Freezing container NanoDrop™ 1000 UV/VIS Spectrophotometer (NanoDrop Software) Nickel Electro Clifton Bath Lab Armor Parafilm Plastipak Syringe disposable (10 ml, 20 ml) Polypropylene universal tubes (30ml) Sanyo CO <sub>2</sub> Incubator MCO-17AIC 164L
Zeiss, Birmingham, UK	AxioCam Hrc Microscope

**Table 2.1 Equipment and software.**

<b>Company</b>	<b>Reagents</b>
Abcam, Cambridge, UK	Anti-cytokeratin 7 antibody (mouse) Anti-ezrin (phospho T567) antibody (rabbit) Anti-ezrin antibody (mouse) Anti-HLA-G (mouse) Anti-IQGAP1 antibody (rabbit) Anti-paxillin antibody (mouse) Anti-S100P (Rabbit) Anti-tubulin antibody (mouse)

Agilent Technologies UK Limited, Cheadle, UK	FITC-conjugated rabbit anti-mouse antibody FITC-conjugated swine anti-rabbit antibody HRP-conjugated rabbit anti-goat antibody TRITC-conjugated rabbit anti-mouse antibody
Bio-Rad, Hemel Hempstead, UK	DC protein assay reagent A DC protein assay reagent B
Carl Zeiss Ltd, Hertfordshire, UK	Immersion oil
CEAC, Aston University, UK	Ethanol, methanol, propanol
Cell Signaling Technology, London, UK	Anti-mouse IgG, HRP-linked antibody Anti-rabbit IgG, HRP-linked antibody
Geneflow Ltd	EZ-PCR Mycoplasma test kit
Melford Laboratories Ltd, Ipswich, UK	Amphotericin B 250 µg/ml solution Gentamicin sulfate
Merck, Feltham, UK	Disodium hydrogen orthophosphate (Na <sub>2</sub> HPO <sub>4</sub> ) Ezrin Inhibitor, NSC668394 – Calbiochem Potassium dihydrogen orthophosphate (KH <sub>2</sub> PO <sub>4</sub> )
Oy Reagentia Ltd, Finland	Quick Diff staining kit
PAN Biotech, Dorset, UK	Ham's F12 without phenol red Trypsin Powder, porcine origin 1:250 Lymphocyte separating medium, Pancoll human, density: 1.077 g/ml

QIAGEN, Manchester, UK

FlexiTube S100P siRNA-1 target sequence:  
CAGGAGGAGGTGGGTCTGAA  
FlexiTube S100P siRNA-4 target sequence:  
TAGCACCATGACGGAAGCTAGA  
FlexiTube S100P siRNA-5 target sequence:  
CAGGCTTCCTGCAGACTGGAA  
FlexiTube S100P siRNA-6 target sequence:  
TAGGCTGAGCCTGCTCATGTA  
FlexiTube ezrin siRNA-5 target sequence:  
AACACCGTGGGATGCTCAAAG  
FlexiTube ezrin siRNA-7 target sequence:  
CAGGACTGATTGAATTACGGA  
FlexiTube ezrin siRNA-8 target sequence:  
AAGAGTGATGGACCAGCACAA  
FlexiTube ezrin siRNA-9 target sequence:  
ACCGTGGGATGCTCAAAGATA:  
FlexiTube IQGAP1 siRNA-1 target sequence  
CTGGGAGATAATGCCCACTTA:  
FlexiTube IQGAP1 siRNA-2 target sequence  
CAGGCGCTAGCTCATGAAGAA:  
FlexiTube IQGAP1 siRNA-3 target sequence  
AAGGCATATCAAGATCGGTTA:  
FlexiTube IQGAP1 siRNA-5 target sequence  
AAGGAGACGTCAGAACGTGGC:  
negative control siRNA

R&D Systems, Abingdon, UK

Anti-S100P (goat)

Scientific Laboratory Supplies, Nottingham,  
UK

Histo-Clear

Sigma Aldrich Co, Dorset, UK

Ham's F12 media  
Kodak® GBX fixer  
2-n-morpholino ethansulfon acid (MES)  
Acrylamide  
Acrylamide/bis-acrylamide (40% w/v)  
Ammonium persulphate (APS)  
Bisacrylamide  
Dimethyl sulphoxide (DMSO)

	Ethylene glycol tetraacetic acid (EGTA)
	Epsilon-aminocaproic acid (ACA)
	Ethylenediaminetetraacetic acid (EDTA)
	Fibronectin from human placenta
	Glycine
	Hydrogen peroxide solution 30% (w/w) in H <sub>2</sub> O
	Kodak® BioMax® light film
	L-Glutamine solution 200 mM
	Luminol 97%
	Magnesium chloride (MgCl <sub>2</sub> )
	MEM (Minimum essential medium)
	N,N,N',N'-Tetramethylethylenediamine (TEMED)
	Nuclease-free water
	Paraformaldehyde (PFA) powder
	Phosphate buffered saline tablets (PBS)
	Poly-L-lysine solution 0.1% (w/v) in H <sub>2</sub> O
	Sodium chloride (NaCl)
	Potassium chloride (KCl)
	Sodium dodecyl sulphate (SDS)
	Triton X-100
	p-Coumaric acid (≥ 98.0%)
Thermo Fisher Scientific, Loughborough, UK	2-Mercaptoethanol (β-mercaptoethanol)
	Alexa Fluor® 568 phalloidin
	Bovine serum albumin powder (BSA)
	Bromophenol blue
	Hygromycin B (50 mg/ml)
	MTT (3-(4,5-Dimethylthiazol-2-yl)-2,5-diphenyltetrazolium bromide)
	Non-essential amino acids solution (100x) (NEAA)
	Opti-MEM® reduced serum medium (no phenol red)
	Prestained Protein Ladder
	RPMI 1640 Medium

	Sodium chloride (NaCl)
	Tris Base Ultra-Pure
	Trypan blue solution, 0.4%
	Weighing boat polystyrene square (250 ml)
	Virkon
Vector Laboratories Ltd, Peterborough, UK	Biotinylated goat anti-rabbit IgG antibody
	Biotinylated goat anti-mouse IgG antibody
	BLOXALL® endogenous peroxidase and alkaline phosphatase blocking solution
	Haematoxylin
	ImmPACT® DAB peroxidase substrate
	VECTASTAIN® avidin-biotin complex (ABC) HRP kit (peroxidase, standard)
	VectaMount® permanent mounting medium
	Vectashield hard set mounting medium containing 4'-6-diamidino-2-phenylindole (DAPI)
VWR International, Leicestershire, UK	INTERFERin® siRNA transfection reagent

**Table 2.2 Reagents.**

## 2.2. Methods

### 2.2.1. Immunohistochemistry (IHC)

All placenta samples were collected following elective termination of pregnancy, using mifepristone and misoprostol (for first and second trimester samples) or from pregnancies delivered by elective Caesarean (third trimester) and were fixed using formaldehyde and embedded into paraffin wax by our colleagues from Aston Medical school: first trimester of gestation (8–11 weeks; n = 3), second trimester (15–20 weeks; n = 3), and third trimester (32–38 weeks; n = 3) or were generous gifts from Prof. Melissa Westwood (University of Manchester and Royal Manchester Children’s Hospital): first trimester of gestation (6 weeks + 3 days, 6 weeks + 3 days and 6 weeks + 4 days; n = 3), second trimester (17 weeks + 2 days, 18 weeks + 2 days, 19 weeks + 2 days; n = 3), and third trimester (39 weeks; n = 4). The ethical approval for collecting and working with human placenta samples was granted by Health Research Authority

(The Research Ethics Committee. (REC) reference number: 15/WM/0284). A copy of the ethical approval confirmation letter can be found in the appendix section.

### **2.2.1.1. Preparing slides from tissue sections**

In order to prepare the slides, glass slides (Thermo Fisher Scientific, UK) were coated with drops of 0.1% (w/v) poly-L-lysine solution (Sigma-Aldrich, UK) in H<sub>2</sub>O and were left to dry on the bench for 30 minutes. The paraffin-embedded sample were chilled on ice to harden the wax, prior to trimming at 30 µm thickness and then cutting at 5 µm thickness, using a microtome (Leica Microsystems Ltd, UK) to obtain section ribbons. The sections were separated with tweezers and flattened on 45°C water surface, using a histology water bath (Leica Microsystems Ltd, UK). The poly-L-lysine covered glass slides were then used to pick the sections out of the water, prior to being dried upright in a slide rack at 37°C overnight.

### **2.2.1.2. Staining**

The dry slides were placed in racks and were warmed up at 60°C for 10 minutes to soften the wax. They were then dewaxed in Histo-clear (Scientific Laboratory Supplies, UK) for 5 minutes, 3 times (in fume hood), hydrated in 100% ethanol for 2 minutes (twice), 70% ethanol 2 minutes (twice), and finally in running tap water and incubated for 5 minutes. For antigen retrieval, the rack containing the hydrated slides was placed into a container with 400 ml 0.01 M sodium citrate buffer (1x) (Table 2.3), covered with two layers of cling film, and were boiled for 10 minutes at full power (800 W) in a microwave. The slides were then left to cool down for 20 minutes at room temperature and then were moved to another container filled with tap water. The sections were marked by drawing a hydrophobic circle around them using a PAP pen (Sigma-Aldrich, UK). The sections were blocked at room temperature using BLOXALL (Vector laboratories, UK) for 10 minutes, washed with PBS for 5 minutes and then were incubated with 2.5% (v/v) goat serum in PBS for 30 minutes. The sections were then incubated with 50 µl desired primary antibody: S100P (Abcam, UK), ezrin (Abcam, UK), IQGAP1 (Abcam, UK), HLA-G (Abcam, UK) or cytokeratin 7 (Abcam, UK) diluted in 2.5% goat serum (dilutions in Table 2.4) at 4°C in a humidified chamber, overnight. Mouse (10µg/ml) and rabbit (5 µg/ml) IgGs (Santa Cruz Biotechnology, USA) were used as negative control for the secondary antibodies. On the next day, the sections were washed with PBS for 5 minutes 3 times and incubated with 200 µl appropriate secondary biotinylated antibodies: anti-mouse or anti-rabbit (Vector Laboratories, UK) diluted in PBS (dilutions in Table 2.4) for 30 minutes at room temperature, following washing with PBS for 5 minutes. While waiting to the secondary antibody incubation, the ABC reagent (Vector Laboratories, UK) was prepared by adding one drop reagent A and one drop B into 5 ml PBS, stirred and incubated at room temperature for 30 minutes prior using. The sections

were then incubated with a drop of ABC reagent for 30 minutes, prior to washing with PBS for 5 minutes. Then, 3,3'-diaminobenzidine (DAB) chromogen was prepared fresh, by adding one drop of DAB peroxidase substrate (Vector Laboratories, UK) into 1 ml diluent (Vector Laboratories, UK) and stirring. Drops of diluted DAB were incubated on each section for 30 seconds, until the brown colour was developed. To stop further staining, the sections were washed with PBS multiple times. For counter staining, the sections were incubated with Haematoxylin (Vector Laboratories, UK) for 1 minute and then were washed with 1x tris-buffered saline (TBS) (Table 2.3). The slides were once again placed in the rack to dehydrate the sections by placing in tab water, then in 70% ethanol for 3 minutes (twice), 95% ethanol for 3 minutes (twice) and 100% ethanol for 3 minutes (3 times). Then, they were moved to Histo-clear for 2, 10 and 20 minutes. Lastly, glass coverslips were mounted on the slides using VectaMount mounting medium (Vector Laboratories, UK) and were left to dry overnight under the fume hood.

<b>Buffers</b>	<b>Ingredients</b>
10x TBS	0.05M Tris base, 3M NaCl in 1 litre deionised (di) H <sub>2</sub> O pH 7.6
0.1 M Citrate buffer (10x)	29.41g sodium citrate in 1 litre diH <sub>2</sub> O pH6.0

**Table 2.3 The buffers used for IHC, and their ingredients.**

<b>Antibodies</b>	<b>Dilution in either 2.5% goat serum (for primary antibodies) or PBS (for secondary antibodies)</b>
Monoclonal anti-ezrin antibody (mouse)	1:200 (5 µg/ml)
Monoclonal anti-IQGAP1 antibody (rabbit)	1:400 (0.5 µg/ml)
Monoclonal anti-HLA-G (mouse)	1:100 (10 µg/ml)
Monoclonal anti-cytokeratin (mouse)	1:100 (10 µg/ml)
Monoclonal anti-S100P (rabbit)	1:1500 (0.578 µg/ml)
Biotinylated goat anti-rabbit IgG (secondary)	1:200
Biotinylated goat anti-mouse IgG (secondary)	1:200
Mouse IgG (negative control)	1:100 (10 µg/ml)

Rabbit IgG (negative control)	1:2000 (5 µg/ml)
-------------------------------	------------------

**Table 2.4 Antibody dilutions for IHC.**

### 2.2.1.3. Analysing IHC images with ImageJ

In order to compare the intensity of the staining for a certain protein (S100P, ezrin or IQGAP1), the images were processed using Fiji-ImageJ (Schindelin et al. 2012), through optical density (OD) calibration, and then the following steps: run Image, Colour, Colour Deconvolution and H DAB. "Colour\_2", which shows the brown DAB staining, and therefore is the equivalent of the expression of the protein of interest, was used to measure the OD. The desired areas in each image were selected through Analyse, Tools, ROI manager and manually choosing the areas with tissues. The OD in each image was measured by selecting Analyse and then Measure. Finally, the average ODs from each trimester were compared with each other.

## 2.2.2. Cell culture

### 2.2.2.1. Used cell lines:

The cell lines used for the study have been listed in Table 2.5 and the specific culture media for each cell type have been listed in Table 2.6.

Name	Description
Jeg-3	Human choriocarcinoma, gift from Dr. Emmanouil Karteris (Brunel University)
BeWo	Human choriocarcinoma, gift from Dr. Emmanouil Karteris (Brunel University)
HTR8/SVneo	Immortalised human first trimester EVT, from chorionic villi, transfected with a plasmid containing the simian virus 40 large T antigen (SV40) (Graham et al. 1993), gift from Prof. Graham Charles (Queen's University, Canada).
Transfected HTR8/SVneo clones	Immortalised human first trimester EVTs, stably transfected with S100P-containing plasmid SGB217 (by in vivo recombination of pcDNA3.1) or control plasmid SGB16 ( <b>mock</b> ), made by Dr. Thamir Ismail, (University of Liverpool, UK).

SW71	Immortalised human first trimester EVT, virally transfected with human telomerase reverse transcriptase hTERT (Straszewski-Chavez et al. 2009), gift from Prof Gil Mor (Yale University, USA)
Saint George's Hospital placental cell lines 4 and 5 (SHPL-4/5)	Immortalised human first trimester EVTs, transfected with SV40 (Choy, St Whitley & Manyonda 2000), gift from Guy St J. Whitley (St George's University of London).

**Table 2.5 Cell lines.**

<b>Cell type</b>	<b>Media</b>
Jeg-3	<p><b>MEM complete</b></p> <p>The medium was made by adding 10% (V/V) FCS (PAA Laboratories Ltd, UK), 1% pen/strep (PAA Laboratories Ltd, UK) and 2 mM L-glutamine (Sigma-Aldrich, UK) into 500 ml MEM (Sigma-Aldrich, UK).</p> <p><b>MEM for serum starvation</b></p> <p>The medium was made by adding 0.5% FCS, 1% pen/strep and 2 mM L-glutamine into 500 ml MEM.</p>
BeWo	<p><b>Ham's F12 complete</b></p> <p>The medium was made by adding 10% FCS, 1% pen/strep and 2 mM L-glutamine into 500 ml Ham's F12 (Sigma-Aldrich, UK).</p> <p><b>Ham's F12 for serum starvation</b></p> <p>The medium was made by adding 0.5% FCS, 1% pen/strep and 2mM L-glutamine into 500ml Ham's F12.</p>
HTR8/SVneo and	<b>RPMI-1640 complete</b>

SGHPL-4/-5	<p>The medium was made by adding 5% (V/V) (for HTR8/SVneo) or 10% (for SGHPL-4/-5) FCS, 1% pen/strep, 2 mM L-glutamine, without (for HTR8/SVneo) or with (for SGHPL-4/-5) 1% NEAA (Thermo Fisher Scientific, UK) into 500 ml RPMI-1640 (Thermo Fisher Scientific, UK).</p> <p>For SGB217 and SGB16 HTR8/SVneo clones, 50 µg/ml Hygromycin B was added to the media mixture as selection marker.</p> <p><b>RPMI-1640 for serum starvation</b></p> <p>The medium was made by adding 0.5% FCS, 1% pen/strep and 2mM L-glutamine into 500 ml RPMI-1640.</p> <p>For SGB217 and SGB16 containing HTR8/SVneo clones, 50 µg/ml Hygromycin B was added to the mixture.</p>
SW71	<p><b>DMEM: F12 complete</b></p> <p>The medium was made by mixing DMEM (PAA Laboratories Ltd, UK) and Ham's F12 at 1:1 ratio and adding 10% FCS, 1% pen/strep, 2 mM L-glutamine and 1% NEAA into the 500 ml mixture.</p> <p><b>DMEM: F12 for serum starvation</b></p> <p>The medium was made by mixing DMEM and Hams F12 at 1:1 ration and adding 0.5% FCS, 1% pen/strep and 2 mM L-glutamine into 500 ml mixture.</p>

**Table 2.6 Cell lines and their culture media.**

### 2.2.2.2. Growing the cells

The cells were grown in T25 flasks and incubated at 37°C in a CO<sub>2</sub> Incubator (Thermo Fisher Scientific, UK). The medium was changed every two days.

### **2.2.2.3. Passaging**

When the cells reached 80-90% confluency in their T25 flask, they were washed with 1 ml warm PBS (Sigma-Aldrich, UK) and detached using 1 ml warm 0.025% (v/v) trypsin- 2.5 mM EDTA (Sigma-Aldrich, UK) for 5-10 minutes. After detaching, 3 ml fresh complete medium was added on top and they were centrifuged using a benchtop centrifuge (Sigma-Aldrich, UK) at 160 x g for 5 minutes. Then, the supernatant was removed and 1/4 - 1/6 of the pellet was seeded back into the flask and topped up with fresh medium to the final volume of 5-6 ml.

### **2.2.2.4. Cryopreservation**

At the times that growing cells was not needed, they were cultured in T75 flasks until they reached 80% confluency, prior to being washed with warm PBS, and then were trypsinised using 3 ml 0.025% (v/v) trypsin- 2.5 mM EDTA for 5-10 minutes or until all cells were detached. 6 ml fresh complete medium was then added to the mixture and the mixture was centrifuged the same way as mentioned previously. After removing the supernatant, the pellet was re-suspended in 4 ml freezing mix made from FCS-10% DMSO (Sigma-Aldrich, UK), and was divided into four cryovials (Greiner Bio-one, UK) and transferred to -80°C in a freezing container (Thermo Fisher Scientific, UK) over-night and then to -196°C in liquid nitrogen tank for long-term storage.

### **2.2.2.5. Culturing cells from frozen**

To regrow the frozen cells, they were thawed quickly, then they were transferred to a T25 culture flasks and warmed-up complete media was gently (drop by droop) added on top. The medium was changed after 2-3 hours, when the cells had attached to the bottom surface of the flask, to reduce the toxic effect of DMSO on the cells.

## **2.2.3. Trypan blue exclusion viability assay**

To measure the cell growth rate, 15,000 Jeg-3 and SW71 cells, or 25,000 non-transfected HTR8/SVneo and transfected HTR8/SVneo clones were seeded in 24-well plates along with the desired treatments: 0.4 µg/ml S100P antibody (R&D Systems, UK), 10 mM epsilon-aminocaproic acid (ACA) (Sigma-Aldrich, UK), 5 nM siRNA targeting ezrin or IQGAP1, 5 µM ezrin inhibitor drug NSC668394 (Merck, UK), 0.01% DMSO, or without any treatment. During the following 24, 48 and 72 hours, the wells were washed once with 400 µl PBS and trypsinised with 200 µl 0.025% (v/v) Trypsin- 2.5 mM EDTA for 5-10 minutes, or until all the cells were detached from the plate. Then, the trypsin was neutralised, using 400 µl complete medium, and the cell suspension was centrifuged at 1180 x g using the 1-14 Microfuge (Sigma-Aldrich, UK)

for 5 minutes. The supernatant was then, discarded and the pellet was re-suspended in 200  $\mu$ l 1:1 mixture of complete medium and trypan blue (Thermo Fisher Scientific, UK). The viable cells, which could be distinguished from the dead cells by not having taken up the blue colour, were counted, using a haemocytometer and the average numbers were compared with each other.

#### **2.2.4. MTT viability assay**

The other way to confirm cell viability was to measure their metabolic activity by the MTT assay. Similar to the exclusion assay, 25,000 HTR8/SVneo and or 15,000 SW71 were seeded in 24-well plates, while being treated or without any treatment as negative control. Their metabolic activity was measured over the next 72 hours by adding 40  $\mu$ l 5 mg/ml (in PBS) MTT (Thermo Fisher Scientific, UK) into each well, followed by mixing and 1 hour of incubation at 37°C. Then, the medium and MTT mixture was aspirated, the wells were washed with 200  $\mu$ l PBS, followed by incubation with 200  $\mu$ l DMSO for 10 minutes at 37°C. Finally, the OD of the solutions at 570 nm was measured, using a plate reader (BioTek Potton, UK).

#### **2.2.5. Primary EVT isolation and culture**

Following elected termination of pregnancy, placental samples, which had been collected surgically by vacuum aspiration, were transferred from Birmingham Women's Hospital to the lab in 50 ml Falcon tubes (Thermo Fisher Scientific, UK) filled with 1:1 mixture of DMEM and Ham's F12 with 1% pen/strep, carried on ice. The samples were emptied on a 150 mm dish (Appleton Woods, UK), and the large clots were removed with forceps, the remaining tissue was placed in a sterile 250 ml bottle with 20 ml Ham's F12 without phenol red (PAN Biotech, UK) and gently stirred for 10 minutes. The samples were then placed in a clean petri dish and after removing the visible blood clots, the villi, which have a feathery appearance, were scraped from the membrane, using a scalpel and placed in a sterile 250 ml bottle with 75 ml EVT isolation trypsin solution (PAN Biotech, UK) (Table 2.7), and stirred on a heated stirrer at 37°C for 9 minutes. Then, to quench the trypsin, the bottle contents were emptied into another sterile 250 ml bottle containing 15 ml FCS and 45 ml Ham's F12 without phenol red, after having passed through a sterile gauze and a funnel. The filtrate was then divided into six universal tubes (Thermo Fisher Scientific, UK) and were centrifuged at 450 x g for 5 minutes. After discarding the supernatant, the pellets from each of the universal tubes were pooled together and resuspended in 20 ml Ham's F12 without phenol red and gently layered on top of two universal tubes containing 8 ml Pancoll lymphocyte separating medium (PAN Biotech, UK). The tubes were centrifuged at 710 x g for 20 minutes with the breaks off. After the spin, a white layer of cells in between the

two layers containing the EVT's, along with some small foetal red cells, mesenchymal core cells and syncytiotrophoblasts was collected and placed in a universal tube, topped up with Ham's F12 without phenol red and centrifuged at 500 x g for 5 minutes. The pellet was resuspended in 2 ml trophoblast complete medium (TCM) (Table 2.7) and seeded in one 35 mm petri dish, previously coated with fibronectin (the fibronectin-coated petri dishes were prepared previously by adding 1 ml 20 µg/ml fibronectin (SIGMA-ALDRICH CO, UK) diluted in diH<sub>2</sub>O and were left to dry for an hour prior to removing the fibronectin solution) and incubated at 37°C for 1 hour for the EVT's to attach, prior to changing the medium. On the next day, the medium was changed again, and the cells were used for further experiments.

<b>Solution</b>	<b>Ingredients</b>
EVT isolation trypsin solution	10.3 g glucose, 12 g NaCl, 0.3 g KCl, 1.725 g, Na <sub>2</sub> HPO <sub>4</sub> (disodium hydrogen orthophosphate), 0.3 g KH <sub>2</sub> PO <sub>4</sub> (potassium dihydrogen orthophosphate) dissolved in 1 litre diH <sub>2</sub> O, the pH was adjusted to 7.4 and then 0.2 g trypsin and 0.2 g EDTA were added to the solution.
Trophoblast complete medium (TCM)	20% FCS, 1x pen/strep, 2 mM L-glutamine dissolved in Ham's F12 without phenol red

**Table 2.7 The solutions used for EVT isolation and their ingredients.**

## **2.2.6. Protein expression measurement by western blot analysis**

All trophoblast cell lines (BeWo, Jeg-3, HTR8/SVneo, SW71, SGHPL-4 and -5) were probed for S100P, ezrin and IQGAP1 by performing western blot as follows:

### **2.2.6.1. Cell lysate preparation**

To collect the cell lysates, the cells growing in 24-well plates were washed with PBS, prior to adding 50 µl of PBS containing 1x protease inhibitor cocktail (Sigma-Aldrich, UK) into each well and the cells were scrapped off, using a plastic cell scraper (Greiner Bio-one, UK) and were transferred into microcentrifuge tubes (Thermo Fisher Scientific, UK). They were then sonicated (Bandelin electronic GmbH & Co, Germany) on the lowest power for 10 seconds to disrupt the cells, followed by spinning down for 20 seconds at 16160 x g. Following the spinning, the pellet makes up the cellular debris, while the supernatant contains the soluble proteins. 5 µl cell lysate

was then taken for protein assay and the rest of the lysate was mixed with 1:3 diluted Laemmli sample buffer (Table 2.8). The samples were stored at -80°C.

### 2.2.6.2. Protein assay

To load desired amounts of cell lysate on sodium dodecyl sulfate-polyacrylamide gel electrophoresis (SDS-PAGE), the protein concentration was measured using detergent-compatible (DC) protein assay kit (Bio-Rad, UK), with an assay similar to the Lowry protein assay (Bio-Rad Laboratories, 2019). For this purpose, 2 µl of cell lysate was loaded into two wells of a 96-well plate (Appleton Woods, UK), along with 0, 1, 2, 5, and 10 µg/ml BSA standard solution (BSA dissolved in diH<sub>2</sub>O) prior to the addition of 25 µl DC protein assay reagent A followed by 200 µl DC protein assay reagent B into each well, and waiting for 15 minutes for the blue colour to develop. Then, the OD of the solution was measured at 570 nm, using a plate reader. The standard curve was then produced in Excel by plotting the standard protein concentration on the x-axis and the OD readings on the y-axis. The trendline was added to the curve and the unknown concentration of the protein was measured using the formula:  $y = mx + b$ , where y is the sample's OD, m is the slope of the trendline, b is the y-intercept, and x is the unknown concentration.

### 2.2.6.3. SDS-PAGE

To separate the bands with desired molecular weights, 15 µg cell lysate was loaded onto either of the two types of polyacrylamide gels:

- 16% (w/v) tricine gel: for bands of 10-60 KDa (S100P, tubulin and ezrin) (Schägger, 2006) (Table 2.8)
- 10% (w/v) polyacrylamide gel: for bands of 50-190 kDa (tubulin, ezrin, phospho-ezrin and IQGAP1) (Table 2.9)

15 µg of each sample was loaded on the appropriate gel using an electrophoresis system (Bio-Rad, UK). The running voltages and their times were: 70 V for 10 minutes, 100 V for 30 minutes, and 150 V for 1 hour or longer.

Buffer	Ingredients
Laemmli sample buffer (4×)	10 ml Tris (1 M, pH 6.8), 4.0 g SDS, 20 ml glycerol, 10 ml β-mercaptoethanol, 0.1 g bromophenol blue, add diH <sub>2</sub> O to 50 ml

16% (w/v) separating gel (x2)	3.3 ml 3x gel buffer, 3.3 ml acrylamide/bisacrylamide mix (48% acrylamide, 1.5% bisacrylamide), 1.36 ml diH <sub>2</sub> O, 2 ml glycerol, 50 µl APS and 6 µl TEME
4% (w/v) stacking gel (x2)	1.2 ml 3x gel buffer, 0.4 ml acrylamide/bisacrylamide mix (48% acrylamide, 1.5% bisacrylamide), 3.36 ml diH <sub>2</sub> O, 40 µl APS and 4 µl TEMED
Sealing gel (x2)	1 ml separating gel (without pre-added APS and TEMED), 20 µl APS and 2 µl TEMED
3x bel buffer (GB)	18.16 g Tris and 0.75 ml 20% SDS in 50 ml diH <sub>2</sub> O (pH 8.45)
Cathode buffer	12.11 g Tris, 17.92 g tricine, and 5 ml 20% SDS in litre diH <sub>2</sub> O (pH 8.25)
Anode buffer	12.11 g Tris in 1 litre H <sub>2</sub> O (pH 8.9)
48% (w/v) acrylamide, 1.5% (w/v) bisacrylamide	24.0 g acrylamide and 0.75 g bisacrylamide in 50 ml diH <sub>2</sub> O

**Table 2.8 SDS-PAGE buffers used for 16% tricine gel and their ingredients.**

<b>Buffer</b>	<b>Ingredients</b>
10% (w/v) separation gel (x2)	2.5 ml 50% glycerol, 2.5 ml 4x tris (pH 8.8), 2.5 ml 40% acrylamide/bisacrylamide, 2.3 ml diH <sub>2</sub> O, 100 µl 10% SDS, 100 µl 10% APS, 9 µl TEMED
4% stacking gel (x2)	1 ml 50% glycerol, 1 ml 4x tris (pH 6.5), 0.5 ml 40% acrylamide/bisacrylamide solution, 1.42 ml diH <sub>2</sub> O, 40 µl 10% SDS, 40 µl 10% APS, 4 µl TEMED
Sealing gel (x2)	1 ml separating gel (without TEMED), 5 µl TEMED
1x Running buffer	3 g Tris base, 14.4 g glycine, 1 g SDS (pH 8.5)

**Table 2.9 SDS-PAGE buffers used for 10% polyacrylamide gel and their ingredients.**

#### 2.2.6.4. Western blot

The separated proteins on the gel were transferred to PVDF membranes (Bio-Rad, UK) using a semi-dry electrotransfer cell (Bio-Rad, UK) for 2 hours at the current of 35 mA per gel (for bands of 10-60 kDa) or 80 mA (for bands of 50-190 kDa), using transfer buffer (Table 2.10). The blots were then washed once in PBS, blocked in 3% (w/v) BSA (Thermo Fisher Scientific, UK) in PBS for 30 minutes on an orbital shaker (Appleton Woods, UK) and incubated with primary antibodies against S100P (R&D Systems, UK), ezrin, phospho-ezrin (Abcam, UK) or IQGAP1, along with anti- $\alpha$ -tubulin (Abcam, UK) (as loading control) on a roller (Thermo Fisher Scientific, UK) at 4°C overnight (antibody dilutions have been listed in Table 2.11). On the next day, the blot was washed three times with PBS, blocked in 3% BSA for the second time and were incubated with secondary HRP-linked anti-goat (Agilent Technologies, UK) and HRP-linked anti-mouse and -rabbit (Cell Signaling, UK) antibodies (dilutions in Table 2.11) for 2 hours on a shaker at room temperature. Following PBS washing for three times, the bands were detected using enhanced chemiluminescence (ECL) detection mix (Table 2.10) either manually on X-ray films (Thermo Fisher Scientific, UK) and exposure times of 3 seconds (for detecting  $\alpha$ -tubulin) or 20 seconds (for detecting the other proteins), or automatically by 6 minutes (standard) exposure on a blot scanner (LI-COR Environmental, UK). The images were then analysed using Image Studio Lite analysis software (LI-COR Environmental, UK), the expression of each protein was normalised to the expression of the house keeping gene ( $\alpha$ -tubulin) and the graphs were produced by Microsoft Excel or Prism 7.04 (GraphPad Software Inc., USA).

<b>Buffer</b>	<b>Ingredients</b>
Electroblot transfer buffer (10x)	0.25 g Tris and 144.0 g glycine in 1 litre diH <sub>2</sub> O.  To prepare 1x: mixed 50 ml of the above with 100 ml methanol and 350 ml diH <sub>2</sub> O
ECL detection mix	1.5 ml 0.5 M Tris, 6 ml diH <sub>2</sub> O, 37.5 µl Luminol, 18.75 µl cumaric acid, and 2.25 µl hydrogen peroxide
Developer	100 ml developer and 360 ml diH <sub>2</sub> O
Fixer	100 ml fixer and 360 ml diH <sub>2</sub> O (kept in the dark)
Stripping buffer	20 ml 10% (w/v) SDS, 12.5 ml 0.5 M tris (pH 6.8), 2.25 µl diH <sub>2</sub> O, and 800 µl β-mercaptoethanol (added in fume hood)

**Table 2.10** The solutions used for western blot transfer and detection.

<b>Antibody</b>	<b>Dilution in 3% BSA</b>
Anti-ezrin (mouse)	1:1000 (0.1 µg/ml)
Anti-phospho ezrin (rabbit)	1:1000 (1 µg/ml)
Ant-IQGAP1 (rabbit)	1:1000 (0.2 µg/ml)
Anti-S100P (goat)	1:1000 (0.5 µg/mL)
Anti-tubulin (mouse)	1:5000
HRP-anti-goat	1:3000
HRP-anti-mouse	1:3000
HRP-anti-rabbit	1:3000

**Table 2.11** Primary and secondary antibody dilutions used in western blot.

### 2.2.6.5. Blot stripping

To detect protein bands with close molecular weights (ezrin and phospho-ezrin), PVDF membranes that had been probed and developed, were reused by stripping all the antibodies and then re-probed with different antibodies. For this purpose, the blots were submerged in stripping buffer (Table 2.10) and incubated for 20 minutes at 50°C with occasional agitation. The blots were washed several times with diH<sub>2</sub>O, to remove any residual stripping buffer, then washed with PBS three times and finally, the blots were blocked with 3% BSA in PBS (w/v) for 30 minutes at room temperature.

## **2.2.7. Protein knock-down**

Protein expression was knocked down by transient gene silencing. This was achieved by transfecting the cells with four different sequences (Table 2.2 Reagents.) of small interfering RNA (siRNA), also known as short interfering RNA or silencing RNA against each of the proteins: S100P (siRNA 1,4, 5, 6), ezrin (siRNA 5, 7, 8, 9) and IQGAP1 (siRNA 1,2, 3, 5).

### **2.2.7.1. Transfecting different cell lines**

60,000 (HTR8/SVneo) or 30,000 cells (all other cell lines) were seeded in 24 well plates. They were left to grow for 24 hours for HTR8/SVneo, Jeg-3, SW71 and six days for the relatively slow-growing BeWo cells. Following the incubation, the media was changed (400  $\mu$ l medium per well). The plate was incubated in the incubator for 30 minutes for the cells to settle. Meanwhile, the siRNA mixture was prepared with 100  $\mu$ l Opti-MEM (Thermo Fisher Scientific, UK), 2  $\mu$ l INTERFERin (VWR International, UK) and 0.5  $\mu$ l siRNA (QIAGEN, UK), per well. The mixture was then added into each well (final siRNA concentration was 5 nM). The control reagent contained Opti-MEM only and mock transfection mixture (as negative control) contained Opti-MEM and INTERFERin, plus a non-specific siRNA sequence, known as negative control siRNA (QIAGEN, UK). The cells were left to grow in the incubator for 48 hours, prior to changing the medium with the desired medium.

## **2.2.8. Boyden chamber assays**

### **2.2.8.1. Motility assay optimisation**

Prior to choosing the most appropriate staining and fixation method for transwell motility assay, 50,000 Jeg-3 cells suspended in 100  $\mu$ l medium were seeded at the bottom of inverted transwells. The transwells were incubated at 37°C in CO<sub>2</sub> incubator for 2 hours and then fixed with either 4% (w/v) PFA or methanol for 10 minutes continued by staining with either the Quick Diff staining kit (Oy Reagent Ltd, Finland), a commercial Romanowski stain variant, using the cytoplasmic (pink) stain and the nuclear (blue) stain, or Vectashield mounting medium containing DAPI (Vector Laboratories Ltd, UK).

The transwells stained with Quick Diff were detected by bright-field microscopy (Nikon Ltd, UK), and the ones stained with DAPI were detected using an inverted epifluorescence microscope (Leica Microsystems Ltd, UK).

To find out what seeding number works best for the transwell assay using trophoblast cell lines, three different seeding numbers were considered at first: 100,000 cells, 50,000 cells and 25,000 cells. To test each of these numbers, three separate groups of Jeg-3 cells were prepared: control, mock transfection and S100P siRNA 4 treated. Each group was adjusted in 100,000, 50,000 or 25,000 cells in 300 µl serum starvation medium and they were seeded in transwells. The transwells were placed on 24 well plates while the lower well was filled with 750 µl complete medium. The plates were incubated at 37°C in a CO<sub>2</sub> incubator for 24 hours, and then the transwells were fixed and stained. The transwell membranes were observed on 20x magnification, the cells on at least 5 random fields were counted and the average number was calculated.

### **2.2.8.2. Boyden chamber motility assay**

Following the previous motility assay optimisations, the motility assay was performed as follows: The cells, which might have been pre-treated or not, were serum-starved for 24 hours, prior to washing with PBS, and trypsinisation for 5-10 minutes or until all cells had been detached from the bottom surface. The trypsin was neutralised with serum starvation medium and the following centrifugation, the cell suspension was adjusted at the following numbers in 300 µl serum starvation medium:

25,000 for SW71 cells.

50,000 for non-transfected and transfected HTR8/SVneo

100,000 Jeg-3 and BeWo cells.

35,0000 primary EVT's

The cell mixture was seeded into 8 µm pore size transwells (Greiner Bio-one, UK), placed on 24-well plates and were incubated at 37°C in CO<sub>2</sub> incubator for 24 ours, while the lower wells were filled with 750 µl complete medium as chemoattractant. Following the incubation, the transwells were washed with PBS, fixed using methanol for 10 minutes, at room temperature and then were stained using the Quick Diff staining kit. The transwell membranes were observed at 20x magnification, the cells on at least 5 random fields were counted and the average number was calculated.

### **2.2.8.3. Invasion assay optimisation**

To find out about the lowest concentration of the Matrigel that can polymerise and solidify to form a gel inside the transwells, the matrix Matrigel (Corning Limited, UK) was diluted with the

appropriate serum free media in the following order of dilutions: 1:1, 1:1.5, 1:2, 1:2.5, 1:3, 1:3.5, 1:4. 100 µl of diluted Matrigel was poured into the transwells and the polymerisation of the Matrigel was tested, the by observation of gel formation, following 2 hours of incubation at 37°C in a CO<sub>2</sub> incubator.

To find out what Matrigel volume and incubation time works best for the cells, 50,000 Jeg-3 cells were seeded on 10, 20 and 30 µl polymerised 1:3 diluted Matrigel and were incubated for 24, 48 and 72 hours. The cells trapped in the transwell membrane were fixed and stained as explained earlier and the non-migratory ones were whipped using cotton swabs. The stained cells were counted using 20x magnification.

#### **2.2.8.4. Boyden chamber invasion assay**

The invasion assay was done in a similar way as the Boyden chamber motility assay (section 2.2.8.2), except for the usage of 20 µl 1:3 diluted Matrigel that was used to coat the transwell membrane, 2 hours prior to seeding the cells inside them.

#### **2.2.8.5. Migration and invasion assays with protein knockdown**

To investigate the role of our different target proteins such as S100P, ezrin and IQGAP1 in motility and or invasion, the cells were treated either with siRNA after serum starvation for 24 hours. Then the seeding numbers were adjusted accordingly, and the cells were left to migrate for 24 hours, prior to fixation and staining.

#### **2.2.8.6. Migration and invasion assays with other treatments (S100P antibody or ezrin inhibitor)**

A T25 flasks with about 80% confluent Jeg-3, SW71 or HTR8/SVneo clones 3 (SGB16), 5 (SGB217) and 7 (SGB217) were serum starved a for 24 hours, prior to trypsinisation (except for primary EVT<sub>s</sub>, which were collected without previous serum starvation). The cell suspensions were seeded inside the transwells, with or without Matrigel coating to test their migration and invasion respectively, as the lower wells contained complete media as chemo-attractant. Both the transwells and the bottom wells contained either of the following the treatments: 0.4 µg/ml goat-anti-S100P (R&D systems, UK) monoclonal antibody, 10 mM ACA, 0.2% (v/v) goat serum as negative control (same volume as anti-S100P antibody), 5 µM ezrin inhibitor NSC668394 (Merck, UK), or 0.01% (v/v) DMSO (the same volume as NSC668394 solution) as negative control. The migration and invasion assays were performed as explained earlier.

### 2.2.9. Immunofluorescence staining

To investigate the localisation and the expression pattern of different cellular markers of either cell motility (paxillin, ezrin, phospho-ezrin and IQGAP1) or in order to confirm HLA-G expression in primary EVT<sub>s</sub>, the cells were stained with immunofluorescence as follows:

Round glass coverslips were incubated with 4 µg fibronectin in 100 µl PBS per well, at room temperature for 1 hour. The unbound fibronectin was aspirated, and the coverslips were washed once with PBS. The coverslips were then placed in the wells of a 24-well plate, then exposed to UV for 15 minutes. 15,000-20,000 cells were seeded and left to attach for 24 hours at 37°C in a CO<sub>2</sub> incubator. The coverslips were then washed with cytoskeleton buffer (CB) (Table 2.12) twice, prior to fixing with 4% (w/v) PFA in CB at 37°C for 10 minutes. Then, to quench any unreacted aldehyde, the cells were incubated with 30 mM glycine solution at room temperature for 10 minutes. Following this, in order to permeabilise the cells, 0.01% (v/v) Triton solution was added and the plate incubated at room temperature for 10 minutes. The cells were then washed 3 times with CB, waiting for 5 minutes each time, at room temperature. Finally, the cells were blocked using 10% (v/v) goat serum in CB for 30 minutes at room temperature. The coverslips were then incubated with 50 µl primary antibodies diluted in 1% (v/v) goat serum in CB (or in 3% (w/v) BSA in PBS for ezrin antibody), for 45 minutes at room temperature (antibody dilutions have been listed in Table 2.13). The excess primary antibody was washed off with 1% (v/v) goat serum (or 3% (w/v) BSA for ezrin) twice and then with diH<sub>2</sub>O once. The cells were then incubated with fluorescein isothiocyanate (FITC) or tetramethylrhodamine (TRITC) conjugated secondary antibodies (Agilent Technologies, UK) diluted in 1% (v/v) goat serum in CB (or 3% BSA for ezrin) (dilutions in Table 2.13), along with 1:100 diluted rhodamine phalloidin (Thermo Fisher Scientific, UK), at room temperature for 45 minutes, to stain F-actin. The cells were washed again with 1% (v/v) goat serum in CB (or 3% BSA for ezrin) twice and once with diH<sub>2</sub>O to remove salt. The coverslips were then mounted onto glass slides with mounting medium containing DAPI, the edges were covered with clear nail varnish and the slides were left to dry for 30 minutes, before viewing under 63x magnification, with immersion oil (Carl Zeiss Ltd, UK) using an inverted epifluorescence microscope.

<b>Solution</b>	<b>Ingredients</b>
Cytoskeleton buffer (CB)	150 mM NaCl, 5 mM MgCl <sub>2</sub> , 5 mM EGTA, 5 mM glucose, 11 mM MES in diH <sub>2</sub> O. pH 7.4
4% PFA	Dilute 16% PFA solution in CB
1x glycine (30 mM)	Dilute 20x glycine solution in CB
0.01% triton-EDTA	Dilute 100x triton-EDTA in CB
10% and 1% goat serum solutions	Dilute goat serum in CB

**Table 2.12 The solutions needed for preparing the cells for immunofluorescence staining.**

<b>Antibody</b>	<b>Dilution in 1% goat serum</b>
Alexa Fluor 568 phalloidin	1:100
FITC secondary conjugate (mouse)	1:200
FITC secondary conjugate (rabbit)	1:200
TRITC secondary conjugate (rabbit)	1:200
Monoclonal anti-ezrin antibody (mouse)	1:100
Monoclonal anti-phospho-ezrin antibody (rabbit)	1:100
Monoclonal anti-HLA-G (mouse)	1:100
Monoclonal anti-IQGAP1 antibody (rabbit)	1:100
Monoclonal anti-paxillin antibody (mouse)	1:100

**Table 2.13 Antibody dilutions used in immunofluorescence staining.**

### 2.2.10. Statistical analysis

GraphPad Prism software or Microsoft Excel were used for statistical analysis. The data are presented as  $\pm$  standard deviation (SD) or  $\pm$  standard error of the mean (SEM) and the groups have been compared to each other by two-tail Student's t-test (two compare two groups of data to each other) or ANOVA (to compare more than two groups of data to each other) along with Dunnett's test (post hoc) to compare the mean of each group to the control mean. The number of

technical replicates (N) as well as the sample size of each experiment is mentioned in the corresponding figure legend.

## Chapter 3.

# S100P regulates trophoblast motility and invasion

### **3.1. Introduction**

S100P, a Ca<sup>2+</sup>-binding protein and a member of S100P family of proteins, is expressed in numerous tissues including oesophagus, trachea, spleen, stomach, duodenum and large intestine, colon, prostate (with highest levels during teenage years), bone marrow and leukocytes (Parkkila et al. 2008). During embryonic stages, S100P has been shown to be expressed as early as week 6, initially in the urogenital sinus as well as the developing gastrointestinal tract, and later in the urethra and bladder as well as the epithelium of the stomach and spleen, along with the allantois and in the hepatic vein (Prca et al. 2016). Its highest expression levels are found in the stomach and placenta, the latter being the organ where it was first discovered (Becker et al. 1992; Parkkila et al. 2008). The role of this protein in the context of this tissue, or indeed in the non-pathological state of any organs is yet unknown.

Similar to S100A 8, 10, and 11, S100P has been shown to be expressed in the endometrium (Baker et al. 2011; Bissonnette et al. 2016; Liu et al. 2006; Zhang et al. 2012). Endometrial S100P shows periodic changes in its expression levels (protein and mRNA) during the menstrual cycle, increasing significantly during the mid-secretory phase of cycle, referred to as the reception-ready phase or the implantation window (from the 20th day till 23rd day of the menstrual cycle), during which the physiological and morphological alterations of the tissue known as decidualisation occur (Dunn, Kelly & Critchley 2003; Tong et al. 2010; Zhang et al. 2012). Endometrial S100P is upregulated even more when pregnancy takes place. It peaks at the time of implantation, enhancing endometrial cell migration as well as embryo adhesion, and therefore promotes implantation (Zhang et al. 2012).

Within the placenta, S100P has been shown to be highly expressed in cyto- and syncytiotrophoblasts during the first trimester, where most of trophoblast proliferation happens (Zhu et al. 2015). Moreover, co-culture of stroma cells with trophoblasts enhances their S100P expression (Popovici et al. 2006).

In this chapter, we aimed to study the expression levels of S100P and characterise its histological localisation in human placenta and its levels during the different stages of pregnancy. We set about to gain further information about its expression in trophoblasts cells in culture and sought to determine its role in trophoblast motility and invasion.

#### **Aim**

To study the role of S100P in trophoblast motility and invasion.

## Objectives

- Establish S100P expression in human placental samples at different stages of gestation
- Establish S100P expression in trophoblast cell lines
- To test whether changes in the trophoblast microenvironment affects S100P expression
- To test whether modulating S100P expression affects trophoblast motility and invasion
- To decipher the molecular mechanisms for S100P-promoted motility and invasion in trophoblast cells

## 3.2. Results

### 3.2.1. Immunohistochemical staining optimisation

The S100P protein was first isolated from placental samples demonstrating that it is endogenously expressed in these tissues (Becker et al. 1992). More specifically, it was later shown to be localised in syncytiotrophoblasts as well as cytotrophoblasts (Parkkila et al. 2008; Zhu et al. 2015), but no information was provided regarding its localisation in the different placental structures. For this aim, we first optimised IHC with different primary antibody concentrations for two trophoblast marker proteins: cytokeratin 7, which is a marker of villous trophoblasts (Maldonado-Estrada et al. 2004), and HLA-G, which is a marker of EVT, a sub-population of trophoblasts that leave the villi, invade the decidua and remodel the maternal arteries (Moser et al. 2011).

In order to find the lowest concentrations of primary antibodies used for the IHC in this part (anti-cytokeratin 7 and anti-HLA-G), dilutions of each antibody were tested for the staining of first trimester samples. Wax-embedded human placenta sections from first trimester human placenta villi were cut, mounted on glass slides prior to preparation and incubation with the following primary antibodies: anti-cytokeratin 7 and anti-HLA-G (20 µg/ml and 10 µg/ml) in 2.5% (v/v) goat serum, prior to secondary antibody incubation and development using avidin-biotin complex and DAB chromogen. The sections were counter stained with haematoxylin.

Both concentrations showed efficient staining for cytokeratin 7 and HLA-G, with even our lowest antibody concentration at 10 µg/ml showing specific labelling (Figure 3.1). Cytokeratin 7 was found to be highly expressed within the cytoplasm of cytotrophoblasts as well as the apical membrane of the multi-nuclear syncytiotrophoblast, and to a lesser extent in the cytoplasm of syncytiotrophoblast as well as their membrane. HLA-G expression was primarily localised within the cytoplasm of the EVTs.

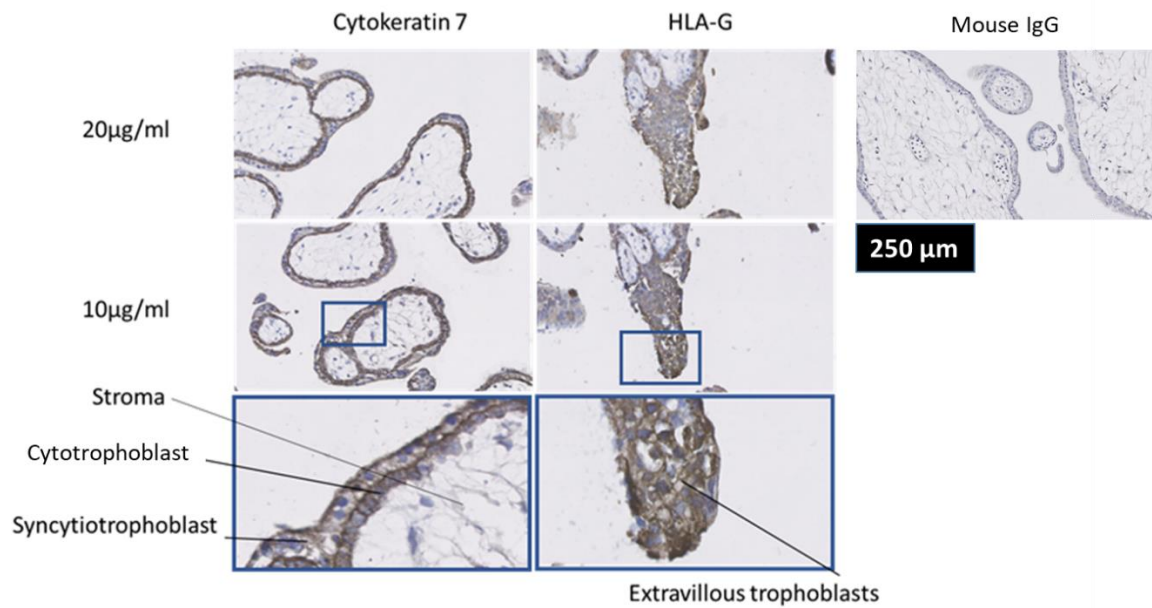


**Figure 3.1 Primary antibody concentration optimisation for IHC.** Wax-embedded human first trimester placental villi sections were prepared and incubated with two concentrations of primary anti-cytokeratin 7, anti-HLA-G and mouse IgG (as negative control), before being incubated with secondary antibodies, and finally were stained using avidin-biotin complex and DAB chromogen and then were counterstained using haematoxylin. The two images on the bottom are magnified fields from cytokeratin 7 and HLA-G staining.

### **3.2.2. Placental S100P expression gradually decreases during gestation**

To compare the expression levels in placenta sections, slides from first trimester, second trimester, and third trimester human placenta sections were prepared and stained by our colleagues in Aston Medical School were studied by taking several images at 20x magnification and analysing by densitometry using Fiji-ImageJ software. The OD from each section was compared with the OD from other sections. The highest levels of S100P expression was detected in samples from the first trimester, which express 40% more S100P compared with the second trimester sections ( $P<0.05$ ), and 50% more than the third trimester sections ( $P<0.01$ ). Third trimester samples showed 10% lower S100P expression compared with the second trimester, but the difference was not significant (Figure 3.2).

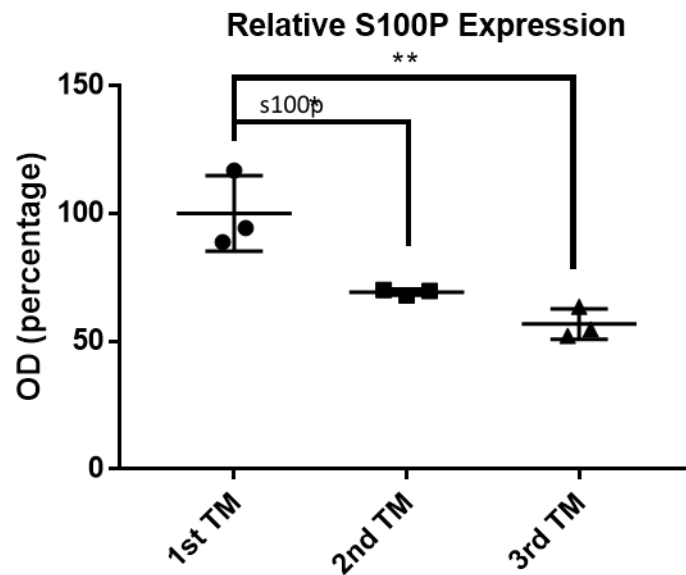
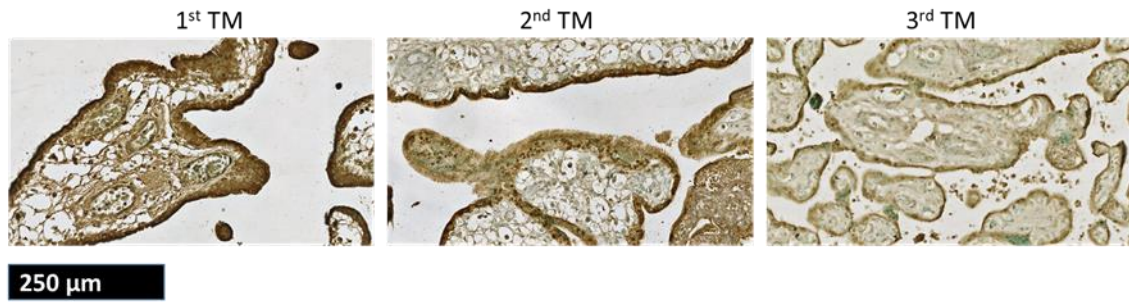


**Figure 3.2 S100P expression in human placenta is the highest during first trimester of gestation.** Relative S100P expression in human placenta sections from first, second and third trimesters (TM), which had been stained for S100P, was measured by densitometry. Panel A shows the images taken at 20x magnification and panel B shows relative S100P expression levels in each of the gestation ages. The error bars represent standard deviation (SD) (\*  $P < 0.05$ , \*\*  $P < 0.001$ ).  $N = 1$ . Sample size = 3 for each condition.

### **3.2.3. S100P is expressed in human trophoblasts and EVT**

After showing that the expression of S100P in placenta is the highest in early stages of placental development and having optimised the IHC staining for trophoblast marker cytokeratin-7 and EVT marker HLA-G, we next wanted to gain insight into S100P localisation within the placental villi, with serial staining for these two markers: cytokeratin 7 and HLA-G.

For this purpose, serial sections of wax-embedded first trimester human placental villi were incubated with the following primary antibodies: anti-S100P, anti-cytokeratin 7 (trophoblast marker) and anti-HLA-G (EVT marker), followed by secondary antibody incubation.

S100P colocalised with cytokeratin 7, confirming its localisation in cyto- and syncytiotrophoblasts, and a small proportion of it colocalised with HLA-G, confirming its localisation in the EVTs. S100P was localised in the cytoplasm of the trophoblasts and was also detectable in the apical plasma membrane of the syncytiotrophoblasts (highest expression level) as well as the EVTs with occasional localisation within the nuclei of the syncytiotrophoblasts and the EVTs. The stroma showed no detectable levels of S100P expression (Figure 3.3).

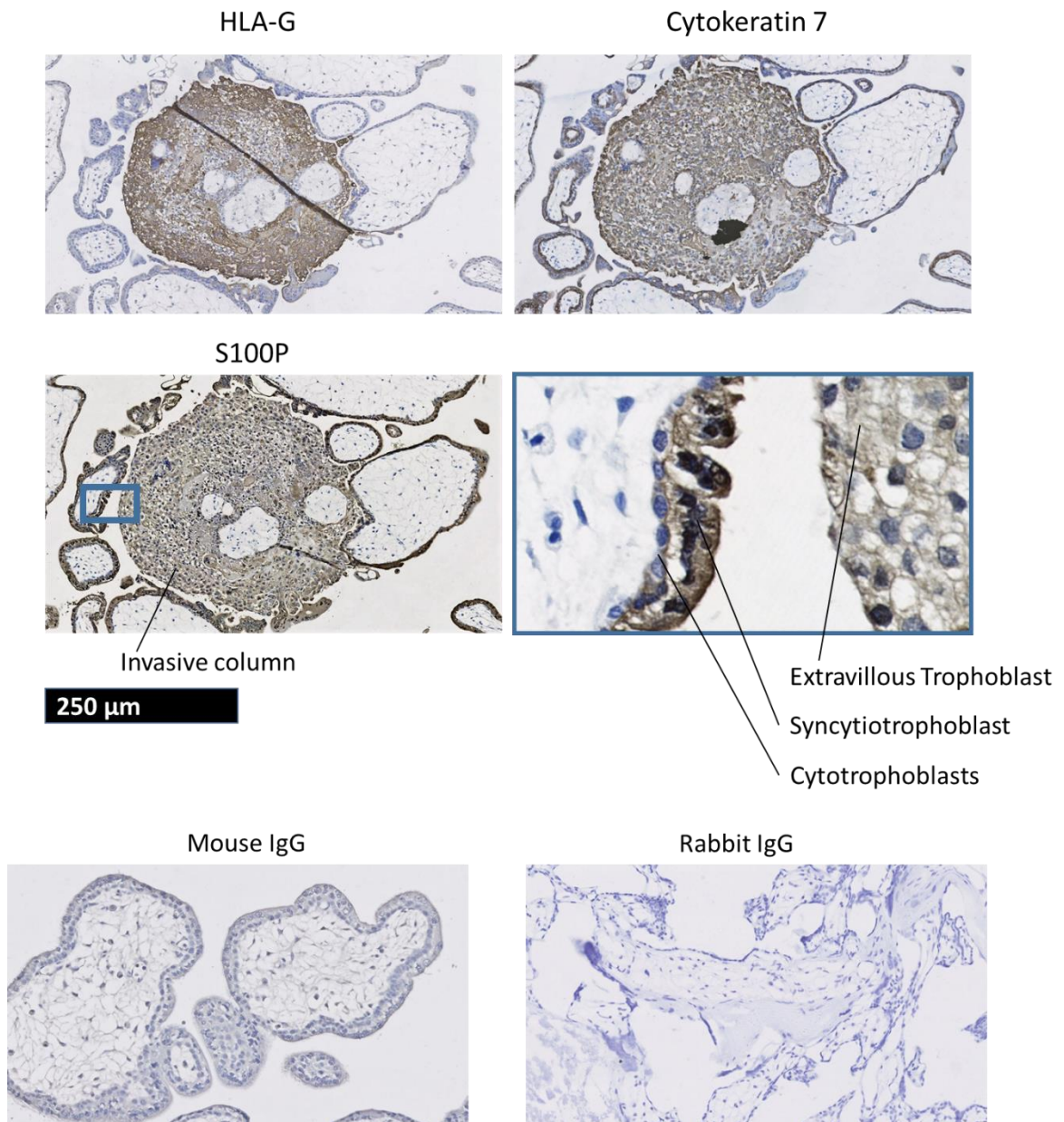


**Figure 3.3 S100P expression in human trophoblasts and EVTs.** Serial sections of wax-embedded human first trimester placental villi were prepared and incubated with primary anti-S100P, anti-cytokeratin 7, anti-HLA-G and mouse and rabbit IgG (as negative control), before being incubated with secondary antibodies, and finally staining using avidin-biotin complex and DAB chromogen and counters-staining using haematoxylin. The images were taken with 20x magnification. The image on the bottom right corner is a magnified field from the S100P staining image.



### 3.2.4. S100P expression in human trophoblast cell lines

Having now demonstrated significant expression of S100P in trophoblasts in placental sections, we wanted to determine if cell lines of trophoblastic origins also demonstrate endogenous expression of S100P.

In this aim, a collection of cell lines was obtained. These corresponds to Jeg-3 and BeWo, which are human choriocarcinoma, from epithelial malignancy of trophoblasts, that have lost their villous organisation (Cheung et al. 2009), as well as a series of immortalised human first trimester EVT cell lines as follows: SW71, virally infected with human telomerase reverse transcriptase hTERT (Straszewski-Chavez et al. 2009), HTR8/SVneo, chorionic villi, transfected with a plasmid containing the simian virus 40 large T antigen (SV40) (Graham et al. 1993), SGHPL-4 and SGHPL-5, which are also transfected with SV40 (Choy, St Whitley & Manyonda 2000).

To determine if S100P was expressed in these trophoblast cells, they were lysed in PBS with 1% (v/v) protease inhibitor cocktail and sonicated prior to proteins being separated by 16% SDS-PAGE. Western blot was performed by transferring proteins on to PVDF membrane prior to incubation with either anti-S100P or anti- $\alpha$ -tubulin antibodies and then incubating with secondary antibodies and ECL detection. S100P expression levels were normalised to the housekeeping gene expression. Endogenous S100P expression was detected, in both of the available human choriocarcinoma trophoblast cell lines, namely Jeg-3 and BeWo, with BeWo expressing 80% higher amounts of S100P, compared with Jeg-3, but not in any of the EVT cell lines: HTR8/SVneo, SW71, SGHPL-4 and SGHPL-5 (Figure 3.4).

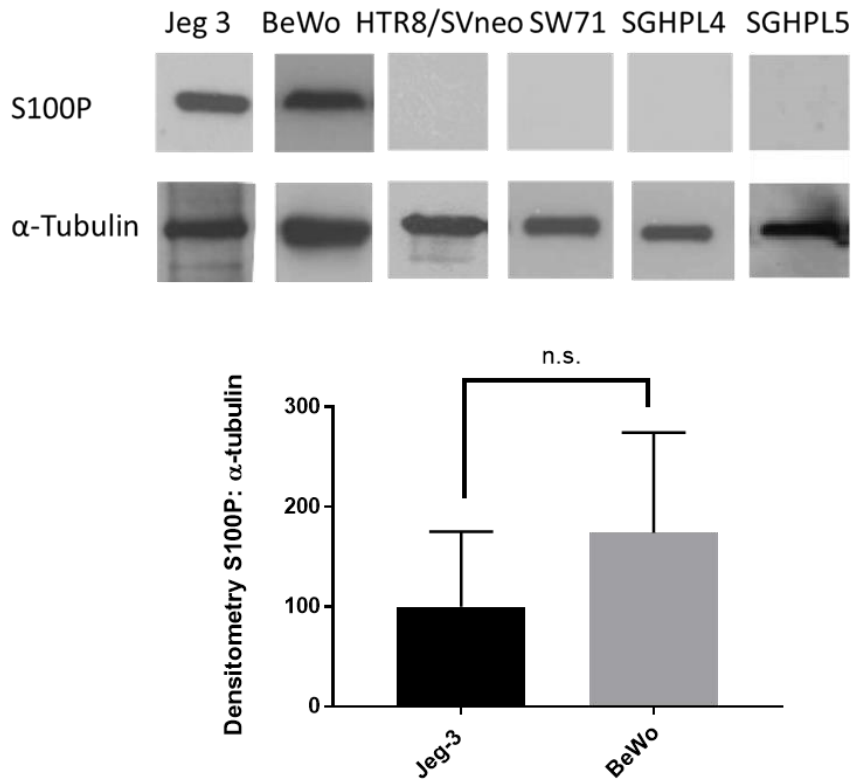


**Figure 3.4 Endogenous S100P expression in different trophoblast cell lines.** Human choriocarcinoma trophoblast cell lines were collected in protease inhibitor cocktail and sonicated, prior to being separated by 16% SDS-PAGE. Then, S100P and  $\alpha$ -tubulin were detected by western blot. Expression levels were quantified by Image Studio Lite software and S100P expression levels were normalised to the housekeeping gene expression. Panel A shows the western blot bands for S100P and  $\alpha$ -tubulin, and panel B shows the densitometry. The error bars represent SD. N.S. = non-significant. N = 2. Sample size = 2 for each cell line.

### **3.2.5. S100P expression in different microenvironments mimicking physiological conditions**

In the previous section, we showed that S100P is expressed in two of our trophoblast cell lines: Jeg-3 and BeWo, but was not found expressed at detectable levels in the EVT cells SW71, HTR8/SVneo, SGHPL-4 and -5. Given that significant S100P expression could be seen in trophoblasts during the early stages of implantation (Figure 3.2), and since trophoblast phenotypes such as proliferation, invasion and motility are controlled by their molecular and cellular interactions with the maternal microenvironment (Staun-Ram & Shalev 2005; Toro et al. 2014), we sought to investigate the effects of changes in trophoblast microenvironment including growing them on fibronectin, Matrigel and different concentrations of gelatine as well 24 hours of serum starvation on S100P expression in the choriocarcinoma cell line Jeg-3 and EVT cell lines: SW71, HTR8/SVneo, SGHPL-4 and SGHPL-5.

Growing Jeg-3 cells on 1% (v/v) fibronectin and 2% (w/v) gelatine, significantly increased S100P levels by 50% compared to non-treated control cells ( $P < 0.05$  and  $P < 0.0001$  respectively), while Matrigel, reduced S100P expression to 70 percent compared to control ( $P < 0.0001$ ). Growing the cells on surfaces covered with lower than 2% (w/v) concentrations of gelatine did not significantly affect S100P levels compared to control ( $P > 0.05$ ). Serum starvation did increase S100P expression by 50% compared with control, this increase, however, was insignificant ( $P > 0.05$ ) (Figure 3.5 A and B). None of these conditions induced S100P expression in the non-S100P-expressing EVT cell lines: HTR8/SVneo, SW71, SGHPL-4 and -5 (Figure 3.5 C).

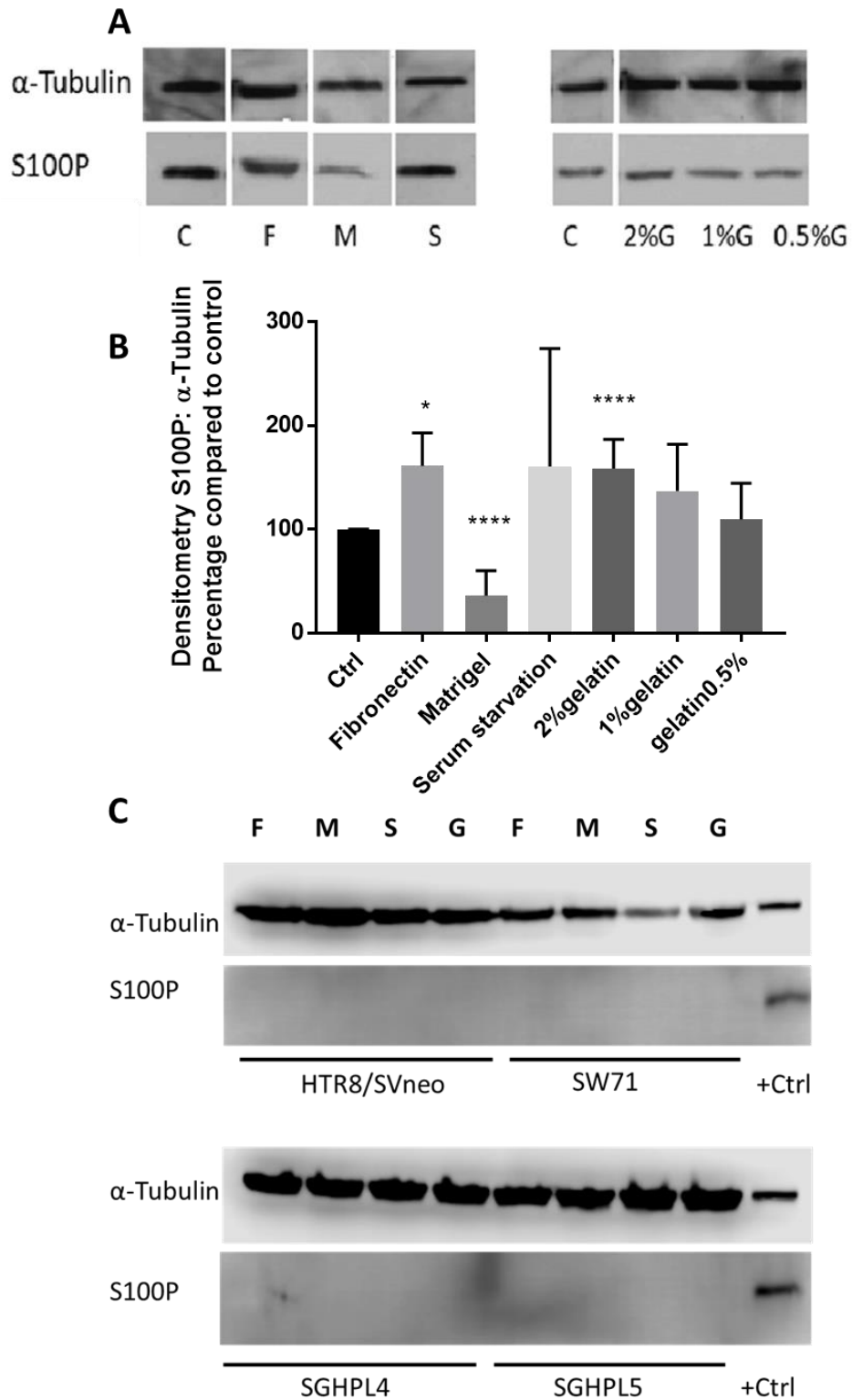


**Figure 3.5 S100P expression in physiological-like conditions enhances S100P expression.** 30,000 Jeg-3 cells were grown on different conditions including: F (on fibronectin coating), M (on Matrigel coating), S (without any coating, with 24 hours serum starvation), and G (on 3 different concentrations of gelatine: 2, 1 and 0.5%). The samples were collected, lysed and

separated by 16% SDS-PAGE and S100P and  $\alpha$ -tubulin were detected by western blot. Expression levels were quantified by Image Studio Lite software. S100P expression levels were normalised to the housekeeping gene expression. Panel A shows S100P expression in Jeg-3 cells grown in different microenvironments and B shows the densitometry. The error bars represent SD (\*  $P < 0.05$ , \*\*\*  $P < 0.0001$ ). Panel C shows the lack of S100P expression in EVT cell lines HTR8/SVneo, SW71, SGHPL-4 and SGHPL-5, when grown in different microenvironments, along with S100P expression in Jeg-3, as positive control. The error bars represent SD.  $N = 3$ . Total sample size = 3 for each condition.

### 3.2.6. S100P expression knockdown

S100P expression has been linked with many cellular functions including proliferation, motility and invasion in cancer cells (Du et al. 2012; Heil et al. 2011; Hsu et al. 2015; Kikuchi et al. 2019; Koltzsch et al. 2003; Mercado-Pimentel et al. 2015; Whiteman et al. 2007), but it is not clear whether it plays any of these roles in trophoblasts. In order to study the role of S100P in trophoblast behaviour, we first optimised siRNA delivery to specifically modulate the expression of S100P in two trophoblast cell lines Jeg-3 and BeWo, where it is found endogenously expressed. To this aim, Jeg-3 and BeWo cells were treated by four different sequences of siRNA (1, 4, 5 and 6) targeting S100P or mock treatment (treated with a nonspecific sequence of siRNA, as negative control). 3 days following the treatment, cell lysate was prepared and was separated by 16% SDS-PAGE, prior to western blot analysis for both  $\alpha$ -tubulin and S100P. S100P expression was normalised to tubulin expression. The expression levels were compared with the non-treated control. S100P was found to be endogenously expressed similarly in both control and mock treated Jeg-3 and BeWo cells, while treatment with a panel of different siRNA targeting S100P led to changes in the levels of protein expression (Figure 3.6). In Jeg-3 cells, siRNA 1 and 5 significantly reduced S100P levels by 70% ( $P < 0.0001$ ), while siRNA 4 and 6 reduced S100P levels by 80% ( $P < 0.0001$ ) compared with non-treated control (Figure 3.6 A1 and A2). In BeWo cells, siRNA 1 and 5 reduced S100P levels by 50% ( $P < 0.05$ ), while siRNA 4 and 6 reduced S100P levels by 60% ( $P < 0.01$ ) (Figure 3.6 B1 and B2), compared with non-treated control. Therefore, it was confirmed that S100P expression knockdown using S100P siRNA transfection (four sequences) was accomplished successfully, and that siRNA 4 and 6 were found to be the most potent in both Jeg-3 and BeWo cell lines.

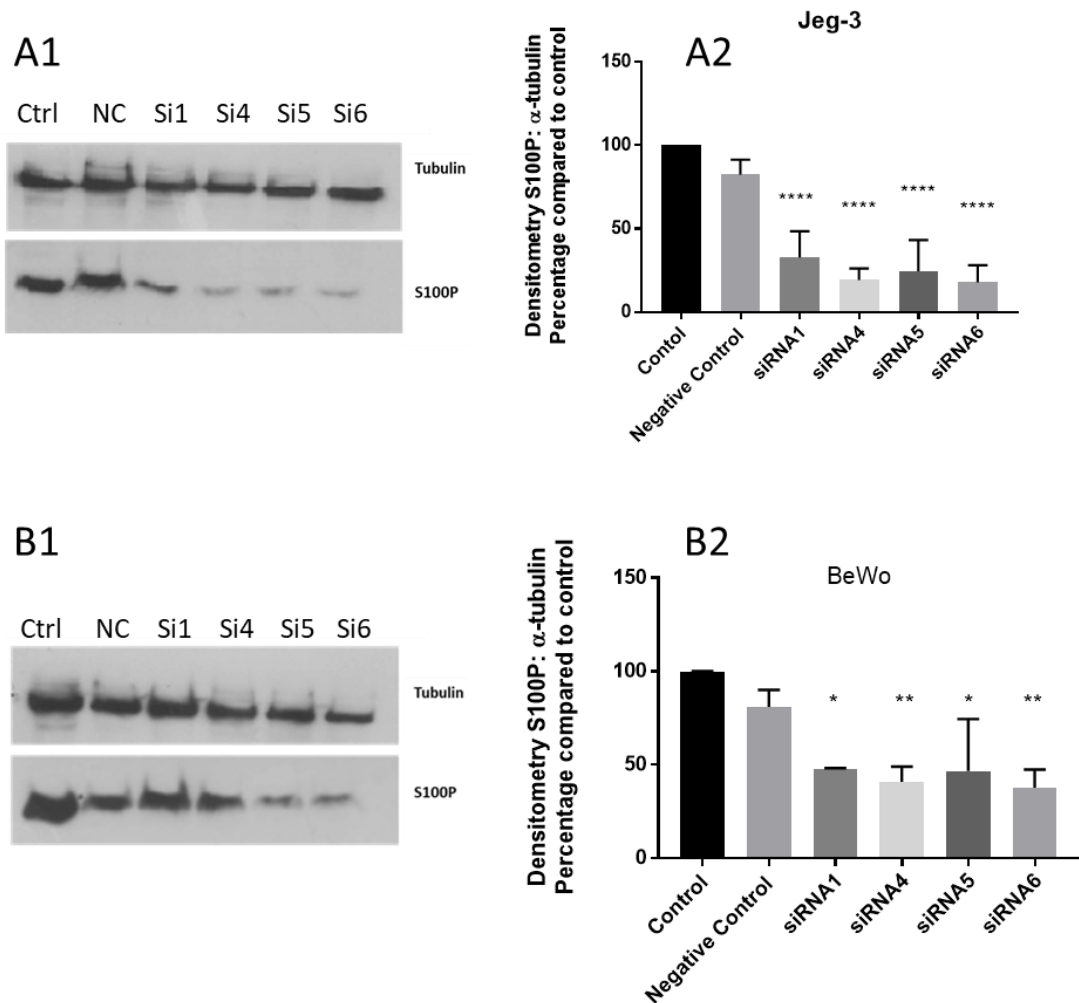


**Figure 3.6 Knocking down S100P expression by siRNA transfection in Jeg-3 and BeWo cells.** Jeg-3 and BeWo cells, were treated with S100P siRNA 1, 4, 5 and 6, along with mock treatment. The treated cells along with non-treated control cells were left to grow for 3 days prior to collection, lysing and sonication. The proteins were separated by 16% SDS-PAGE and S100P and  $\alpha$ -tubulin bands were detected by western blot. Expression levels were quantified by Image Studio Lite software and S100P expression levels were normalised to the housekeeping gene expression. Panels A1 and B1 show S100P and  $\alpha$ -tubulin bands in Jeg-3 and BeWo cells, respectively, while panels A2 and B2 show the densitometry in the mentioned cells in the same order. The error bars represent SD. (\*  $P < 0.05$ , \*\*  $P < 0.01$  and \*\*\*\*  $P < 0.0001$ ).  $N = 3$ . Total sample size = 3 for each cell line.

## 3.2.7. Boyden chamber assay optimisation

### 3.2.7.1. Migration assay optimisation

Both cellular motility and invasion measurements can be performed using a plethora of techniques. In this study, we sought to assess the cells' ability to migrate and invade using the Boyden chamber assays. In order to optimise transwell migration assay for trophoblast cell line Jeg-3, 100,000 cells were seeded in transwells and were left to migrate for 24 hours, before being fixed by two different fixation (4% PFA and ice-cold methanol) and staining methods (Quick Diff staining kit containing eosinophilic and basophilic staining reagents along with Vectashield mounting medium containing DAPI). The trapped cells inside the transwell membrane pores could be observed when either 4% PFA (Figure 3.7 A and C) or ice-cold methanol (Figure 3.7 B and D) were used as fixatives. However, methanol, which is less hazardous, was used for further experiments. Both DAPI (Figure 3.7 C and D) and Quick Diff staining (Figure 3.7 A and B) could stain the cells, but Quick Diff staining was used for further experiments due to its more convenient procedure.

In order to establish an appropriate and workable number of cells migrating or invading throughout the transwells, we sought to determine the most appropriate cell seeding number to analyse motility capabilities of trophoblast using transwell assays. Therefore, three different seeding numbers were tested: 25,000, 50,000 and 100,000. The cells were then treated with S100P siRNA 4, which was shown to significantly reduce S100P expression (Figure 3.6), or negative control siRNA (mock transfection), along with non-treated control. 48 hours after the transfection, the media was replaced with serum starvation media and the cells were left to grow for one more day, before being collected. The collected cells (control, negative control and siRNA 4 treated) were resuspended in serum starvation medium and the above-stated number of cells were seeded in transwells, while the lower wells contained complete media as chemoattractant, and were left to migrate for 24 hours, followed by fixation and staining. The cells were counted in six different files with 20x magnification and the average number of negative control and siRNA 4 treated cell counts were compared with the non-treated control of each group of cell counts. When 100,000 and 50,000 cells were seeded, there was a 70% reduction in Jeg-3 migration in the S100P-knockdown cells compared with the control ( $P < 0.01$  for 100,000 and  $P < 0.05$  for 50,000), while seeding 25,000 cells did not show a significant change in migration due to S100P knock-down ( $P > 0.05$ ) (Figure 3.7 E). Therefore, these two seeding numbers (100,000 and 50,000) were chosen as suitable numbers for further experiments.

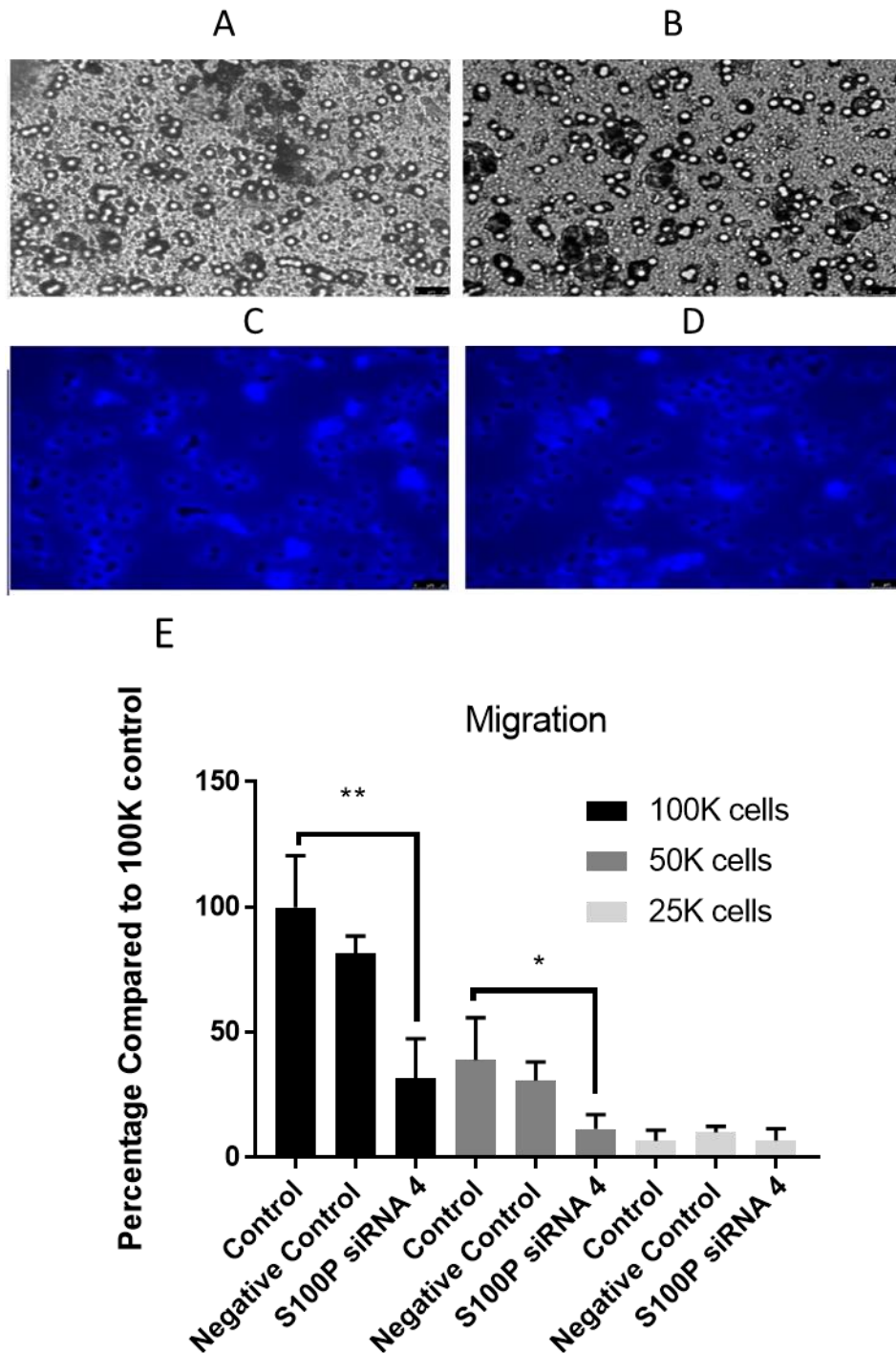


**Figure 3.7 Transwell migration assay optimisation results.** In the above panel, JEG-3 cells were seeded on the bottom of inverted transwells and were incubated at 37°C for 2 hours before they were fixed with either 4% PFA (panels A and C) or 100% methanol (panels B and D) and stained with either Quick Diff staining kit (panels A and B) or DAPI (panels C and D). The images were taken at 40x magnification using bright field (A and B) or fluorescent (C and D) microscopy. The lower panel (E) shows average cell count percentage for control, negative

control and S100P siRNA 4 treated samples with three different seeding numbers: 100,000 (black bars); 50,000 (dark grey bars); 25,000 (light grey bars) in six random fields of the transwell membrane at 20x magnification. The error bars represent SD (\* P<0.05, \*\* p<0.01). N = 1. Sample size = 6 for each condition.

### **3.2.7.2. Invasion assay optimisation**

To optimise the invasion assay in our hands, 1:3 diluted Matrigel was used to cover the bottom of the transwells (as the Matrigel quickly forms a gel at room temperature, it is more convenient to dilute it with the medium used for cell growth). Matrigel was polymerised and formed a gel after 2 hours of incubation at 37°C. The gel forms only when the proportion of Matrigel to medium is 1:3 or higher (data not shown).

To find the maximum volume of Matrigel that the Jeg-3 trophoblast cells are able to digest and pass through and how much time they need for invasion, three different Matrigel volumes and three different incubation times were tested. The cells could digest 10 µl and 20 µl of polymerised Matrigel, while none of the incubation times (24 or 48 hours) were enough for the cells to digest 30 µl of Matrigel (Figure 3.8). For further experiments, 20 µl diluted Matrigel was chosen as it is easier to spread on the membrane compared to 10 µl. As for the incubation time, 24 hours seemed to give the best results (Figure 3.8) as a longer incubation time lead to cells forming a clump of cells in the centre of the transwells and being too numerous and dense to count (Figure 3.8).

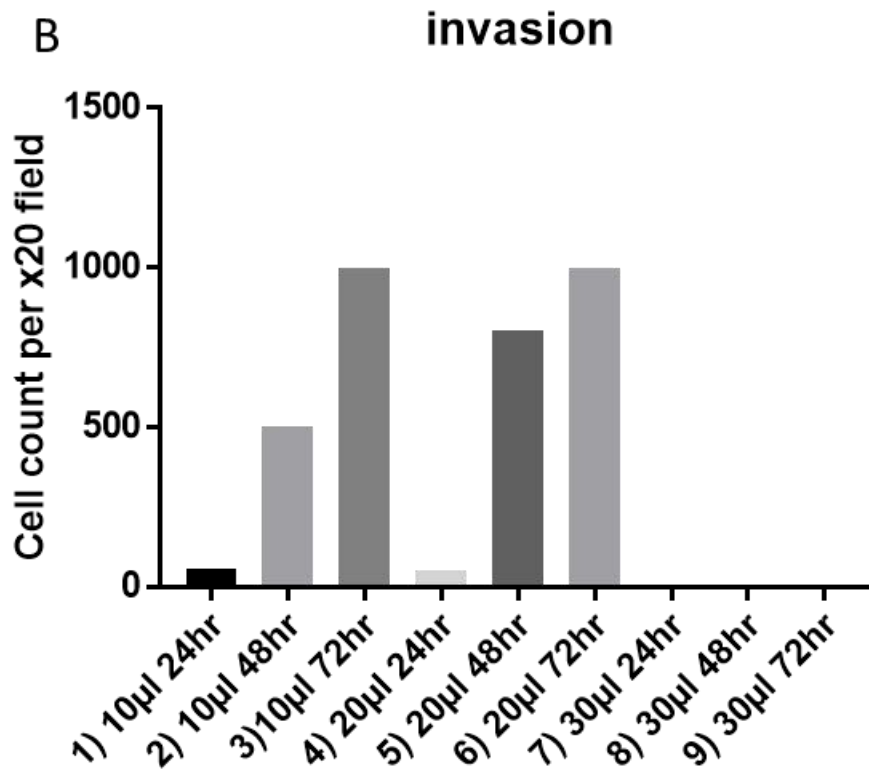
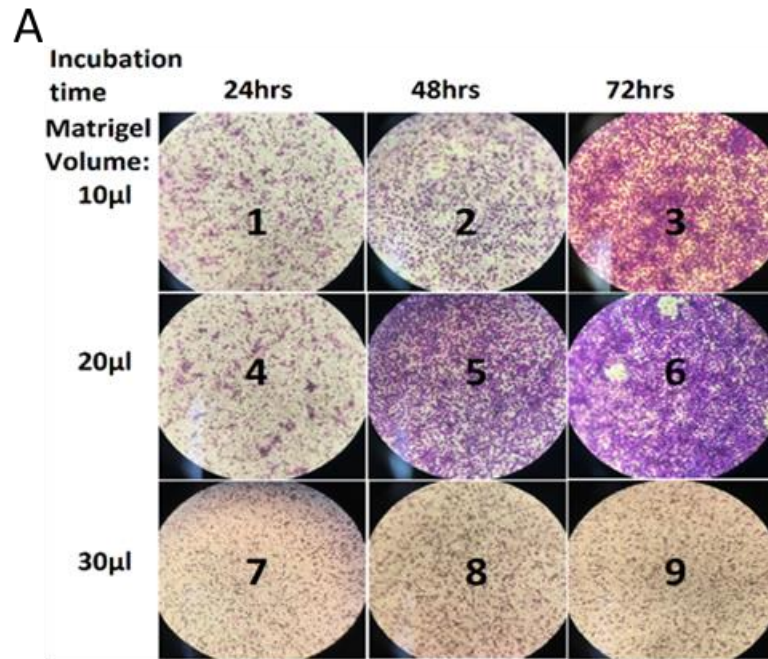


**Figure 3.8 Transwell invasion assay optimisation results.** 50,000 Jeg-3 cells were seeded in transwells coated with 10, 20 and 30  $\mu$ l polymerised Matrigel (three transwells for each volume, total of nine transwells) and each of them were incubated for either 24, 48 and 72 hours prior to

fixation and staining with Quick Diff kit. The images were taken at 20x magnification (A) and the graph shows cell count per 20x field (B). N = 1. Sample size = 1 for each condition.

### **3.2.8. Knocking down S100P reduces trophoblast motility**

S100P has been shown to be a key regulator of cell motility in cancer cells (Austermann et al. 2008; Du et al. 2012; Hsu et al. 2015). Therefore, we sought to determine whether S100P could equally regulate trophoblast motility. Given our ability to knock down S100P expression in trophoblast cell lines, Jeg-3 and BeWo using siRNA delivery, we now sought to establish whether such reduction would correlate with changes in motility.

For this purpose, Jeg-3 and BeWo cells were treated with S100P siRNA (four different sequences) or negative control siRNA. 72 hours following the treatment, the cells were seeded in transwells and were left to migrate for 24 hours. The transwells were then fixed and stained and the migrated cells were counted in six random fields at 20x magnification. Knocking down S100P expression in Jeg-3 and BeWo cells, reduced cell migration compared with the controls in both cell types. This reduction was more significant for Jeg-3 (50% reduction for siRNA 1, 4, 5 and 60% for siRNA 6) ( $P < 0.0001$ ), than BeWo (50% reduction for siRNA1, 40% for siRNA4 and 60% for siRNA6) ( $P < 0.01$  for siRNA 1,  $P < 0.05$  for siRNA 4,  $P > 0.05$  for siRNA 5 and  $P < 0.001$  for siRNA 6) (Figure 3.9).

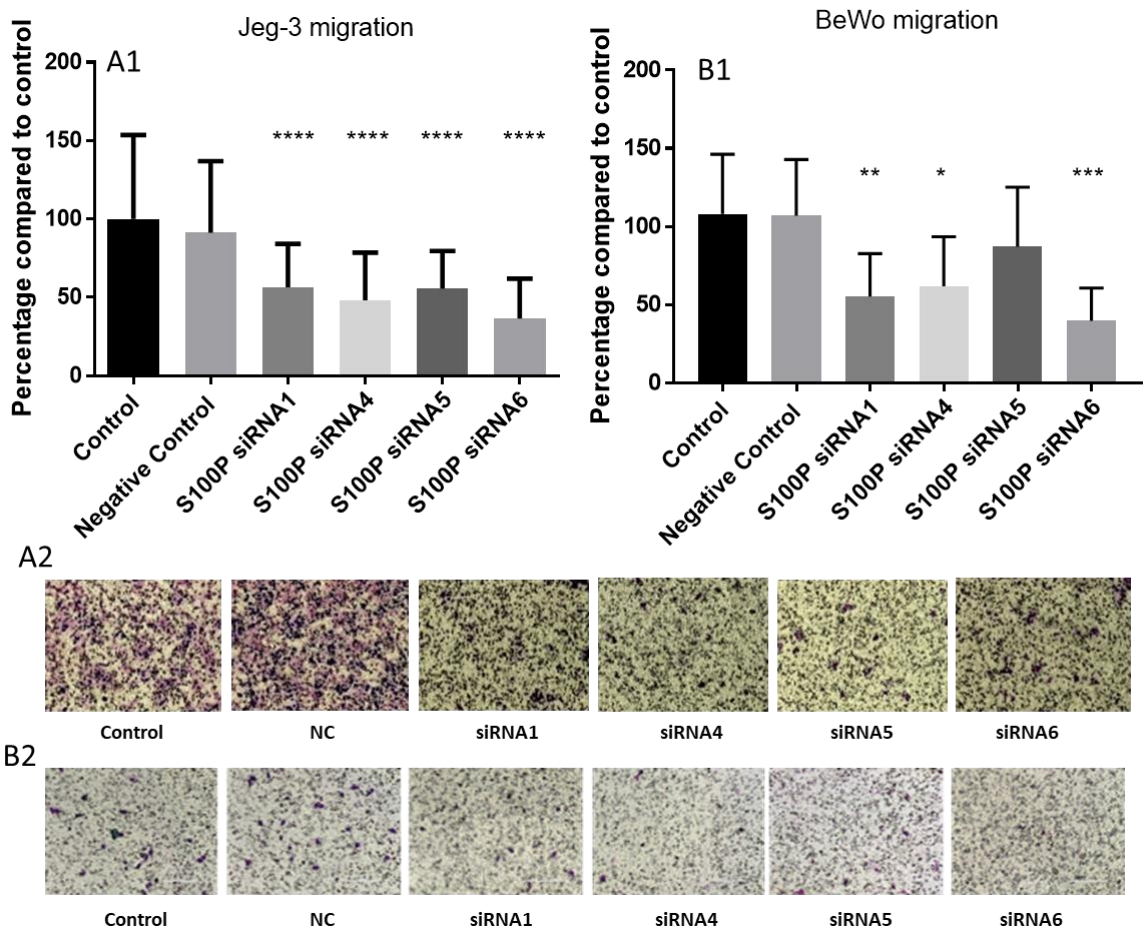


**Figure 3.9 S100P knockdown reduces trophoblast migration.** Jeg-3 (A) and BeWo (B) cells were seeded in 24 well plates and treated with S100P siRNA 1, 4, 5 and 6, along with mock treatment and not treated control. They were left to grow for 48 hours before being serum starved. After another 24 hours of incubation, the cells were collected and were seeded in transwells. On the next day the transwells were fixed and stained. The cells were counted in fields of 20x magnification. Graphs A1 and B1 show average cell count percentage compared with control in Jeg-3 and BeWo cells respectively and the bars represent standard error of the mean (SEM) (\*  $P < 0.05$ , \*\*  $p < 0.01$  and \*\*\*\*  $p < 0.0001$ ). Panels A2 and B2 show representative fields of fixed and stained transwells for Jeg-3 and BeWo, respectively.  $N = 3$  for each cell line. Total sample size = 18 for each cell line.

### **3.2.9. Knocking down S100P reduces trophoblast invasion**

S100P has been shown to be a key regulator of cell invasion, mainly in cancer lines, and its expression correlates with both cellular invasion (Mercado-Pimentel et al. 2015; Whiteman et al. 2007) and overall metastasis (Arumugam et al. 2005) and poor prognosis (Wang et al. 2015). Given that S100P knockdown was shown to reduce trophoblast migration (Figure 3.9), here we sought to test the role of S100P protein on trophoblast invasion.

For this purpose, Jeg-3 and BeWo cells were treated with S100P siRNA (four different sequences) or negative control siRNA. 72 hours following the treatment, the cells were seeded in transwells coated with Matrigel and were left to invade for 24 hours. The transwells were then fixed and stained and the migrated cells were counted in two fields at 20x magnification. Knocking down S100P expression in Jeg-3 and BeWo cells, reduced cell invasion in both Jeg-3 and BeWo cells, compared with control cells. In Jeg-3 there was a 60% reduction in invasion for siRNA 1 and 70% reduction for siRNA 4, and 6 ( $P < 0.0001$ ). In BeWo on the other hand, there was 60% reduction in invasion for siRNA 4 and ( $P < 0.0001$ ) and 50% reduction for siRNA 6 ( $P < 0.001$ ), while siRNA 1 and 5 did not significantly affect invasion (Figure 3.10).

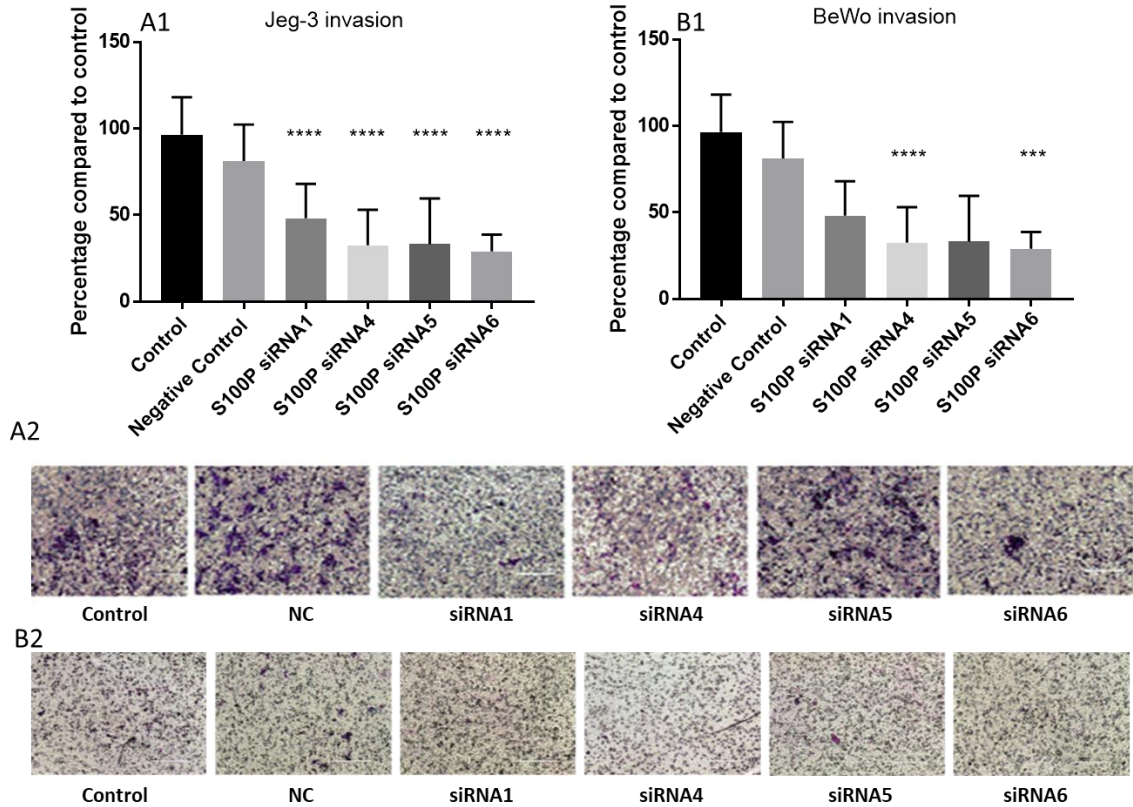


**Figure 3.10 The effect of S100P knockdown on trophoblast invasion.** Jeg-3 (A) and BeWo (B) cells were seeded in 24 well plates and treated with S100P siRNA 1, 4, 5 and 6, along with mock treatment and not treated control. They were left to grow for 48 hours before serum starvation. After another 24 hours of incubation, the cells were collected and were seeded in Matrigel-coated transwells. On the next day the transwells were fixed and stained. The cells were counted in fields of 20x magnification. Graphs A1 and B1 show average cell count percentage compared with control in Jeg-3 and BeWo cells respectively and the bars represent SEM (\*\*\*)  $p < 0.001$  and \*\*\*\*)  $p < 0.0001$ ). Panels A2 and B2 show representative files of fixed and stained transwells for Jeg-3 and BeWo, respectively. N = 3 for each cell line. Total sample size = 6 for each cell line.

### 3.2.10. Stable S100P transfection

Initial work carried out with EVT cell lines (HTR8/SVneo, SW71, SGHPL-4 and SGHPL-5), did not show detachable levels of S100P expression in these cells (Figure 3.4). Therefore, HTR8/SVneo cell lines were stably transfected with SGB217 plasmid containing S100P or SGB16 control plasmid. To confirm S100P expression in the clones transfected with S100P-containing plasmid SGB217, the cells were collected, lysed and separated by 16% SDS-PAGE, before performing western blot analysis for both  $\alpha$ -tubulin and S100P. S100P expression level was normalised to tubulin expression. HTR8/SVneo clones expressed different levels of S100P (Figure 3.11 A1 and A2): SGB217 clones 2, 5, 7, 14 and pools of SGB217 clones express moderate levels (300000-500000% compared to clone 1 baseline), clones 1, 8 and 12 express low or undetectable levels, and clones 3, 4, 9 and 10 express high amounts (900000-1100000% compared to clone 1 baseline), while the mock clone and the mock clones pool, which were transfected with SGB16 plasmid, do not show any detectable levels of S100P. Moreover, lysates of clones 5 and 7 (SB217) were loaded on the same gel along with Jeg-3 (which expresses S100P) as well as the mock clone (SGB16) and were probed for S100P and  $\alpha$ -tubulin as before, to compare S100P expression in these two HTR8/SVneo clones with the endogenous expression of Jeg-3. HTR8/SVneo clones 5 and 7 show similar expression levels of S100P, when compared with Jeg-3 (Figure 3.11 B1 and B2).

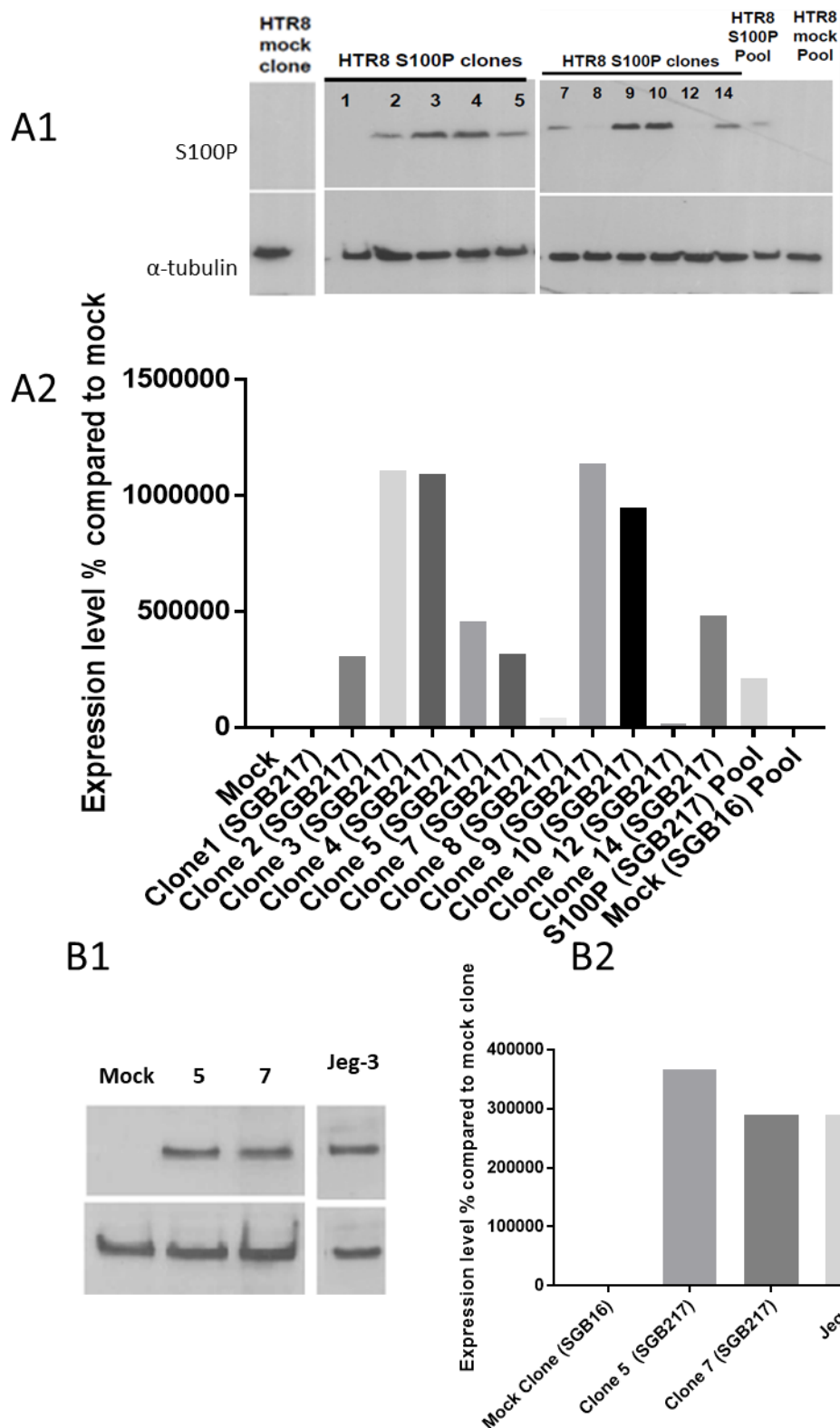


**Figure 3.11 S100P expression in HTR8/SVneo SGB217 clones and their levels compared with Jeg-3 HTR8/SVneo clones 1, 2, 3, 4, 5, 7, 8, 9, 10, 12, 14 (SGB217), pool of SGB217 clones and pool of SGB16, and the mock clone (SGB16) as well as Jeg-3 samples were collected, lysed,**

sonicated and loaded on 16% tricine gel. The bands were detected with ECL (panels A1 and B1) and the expression levels were quantified with Image Studio Lite software (panels A2 and B2). S100P signals were normalised to  $\alpha$ -tubulin signals. N = 1. Sample size = 1 for each cell line.

### **3.2.11. Moderate levels of S100P expression enhance trophoblast**

#### **motility**

Endogenous S100P expression promotes motility and invasion in cancer cell motility (Austermann et al. 2008), and in trophoblasts (Figure 3.9 and Figure 3.10). Here, to further study the effect of exogenous S100P expression on trophoblast motility, HTR8/SVneo EVT clones with different levels of S100P expression (containing SGB217 plasmid): 250-300% higher (clones 9 and 10), 90% lower (clone 12) and similar to Jeg-3 expression levels (clones 5 and 7) along with the mock clone (SGB16) were serum starved for 24 hours and then seeded in transwells (50,000 cells per transwell) and were left to migrate for 24 hours. The transwells were then fixed and stained, prior to counting the migrated cells. S100P expression showed a hormetic effect on the migration of HTR8/Svneo cells. There was a significant increase in the migration of clones 5 (250%) ( $P < 0.0001$ ) and 7 (50%) ( $P < 0.05$ ), when compared with mock clone (SGB16). Clones 12 with lower S100P than Jeg-3, showed no difference in migration. Clones 9 and 10 with higher S100P than Jeg-3 levels showed a significant 50% and 80% reduction, respectively, when compared with the mock clone ( $P < 0.05$  for clone 9 and  $P < 0.0001$  for clone 10) (Figure 3.12).

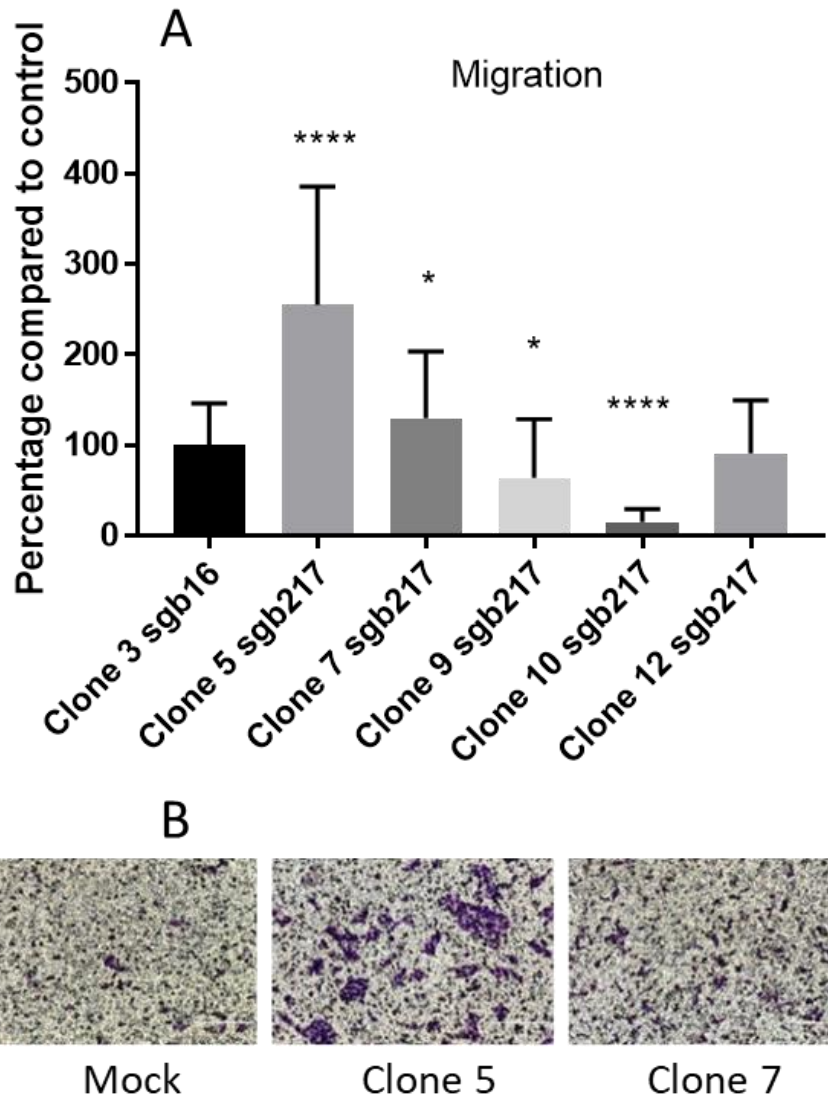


**Figure 3.12 S100P expression and trophoblast migration.** S100P-expressing HTR8/SVneo clones with different levels of S100P expression: clones 9 and 10 (high), clone 12 (low) and clones 5 and 7 (similar to Jeg-3), were tested for migration (compared with the mock clone) by transwell migration assay. For this aim, the cells were serum starved for a day, before being collected. They were then seeded into transwells. The transwells were fixed and stained after 24 hours. Panel A shows the average cell count for HTR8/SVneo clones 3 (SGB16), and SG217 clones 5, 7, 9, 10 and 12, while panel B shows representative fields from migrated HTR8/SVneo clones 3 (SGB16), 5 (SGB217) and 7 (SGB217) at fields of 20x magnification. The error bars represent SEM (\*  $p < 0.05$  and \*\*\*\*  $p < 0.0001$ ).  $N = 3$ . Total sample size = 18 for each cell line.

### **3.2.12. Moderate levels of S100P expression enhances trophoblast invasion**

Moderate S100P expression was shown to enhance trophoblast migration, previously. Here, to study the effect of exogenous S100P expression on trophoblast invasion, HTR8/SVneo EVT clones with different levels of S100P expression (containing SGB217 plasmid): 250-300% higher (SGB217 clones 9 and 10), 90% lower (clone 12) and similar to Jeg-3 levels (clones 5 and 7) along with the mock clone (SGB16) were serum starved for 24 hours and then seeded in Matrigel-coated transwells and were left to invade for 24 hours. The transwells were then fixed and stained, prior to counting the invaded cells. clones 5 and 7 (SGB217), with the same levels of S100P as in Jeg3 showed significantly enhanced invasiveness (by 700% and 500%, respectively) compared to mock clone (SGB16) ( $P < 0.0001$  for both), while the other clones (9, 10, 12 SGB217) with either higher or lower levels were not significantly different from the mock clone (SGB16) in invasion (Figure 3.13).

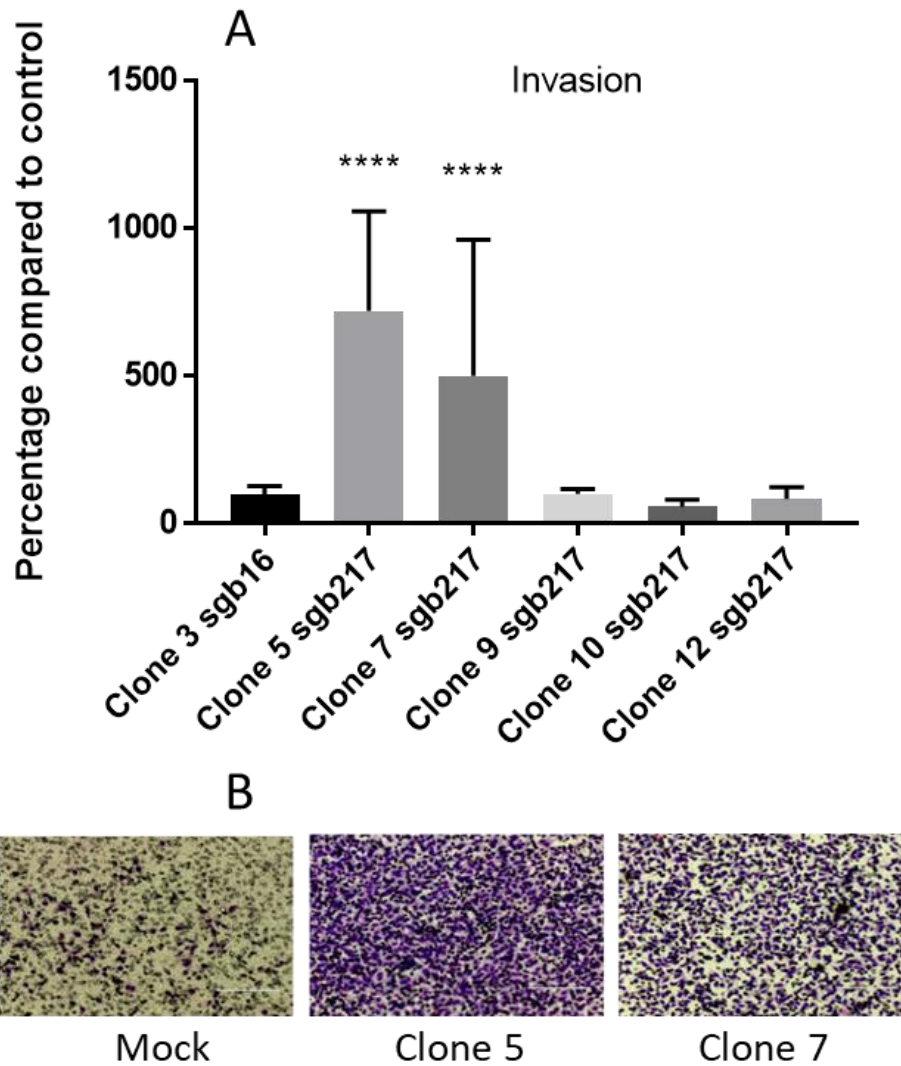


**Figure 3.13 S100P expression and trophoblast invasion.** S100P-expressing HTR8/SVneo clones with different levels of S100P expression: clones 9 and 10 (high), clone 12 (low) and clones 5 and 7 (similar to Jeg-3), were tested for invasion (compared with the mock clone) by transwell invasion assay. For this aim, the cells were serum starved for a day, before being collected and resuspended in serum starvation medium. 50,000 cells were then seeded into Matrigel-coated transwells, while the bottom wells contained complete medium. The transwells were fixed and stained after 24 hours. Panel A shows the average cell count for HTR8/SVneo clones 3 (SGB16), and SG217 clones 5, 7, 9, 10 and 12, while panel B shows representative fields from invaded HTR8/SVneo clones 3 (SGB16), 5 (SGB217) and 7 (SGB217) at fields of 20x magnification. The error bars represent SEM (\*\*\*\*  $p < 0.0001$ ).  $N = 3$ . Total sample size = 6 for each cell line.

### 3.2.13. S100P expression reduced the size and the number of focal adhesions

Knocking down S100P in Jeg-3 and BeWo cells was shown previously to increase the number and the size of the FAs (Tabrizi et al. 2018). Here we sought to test whether S100P expression in HTR8/SVneo clones 5 and 7, which were shown to be significantly more motile and invasive than the mock clone (SGB16) (Figure 3.12 and Figure 3.13), also affects the number and/or the size of FAs, by staining the cells for paxillin, one of the components of the FA complex. For this aim, 10,000 HTR8/SVneo mock clone (control) and S100P-expressing clones 5 and 7 were seeded on fibronectin-coated coverslips and were left to grow for 48 hours, before fixing and permeabilisation. They were then incubated with primary anti-paxillin and then secondary antibody as well as phalloidin. The staining showed FAs formed on the cell surface, mostly along the actin bundles (Figure 3.14). There a significant 30% reduction in the average number of the FAs (Table 3.1) in S100P-expressing clones 5 ( $P < 0.01$ ) and 7 ( $P < 0.05$ ) compared to the mock clone, and the FAs look relatively smaller in clones 5 and 7 compared with 3 (Figure 3.14).

	Percentage focal adhesions per cell $\pm$ SEM (n=34)	P value (compared with control)
Mock clone (SGB16)	100 $\pm$ 6.66	N/A
Clone 5 (SGB217)	75.63 $\pm$ 4.24	0.0030
Clone 7 (SGB217)	72.34 $\pm$ 3.60	0.0183

**Table 3.1** The average number of focal adhesions per cell in HTR8/SVneo clones, represented as percentages

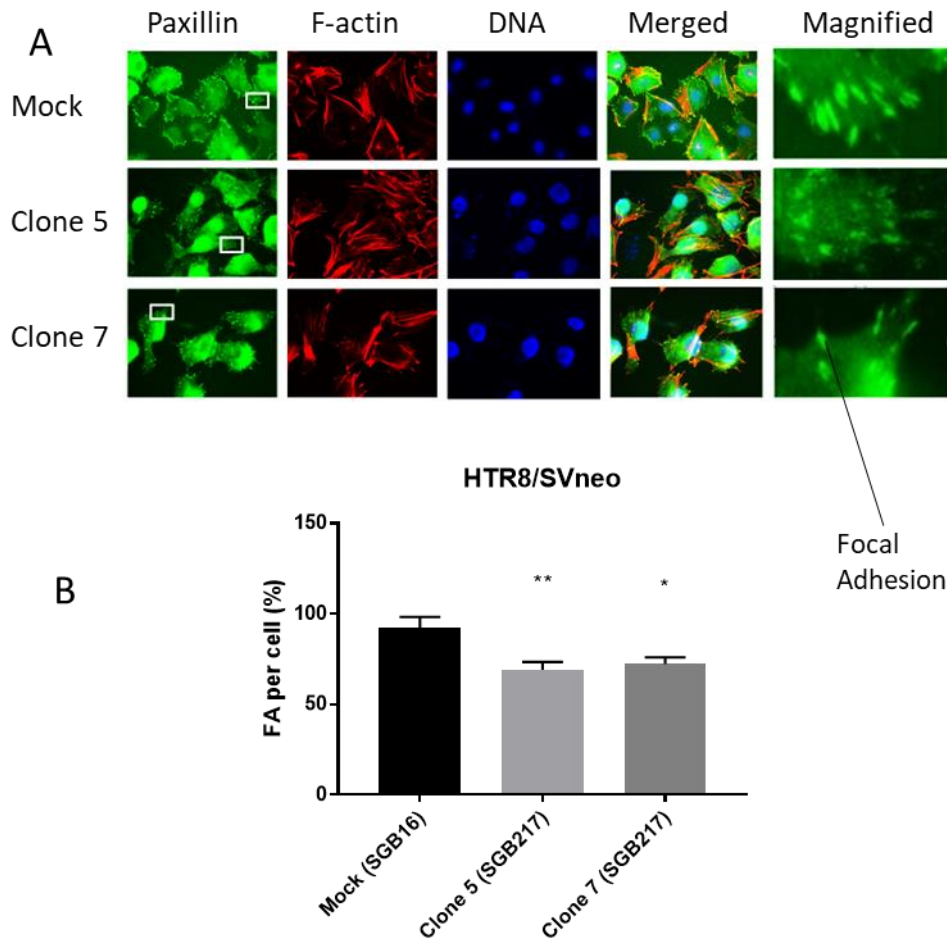


**Figure 3.14** The effect of exogenous S100P expression on focal adhesions in HTR8/SVneo EVT cells. HTR8/SVneo mock clone (containing the control SGB16 plasmid) as well as clones 5 and 7 (containing S100P-expressing SGB217 plasmid) were seeded on fibronectin-coated coverslips and FAs were visualised with immunofluorescence staining on paxillin, a marker of FAs, along with rhodamine phalloidin to stain F-Actin and DAPI to visualise DNA. The images were taken with 63x magnification (panel A). Panel B shows the average FA count per cell in each of the clones. The error bars represent standard SEM (\*  $p < 0.5$ , \*\* $P < 0.01$ ).  $N = 1$ . Sample size (number of images) = 34 for each cell line.

### **3.2.14. S100P expression does not affect the viability of**

#### **HTR8/SVneo**

Migration and invasion abilities can sometimes be the result of cell growth. Moreover, S100P expression has been shown to promote proliferation in cancer cells (Arumugam et al. 2004, 2005; Guo et al. 2014; Liu et al. 2017). We already had shown that knocking down S100P in Jeg-3 and BeWo trophoblast cells does not affect their viability (Tabrizi et al. 2018). Since previously, it was shown that moderate levels of S100P expression in HTR8/SVneo EVT cell lines, significantly enhances their migration and invasion (Figure 3.12 and Figure 3.13), here, to rule out the possibility of changes in cell viability and proliferation due to S100P expression, we sought to find out whether S100P expression in HTR8/SVneo EVT cells, affects their viability compared to the control counterpart. For this aim, an equal number of seeded HTR8/SVneo clones 3 (SGB16), and clones 5 and 7 (SGB217) were left to grow and their viability was tested during the next 24 and 48 hours, by the trypan blue assay. The assay showed that S100P-expressing HTR8/SVneo clones have similar growth rates to the mock clone (Figure 3.15), validating that the S100P-induced increase in migration and invasion of HTR8/SVneo clones is not due to a difference in their viability.

### Cell proliferation percentage in HTR8/SVneo clones

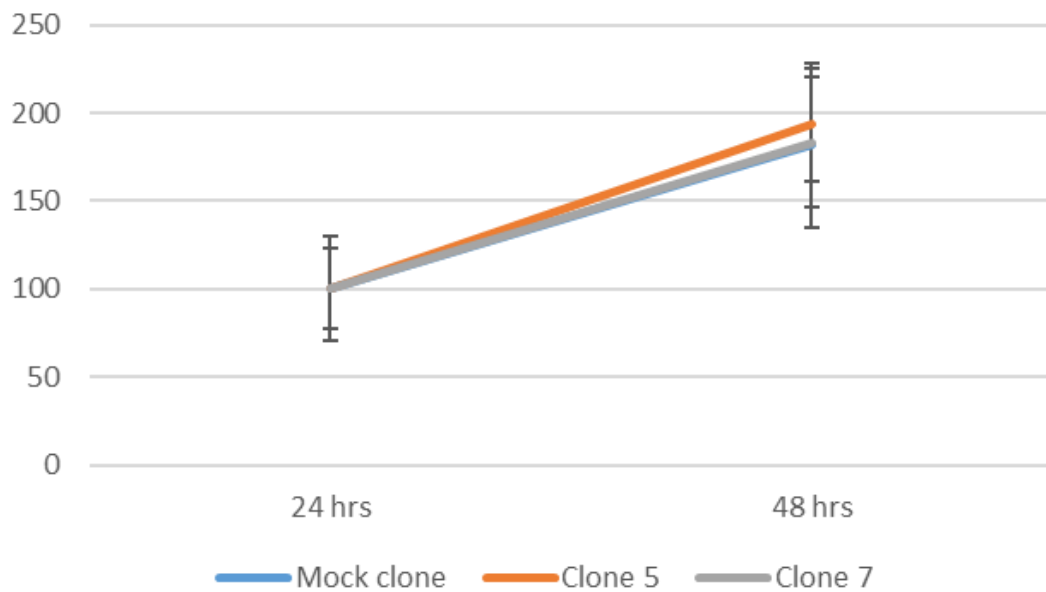


**Figure 3.15 S100P expression does not affect the viability of HTR8/SVneo clones.** HTR8/SVneo clones 3 (with control SGB16 plasmid), and clones 5 and 7 (with SGB217 S100P-expressing plasmid) were seeded in 24-well plates and their viability was measured by trypan blue exclusion assay during the next 24 and 48 hours. The error bars represent SD. N = 3. Total sample size = 60 for each cell line.

### **3.2.15. Reversing the motile/invasive phenotype in HTR8/SVneo clones**

We have shown that expression of S100P results in increased levels of migration and invasion in the HTR8/SVneo cell background after stable transfection. To further demonstrate that this effect is due to the sole expression of S100P as opposed to clonal selection, we sought to further validate that the increase in migration and invasion of HTR8/SVneo clones 5 and 7 (SGB217) compared with mock clone (SGB16) is S100P-specific, via knocking down S100P expression and investigating its effect on migration/invasion of these cells, as follows:

#### **3.2.15.1. S100P knock-down in S100P-expressing HTR8/SVneo clones**

To achieve S100P knockdown, S100P-expressing HTR8/SVneo clones 5 and 7 (SGB217) were seeded and treated with four different sequences of siRNA (1, 4, 5 and 6) targeting S100P along with mock treatment (treatment with a nonspecific sequence of siRNA, as negative control) and non-treated control. The cells were left to grow for 72 hours, then the lysates were collected, loaded on 16% tricine gels and were then probed for S100P and  $\alpha$ -tubulin by western blot. S100P expression levels were normalised to  $\alpha$ -tubulin expression. Both siRNA 4 and 5 have significantly reduced S100P expression by 60% ( $P < 0.05$ ), in both clones 5 (black bars) and 7 (grey bars) compared with the non-treated control, while siRNA 1 and 6 had no significant effect in neither of the clones ( $P > 0.05$ ) (Figure 3.16).

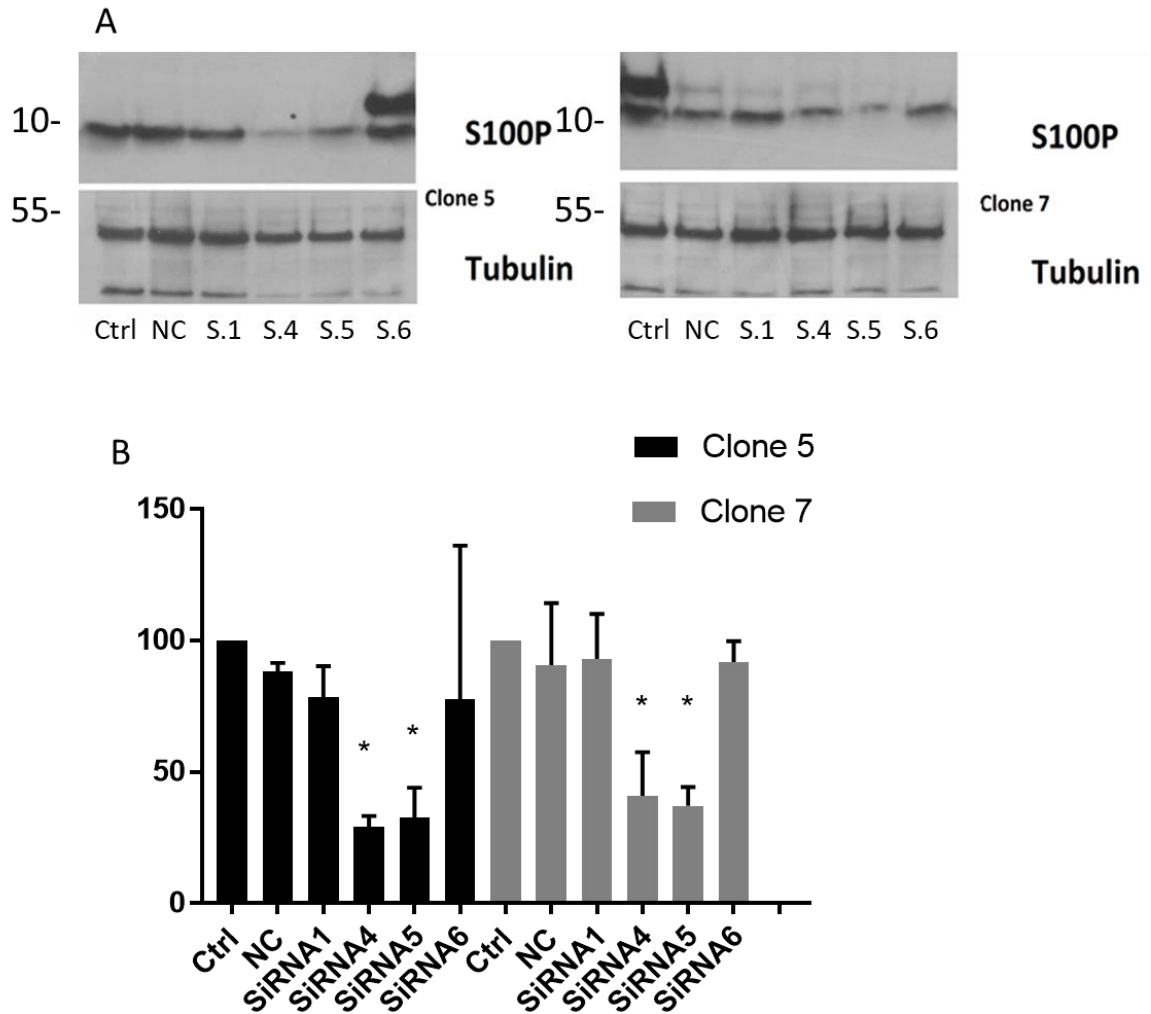


**Figure 3.16 Knocking down S100P expression in S100P-expressing HTR8/SVneo clones.** HTR8/SVneo clones 5 and 7 (SGB217) were treated with S100P siRNA 1, 4, 5 and 6, or negative control siRNA (NC) for 72 hours, before being collected, lysed and separated by 16% SDS-PAGE. S100P and  $\alpha$ -tubulin were detected by western blot. Expression levels were quantified by Image Studio Lite software. S100P expression levels were normalised to the housekeeping gene expression. Panel A shows western blot bands for S100P and  $\alpha$ -tubulin in HTR8/SVneo clones 5 and 7, while panel B shows relative S100P expression levels in these cells. The error bars represent SD (\*  $p < 0.05$ ). The double bands are artefacts that were seen only occasionally. N = 3. Total sample size = 3 for each condition.

### **3.2.15.2. S100P knock-down does not affect the viability of HTR8/SVneo clones**

To investigate the effect of S100P knockdown on mock HTR8/SVneo clones (SGB16 control) and clones 5 and 7 (S100P-expressing SGB217), the cells were treated with S100P siRNA 4, which was shown to significantly reduce S100P expression by 60%, as well as a nonspecific negative control siRNA (mock transfection), or without any treatment, as control. Following the transfection, an equal number of seeded cells were left to grow and their viability was tested during the next 48 and 72 hours, by performing the trypan blue exclusion assay. The assay revealed that there was no difference in the growth rate of the three clones without treatment (black bars), but there was a 50% decrease in mock transfection (dark grey bars) and siRNA 4 treated samples (light grey bars) compared with the no treatment control samples (black bars) in all three clones. Comparing the mock treated samples and their siRNA 4 treated counterparts showed that there was no significant difference between these two, 48 or 72 hours following the treatment (Figure 3.17), validating the ineffectiveness of the siRNA treatment on HTR8/SVneo clones viability.

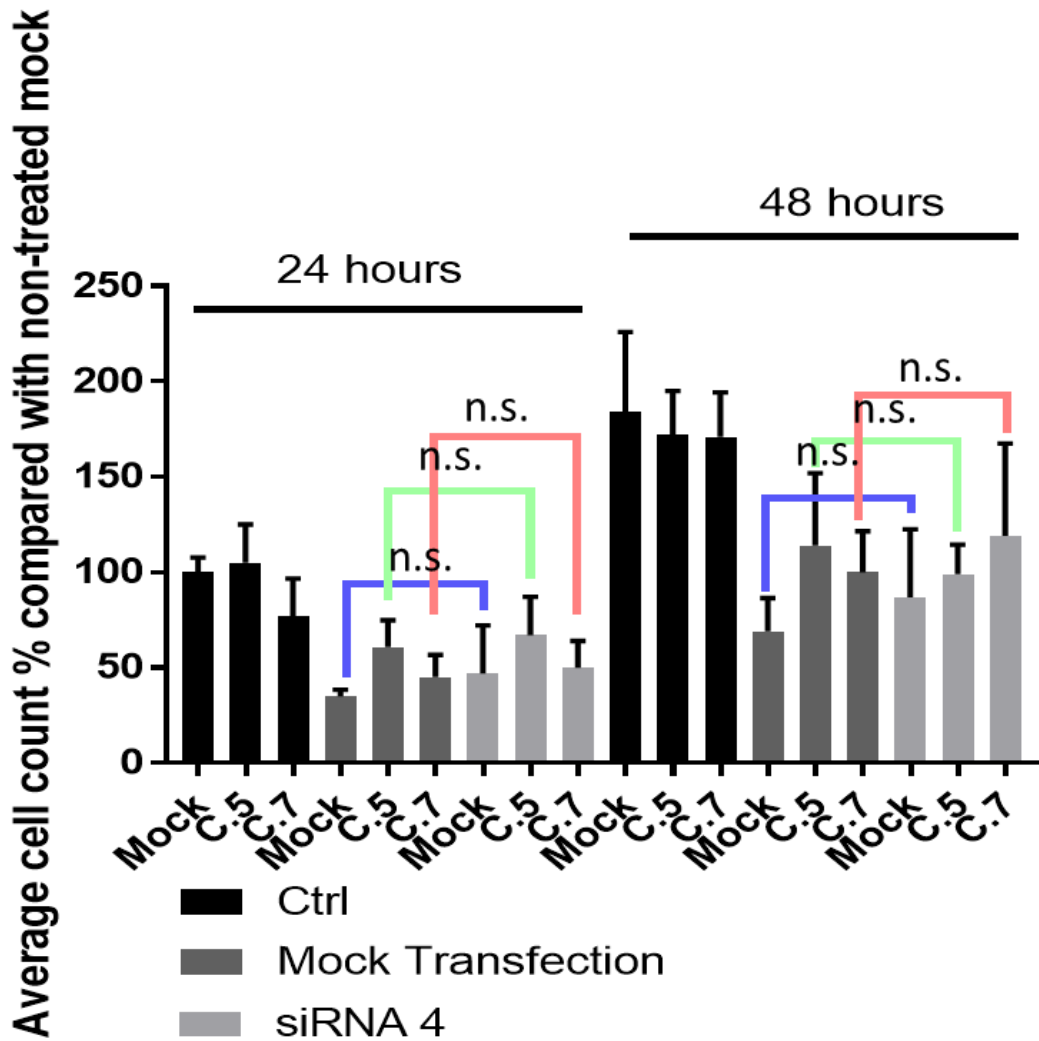


**Figure 3.17 S100P expression and S100P knockdown do not affect the viability of HTR8/SVneo clones.** Mock HTR8/SVneo clone (with control SGB16 plasmid), and clones 5 and 7 (with SGB217 S100P-expressing plasmid) were seeded in 24 well plates and were treated with S100P siRNA 4, or with negative control siRNA (mock), along with non-treated control. The viability of the cells was measured by the trypan blue exclusion assay 48 and 72 hours following the transfection. The differences between mock treated and their siRNA treated counterparts have been marked by different colours. The error bars represent SD (P-values are as follows. Between mock and mock after 24 hours = 0.35, between clone 5 and clone 5 after 24 hours = 0.60, between clone 7 clone after 24 hours 7 = 0.56, between mock and mock after 48 hours = 0.35, between clone 5 and clone 5 after 48 hours = 0.45, between clone 7 clone after 48 hours 7 = 0.64. N = 1. Sample size = 5 for each condition.

### **3.2.15.3. Knocking down S100P can reverse motile/invasive phenotype in S100P-expressing HTR8/SVneo clones**

We have shown that high expression of S100P results in increased levels of migration and invasion in HTR8 clones. To demonstrate that this effect is due to the sole expression of S100P, and not as the result of other mutations, we sought to further validate that the increase in migration and invasion of HTR8/SVneo clones 5 and 7 (SGB217) compared with mock clone (SGB16), is S100P specific, via S100P knockdown and investigating its effect on migration/invasion.

For this, HTR8/SVneo clones 5 and 7 (SGB217) were treated with S100P siRNA 5, which was shown to significantly reduce S100P expression (Figure 3.16), along with negative control siRNA (mock transfection) for 48 hours. The cells were seeded in transwells with (for invasion assay) and without Matrigel (for migration assay). The cells were left to migrate and invade for 24 hours, before fixation and staining and counting the migrated/invaded cells. The results showed that there was a significant ( $P < 0.0001$ ) 300% (for clone 5) and 200% (for clone 7) reduction in migration and 300% (for clone 5) and 250% (for clone 7) reduction in invasion, when the clones were treated with S100P siRNA 5, which brought both the migration and the invasion down to almost same levels as the mock clone (Figure 3.18), validating that the increase seen in both migration and invasion of clones 5 and 7 compared with the mock clone, was indeed S100P-dependent.

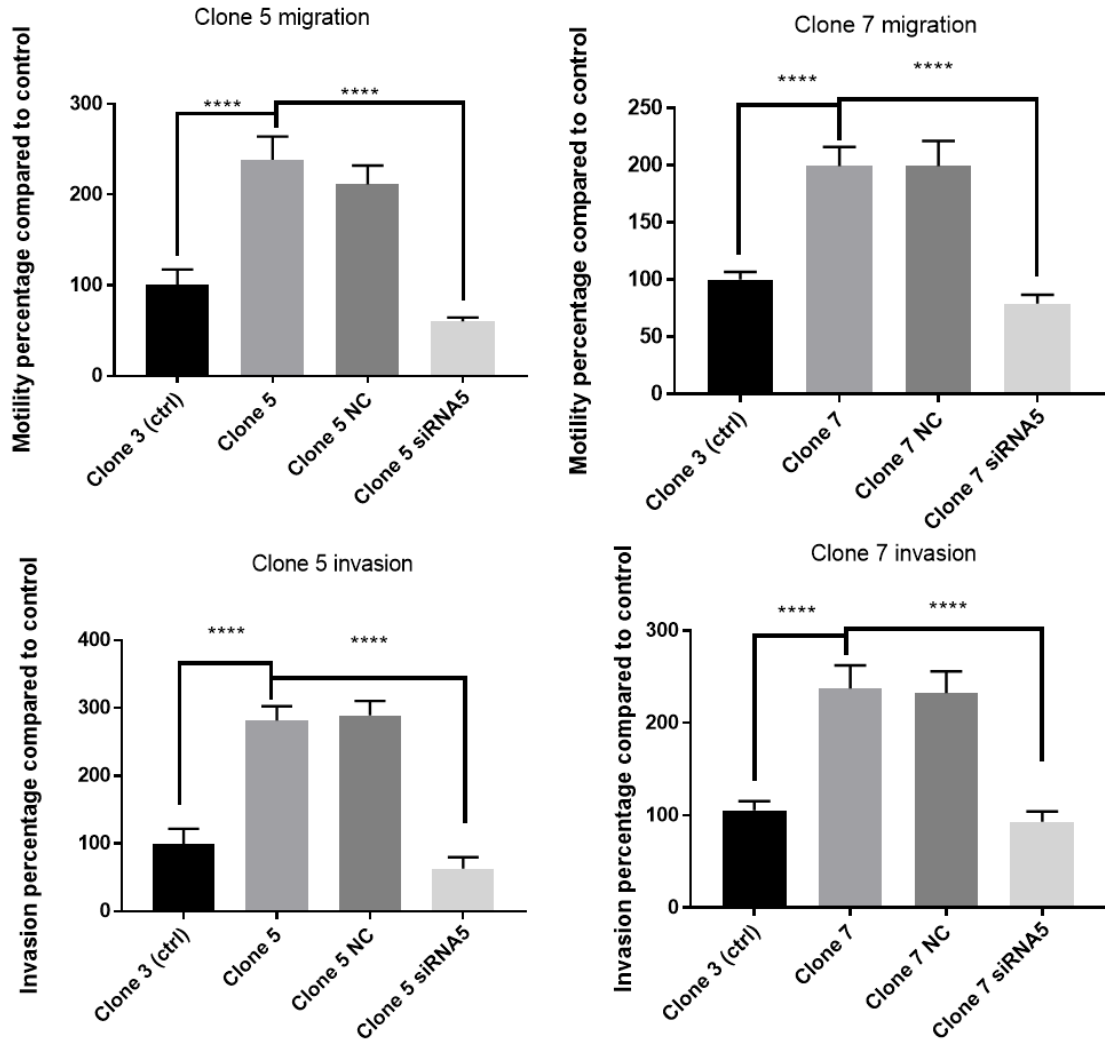


**Figure 3.18 S100P knockdown in S100P-expressing HTR8/SVneo clones brings migration and invasion down to same levels as the control clone.** HTR8/SVneo clone 5 and 7 (with SGB217 S100P-expressing plasmid) were seeded in 24 well plates and were treated with S100P siRNA 5, or negative control siRNA (NC), along with non-treated control. The treated cells were then seeded in transwells with (for invasion) and without Matrigel coating (for migration). The error bars represent SD (\*\*\*\*  $p < 0.0001$ ).  $N = 3$  for each condition. Total sample size for each condition: 18 (migration) and 6 (invasion).

### 3.2.16. Regression analysis

Predicting phenotypical traits based on gene expression in living organism is possible using mathematical modelling but remains challenging due to the complex nature of genetics (Carter et al. 2007; Hao et al. 2014). Here, we aimed to see whether there is a meaningful correlation between S100P expression and migration/invasion in our trophoblast cells, by regression analysis. To do this, S100P expression levels in trophoblast cells Jeg-3 and BeWo, with four sequences of S100P siRNA (1, 4, 5 and 6), mock transfection (with negative control siRNA), along with non-treated control (Figure 3.6) were correlated with their migration (Figure 3.9) and invasion (Figure 3.10). For HTR8/SVneo EVT cells, mock clone (with control SGB16 plasmid) and clones 5 and 7 (with S100P-expressing GB217 plasmid) were used for the comparison between S100P-expression (Figure 3.11) and migration (Figure 3.12) as well as invasion (Figure 3.13). Other clones with lower and higher expression levels than Jeg-3, which did not positively affect migration and invasion, were not used in the regression analysis. Pearson correlation coefficient,  $r$ , which can take a range of values from -1 to +1, was calculated and Student's  $t$ -distribution was used to test the significance of the correlation. Regression analysis showed a positive correlation ( $r > 0$ ) between S100P expression and cell migration/invasion for all trophoblast cells: S100P expression and Jeg-3 migration  $r = 0.97$  and invasion  $r = 0.96$ , S100P expression and BeWo migration  $r = 0.76$  and invasion  $r = 0.49$ , S100P expression and HTR8/SVneo migration  $r = 0.88$  and invasion  $r = 0.99$ . The correlation however, was only significant for Jeg-3 migration ( $P < 0.001$ ) and invasion ( $P < 0.001$ ) as well as HTR8/SVneo invasion ( $P < 0.01$ ) (Figure 3.19).

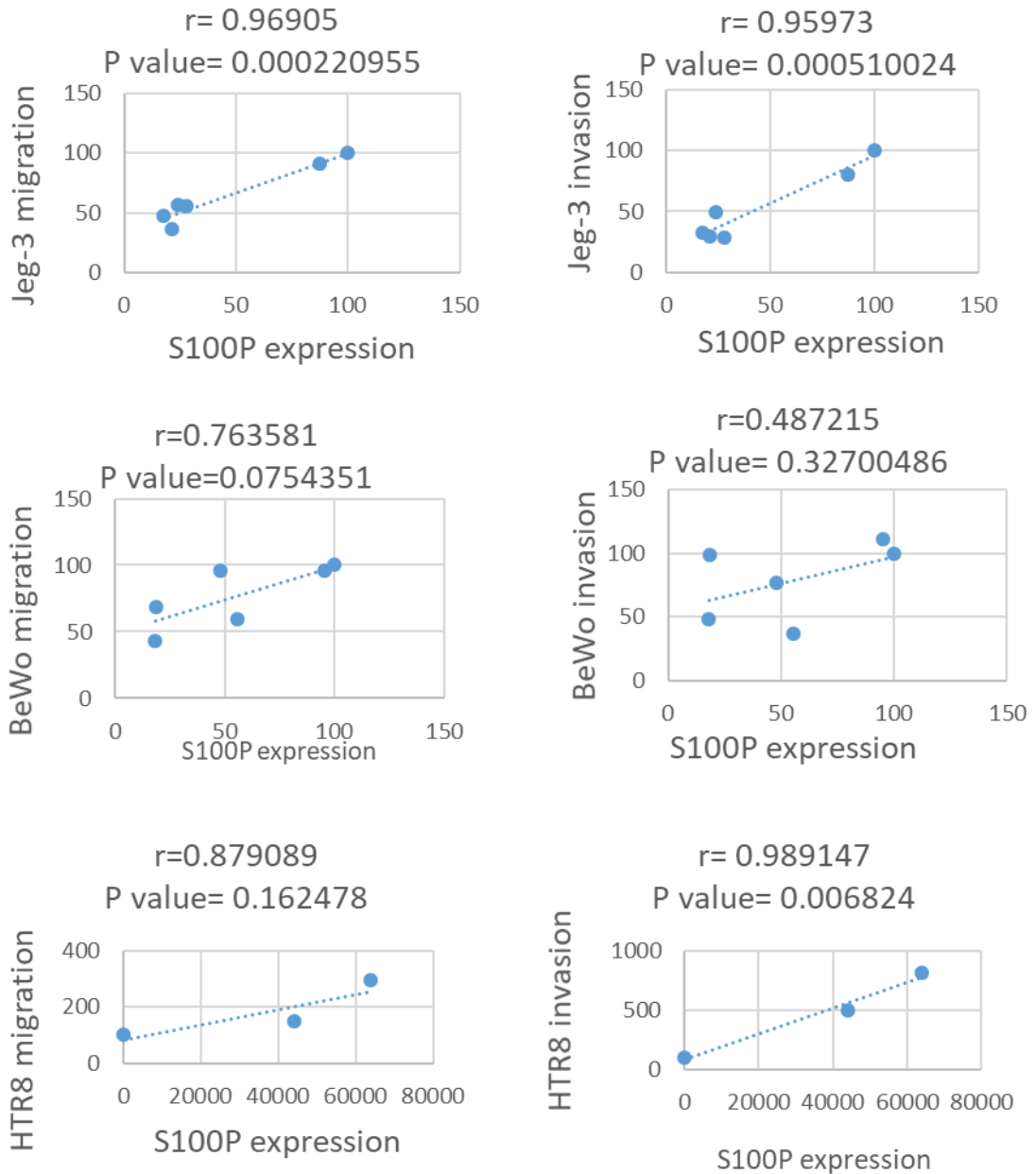


**Figure 3.19 Positive correlation between trophoblast migration/invasion and S100P expression.** S100P expression levels in trophoblast cell lines Jeg-3, BeWo and HTR8/SVneo (mock and clones 5 and 7) were correlated with migration and invasion and Pearson correlation coefficient,  $r$ , was calculated. 's t-distribution was used to test the significance.

### **3.2.17. Extracellular S100P promotes trophoblast migration and invasion**

Our work so far clearly shows that high levels of S100P promote an increase in both cellular migration and invasion in all trophoblast cells tested to date. We do not however have any information about the possible mechanisms of this regulation.

The majority of the S100P-interacting partners identified so far (Table 1.1) suggest an internal localisation for the protein, with only two extracellular membrane-bound binding partners i.e. RAGE (Mercado-Pimentel et al. 2015) and integrin  $\alpha 7$  (Hsu et al. 2015). Therefore, we aimed to investigate whether S100P regulates trophoblast migration and invasion while being located on the cell-surface or the extra-cellular environment. Moreover, S100P includes a C-terminal lysine in its amino acid sequence (Clarke et al. 2017), and therefore we hypothesised that it might regulate cell invasion (and possibly migration) through a pathway that involves an interaction with plasminogen (which has a lysine-binding site) and/or plasminogen activators (PAs), leading to the break-down of the ECM by plasmin (plasminogen's active form) and MMPs, which are activated by plasmin (Holst-Hansen et al. 1996).

In order to test our hypothesis (extracellular localisation of S100P and interaction with the plasminogen pathway), we aimed to study the effect of anti-S100P antibody and Epsilon-aminocaproic acid (ACA), which is a derivative of the amino acid lysine and acts as a plasminogen inhibitor (Purwin et al. 2009), on trophoblast cell invasion and migration.

#### **3.2.17.1. S100P antibody and ACA do not affect trophoblast viability**

Prior to testing the effect of S100P antibody and ACA on trophoblast migration and invasion, we aimed to study how S100P antibody and ACA affect the viability of Jeg-3 cells and HTR8/SVneo clones 3 (non-S100P-expressing control SGB16) and clones 5 and 7 (S100P-expressing SGB217), to rule out toxicity. For this aim, 15,000 trophoblast cell lines Jeg-3, and 25,000 HTR8/SVneo clones 3 (non-S100P-expressing control SGB16) and clones 5 and 7 (S100P-expressing SGB217) were seeded and treated with either 0.4  $\mu\text{g/ml}$  anti-S100P, or 10 mM plasminogen inhibitor ACA, along with non-treated control cells. The cells were left to grow, and their viability was measured during the next 24 and 48 hours following the treatment, by the trypan blue exclusion assay. The assay showed that the growth rates of Jeg-3, HTR8/SVneo mock clone (SGB16), HTR8/SVneo clone 5 (SGB217) and HTR8/SVneo clone 7 (SGB217) are not affected by either S100P antibody or ACA treatment, compared with control (Figure 3.20).

Therefore, the possibility of toxicity caused by these two compounds (S100P antibody and ACA) was ruled out.

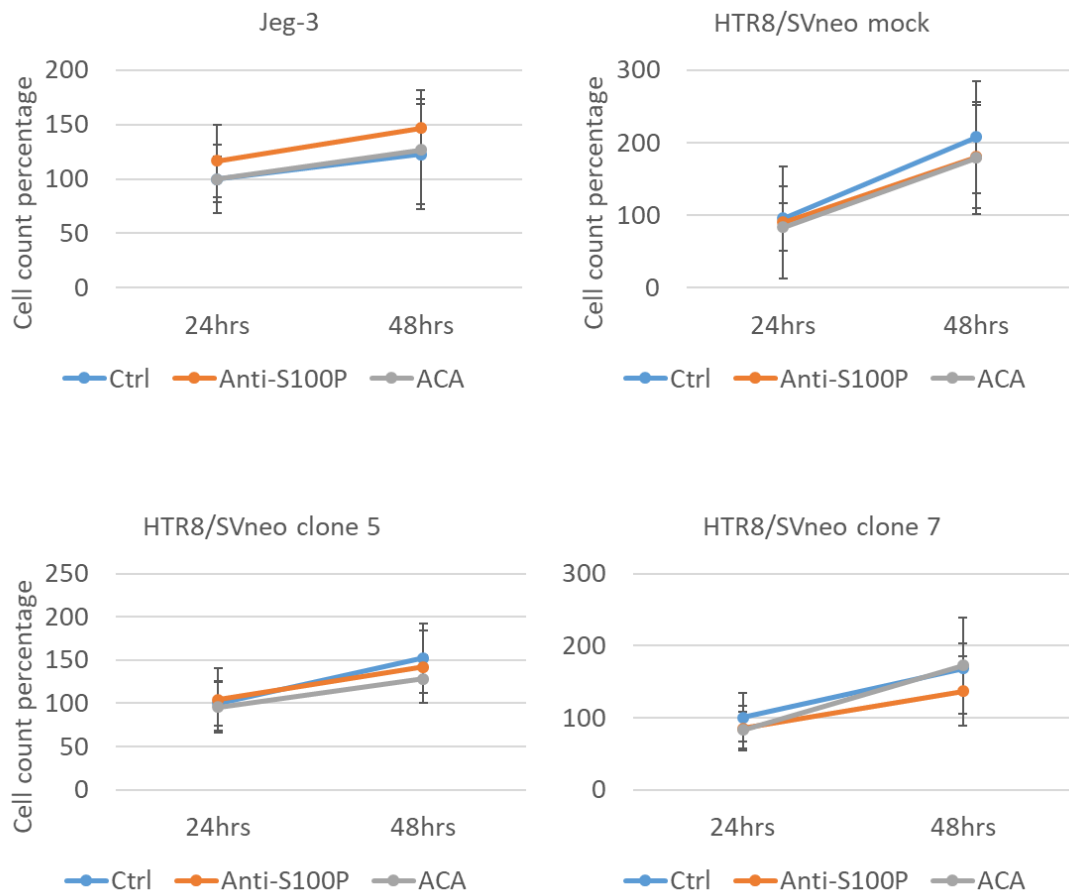


**Figure 3.20 S100P antibody and ACA do not affect the viability of trophoblast cell lines Jeg-3 and HTR8/SVneo clones 3, 5 and 7.** Jeg-3, HTR8/SVneo mock clone (SGB16) S100P-expressing clones 5 and 7 (SGB217) were seeded in 24-well plates, while being treated with anti-S100P, plasminogen inhibitor, or without any treatment as control. Their viability was tested during the next 24 and 48 hours. The error bars represent SD. N = 3. Total sample size for each condition: 36 (for Jeg-3) and 24 (for each HTR8/SVneo clone).

### **3.2.17.2. The role of S100P antibody and ACA on trophoblast motility**

To investigate whether S100P can regulate trophoblast motility, while being localised on the cell surface and/or being soluble extracellularly, trophoblast cell lines Jeg-3 and HTR8/SVneo mock clone (non-S100P-expressing control SGB16) and clones 5 and 7 (S100P-expressing SGB217) were serum starved for 24 hours, before collection and resuspension in serum starvation medium and seeding in transwells with either 0.4 µg/ml anti-S100P or 0.2% (v/v) goat serum, as negative control (S100P antibody was raised in goat). The cells were left to migrate for 24 hours, before fixing, staining and being counted. When compared with the non-treated control, S100P antibody reduced migration by 30% in Jeg-3 ( $P < 0.0001$ ) and by 20% in HTR8/SVneo clones 5 and 7 ( $P < 0.05$ ), while the mock clone was not significantly affected (Figure 3.21).

To test the involvement of plasminogen pathway in trophoblast migration, the same cells (Jeg-3 and HTR8/SVneo clones) were treated with 10 mM plasminogen inhibitor ACA and their migration was measured as stated above. When compared with the non-treated control, ACA reduced migration by 30% in Jeg-3 ( $P < 0.0001$ ), the non-S100P-expressing HTR8/SVneo mock clone ( $P < 0.01$ ) and the S100P-expressing HTR8/SVneo clones 5 and 7 ( $P < 0.01$  and  $P < 0.0001$ , respectively) (Figure 3.21).

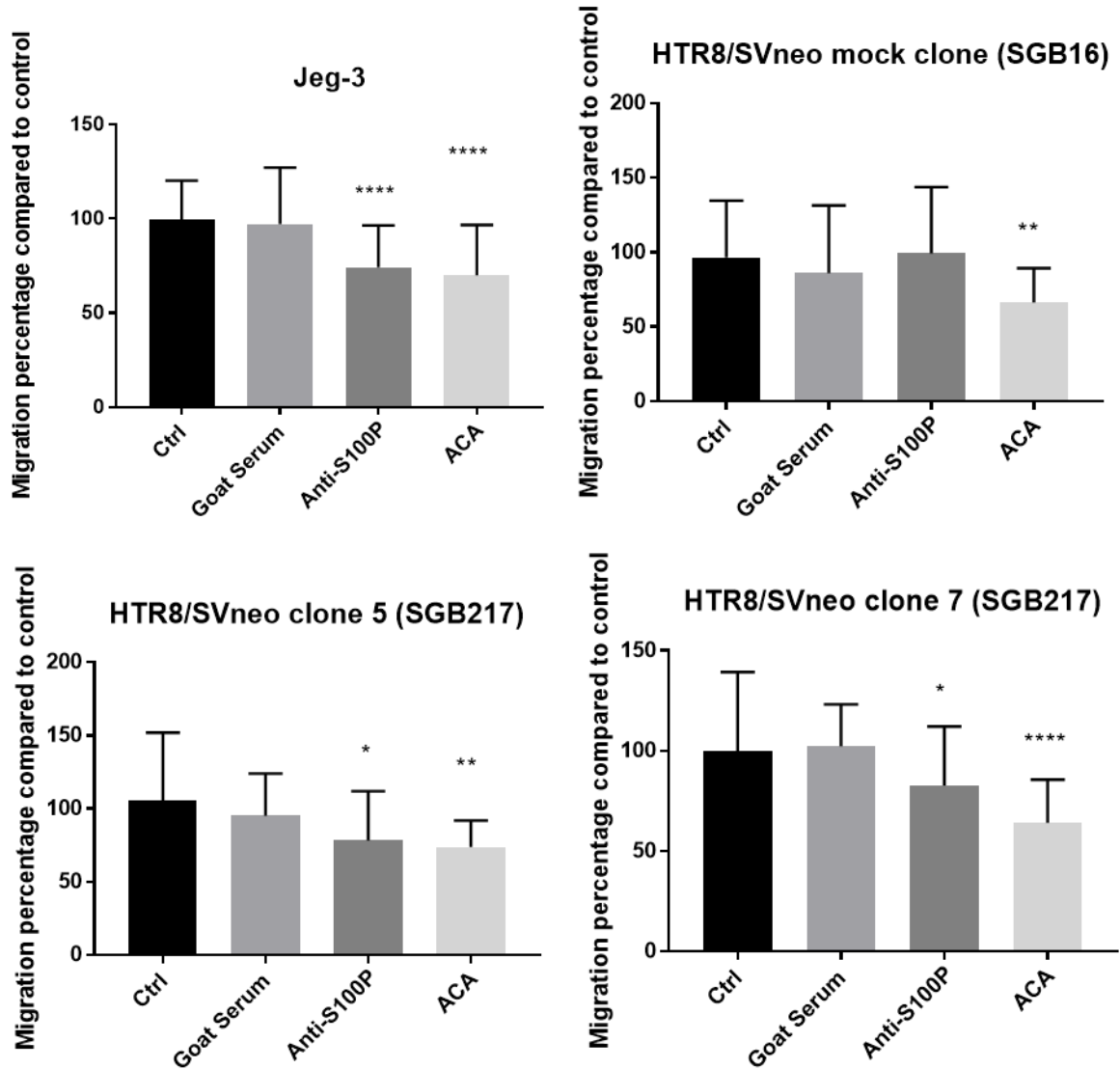


**Figure 3.21** The effect of S100P antibody and ACA on the migration of Jeg-3 and HTR8/SVneo clones Trophoblast-line Jeg-3, non-S100P-expressing HTR8/SVneo mock clone (SGB16), and S100P-expressing HTR8/SVneo clones 5 and 7 SGB217 were serum starved for 24 hours and then were collected and seeded in transwells (while the lower wells contained complete medium as chemoattractant), while being treated with S100P antibody, ACA, or goat serum (as negative control), along with non-treated control, for 24 hours prior to fixation, staining and counting. The error bars represent SEM (\* p<0.05, \*\* p<0.01, \*\*\* p<0.001, \*\*\*\* P<0.0001). N = 3 for each condition. Total sample size = 18 for each condition.

### **3.2.17.3. The role of S100P antibody and ACA on trophoblast invasion**

After showing the inhibitory effect of S100P antibody and ACA on migration in Jeg-3 and HTR8/SVneo trophoblast cells, we aimed to test their effect on trophoblast invasion. For this purpose, trophoblast cell lines Jeg-3 and HTR8/SVneo mock clone (non-S100P-expressing control SGB16) and clones 5 and 7 (S100P-expressing SGB217) were serum starved for 24 hours, before collection and resuspension in serum starvation medium and seeding in Matrigel-coated transwells with either 0.4 µg/ml anti-S100P or 0.2% (v/v) goat serum, as negative control (S100P antibody was raised in goat). The cells were left to invade for 24 hours, before fixing, staining and being counted. When compared with the non-treated control, S100P antibody reduced invasion by 50% in jeg-3 ( $P < 0.0001$ ) and by 20% in S100P-expressing HTR8/SVneo clones 5 and 7 ( $P < 0.05$  for clone 5 and  $P < 0.01$  for clone 7), while the mock clone was not significantly affected (Figure 3.22).

To test the involvement of plasminogen pathway in trophoblast invasion, the same cells (Jeg-3 and HTR8/SVneo clones) were treated with plasminogen inhibitor ACA and their invasiveness was measured as stated above. When compared with the non-treated control, ACA reduced invasion by 40% in Jeg-3 ( $P < 0.0001$ ), and by 30% in HTR8/SVneo clones 5 and 7 ( $P < 0.01$  for clone 5 and  $P < 0.0001$  for clone 7), while the mock clone was not significantly affected (Figure 3.22).

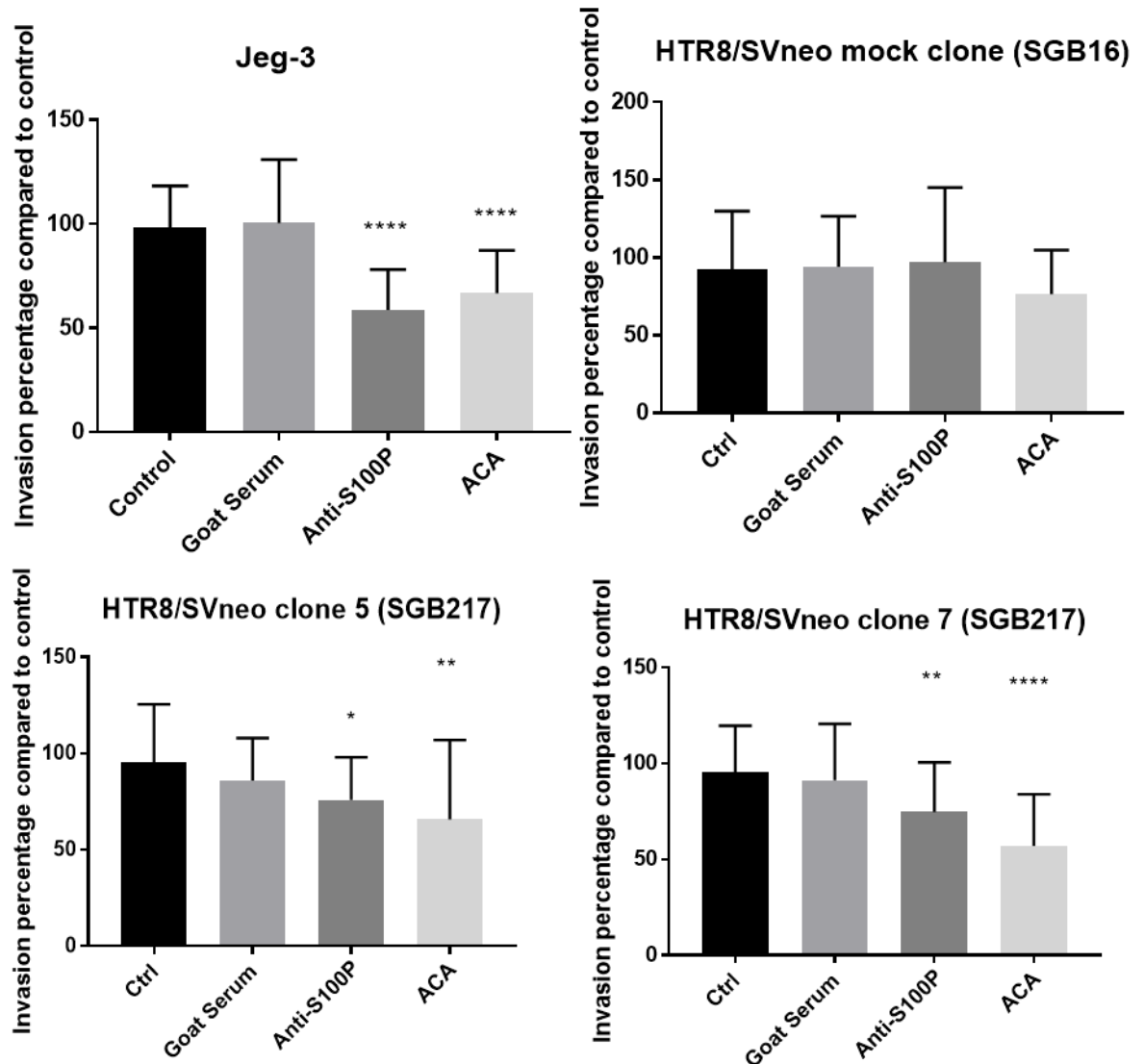


**Figure 3.22** The effect of S100P antibody and ACA on the invasion of Jeg-3 and HTR8/SVneo clones. Trophoblast-line Jeg-3, non-S100P-expressing HTR8/SVneo mock clone (SGB16), and S100P-expressing HTR8/SVneo clones 5 and 7 SGB217 were serum starved for 24 hours and then were collected and seeded in Matrigel-coated transwells (while the lower wells contained complete medium as chemoattractant), while being treated with S100P antibody, ACA, or goat serum (as negative control), along with non-treated control, for 24 hours prior to fixation, staining and counting. The bars represent SEM (\*  $p < 0.05$ , \*\*  $p < 0.01$ , \*\*\*  $p < 0.001$ , \*\*\*\*  $P < 0.0001$ ). N = 3 for each condition. Total sample size = 6 for each condition.

### 3.2.17.4. Extracellular S100P inhibition does not affect the focal adhesions

S100P knockdown in Jeg-3 cells has been shown increase the numbers and the size of FAs (Tabrizi et al. 2018). Here, we sought to test whether the extracellular S100P inhibition, which was shown to reduce trophoblast migration and invasion, also takes place with due to a similar effect on FA dynamics. For this aim, Jeg-3 cells were seeded on fibronectin-coated coverslips, while being treated with 0.4  $\mu\text{g/ml}$  anti-S100P antibody, goat serum as negative control, or without any treatment as control, and were left to grow for 24 hours, before fixing and permeabilisation. They were then incubated with 1% (v/v) primary anti-paxillin antibody and 0.5% (v/v) secondary antibody. The staining showed FAs formed on the cell surface, mostly along the actin bundles (Figure 3.23). There was no difference in the number or the relative size of the FAs (Table 3.2) in control and the anti-S100P treated cells (Figure 3.23).

	Percentage focal adhesions per cell $\pm$ SEM (n=8)	P value (compared with control)
Control	100 $\pm$ 11.17	N/A
Goat Serum	108.14 $\pm$ 9.27	0.72939
Anti-S100P	101.14 $\pm$ 8.33	0.9949

**Table 3.2 The average number of focal adhesions per cell in Jeg-3 cells, represented as percentages**

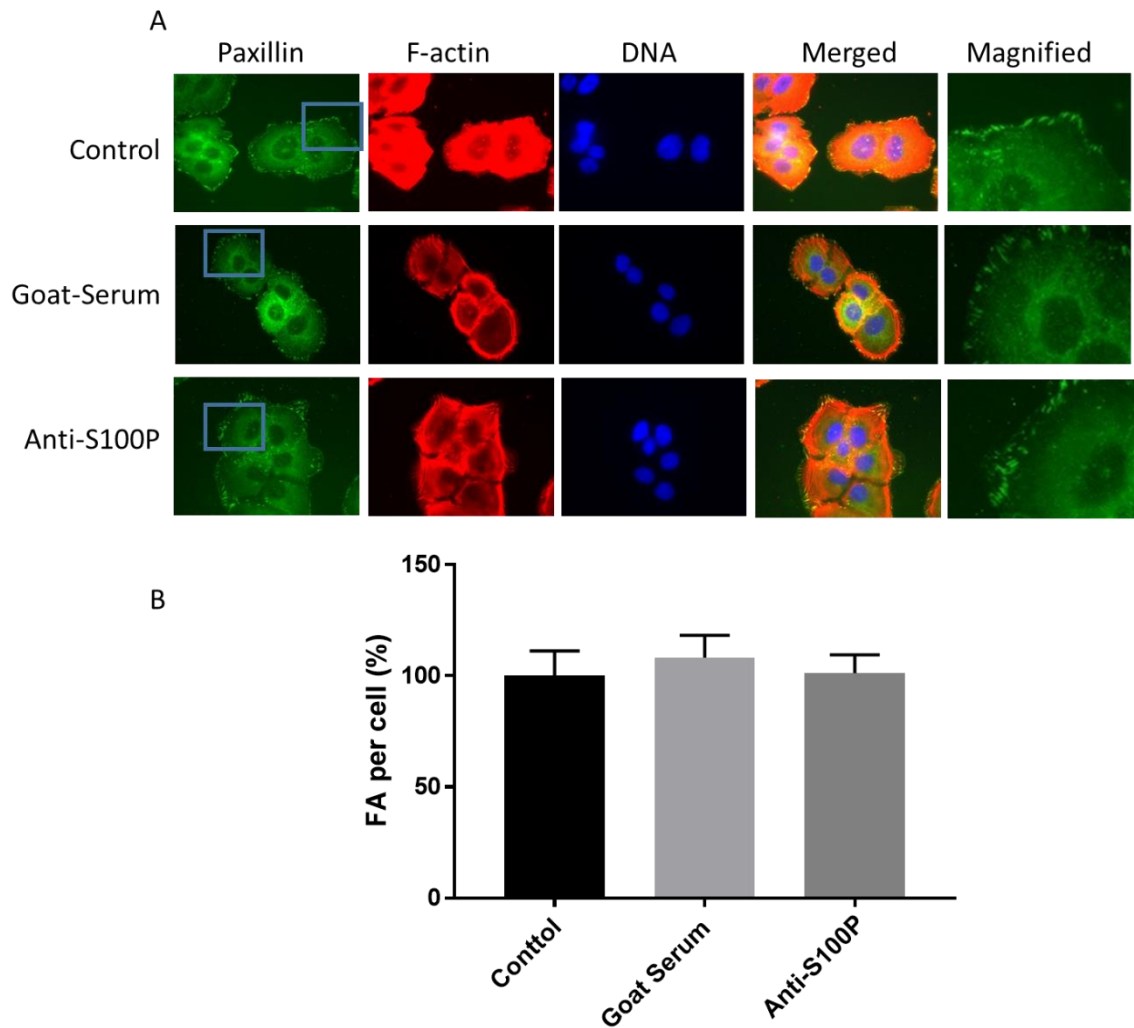


**Figure 3.23 Extracellular S100P inhibition does not affect focal adhesions in Jeg-3 cells.** Jeg-3 cells were seeded on fibronectin-coated coverslips, while being treated with anti-S100P antibody, goat serum or without any treatments as control. The FAs were visualised with immunofluorescence staining on paxillin, a marker of FAs, along with rhodamine phalloidin to stain F-Actin and DAPI to visualise DNA. The images were taken at 63x magnification (panel A). Panel B shows the average FA count per cell in each condition. The error bars represent standard SEM. N = 3. Total sample size for each condition: 13 (control), 18 (goat serum) and 20 (anti-S100P).

### **3.2.18. Primary EVT isolation**

S100P expression in human placenta was confirmed by IHC, showing strong expression of the protein in first trimester trophoblasts including in the EVTs. Endogenous S100P expression was also confirmed in our choriocarcinoma cell lines: Jeg-3 and BeWo, but to our surprise none of our EVT cell lines, HTR8/SVneo, SW71, SGHPL-4 and SGHPL-5, showed detectable levels of the protein.

To confirm S100P expression in human EVTs, even after they have been isolated from their surrounding placenta tissues, primary EVT cells were prepared from placenta samples with 12 weeks of gestation age, collected by elective termination of pregnancy. The placenta samples were brought to the lab and the villi were scrapped off and digested with trypsin, and the EVTs were separated from the other cell populations, using lymphocyte separation medium. The isolated EVTs were cultured on fibronectin-coated plates and were left to attach overnight (Figure 3.24). The cultured EVTs look slightly elongated, with some EVTs looking more elongated than others.

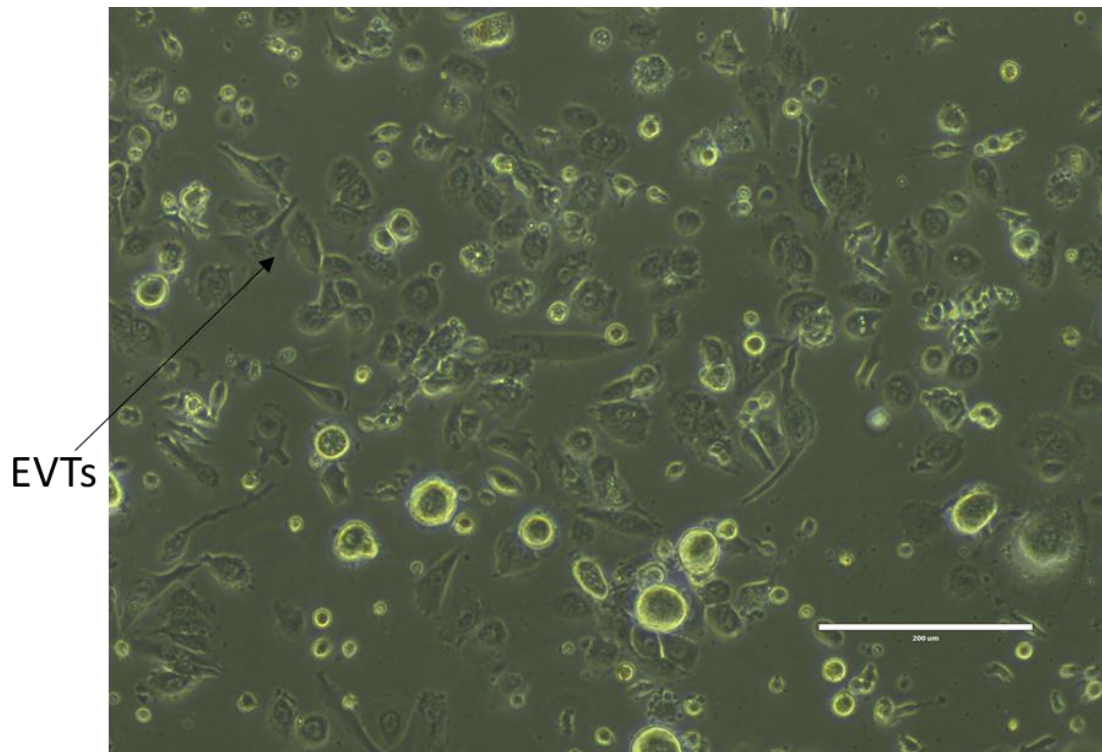


**Figure 3.24 Primary EVT culture.** Primary EVTs were isolated from first trimester placenta samples and cultured on fibronectin-coated coverslips. The image was taken at 40x magnification

### **3.2.18.1. HLA-G expression in primary EVT**

To confirm that the isolated cells are EVTs, the cells were seeded on fibronectin-coated dishes. On the next day, the EVTs were collected and seeded on fibronectin-coated coverslips and were left to attach for 24 hours, prior to fixation and permeabilisation and eventually stained for HLA-G (EVT marker), F-actin and DNA. HLA-G expression was detected in about 80% of the cells (Figure 3.25).

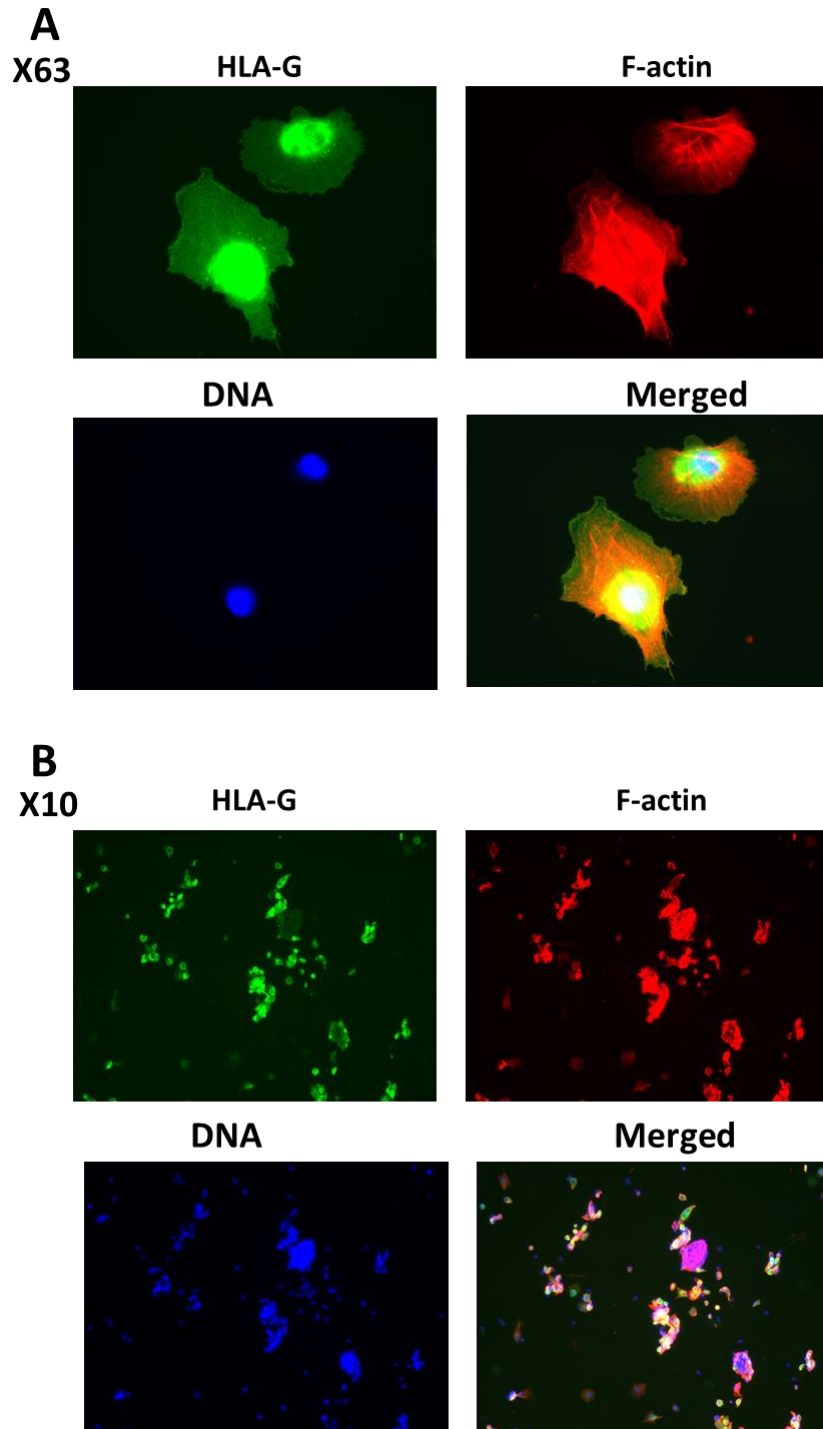


**Figure 3.25 HLA-G staining in primary EVT.** Primary EVT were fixed, permeabilised and stained for HLA-G, F-actin and DNA. Panel A shows HLA-G staining on EVT at 63x magnification. Panel B shows the cells at 10x magnification.

### **3.2.18.2. S100P is expressed in primary EVT<sub>s</sub>**

To confirm S100P expression in primary EVT<sub>s</sub>, the cells were probed for the protein by western blot. For this purpose, the primary EVT<sub>s</sub> were collected a day after their isolation and the cell lysate was prepared in protease inhibitor cocktail and sonicated. The cell lysate was loaded on 16% tricine gel along with HTR8/SVneo clone 7, as positive control, and the blot was probed for S100P and  $\alpha$ -tubulin. Both HTR8/SVneo clone 7 and the EVT<sub>s</sub> showed S100P expression, with EVT<sub>s</sub> expressing 30 times higher than the clone (Figure 3.26).

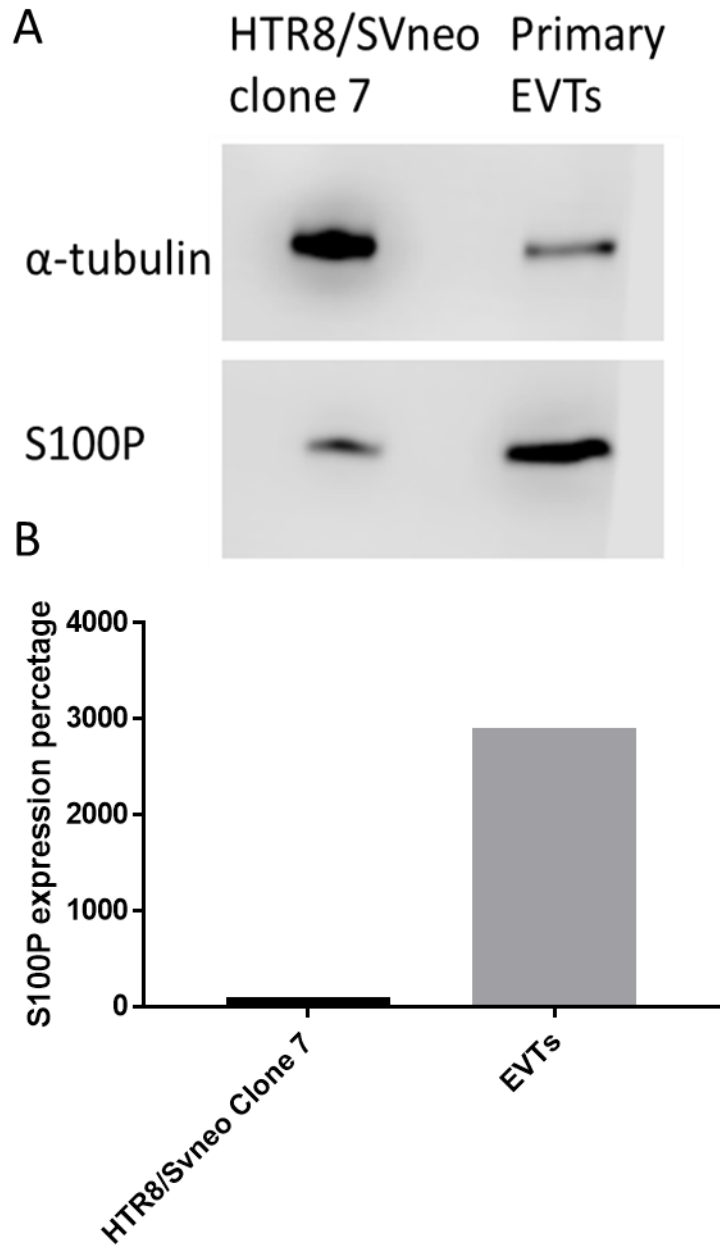


**Figure 3.26 S100P expression was detected in primary EVT<sub>s</sub>.** EVT cells were collected, lysed and separated by 16% SDS-PAGE and S100P and  $\alpha$ -tubulin were detected by western blot (A), and the expression levels of S100P were normalised to  $\alpha$ -tubulin levels (B). N = 1. Sample size = 1 for each cell type.

### 3.3. Discussion

Over-expression and ectopic expression of S100P protein has been well-documented in a variety of malignancies, making it a potential tumour marker (Parkkila et al. 2008). S100P has been shown to regulate cellular behaviours such as, proliferation (Arumugam et al. 2004; Guo et al. 2014; Kim et al. 2009), motility (Austermann et al. 2008; Du et al. 2012; Hsu et al. 2015) and invasion (Mercado-Pimentel et al. 2015; Whiteman et al. 2007). In a more physiological context, its expression also has been associated with receptivity and decidualisation of the endometrium, an important contributor to successful embryo implantation (Zhang et al. 2012). However, there does not seem to be a clear definition for the role of S100P with regards to the organ of its origin, placenta, where it also shows the highest expression levels compared with any other organ (Becker et al. 1992; Emoto et al. 1992) and was therefore part of this section of the research project.

Through our work, and making use of different human placental samples available such as embedded parafilm sections, we demonstrated that S100P protein expression is at its highest levels during the first trimester (Figure 3.2). At this stage, most trophoblast invasion and placenta development takes place (Caniggia et al. 2000), reducing gradually along the second and then the third trimesters, as demonstrated both by staining intensities of the DAB signal as well as following protein level determination with western blotting on samples from different stages of gestation (Tabrizi et al. 2018).

In an effort to learn more about the localisation of the protein in cells, as well as further understanding about cell types that express it, in the context of placental samples, further analysis was carried out using IHC along with other trophoblast markers such as HLA-G and cytokeratin-7 (Figure 3.3). Previously, S100P was shown to be localised within the trophoblast cytoplasm and nuclei (Zhu et al. 2015). Similarly, in this work, we detected the protein within the cytoplasm of the first trimester cyto- and syncytiotrophoblasts as well as EVT, with occasional nuclear localisation in the last two (Figure 3.3). It has been suggested previously that trophoblasts might gain the ability to transport S100P into the nucleus, along their differentiation (Zhu et al. 2015). Interestingly, we also detected a strong signal in the apical membrane of the syncytiotrophoblasts and the EVTs, but not the cytotrophoblasts (Figure 3.3).

Having demonstrated the high expression levels of S100P in trophoblast cells in human placental sections, we next wanted to establish cell culture models of trophoblast to further analyse the role of S100P. A number of cell lines were obtained (Jeg-3, BeWo, HTR8/SVneo, SW71, SGHPL-4 and SGHPL-5) and the levels of S100P expression was determined using western blotting

techniques (Figure 3.4) and mRNA amplification (Tabrizi et al. 2018). We showed S100P expression in the choriocarcinoma cell lines Jeg-3 and BeWo. To our surprise, none of our first trimester trophoblast cell lines i.e. HTR8/SVneo, SW71, SGHPL-4 and SGHPL-5, expressed detectable levels of the protein (Figure 3.4), whilst isolated primary first trimester EVT<sub>s</sub> demonstrated high levels of S100P expression (Figure 3.26). This brought us to the question of why none of our EVT cell lines showed detectable amounts of S100P. Changes in gene expression could happen at different stages and be due to protein stability, changes in mRNA levels, translation regulation or epigenetic modifications (Arcondeguy et al. 2013), all of which are possible mechanisms that could be regulated in these cells to prevent/reduce S100P expression. For instance we know that trophoblast phenotypes are associated with their microenvironment (Staun-Ram & Shalev 2005; Toro et al. 2014). As such, the presence of fibronectin in the trophoblast microenvironment has been shown to enhance their invasive capabilities, through interacting with integrin- $\alpha$ 5 (Zeng et al. 2007). Matrigel, a gelatinous protein mixture secreted by mouse sarcoma cells, and mimics the ECM in the basement membrane, has been shown to have a similar effect on trophoblast invasiveness by modifying their protease expression pattern (Tarrade et al. 2002; Toro et al. 2014). Serum starvation has also been shown to affect the protein expression profile (both structural proteins and enzymes) in HTR8/SVneo cell lines (Novoa-Herran et al. 2016) and hypoxia has been shown to affect trophoblast differentiation, metabolism and invasion (Esterman et al. 1997; Rosario, Konno & Soares 2008; Wakeland et al. 2017). It is unclear at this stage whether any of these regulations seen for other proteins may equally be linked to S100P expression. Further work was therefore carried out to establish whether cells incubated with different matrices would show changes in S100P expression. We showed that growing Jeg-3 cells on fibronectin and gelatine increased S100P expression, while growing them on Matrigel reduced S100P expression. None of these changes induced S100P expression in non-S100P-expressing EVT cell lines (Figure 3.5). However, we cannot rule out the possibility of S100P expression induction in these cells, provided that they are grown in an alternative microenvironment for a longer period of time. Likewise, a study reported the time-dependence of S100P expression levels in the presence of prostaglandin E<sub>2</sub> (Chandramouli et al. 2010). Moreover, S100P expression been reported to be upregulated in response to stimulation with non-steroidal anti-inflammatory drugs (Namba et al. 2009) and prostaglandin E<sub>2</sub> (Chandramouli et al. 2010), but downregulated in response to androgen deprivation (Averboukh et al. 1996).

Similar to other studies (L. Dong et al. 2016; Gong et al. 2017; C.-C. Wu et al. 2018; L. Wu et al. 2018), this work showed that Jeg-3, BeWo and HTR8/SVneo cell lines are appropriate model systems to use to study trophoblast migration and invasion. We set about to see if modulating expression of S100P could be achieved in such cell systems. For the loss of function experiments,

siRNA delivery was found to be an effective method to knockdown S100P (Figure 3.6 and Figure 3.16) with all cells tested and siRNA sequences used. It is interesting to note that although all siRNA sequences that we used were able to reduce S100P expression, there were cell-specific differences in their efficacies. SiRNA 4 and siRNA 6 were found to induce the highest level of expression downregulation in Jeg-3 and BeWo (Figure 3.6), while siRNA 4 and 5 were the most efficient in S100P-expressing HTR8/SVneo clones (Figure 3.16). SiRNA gene regulation was reported to be a reliable method at the concentration that was used in this study (5 nM), as its administration at <20 nM was reported to eliminate non-specific responses (Semizarov et al. 2003). However, there is always a chance of unwanted siRNA interactions with proteins (aptameric effect), which could potentially reduce its availability and therefore result in silencing its effect (Brukner & Tremblay 2000). Therefore, variations in the effectiveness of different siRNA sequences targeting different areas of the same gene might be a cell specific phenomenon, due to the complex nature of protein content in each cell type.

We were able to significantly reduce both the motile (Figure 3.9) and invasive (Figure 3.10) properties of Jeg-3 and BeWo choriocarcinoma cell lines, by S100P knockdown, using siRNA delivery. Whilst this is the first time such an observation has been made in the context of trophoblast cells, short-term (siRNA delivery) (Arumugam et al. 2005; Liu et al. 2017) and long-term (lentiviral vector-mediated RNA interference) (Jiang et al. 2011) post-transcriptional S100P gene silencing methods have been reported to induce similar effects on tumour cell motility and invasion.

Through gain of function experiments, we were successful in obtaining permanent transfection of HTR8/SVneo cells with a S100P expressing plasmid, and interestingly showed that S100P expression at levels similar to S100P levels in Jeg-3 cells correlated with an increase in the motile (Figure 1.12) and invasive (Figure 3.13) features of the cells. S100P expression levels lower than jeg-3 did not affect invasion and migration. Higher S100P expression levels than Jeg-3 did not affect migration but significantly reduced invasion in HTR8/SVneo clones.

In an effort to further characterise the possible molecular pathways leading to such changes in migration, we investigated possible changes in cell adhesion to the ECM, through FA dynamics. FAs are multi-protein complexes that are recruited the cytoplasmic part of the clustered integrins (attaching the cell to the ECM) (Petit & Thiery 2000). FA-associated adaptor proteins such as paxillin and vinculin, link the protein complex to the actin cytoskeleton and provide the cell with the tension required for traction and morphological alterations necessary for cell movement, while signalling protein, recruited to FAs, such as focal adhesion kinase, transmit the signals from the ECM into the cell and regulate pathways such as cell migration and proliferation (Nagano et al.

2012). In general, during direction cell migration, rapid formation and turnover of the FAs, seen at the leading edge of the cells, pulls the cell body forward, while their rapid turnover at the rear end makes the detachment from the ECM possible. In contrast, stationary cells, which are strongly attached to the ECM, show a higher ratio of FA formation relative to turnover (Nagano et al. 2012).

We showed that the increase in HTR8/SVneo migration, upon S100P expression, was linked with a decrease in the number and the relative size of paxillin-containing, actin-terminating FAs (Figure 3.14). This could indicate the rapid turnover and formation of the FAs in the S100P-expressing clones, while the larger and more mature FAs seen in non-S100P expressing control clone indicates their relative stationary state. This goes in line with the previously reported S100P knockdown-induced increase in the size and number of FAs in trophoblasts (Tabrizi 2014) and cancer cells (Du et al. 2012).

The S100P-induced increase in the migration and invasiveness of HTR8/SVneo clones was reversible upon S100P knockdown (Figure 3.18) and brought migration and invasion levels of the S100P-expressing HTR8/SVneo clones down to similar levels as the mock clone, confirming the role of S100P, alone, in the induction of such phenotypical changes, rather than another mutation that might have taken place during cloning.

To rule out the possibility of increased cell proliferation affecting our migration and invasion assays, cell viability assays were performed on HTR8/SVneo clones with and without S100P expression (Figure 3.15) and revealed the ineffectiveness of S100P expression on the viability of trophoblasts. Similarly, we showed the ineffectiveness of S100P knockdown on the viability of trophoblasts with both endogenous (Tabrizi et al. 2018) and exogenous S100P expression (Figure 3.17). In cancer cells however, while many reports have shown the ineffectiveness of S100P expression on cell viability (Barry et al. 2013; Du et al. 2012; Hsu et al. 2015), others have indicated otherwise (Arumugam et al. 2004, 2005; Guo et al. 2014; Liu et al. 2017).

Other than affecting trophoblast migration and invasion, through regression analysis, we demonstrated that there is a strong correlation between S100P expression levels and trophoblast migration and trophoblast invasion (Figure 3.19). The correlation was significant for migration and invasion in Jeg-3, and invasion in HTR8/SVneo clones. This new finding, which is to our knowledge, the first in its kind, not only in trophoblast cell lines but indeed in any other cells, highlights a proportionality between S100P levels and motile/invasive features.

Having demonstrated that S100P is an overall regulator of migration and invasion in Jeg-3, BeWo and HTR8/SVneo cells, we next wanted to understand more about the mechanisms involved and how this protein regulates these behaviours. As stated earlier, a high percentage of S100P expression was detected within the apical membrane of syncytiotrophoblasts and the EVT's (Figure 3.3). However, there has been no direct evidence of S100P expression on the trophoblast cell surface. To this end, Jeg-3 cells with endogenous and HTR8/SVneo clones 5 and 7 with exogenous S100P expression were treated with S100P antibody. This resulted in a significant reduction in their migration (Figure 3.21) and invasion (Figure 3.22), while no effect was seen on the motility (Figure 3.21) and invasion (Figure 3.22) of the control non-S100P-expressing HTR8/SVneo clone. This observation validates the importance of extracellularly-localised (either secretory or membrane-bound) S100P in regulating trophoblast motility and invasion, which is in line with the reported possibility of the extracellular localisation of S100P in cancer (Arumugam et al. 2004; Mercado-Pimentel et al. 2015). Furthermore, we equally showed that addition of ACA, which is an analogue of the amino acid lysine and an inhibitor of the plasmin/plasminogen cascade, equally resulted in a similar reduction in both trophoblast motility (Figure 3.21) and invasion (Figure 3.22) in S100P-expressing trophoblast cell lines (Jeg-3 and HTR8/SVneo clones 5 and 7), similar to the reduction levels seen with S100P antibody treatment. ACA also reduced the motility of our non-S100P expressing mock clone (Figure 3.21), while showed no effect on its invasion (Figure 3.22). The ACA-induced reduction in the motility of both S100P-expressing and non-S100P expressing HTR8/SVneo cells indicates that the plasmin/plasminogen cascade regulates trophoblast motility, at least partially, in a S100P-independent manner, while the effectiveness of the drug on the invasion of S100P-expressing cells along with its ineffectiveness on non-S100P-expressing cell invasion, confirms the importance S100P in plasmin-induced trophoblast invasion.

The interaction of plasmin with integrin  $\alpha 5\beta 3$  (vitronectin receptor) has been shown to promote stress fibre formation and migration (Tarui et al. 2002). Although no reports have shown the interaction between S100 proteins and these two integrin subunits so far, S100P has been shown to bind to integrin  $\alpha 7$  (Hsu et al. 2015). Plasmin has been shown to promote invasion by degrading ECM components, directly and indirectly by activating the MMPs (Lijnen et al. 1998) and urokinase-type plasminogen activator (uPA) has been shown to regulate trophoblast motility and invasion (Liu et al. 2015). Annexin II, which induces plasminogen activation, binds to S100 proteins, including S100P (Hajjar & Krishnan 1999; Liu, Myrvang & Dekker 2015). The S100P amino acid sequence includes a lysine residue at its C-terminus, which has the potential to bind to the lysine-binding site of the plasmin. Based on the mentioned reports, we propose a novel mechanism for S100P-induced invasiveness and possibility motility in trophoblasts, which

includes a potential interaction between surface S100P and plasmin/PAs. Indeed, S100P, similar to other S100 proteins (S100A4 and S100A1) was shown to induce invasion via activating the above stated pathway through interacting with plasminogen and tPA as well as stimulating tPA in cancer cells (Clarke et al. 2017; Kwon et al. 2005; Semov et al. 2005).

Extracellular S100P, however, might not be regulating trophoblast motility and invasion via the same pathway as the total pool. Unlike the effect of changing expression in HTR8/SVneo, BeWo and Jeg-3 (Tabrizi et al. 2018), here S100P antibody treatment showed no effect on either the relative size or the number of FAs in Jeg-3 cells. Moreover, despite showing the role of extracellular and/or membrane-bound S100P in trophoblast motility and invasion, we still are not sure how this transport to the outside takes place. Submitting the S100P amino acid sequence (FASTA format) to the Phobius, a transmembrane topology and signal peptide predictor at <http://phobius.sbc.su.se/> showed zero chance of the existence of a signal peptide in the protein. This however, does not rule out the possibility of S100P secretion by non-classical secretion pathways, which do not involve ER-to-Golgi transport, such as transport via membrane pores or ABC transporters, or the ability of transmembrane proteins to reach the membrane via by-passing the Golgi (Kim, Gee & Lee 2018).

In conclusion, we report that due to its expression pattern in placental villi throughout the gestation period and its role in trophoblast motility and invasion, S100P might potentially play an important role in early placenta development and implantation.

## Chapter 4.

# Ezrin regulates trophoblast motility and invasion

## 4.1. Introduction

Ezrin is a member of the ERM protein family, mainly located at cellular protrusions such as microvilli and under the membrane. Ezrin links the plasma membrane to the cytoskeleton, and regulates cell morphology, polarity, cytokinesis and motility (Fehon, McClatchey & Bretscher 2010; Tsukita, Yonemura & Tsukita 1997). The majority of the work done on ezrin relates to its function in pathological conditions; consequently, ezrin has been implicated in various human cancers as its over-expression in malignant melanoma and sarcomas has been linked with metastasis and poor survival (Ilmonen et al. 2005; Khanna et al. 2004) and its under-expression has been linked with poor survival in patients with ovarian cancer (Moilanen et al. 2003). In the physiological context, ezrin is highly expressed in the immune system (Pore & Gupta 2015), gastrointestinal (Casaletto et al. 2011) and urinary tract (Andersson et al. 2014). During the early stages of human embryonic and foetal development, ezrin shows tissue and time specificity in its expression: it is first detected in the neural tube at 4 weeks of gestation, and it is highly expressed in the nerve cells of the neural tube. In later stages of gestation, it is undetectable in the derivative tissues such as cerebral tissue as well as in adult nervous tissue (Woods, Perez-Garcia & Hemberger 2018). In the endometrium, ezrin expression has been reported in the glandular cells and microvilli of non-pregnant endometrium in both human and cow, mostly localised at apical cell poles and intercellular borders of the epithelium, and at lower levels in the epithelial cytosol as well as the stroma (Haeger et al. 2015; Tan et al. 2012), reaching at its highest levels during the secretory phase of the endometrium (around day 21 of a 28-day cycle, where it reaches the maximum thickness) (Tan et al. 2012). In bovine gestation, there is a reduction in endometrial ezrin in the early stages of the pregnancy, with minimal levels at around day 20 of the of the total 283 gestation days and a complete depletion of cytosol and stromal ezrin, followed by a consequent increase back to normal levels after gestational day 35, when implantation occurs (Haeger et al. 2015).

In human placenta, ezrin is highly concentrated at the plasma membrane of the microvilli of epithelial cells, especially in syncytiotrophoblasts (Berryman, Franck & Bretscher 1993; Pidoux et al. 2014). It has been suggested that the protein plays a role in the fusion of cytotrophoblasts into syncytiotrophoblast as well as formation of gap junctions (Firth, Farr & Bauman 1980; Pidoux et al. 2014). In rat placenta, ezrin is localized at the apical membrane of the trophoblasts and its expression increases during pregnancy, peaking at days 14-18 of the total of 21 gestational days, and then gradually decreases afterwards, thus correlating with the morphogenesis of the placental villi (Higuchi et al. 2010). In mouse, ezrin has been found in the trophoblasts of activated blastocysts at higher intensity in implantation-competent than in dormant blastocysts.

In dormant blastocysts the metabolism is naturally reduced, awaiting stimuli from the uterus for further development and subsequent implantation (Matsumoto et al. 2004).

The true functions of ezrin in cellular behaviours are not clear, but its ability to interact with the membrane and the actin cytoskeleton have linked it to cellular motility. Ezrin has been found to localise at the leading edge of cells where it controls actin polymerisation (Arpin et al. 2011). Ezrin may also play a role in invasion, through regulating MMP expression (Jiang, Wang & Chen 2014; Tang et al. 2019), and therefore can promote metastasis (Hunter 2004). The mechanism by which ezrin regulates cellular motility and invasion remains unclear and the possible functions of the protein in regulating these cellular processes in a non-pathological context are not known. As before, we set about to determine whether ezrin, a known metastasis inducing protein, has any roles in trophoblast motility and invasion, two of the main processes involved in embryo implantation, based on evidence that it is expressed during the early stages of placental formation (Berryman, Franck & Bretscher 1993; Pidoux et al. 2014).

## **Aim**

To study the role of ezrin in trophoblast motility and invasion.

## **Objectives**

- Establish ezrin expression in human placental samples at different stages of gestation
- Establish ezrin expression in trophoblast cell lines
- To regulate ezrin expression and activity by:
  - 1) Testing whether modulating ezrin expression affects trophoblast motility and invasion
  - 2) Testing whether ezrin inhibition affects trophoblast motility and invasion
- To decipher the molecular mechanisms for the enhancement of motility and invasion by ezrin in trophoblasts

## **4.2. Results**

### **4.2.1. Immunohistochemical staining optimisation**

Having shown, in the previous chapter, that S100P expression is important for trophoblast motility/invasion and that its levels can be clearly seen to decrease in human placenta during gestation, we aimed to follow a similar approach in relation to ezrin, another known metastatic-associated protein with no real physiological functions and establish its expression in human placenta. We sought to first gain more information about both the localisation and expression levels of ezrin in samples of first, second and third trimester human placental villi.

Optimisation for the use of the primary antibody against ezrin was first carried out, to find the lowest concentration of anti-ezrin antibody. For this aim, wax-embedded human placenta sections from first trimester human placenta villi were prepared and incubation with 10 µg/ml and 5 µg/ml anti-ezrin overnight, along with mouse IgG as negative control, followed by secondary antibody incubation and development using avidin-biotin complex and DAB chromogen. The sections were counter stained with haematoxylin before viewing.

Both concentrations showed efficient staining for ezrin, which was localised within the trophoblasts, the cells that surround the villi, being highly detectable in the outer membrane of the syncytiotrophoblasts and to a lesser extent within the cytoplasm of cyto- and syncytiotrophoblasts, with weak staining detectable in some parts of the stroma, located at the core of the villi (Figure 4.1).

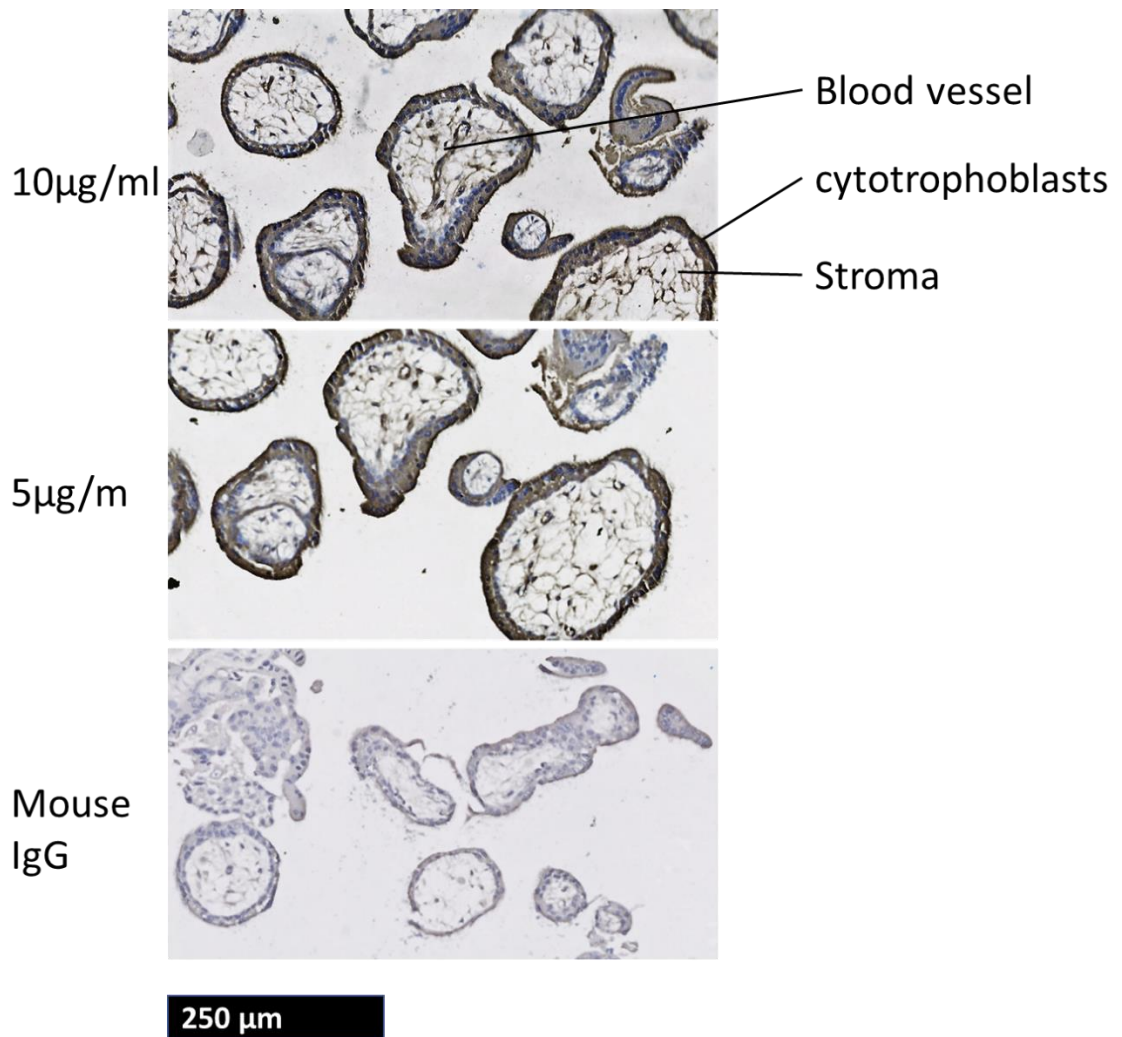


**Figure 4.1 Primary ezrin antibody concentration optimisation for IHC.** Wax-embedded human first trimester placental villi sections were prepared and incubated with two concentrations of primary anti-ezrin, before being incubated with secondary antibody, and finally staining using avidin-biotin complex and DAB chromogen and counter-staining using haematoxylin.

#### **4.2.2. Placental ezrin expression decreases gradually during gestation**

Having optimised staining for ezrin, we then wanted to determine how ezrin levels were affected during gestation as well as its localisation during placental development. To this end, three samples from first trimester, three from second trimester and four from third trimester placenta samples were stained for ezrin as detailed earlier. Images were analysed by densitometry using Fiji-ImageJ software. The staining showed that during the first trimester, ezrin expression can be detected in the cytoplasm of cytotrophoblasts, very intensely in the apical membrane of syncytiotrophoblasts, and to a lesser extent in the cytoplasm of syncytiotrophoblasts (Figure 4.2B). The expression of ezrin in the first and the second trimesters was not significantly different ( $P>0.05$ ). Ezrin expression during the third trimester, however, was 50 lower than the first and second trimesters ( $P<0.001$ ). (Figure 4.2 A and C).

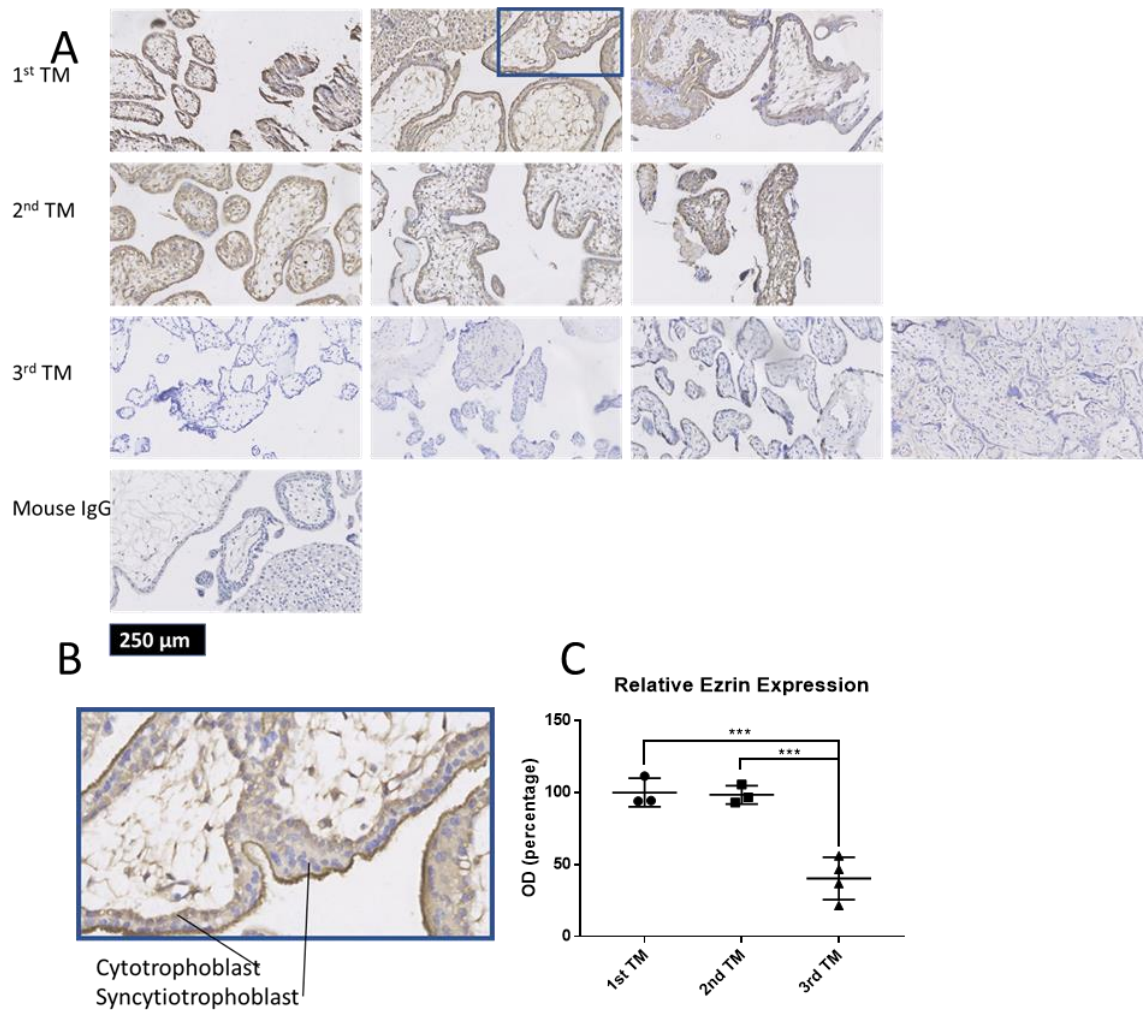


**Figure 4.2 Ezrin expression in human placenta is the highest during the first and second trimesters of gestation.** Wax-embedded human first trimester placental villi sections were prepared and incubated with anti-ezrin antibody, before being incubated with secondary antibody, and finally staining using avidin-biotin complex and DAB chromogen and counter-staining using haematoxylin. Panel A shows representative images of human placental sections from first and second and third trimesters, panel B shows a magnified image of one of the first trimester placenta sections, and panel C shows the average ezrin expression (calculated by densitometry) in different samples. The error bars represent SD. (\*\*\*)  $P < 0.001$ .  $N = 2$ . Total sample size for each trimester: 6 (1<sup>st</sup>), 6 (2<sup>nd</sup>) and 8 (3<sup>rd</sup>).

### 4.2.3. Ezrin is expressed in human trophoblasts and EVTs

Having shown that expression of ezrin in placenta is highest in the earlier stages of placental development, we wanted to learn more about its localisation and where it is expressed in first

trimester samples using markers for trophoblasts (cytokeratin 7) and more specifically to identify EVT<sub>s</sub> (HLA-G). Serial sections of wax-embedded first trimester human placental villi were prepared and incubation with the following primary antibodies: anti-ezrin, anti-S100P, anti-cytokeratin 7, anti-HLA-G or mouse and rabbit IgGs (as negative control), prior to secondary antibody incubation and development using avidin-biotin complex and DAB chromogen. The sections were counter-stained with haematoxylin. Following staining, ezrin was shown to colocalise with cytokeratin-7 as well as S100P in cyto- and syncytiotrophoblasts as well as EVT<sub>s</sub>. It colocalised with HLA-G in the cytoplasm and the apical membrane of a sub-population of the trophoblasts (EVT<sub>s</sub>) located in trophoblastic columns (Figure 4.3).

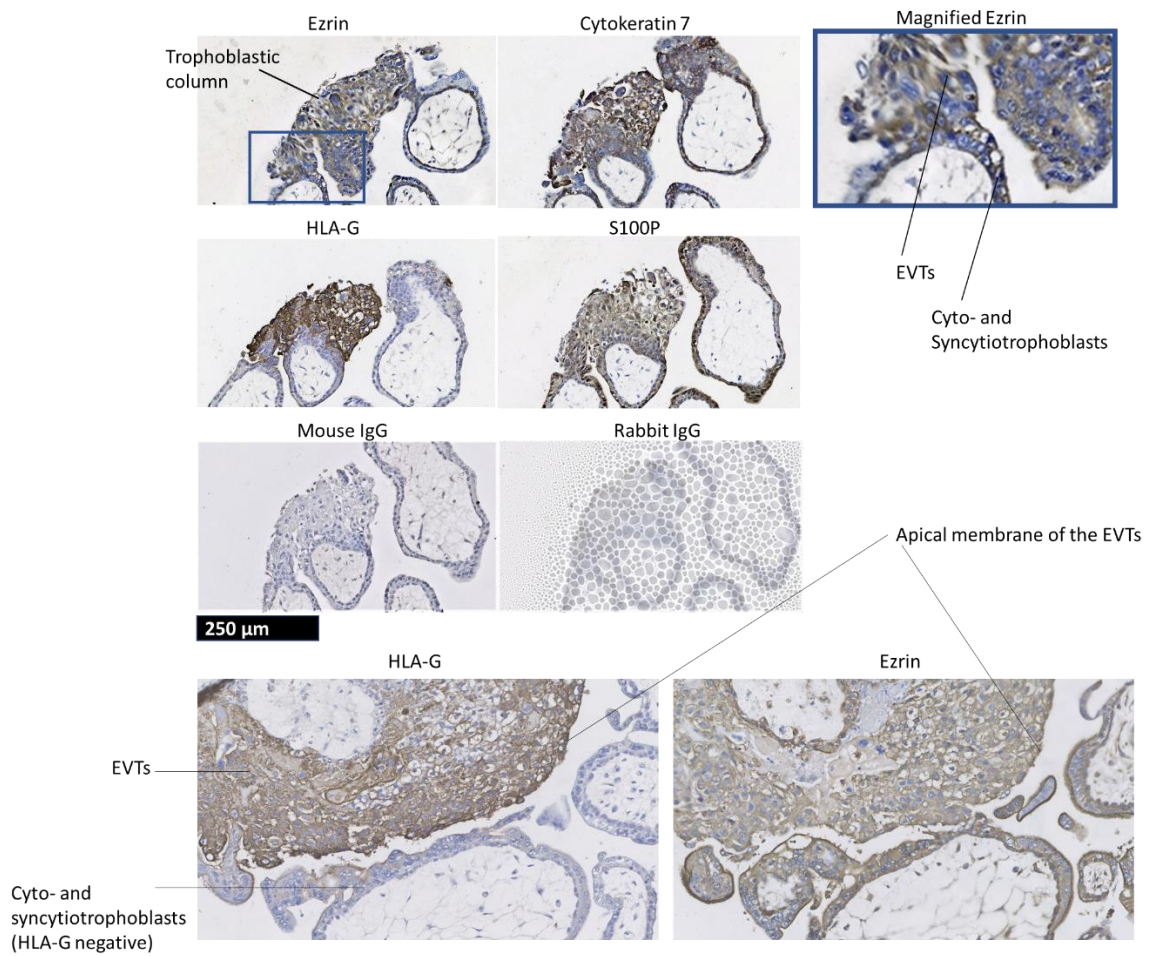


**Figure 4.3 Ezrin expression in human trophoblasts and EVTs.** Serial sections of wax-embedded human first trimester placental villi were prepared and incubated with primary anti-ezrin, anti-cytokeratin 7, anti-HLA-G, and anti-S100P, as well as mouse and rabbit IgGs as negative controls, before being incubated with secondary antibodies, and finally staining using avidin-biotin complex and DAB chromogen and counters-staining using haematoxylin. The images were taken at 20x magnification.

#### 4.2.4. Ezrin is expressed in human trophoblast cell lines

Having demonstrated ezrin expression in human placenta and more specifically in trophoblast and EVT<sub>s</sub>, we aimed to investigate whether ezrin could also be detected in trophoblast cell lines. We sought to investigate the levels of ezrin expression in trophoblast cell lines, i.e. Jeg-3 and BeWo, as well as a series of human first trimester EVT cell lines SW71, HTR8/SVneo, SGHPL-4 and SGHPL-5. Cell lysates were loaded on 10% polyacrylamide gel. Ezrin, phospho-ezrin (the active form of ezrin) and  $\alpha$ -tubulin bands were detected by western blot and ezrin signals were normalised to the housekeeping gene expression.

Ezrin was found to be highly expressed in the human trophoblast cell lines: Jeg-3, BeWo, HTR8/SVneo, SW71, SGHPL-4 and SGHPL-5. Protein levels were seen to be relatively harmonious across all cells, with Jeg-3 cells expressing 50% higher levels ( $P > 0.05$ ) of the protein compared with the others (Figure 4.4). Phospho-ezrin showed a different expression pattern amongst the cell lines: BeWo, Jeg-3 and SGHPL-4 expressed relatively similar levels of phospho-ezrin expression, while SW71 and SGHPL-4 showed about 50-70% lower levels of expression ( $P > 0.05$ ), and HTR8/SVneo showed the highest expression level ( $P > 0.05$ ) compared to other cells (Figure 4.4).

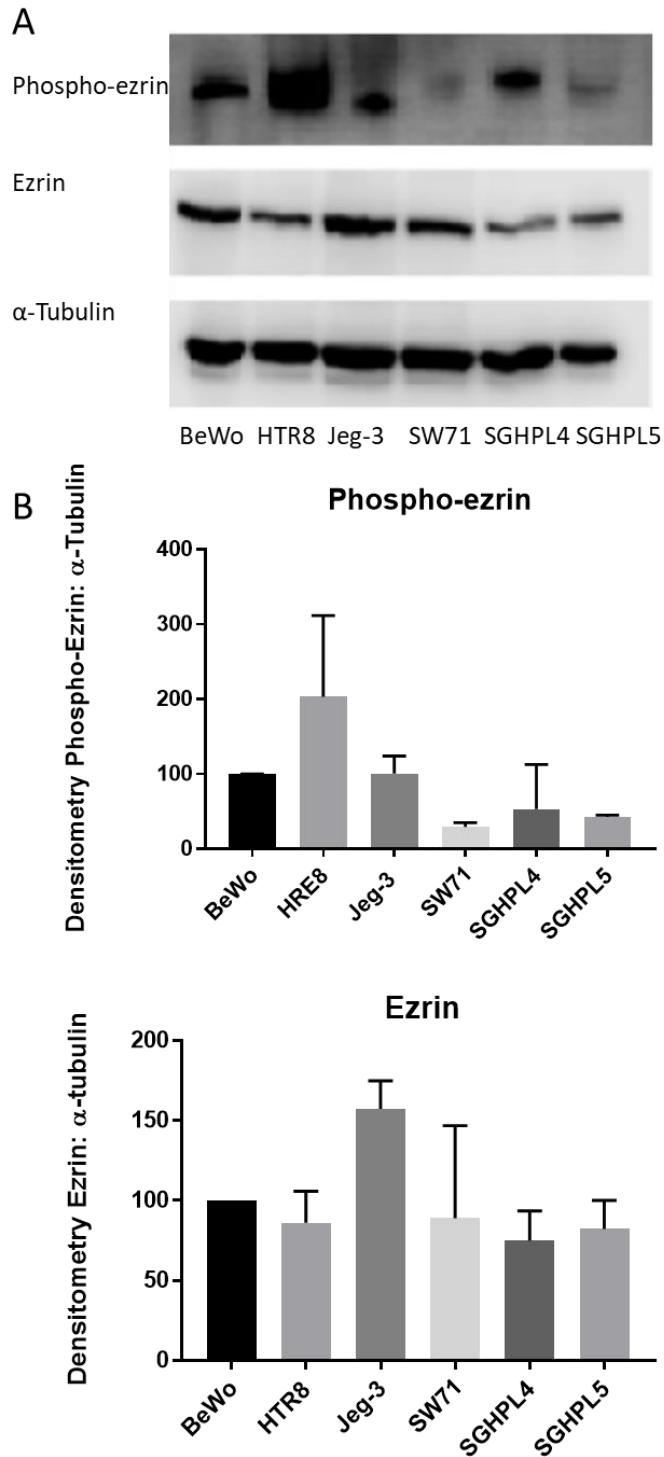


**Figure 4.4 Ezrin and phospho-ezrin expression in human trophoblast cell lines.** Human trophoblast cell lines BeWo, HTR8/SVneo, Jeg-3, SW71, SGHPL-4 and SGHPL-5, were collected in protease inhibitor cocktail and sonicated, prior to being separated by 10% SDS-PAGE, prior to protein transfer and western blot against ezrin, phospho-ezrin and  $\alpha$ -tubulin. Expression levels were quantified by Image Studio Lite software and ezrin and phospho-ezrin

expression levels were normalised to the housekeeping gene expression. Panel A shows the western blot bands for ezrin, phospho-ezrin and  $\alpha$ -tubulin, and panel B shows the densitometry. The error bars represent SD. N = 2, therefore the differences are non-significant. Total sample size = 2 for each cell line.

#### **4.2.5. Ezrin localisation in trophoblast cell lines**

Having shown that ezrin is expressed in different trophoblast cell lines, we wanted to learn more about its cellular localisation. To do this, trophoblast cells (HTR8/SVneo, SW71, SGHPL-4, SGHPL-5, Jeg-3 and BeWo) were seeded on to fibronectin-coated glass coverslips and left to attach for 24 hours. The coverslips were then fixed before permeabilisation, blocking and incubation with primary anti-ezrin antibody followed by secondary FITC-conjugated antibody and rhodamine phalloidin, prior to mounting and viewing. In the EVT cell lines HTR8/SVneo, SW71, SGHPL-5 and choriocarcinoma cell line BeWo, ezrin was highly detectable within the membrane protrusions, colocalising with actin at the leading edge of the cells, and in the cytoplasm to a lower extent, while showing a different pattern of localisation in EVT cell lines SGHPL-4 and choriocarcinoma cell lines Jeg-3, localising within the cytoplasm only. HTR8/SVneo and SW71 also showed nuclear localisation of the protein (Figure 4.5).

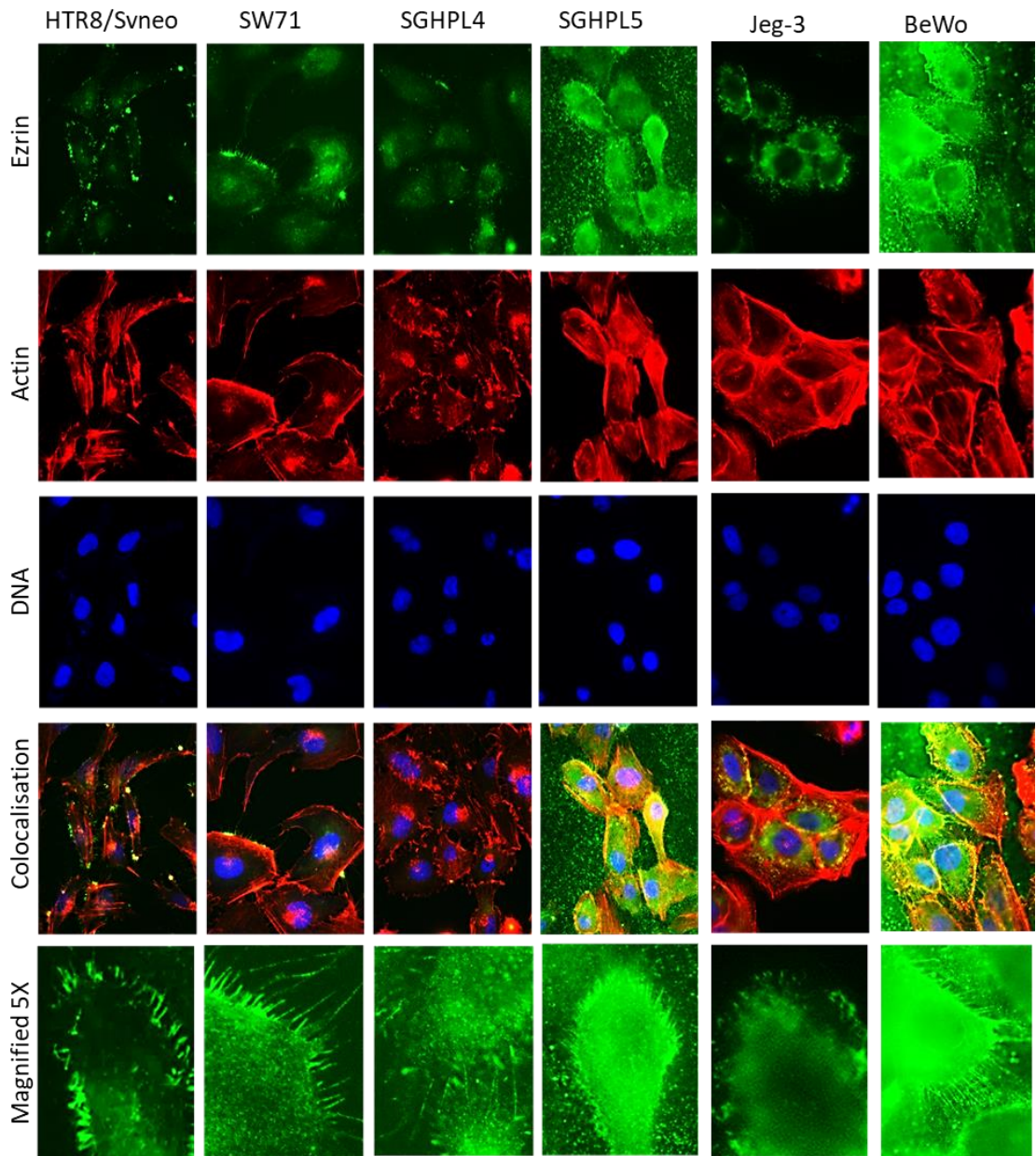


**Figure 4.5 Ezrin expression and localisation in trophoblast cell lines.** EVT cell lines HTR8/SVneo, SW71, SGHPL-4 and SGHPL-5 along with choriocarcinoma cell lines Jeg-3 and BeWo were seeded on fibronectin-coated coverslips. The cells were stained for ezrin, F-actin and DNA by immunofluorescence. The images were taken at 63x magnification.

#### 4.2.6. Ezrin expression knockdown

Having confirmed the expression of ezrin in EVT and choriocarcinoma cells-lines, and in order to decipher the roles that might be associated with the expression of this protein in trophoblast cell lines, we aimed to manipulate its expression to further study some of the cellular changes induced by such regulation. For this purpose, HTR8/SVneo and SW71 EVT cell lines, which showed the highest amount of ezrin within their protrusions as well as Jeg-3 choriocarcinoma cell lines, which had been found to express the highest amount of ezrin compared to the rest of our trophoblast cell lines were chosen for the experiment, as follows.

EVT cell lines HTR8/SVneo and SW71 as well as choriocarcinoma cell lines were treated with a panel of four different siRNA (5, 7, 8 and 9) targeting ezrin, along with a non-specific sequence of siRNA as negative control, for 72 hours. Then, the cells were collected and loaded on 10% polyacrylamide gel and was probed for ezrin and  $\alpha$ -tubulin by western blot. Ezrin and  $\alpha$ -tubulin expression in each condition were calculated by densitometry, ezrin expression was normalised to  $\alpha$ -tubulin (housekeeping gene) expression.

The treatment of the different cells with ezrin siRNA was found to reduce its expression in all cell lines tested. In HTR8/SVneo, siRNA 7 and 9 were the most effective and reduced ezrin expression significantly by 60% and 70%, respectively ( $P < 0.01$ ) compared with control, while siRNA 5 and 8 did not significantly affect ezrin expression. In SW71, once again siRNA 7 and 9 were the most effective and reduced ezrin expression by 70% and 80%, respectively ( $P < 0.001$ ), and siRNA 8 by did so by 50% ( $P < 0.01$ ) compared with control, while siRNA 5 did not significantly affect ezrin expression. In Jeg-3, siRNA 7 and 8 brought ezrin expression down to 10% and siRNA 9 reduced the expression of the protein by 50% compared with the control, however, none of these reductions were statistically significant. Ezrin expression levels in negative control samples remained similar to control samples in all three cell lines (Figure 4.6).

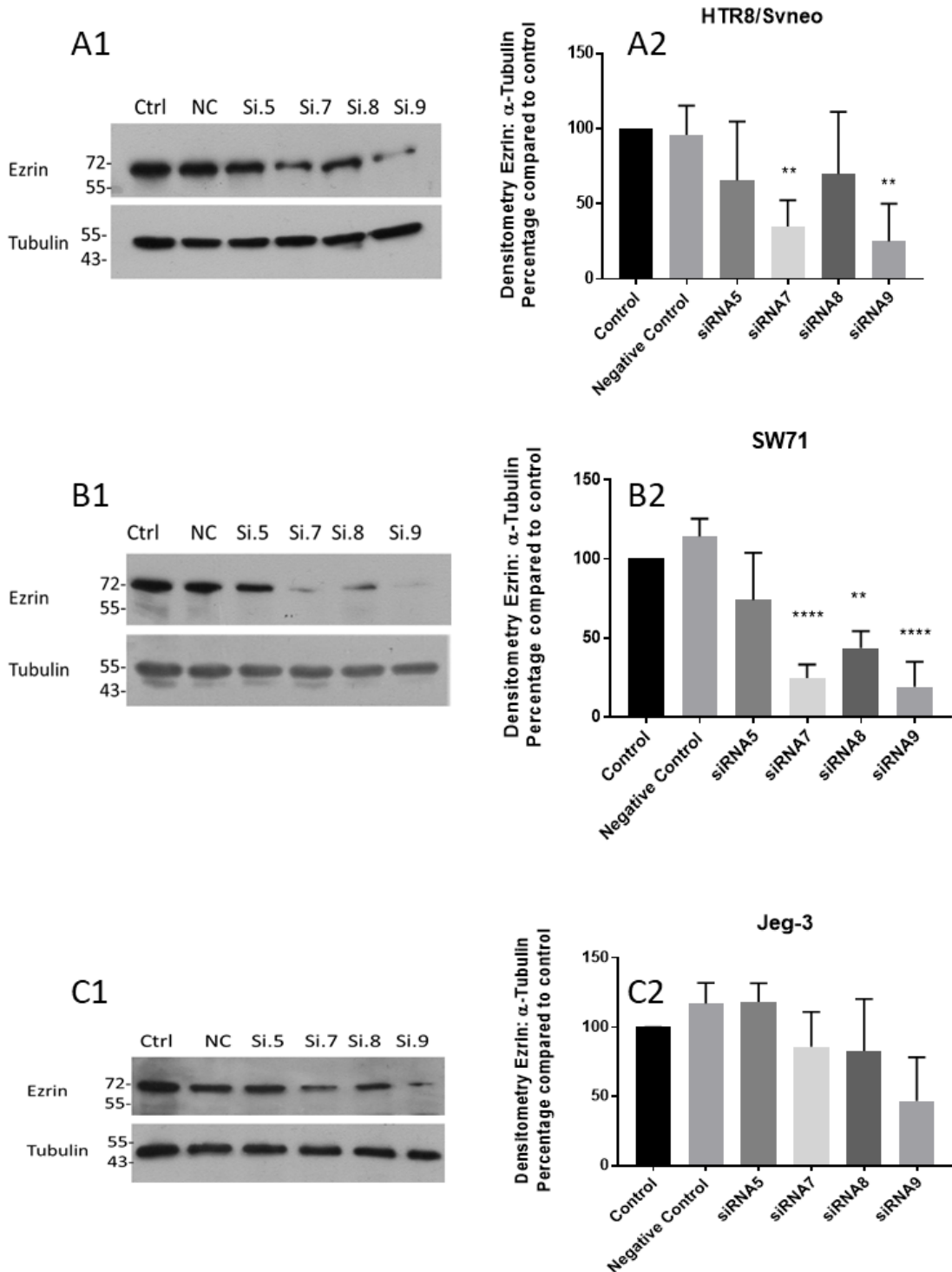


**Figure 4.6 Ezrin siRNA treatment knocks down ezrin expression in trophoblast cell lines.** HTR8/SVneo, SW71 and Jeg-3 cells, were treated with ezrin siRNA 5, 7, 8 and 9, along with mock treatment. The treated cells along with non-treated control cells were left to grow for 3 days prior to collection, lysing and sonication. The proteins were separated by 10% SDS-PAGE and ezrin and  $\alpha$ -tubulin bands were detected by western blot. Expression levels were quantified by

Image Studio Lite software and ezrin expression levels were normalised to the housekeeping gene expression. Panels A1, B1 and C1 show ezrin and  $\alpha$ -tubulin bands in HTR8/SVneo, SW71 and Jeg-3 cells, respectively, while panels A2, B2 and C2 show the densitometry in the mentioned cells in the same order. The error bars represent SD. (\*\*P<0.01, \*\*\*P<0.001, \*\*\*\*P<0.0001). N = 3 for each cell line. Total sample size = 3 for each condition.

#### **4.2.7. Ezrin knockdown does not affect trophoblast viability**

Ezrin has been shown to promote proliferation in cancer (Jeong et al. 2019; Kong et al. 2016) and fibroblast-like cells (Huang et al. 2011). Having successfully knocked down ezrin expression in EVT cell lines HTR8/SVneo and SW71, we sought to find out whether this can affect the viability of these cells over time. To achieve this, HTR8/SVneo and SW71 cells were treated with ezrin siRNA 7 and 9, which were shown to be the most effective in reducing ezrin expression in these cells (Figure 4.6), as well as a non-specific siRNA sequence as negative control. 72 hours following the treatment, the viability of the cells as well as their metabolic activity were studied by trypan blue exclusion and MTT assays, respectively. Trypan blue assay indicated that HTR8/SVneo cells increased in cell number by 100% over the second 24 hours following the seeding and then by 50% over the third 24 hours, and SW71 increased by 50% over the second 24 hours following the seeding and then by 50% over the third 24 hours in all four conditions. The MTT assay, showed that the HTR8/SVneo and SW71 increased in cell number by 50% over the second as well as the third 24 hours following the seeding, in all four conditions. Ezrin knockdown, using either siRNA 7 or 9, did not show any significant effect on the growth rate of the cells, as their viability or the metabolic activity seemed to have followed a similar pattern as the control and the negative control cells (Figure 4.7).

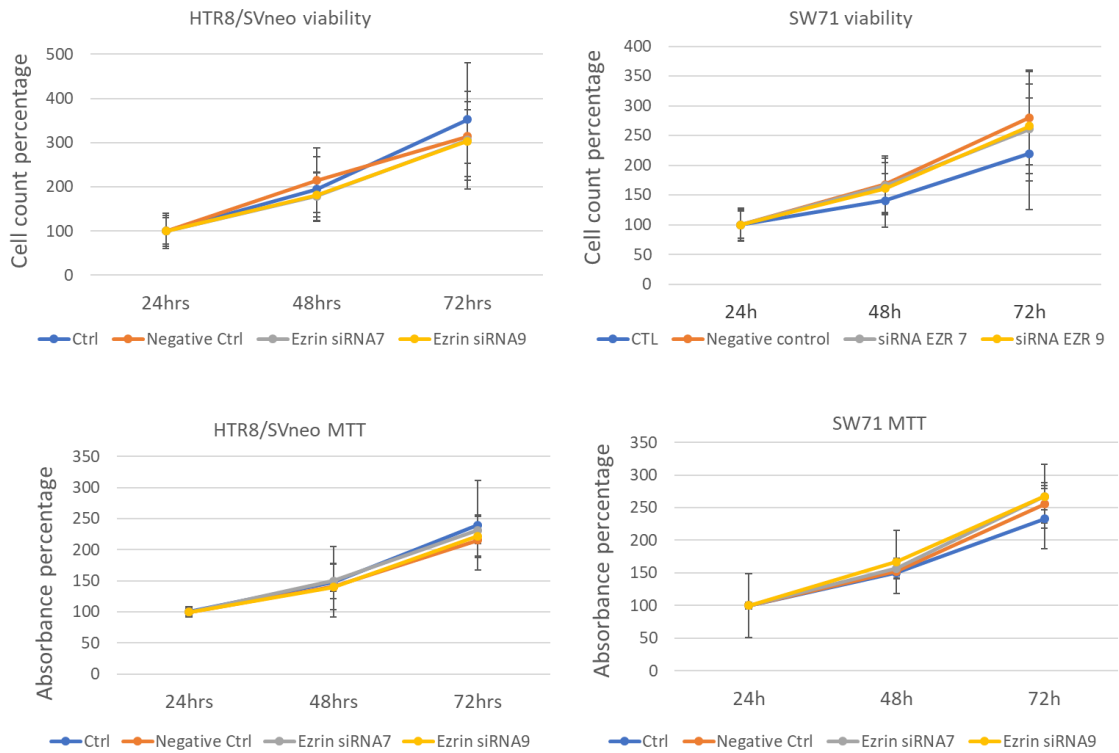


**Figure 4.7 Trophoblast viability with ezrin knockdown.** HTR8/SVneo and SW71 cells were treated with ezrin siRNA 7 and 9, along with a non-specific siRNA sequence, as negative control, for 72 hours. The cells were then collected and reseeded and their viability and metabolic activity (MTT assay) was tested over the next 72 hours. N = 3 for each condition. Total sample size for each condition: 60 (viability) and 6 (for MTT).

#### **4.2.8. Ezrin knockdown reduces trophoblast motility**

Ezrin over-expression has been reported to lead to increased cell motility and invasion in many tumours (Bruce et al. 2007; Geiger et al. 2000; Huang et al. 2010; Khanna et al. 2004; Yu et al. 2004; Zhou et al. 2014). However, it is not clear whether ezrin plays a similar role in trophoblast cells or not. To investigate this, HTR8/SVneo and SW71 EVT and Jeg-3 choriocarcinoma cell lines were treated with ezrin siRNA 7 and 9, which were shown to be the most effective in reducing ezrin expression (Figure 4.6). The cells were collected after 72 hours and were seeded in transwells. After 24 hours of incubation, the migrated cells were fixed and stained using Quick Diff staining kit, the cells were counted on random fields at 20x magnification and the average number of migrated treated cells were compared with non-treated cells. While negative control cells showed similar migratory capabilities to control cells in all three cell lines, knocking down ezrin significantly reduced motility in HTR8/SVneo EVT cell lines by 20%, with siRNA 7 ( $P<0.05$ ) and 50% with siRNA 9 ( $P<0.0001$ ) and in SW71 by 40% with siRNA 7 ( $P<0.0001$ ) and 50% with siRNA 9 ( $P<0.0001$ ) (Figure 4.8). In Jeg-3 cells however, the reduction was not significant (Figure 4.8).

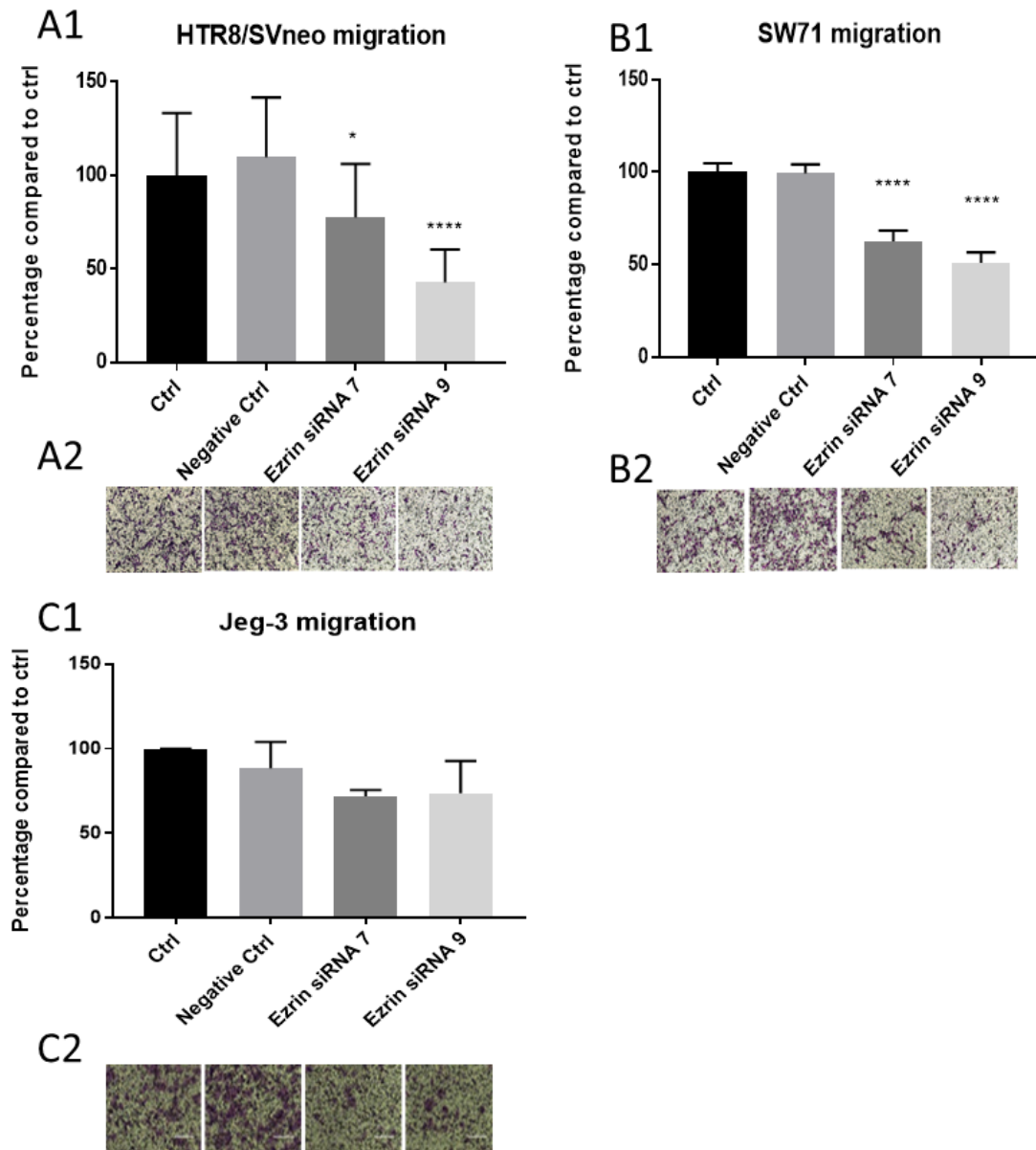


**Figure 4.8 The effect of ezrin knockdown on trophoblast migration.** HTR8/SVneo, SW71 and Jeg-3 cells were seeded in 24 well plates and treated with ezrin siRNA 5,7, 8 and 9, along with mock treatment and not treated control. They were left to grow for 48 hours before the medium was replaced with serum starvation medium. After another 24 hours of incubation, the cells were collected and were seeded in transwells. After 24 hours of incubation, the transwells were fixed and stained. The cells were counted in fields of 20x magnification. Panels A1, B1 and C1 show average cell count percentage compared with control in HTR8/SVneo, SW71 and Jeg-3 cells, respectively and the error bars represent SEM (\*  $P < 0.05$ , \*\*\*\*  $p < 0.0001$ ). Panels A2, B2 and C2 show representative fields of fixed and stained transwells for HTR8/SVneo, SW71 and Jeg-3 cells, respectively.  $N = 3$  for each cell line. Total sample size = 18 for each condition.

#### **4.2.9. Ezrin knockdown reduces trophoblast invasion**

Ezrin has been specifically linked with tumour cell invasion by enhancing MMP expression (Jiang, Wang & Chen 2014; Tang et al. 2019). Having shown the role of ezrin in trophoblast motility we next wanted to evaluate a possible role of ezrin in trophoblast invasion. HTR8/SVneo, SW71 (EVT) and Jeg-3 (choriocarcinoma) cell lines were treated with ezrin siRNA 7 and 9, which were shown to be the most effective in reducing ezrin expression (Figure 4.6), along with a non-specific sequence of siRNA as negative control. The cells were then seeded in transwells, coated with Matrigel. The cells were left to invade for 24 hours, before being fixed and stained. The cells were counted on random fields at 20x magnification and the average number of invaded treated cells were compared with non-treated control cells. Similar to motility, the negative control cells showed similar invasiveness to the control cells, but knocking down ezrin significantly reduced invasion in HTR8/SVneo EVT cell lines by 20% with siRNA 7 ( $P<0.05$ ) and 50% with siRNA 9 ( $P<0.0001$ ) compared with control, and in SW71 by 40% with siRNA 7 ( $P<0.01$ ) and 50% with siRNA 9 ( $P<0.001$ ), while invasion in Jeg-3 choriocarcinoma cells was not reduced significantly upon ezrin knockdown (Figure 4.9).

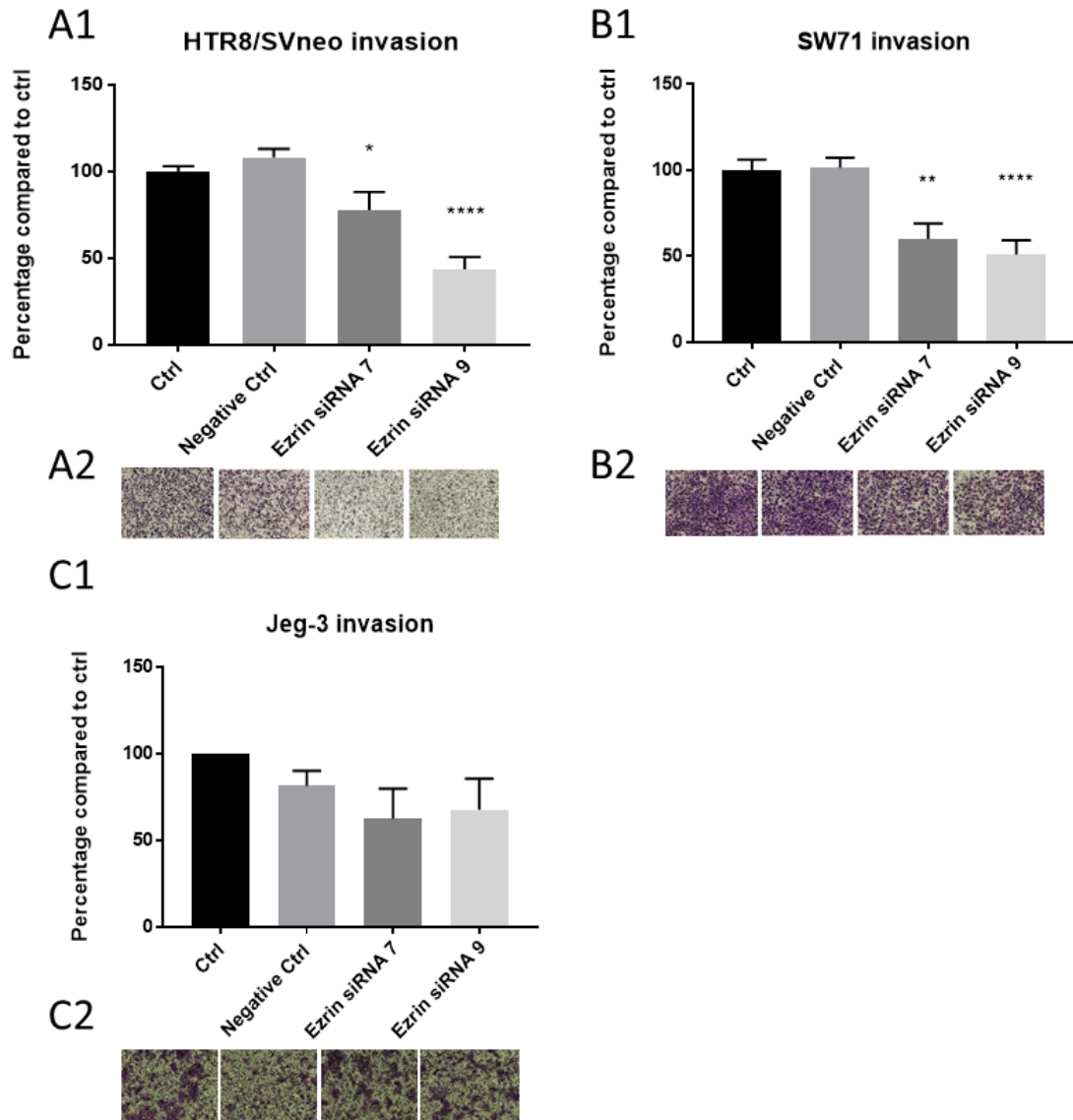


**Figure 4.9 The effect of ezrin knockdown on trophoblast invasion.** HTR8/SVneo, SW71 and Jeg-3 cells were seeded in 24 well plates and treated with ezrin siRNA 5,7, 8 and 9, along with mock treatment and not treated control. They were left to grow for 48 hours before the medium was replaced with serum starvation medium. After another 24 hours of incubation, the cells were collected and were seeded in Matrigel-coated transwells. After 24 hours of incubation, the transwells were fixed and stained. The cells were counted in fields of 20x magnification. Graphs A1, B1 and C1 show average cell count percentage compared with control in HTR8/SVneo, SW71 and Jeg-3 cells, respectively and the error bars represent SEM (\* P<0.05, \*\* P<0.01, \*\*\* p<0.0001). Panels A2, B2 and C2 show representative fields of fixed and stained transwells for HTR8/SVneo, SW71 and Jeg-3 cells, respectively. N = 3 for each cell line. Total sample size = 6 for each condition.

#### 4.2.10. Regression analysis

Having shown the effect of ezrin down regulation on trophoblast cell line motility and invasion, we next aimed to see whether there is a meaningful correlation between ezrin expression and migration/invasion in these cells, by regression analysis. To do this, ezrin expression levels in trophoblast cells HTR8/SVneo and SW71, with two sequences of ezrin siRNA (7 and 9), mock negative control, along with non-treated control (Figure 4.6) were correlated with their migration (Figure 4.8) and invasion (Figure 4.9). Pearson correlation coefficient,  $r$  was calculated, and Student's  $t$ -distribution was used to test the significance of the correlation. Regression analysis showed a positive correlation ( $r > 0$ ) between ezrin expression and cell migration/invasion for both trophoblast cells: ezrin expression and HTR8/SVneo migration  $r = 0.86$  and invasion  $r = 0.86$ , ezrin expression and SW71 migration  $r = 0.94$  and invasion  $r = 0.96$ . The correlation however, was only significant for SW71 motility ( $P < 0.05$ ) and invasion ( $P < 0.01$ ) (Figure 4.10).

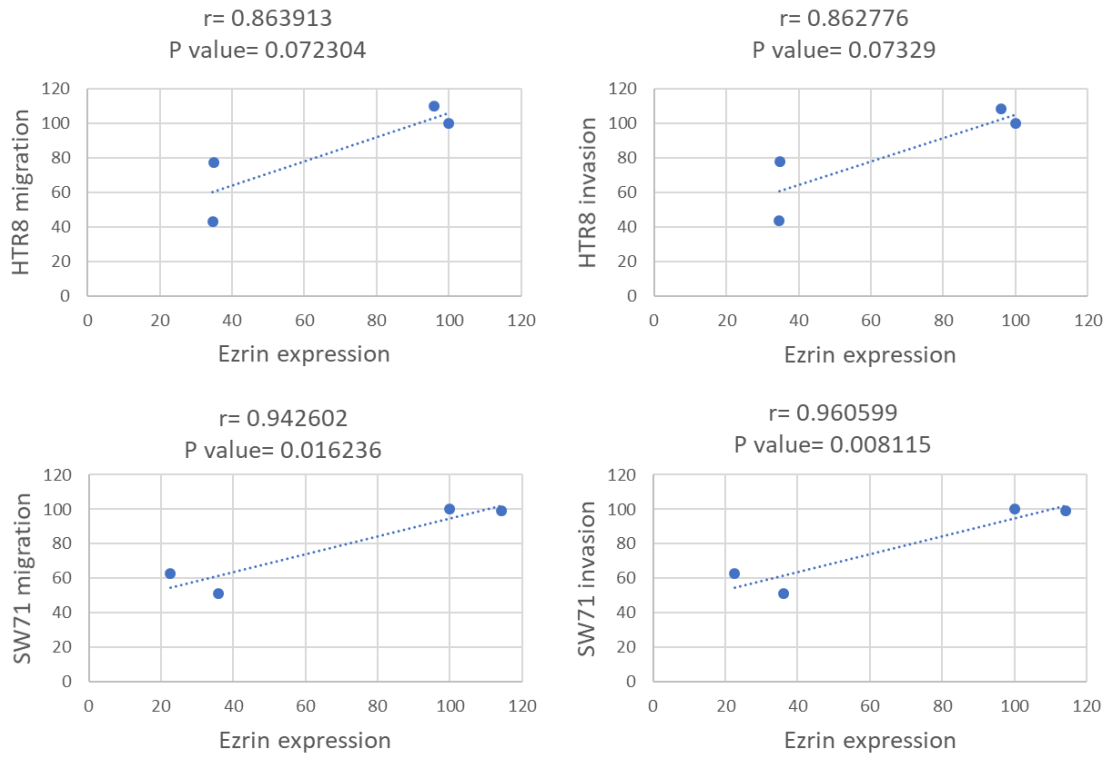


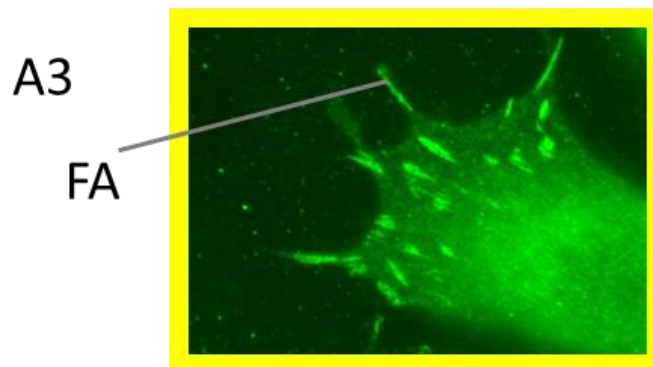
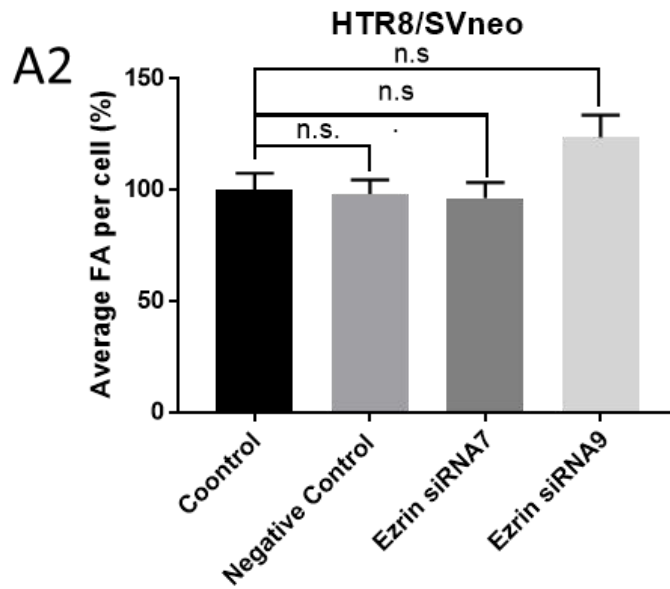
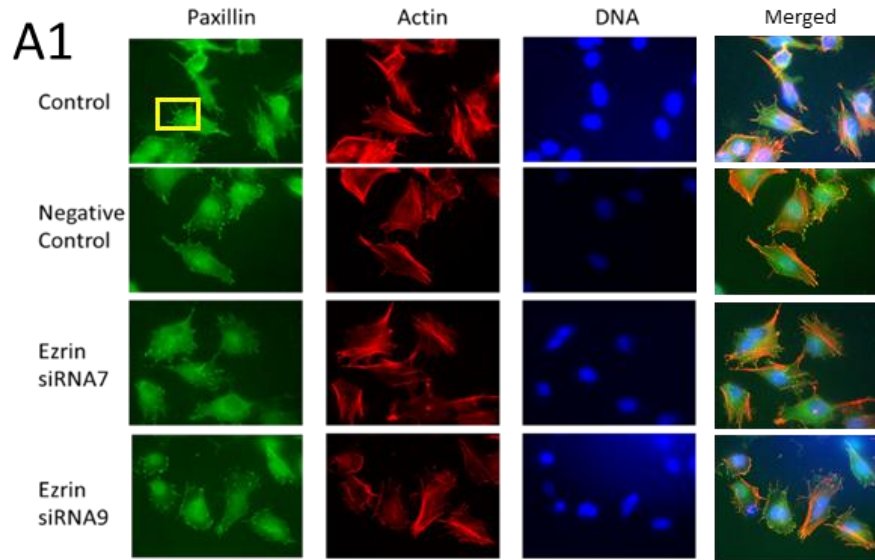
**Figure 4.10 Positive correlation between trophoblast migration/invasion and ezrin expression.** Average ezrin expression levels in trophoblast cell lines HTR8/SVneo and SW71 were correlated with motility and invasion and Pearson correlation coefficient,  $r$ , was calculated. Student's t-distribution was used to calculate the P-values.

#### 4.2.11. Ezrin knockdown does not affect FAs

Ezrin depletion in breast cancer cells has been shown to reduce the number and size of FAs as well as their invasion (Hoskin et al. 2015). Here, we hypothesised that the motility and invasion of trophoblast cells might also be regulated by ezrin through a similar mechanism. For this purpose, HTR8/SVneo and SW71 cells were treated with ezrin siRNA 7 and 9, which were shown to reduce both motility and invasion in these two cell lines along with a non-specific siRNA sequence as negative control. 72 hours after knocking down ezrin, the cells were seeded on fibronectin-coated coverslips and were left to attach for 24 hours. Following preparation, the coverslips were incubated with primary anti-paxillin (a component of the FA complex) antibody followed by secondary FITC-conjugated antibody and rhodamine phalloidin, before mounting and viewing. Control samples do not show a significant difference in the number (Table 4.1) or the relative size of FAs when compared with negative control and ezrin siRNA treated samples in either HTR8/SVneo or SW71 cells (Figure 4.11).

	Percentage focal adhesions per cell $\pm$ SEM (n=10)	P value (compared with control)
HTR8/SVneo Control	100 $\pm$ 7.34	N/A
HTR8/SVneo Negative Control	98.23 $\pm$ 6.26	0.9970
HTR8/SVneo Ezrin siRNA 7	96.34 $\pm$ 6.97	0.9750
HTR8/SVneo Ezrin siRNA 9	123.60 $\pm$ 9.91	0.0962
SW71 Control	100 $\pm$ 11.53	N/A
SW71 Negative Control	78.85 $\pm$ 4.72	0.1740
SW71 Ezrin siRNA 7	89.59 $\pm$ 5.52	0.6898
SW71 Ezrin siRNA 9	110.10 $\pm$ 9.11	0.7149

**Table 4.1 Average FA count per cell in HTR8/SVneo and SW71 cells.** HTR8/SVneo and SW71 trophoblast cell lines were treated with ezrin siRNA 7 and 9 for 48 hours before collection. The cells were then seeded on fibronectin-coated coverslips, were left to attach for 24 hours, and finally, were stained for paxillin. The FAs were counted on all cells in each image.



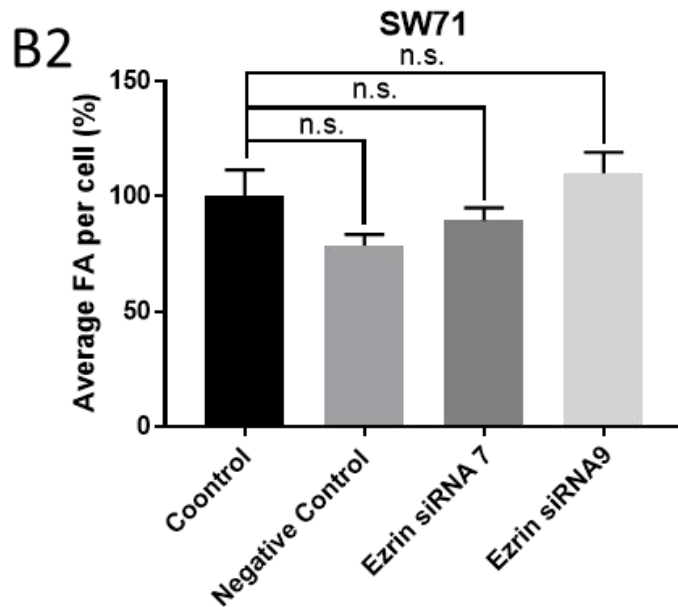
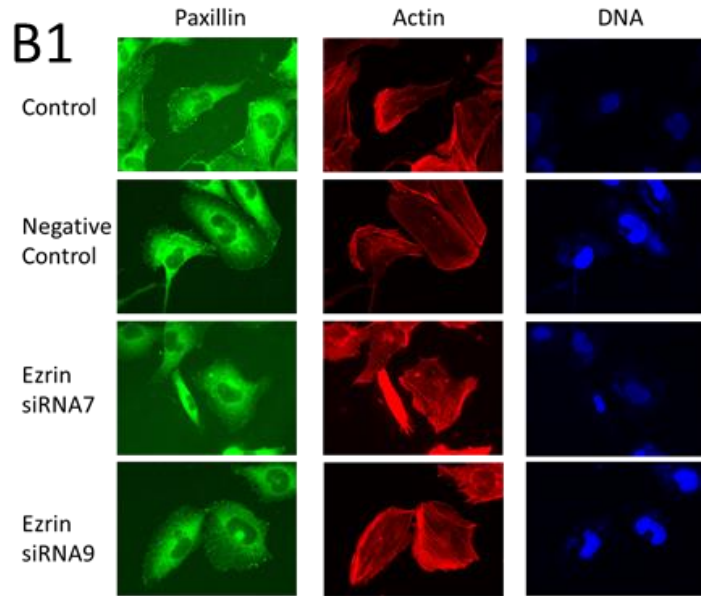


**Figure 4.11 Knocking down ezrin does not affect the FAs.** HTR8/SVneo and SW71 trophoblast cell lines were treated with ezrin siRNA 7 and 9 for 48 hours before collection and being seeded on fibronectin-coated coverslips and were left to attach for 24 hours. The cells were stained for paxillin, F-actin and DNA by immunofluorescence. The images were taken with 63x magnification. Panels A1 (previous page) and B1 show the staining on HTR8 and 9SW71 cells, respectively. Panels B2 (previous page) and B2 show average FA count (in percentage) in treated cells compared with the non-treated controls in HTR8/SVneo and SW71, respectively. The error bars represent SEM. Panel A3 on the first part of the image shows a zoomed-in part of control

HTR8/SVneo cells. N = 1 for each cell line. Total sample size for each condition: 10 (HTR8/SVneo) and 20 (SW71).

#### **4.2.12. Ezrin phosphorylation inhibition**

Like other ERM protein family members, ezrin requires phosphorylation of a conserved threonine residue (Thr567), to switch to its open and active conformation (Fehon, McClatchey & Bretscher 2010). Changes in ezrin phosphorylation have been reported to result in changes its sub-cellular localisation (Zhou et al. 2005). To assess the role of ezrin phosphorylation in trophoblasts, we aimed to measure the amount of phospho-ezrin as well as its localisation upon treatment with ezrin inhibitor, NSC668394, a chemical compound, which binds to ezrin ( $K_d = 12.59 \mu\text{M}$ ), preventing its phosphorylation at Thr567 (Bulut et al. 2012).

##### **4.2.12.1. Ezrin inhibitor reduces phospho-ezrin in HTR8/SVneo**

To evaluate phospho-ezrin levels in ezrin inhibited trophoblasts, 100,000 HTR8/SVneo and 50,000 SW71 cells were seeded in 24-well plates, while being treated with 5 $\mu\text{M}$  ezrin inhibitor NSC668394 (dissolved in DMSO), or with 0.1% DMSO (same volume as NSC668394), as negative control for 24 hours. After treatment, HTR8/SVneo and SW71 EVT cells were collected and loaded on 10% SDS-PAGE. Phospho-ezrin and  $\alpha$ -tubulin bands were detected by western blot. The expression levels were measured by densitometry and phospho-ezrin expression was normalised to  $\alpha$ -tubulin expression levels. In HTR8/SVneo cells, NSC668394 significantly reduced phospho-ezrin expression by 70% ( $P < 0.001$ ) compared with non-treated control cells, while in SW71, phospho-ezrin levels remained unchanged upon treatment with the inhibitor (Figure 4.12). In both cell lines, DMSO treated samples expressed the same amount of ezrin as the controls.

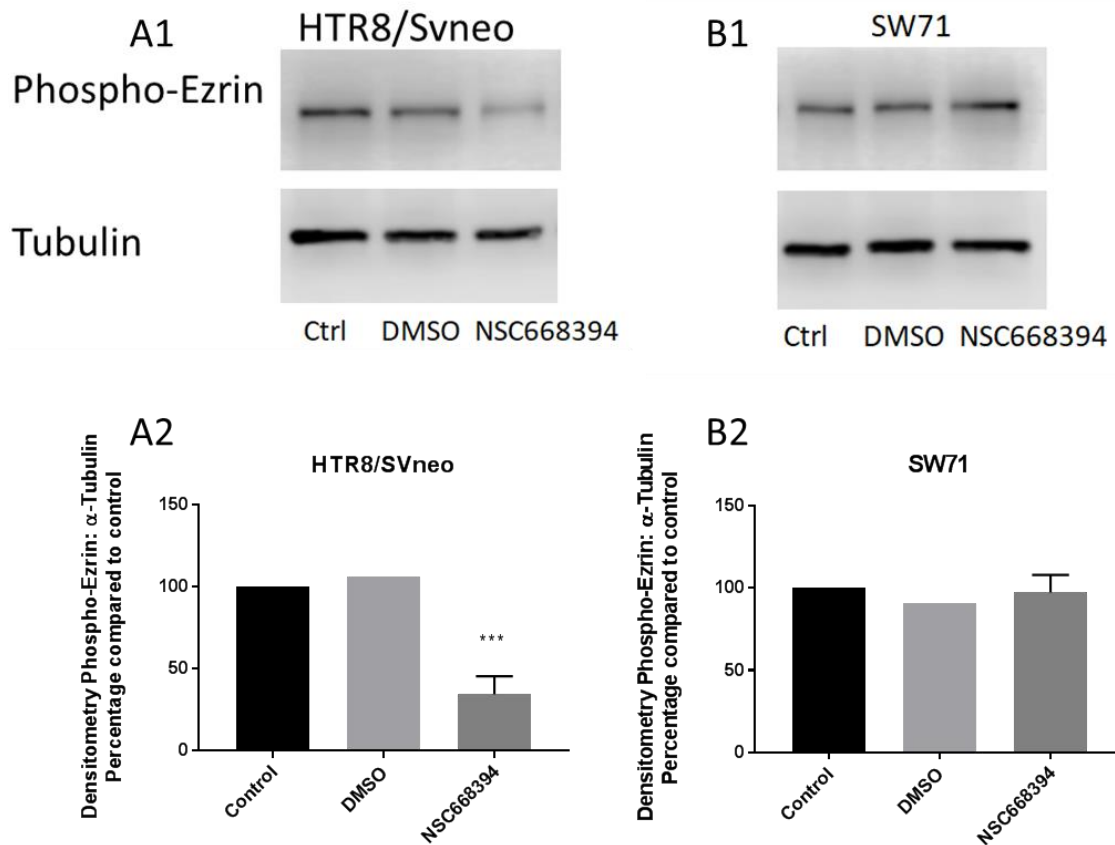


**Figure 4.12 The effect of ezrin inhibition on phospho-ezrin levels.** HTR8/SVneo and SW71 cells were treated with NSC668394 or DMSO (as negative control) for 24 hours prior to being collected in protease inhibitor cocktail and sonication. The cell lysates were then loaded on 10% SDS-PAGE and then phospho-ezrin and  $\alpha$ -tubulin bands were detected by western blot. A1 and B1 show the bands for phospho-ezrin in HTR8/SVneo and SW71 cells, respectively, while A2 and B2 show phospho-ezrin expression levels normalised to  $\alpha$ -tubulin in these cells. The error bars represent SD (\*\*\*)  $P < 0.001$ .  $N = 3$  for each cell line. Total sample size = 3 for each condition.

#### **4.2.13. Ezrin inhibition modifies the localisation of ezrin and phospho-ezrin in HTR8/SVneo**

Having shown the effectiveness of the ezrin inhibitor drug NSC668394 in reducing phospho-ezrin in HTR8/SVneo EVT cell lines, here we aimed to see whether the drug can cause a change in the localisation of ezrin and/or phospho-ezrin in HTR8/SVneo and SW71 cell lines. For this purpose, the cells were seeded on fibronectin-coated glass coverslips, while being treated with 5  $\mu$ M NSC668394, or without treatment. The cells were left to attach for 24 hours. The coverslips were then prepared and incubated with primary anti-phospho-ezrin and anti-ezrin antibodies followed by incubation with secondary TRITC (for ezrin) and FITC-conjugated (for phospho-ezrin) antibodies, before mounting and viewing. Both ezrin (red) and phospho-ezrin (green) were shown to be mainly localised within the protrusions in control HTR8/SVneo and SW71 cells. Both ezrin and phospho-ezrin show reduced membrane localisation upon treatment with NSC668394 in HTR8/SVneo cells. In SW71 however, there are no distinctive changes in the localisation of ezrin and phospho-ezrin following the treatment. Ezrin and phospho-ezrin also showed nuclear localisation, which was reduced in HTR8/SVneo cells upon ezrin inhibition (Figure 4.13).

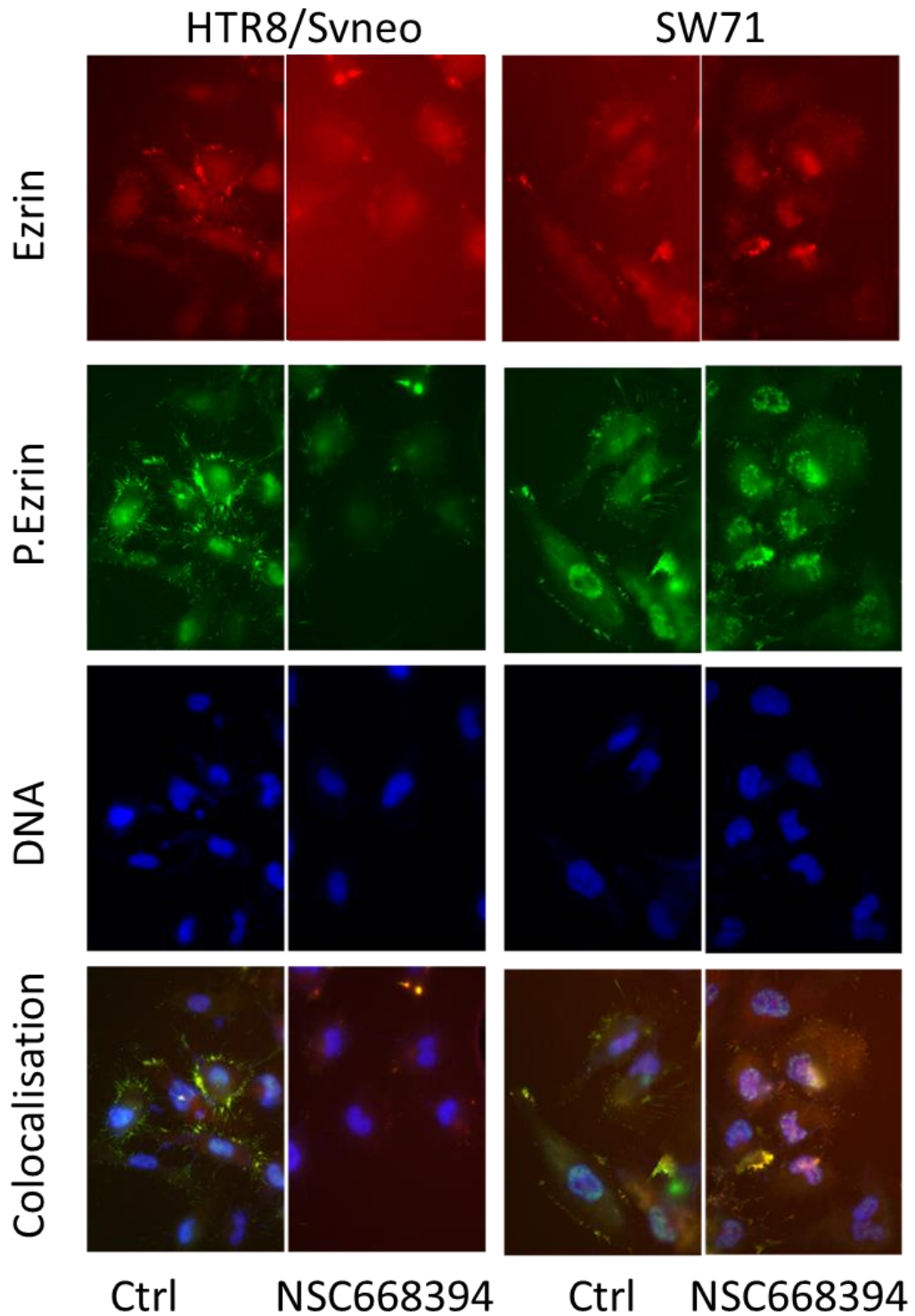


**Figure 4.13** The effect of ezrin inhibition on ezrin and phospho-ezrin localisation in EVT cell lines. EVT cell lines HTR8 and SW71 were seeded on fibronectin-coated coverslips, while being treated with NSC668394 along with non-treated control. After 24 hours of incubation, ezrin

was visualised with TRITC, phospho-ezrin with FITC, and DNA with DAPI. The images were taken at 63x magnification.

#### **4.2.14. Ezrin inhibition does not affect trophoblast viability**

The ezrin inhibitor NSC668394 has been shown to affect cell proliferation in different ways. While it was shown to reduce the viability of human glioblastoma cells (Hilliard et al. 2017), it was not shown to affect the viability of osteosarcoma cells (Bulut et al. 2012). Here, we aimed to find out if ezrin inhibition affects trophoblast cell lines' viability. For this purpose, HTR8/SVneo and SW71 cells were treated with 5  $\mu$ M NSC668394, or with 0.1% (v/v) DMSO as negative control. Over the next 72 hours, the viability of the cells was assessed by trypan blue exclusion assay and the metabolic activity of the cells was assessed by MTT assay. Trypan blue assay indicated that HTR8/SVneo cells increased in cell number by 100% over the second 24 hours following the seeding then by 50% over the third 24 hours, and SW71 increased by 50% over the second 24 hours following the seeding and then by 50% over the third 24 hours in all four conditions. The MTT assay showed that the HTR8/SVneo increased in cell number by 20% over the second and then by 30% over the third 24 hours following the seeding, while SW71 increased in cell number by 50% over the second as well as the third 24 hours following the seeding in all four conditions. Ezrin inhibition was not shown to significantly affect the viability or the metabolic activity of neither the HTR8/SVneo nor the SW71 cells (Figure 4.14).

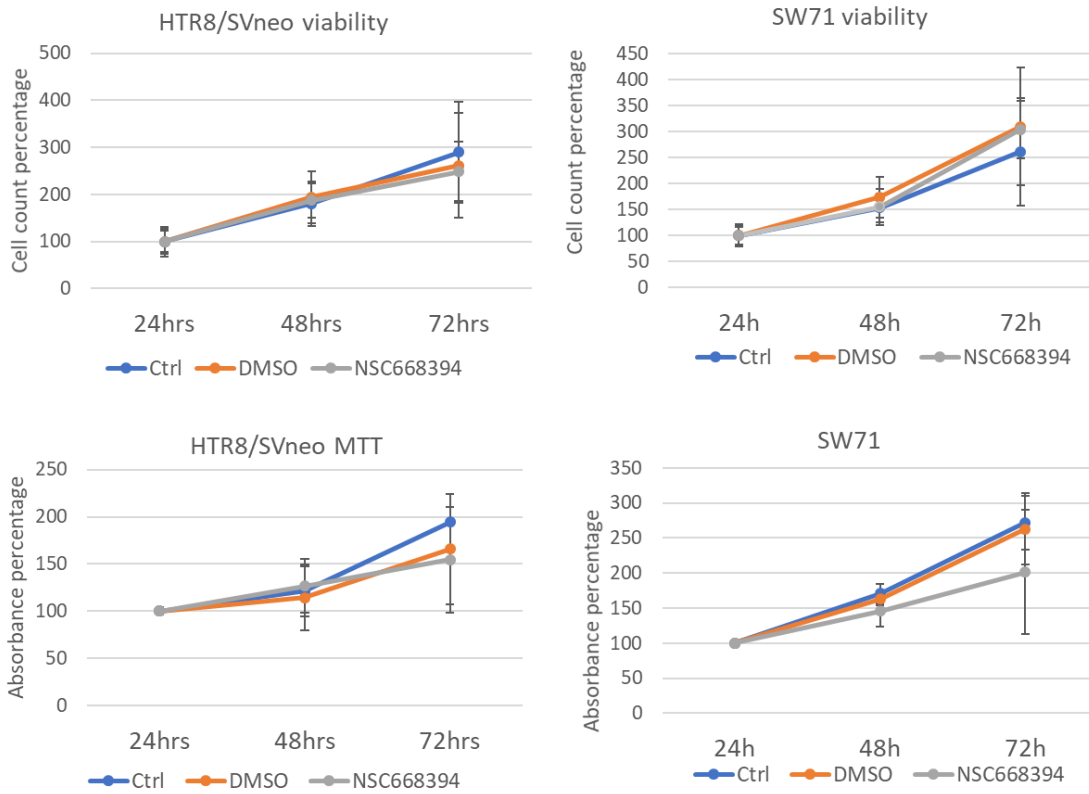


**Figure 4.14 Trophoblast viability with ezrin inhibition.** HTR8/SVneo and SW71 cells were seeded and treated with ezrin inhibitor NSC668394 or DMSO for 24 hours. Their viability and metabolic activity were tested during the next 3 days, by trypan blue exclusion and MTT assays, respectively. The error bars represent SD. The numbers have been reported as percentages. N = 3 for each condition. Total sample size for each condition: 60 (viability) and 6 (for MTT).

#### **4.2.15. The effect of ezrin inhibition on trophoblast motility**

Ezrin inhibitor, NSC668394, has been shown to inhibit motility and invasion of osteosarcoma cells (Bulut et al. 2012). Here we aimed to study the effect of ezrin phosphorylation inhibition on trophoblasts. For this purpose, HTR8/SVneo and SW71 cells were serum starved for 24 hours, and then were seeded into transwells without treatment (control), with 0.1% (v/v) DMSO (as negative control), or with 5  $\mu$ M NSC668394, followed by 24 hours incubation. The transwells were then fixed and stained and the cells were counted on random fields at 20x magnification. NSC668394 significantly reduced HTR8 migration by 80% ( $P < 0.0001$ ), while it did not significantly affect SW71, indicating a proportionality between phospho-ezrin levels (Figure 4.15) and EVT migration.

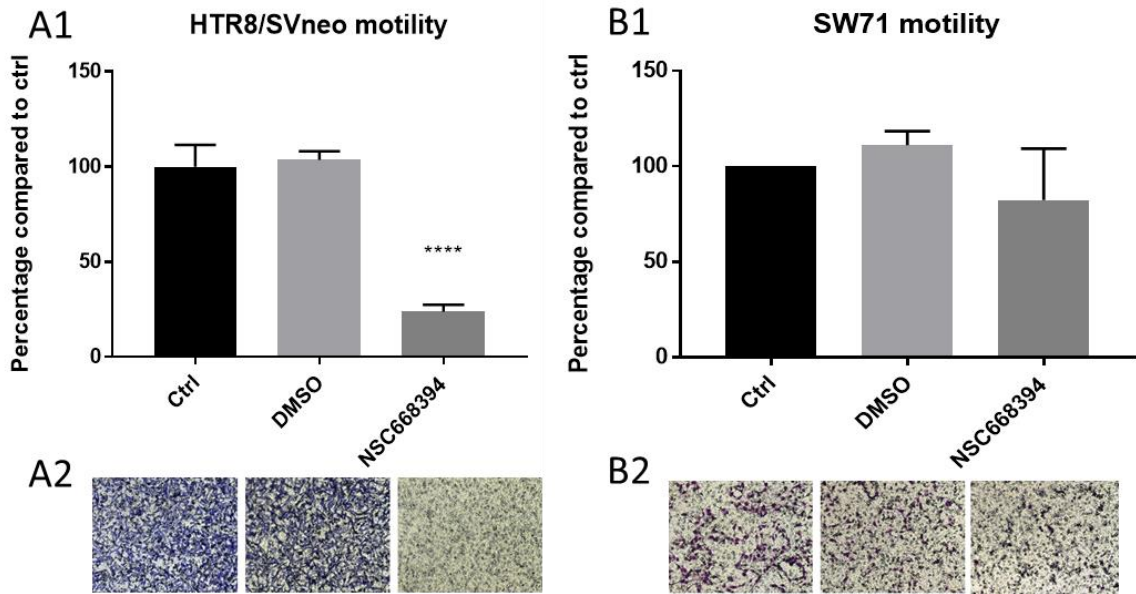


**Figure 4.15 Ezrin phosphorylation inhibition reduces trophoblast motility.** HTR8/SVneo and SW71 EVT cell lines were serum starved for 24 hours prior to being collected and resuspended in serum starvation medium. The cells were seeded in transwells while being treated with NSC668394, DMSO (as negative control) or without any treatment. After 24 hours, the transwells were fixed, stained and the stained cells were counted on random fields at 20x magnification. The graphs show average cell count percentage compared with control in HTR8/SVneo (A1) and SW71 (B1) and the error bars represent SEM (\*\*\*\*  $p < 0.0001$ ). Panels A2 and B2 and show representative fields of fixed and stained transwells.  $N = 3$  for each cell line. Total sample size = 18 for each condition.

#### **4.2.16. The effect of ezrin inhibition on trophoblast invasion**

Having shown the effect of ezrin inhibition on trophoblast motility, here we sought investigate the effect of ezrin inhibition on trophoblast invasion. For this aim, HTR8/SVneo and SW71 cells were seeded into Matrigel-coated transwells without treatment (control), with 0.1% (v/v) DMSO (as negative control), or with 5  $\mu$ M NSC668394, followed by 24 hours of incubation. The transwells were then fixed and stained and the cells were counted on random fields at 20x magnification. NSC668394 significantly reduced HTR8 invasion by 70% ( $P < 0.0001$ ), while it did not significantly affect SW71 (Figure 4.16).

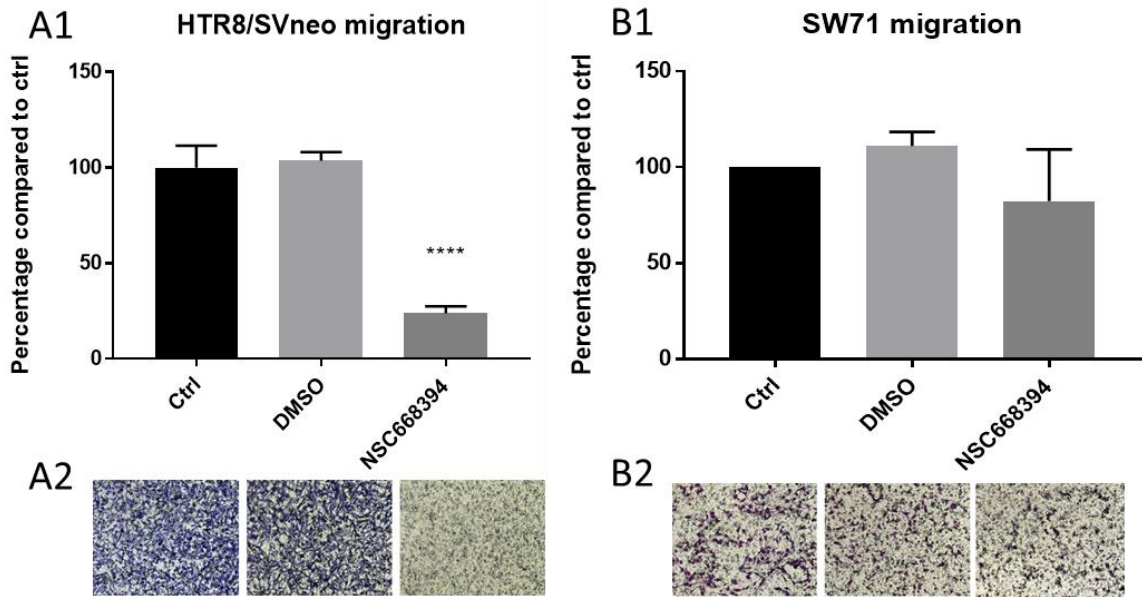


**Figure 4.16 Ezrin phosphorylation inhibition reduces trophoblast invasion.** HTR8/SVneo and SW71 EVT cell lines were serum starved for 24 hours prior to being collected and resuspended in serum starvation medium. The cells were seeded in Matrigel-coated transwells while being treated with NSC668394, DMSO (as negative control) or without any treatment. After 24 hours, the transwells were fixed, stained and the stained cells were counted at 20x magnification. The graphs show average cell count percentage compared with control in HTR8/SVneo (A1) and SW71 (B1) and the error bars represent SEM (\*\*\*  $p < 0.001$ ). Panels A2 and B2 show representative fields of fixed and stained transwells. N = 3 for each cell line. Total sample size = 6 for each condition.

#### 4.2.17. Ezrin inhibition affects FA number and size in

##### HTR8/SVneo

Knocking down ezrin in the previous section (4.2.11) was not shown to affect the size or the number of FAs. In this section, we aimed to study the effect of ezrin inhibition on FAs in HTR8/SVneo, which was shown to reduce motility and invasion in the mentioned cells. For this purpose, HTR8/SVneo cell lines were seeded on fibronectin-coated glass coverslips, while they were treated with 5  $\mu$ M NSC668394, along with non-treated control cells. After 24 hours, the coverslips were prepared and incubated with primary anti-paxillin antibody followed by incubation with secondary FITC-conjugated antibody and rhodamine phalloidin, before mounting and viewing. Control samples were shown to have significantly ( $P < 0.0001$ ) 60% lower numbers of FAs (Table 1.1), which looked relatively smaller as well, compared with the treated cells (Figure 4.17).

	Percentage focal adhesions per cell $\pm$ SEM (n=20)	P value (compared with control)
Control	100 $\pm$ 5.47	N/A
NSC668394	162.11 $\pm$ 7.94	<0.0001

**Table 4.2 Average FA count per cell in HTR8/SVneo cells, following ezrin inhibition.**

HTR8/SVneo trophoblast cell lines were seeded on fibronectin-coated coverslips, while being treated with NSC668394 ezrin-inhibitor and were left to attach for 24 hours. The cells were then fixed and stained for paxillin. The FAs were counted on all cells in each image.

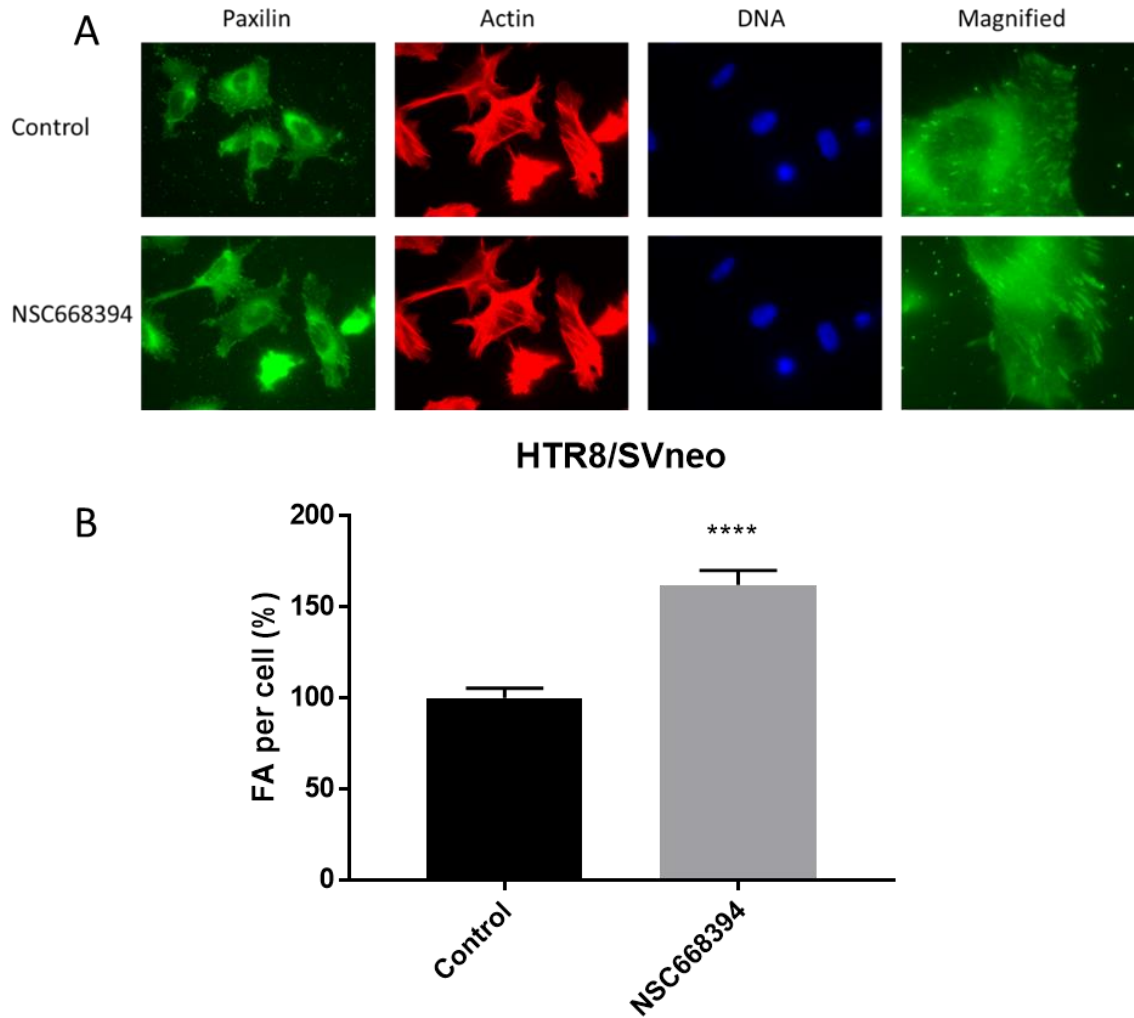


**Figure 4.17 Ezrin inhibition affects the FAs in HTR8/SVneo.** HTR8/SVneo cells were seeded on fibronectin-coated coverslips while being treated with the ezrin inhibitor NSC668394 along with non-treated control and were left to attach for 24 hours. Paxillin was visualised with FITC, F-actin with rhodamine phalloidin and DNA with DAPI. The images were taken at 63x magnification. Panel A shows staining on paxillin, F-actin and DNA. Panel B shows average FA count in NSC668394-treated HTR8 cells compared with the non-treated control. The error bars represent SEM (\*\*\*\*  $P < 0.0001$ ).  $N = 2$ . Total sample size = 20 for each condition.

#### **4.2.18. Ezrin expression and localisation in primary EVT**

Having shown ezrin expression in all trophoblast cell lines, here we aimed to look for the expression of the protein in primary EVT cells, which were isolated from first trimester human placenta. For this purpose, the cells were collected, a day following the isolation of EVTs and cell lysate was prepared in 10% protease inhibitor cocktail and sonicated. The lysate was separated by 10% SDS-PAGE and was probed for ezrin, phospho-ezrin and  $\alpha$ -tubulin by western blot. Ezrin signal and a strong phospho-ezrin signal were obtained when expression was measured by western blotting (Figure 4.18 A).

To find out more about the localisation of ezrin in primary EVTs, the cells were fixed on fibronectin-coated glass coverslips and incubated with primary anti-ezrin antibody followed by incubation with secondary FITC-conjugated antibody, as well as rhodamine phalloidin, before mounting and viewing. The immunofluorescence staining showed the localisation of the protein in the EVT cytoplasm as well as the cell membrane and membrane projections (Figure 4.18 B).

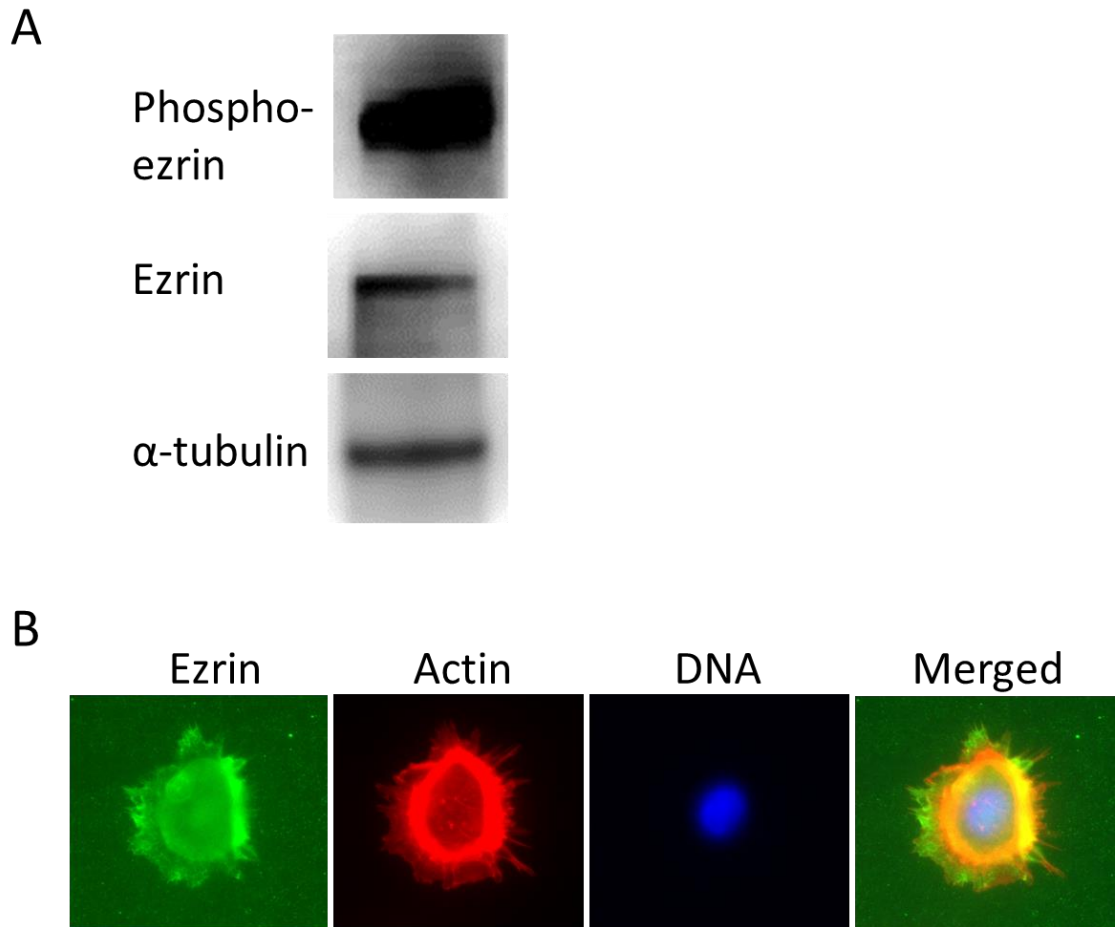


**Figure 4.18 Ezrin expression and localisation in primary EVT.** For expression analysis (panel A) EVT cells were collected, lysed and separated by 10% SDS-PAGE, and probed for ezrin, phospho-ezrin and  $\alpha$ -tubulin by western blotting. For the localisation experiment, (panel B) the EVT cells were seeded on fibronectin-coated coverslips and incubated for 24 hours. Ezrin was visualised by immunofluorescence with FITC and actin with rhodamine phalloidin and DNA with DAPI. The images were taken at 63x magnification.

#### 4.2.19. Phospho-ezrin localisation in first and second trimester

##### EVTs

Having shown the differential expression of ezrin proteins over the course of gestation, with higher levels being seen in first and second trimesters compared with the third, but no significant difference between the first two, we sought to determine whether changes could be seen in the levels of ezrin activation, such as its phosphorylated state over the early stages of implantations. Consequently, we aimed to compare at the localisation of phospho-ezrin (active form) in primary EVT<sub>s</sub> isolated from first (weeks 9) and second trimester (16 weeks) placenta samples. The cells were seeded on fibronectin-coated glass coverslips and incubated with anti-phospho-ezrin and then secondary FITC-conjugated secondary antibody as well as phalloidin. The staining showed strong phospho-ezrin localisation within membrane protrusions of both the first trimester and second trimester EVT<sub>s</sub>, while the cells from earlier gestational age showed a stronger nuclear localisation. EVT morphology also looked different between these two gestational ages, as there were 40% more (Table 4.3) membrane protrusions in the first trimester EVT<sub>s</sub> ( $P < 0.05$ ) and they looked more elongated compared with the older cells (Figure 4.19).

	Membrane projection count per cell as percentage $\pm$ SEM (n=12)	P value (compared with control)
1 <sup>st</sup> TM	100 $\pm$ 10.43	N/A
2 <sup>nd</sup> TM	66.07 $\pm$ 8.94	0.023682135

**Table 4.3 Average membrane projection count per cell in primary first and second trimester EVT<sub>s</sub>.** Primary EVT<sub>s</sub> from first and second trimesters were seeded on fibronectin-coated coverslips and were left to attach for 24 hours. The cells were then fixed and stained for phospho-ezrin. The membrane projections were counted on all cells in each image.

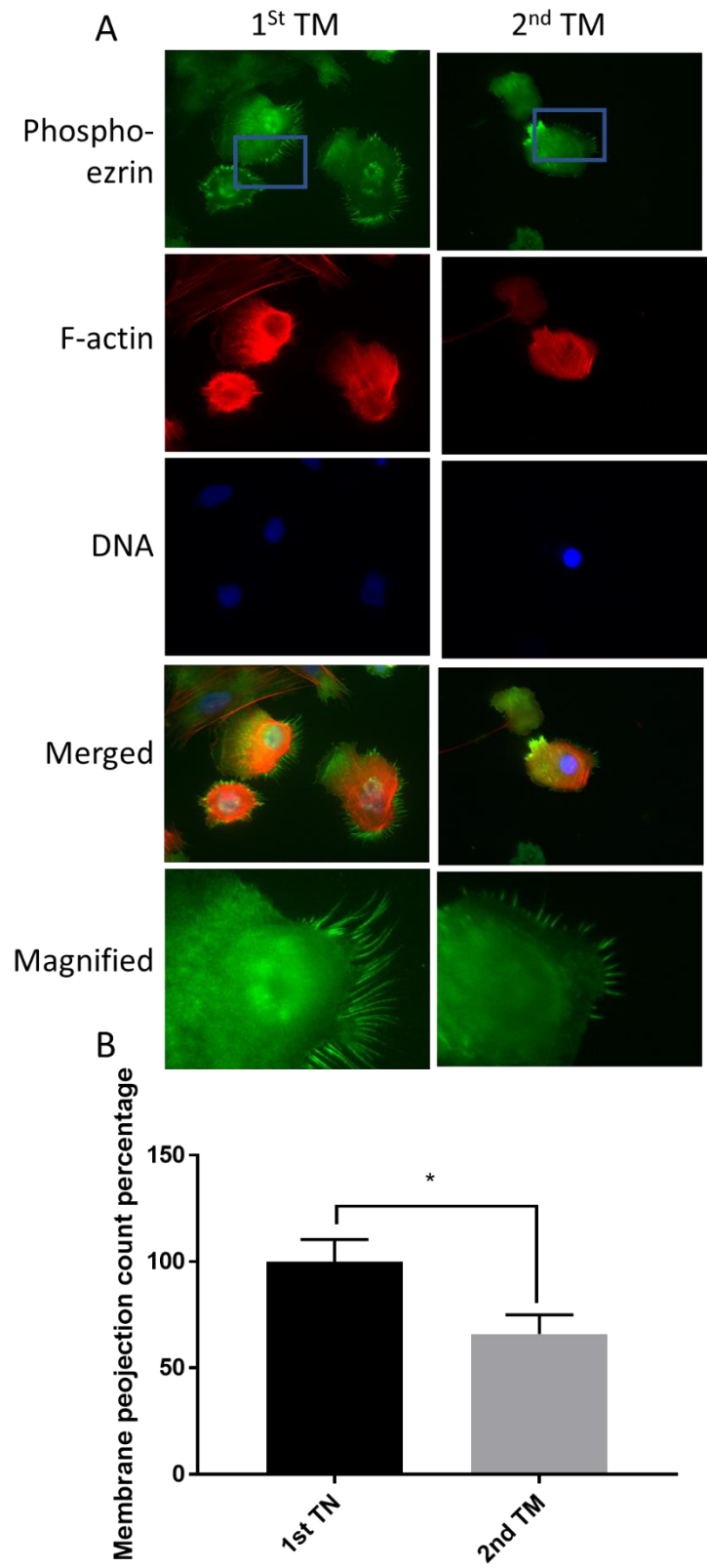


**Figure 4.19 Phospho-ezrin localisation in EVT<sub>s</sub> from first and second trimester.** The primary EVT<sub>s</sub> from week 9 (first trimester) and week 16 (second trimester) of gestation were seeded on

fibronectin-coated coverslips and incubated for 24 hours. Panel A shows phospho-ezrin visualised with FITC, F-actin with rhodamine phalloidin and DNA with DAPI. The images were taken at 63x magnification. Panel B shows the average memorable projection count per cell, represented as percentage. The error bars represent SEM (\* P<0.05). N = 1. Total sample size = 12 for each condition.

#### 4.2.20. Ezrin inhibition in primary EVT<sub>s</sub>

Having shown the effect of ezrin inhibition in EVT cell lines and the subsequent effects on their motility and invasion, we next aimed to carry out loss of function experiments in primary EVT<sub>s</sub>. To facilitate this, and in view of the key requirement for ezrin to be phosphorylated at residue Thr567, a step that is necessary for its association with the membrane and actin cytoskeleton, we set about to inhibit this through the use of the ezrin inhibitor NSC668394 as previously explained. For this aim, primary EVT<sub>s</sub>, isolated from first trimester human placenta, were seeded on fibronectin-coated glass coverslips while being treated with 5 µM ezrin inhibitor NSC668394, or with no treatment as control. 24 hours following seeding, the cells were incubated with anti-phospho-ezrin and then secondary FITC-conjugated secondary antibody as well as phalloidin. The inhibitor altered the localisation pattern of the protein by significantly (P<0.001) reducing the microvillous structures, by 60% (Table 4.4) and by making it relatively more abundant within the cytoplasm, rather than the membrane (Figure 4.20).

	Membrane projection per cell as percentage ± SEM (n=12)	P value (compared with control)
Control	100 ± 10.43	N/A
NSC668394	44.88 ± 7.07	0.0004

**Table 4.4 Average membrane projection count per cell in primary EVT<sub>s</sub>.** Primary first trimester EVT<sub>s</sub> were seeded on fibronectin-coated coverslips, while being treated with NSC668394 ezrin-inhibitor and were left to attach for 24 hours. The cells were then fixed and stained for phospho-ezrin. The microvillous projections were counted on all cells in each image.

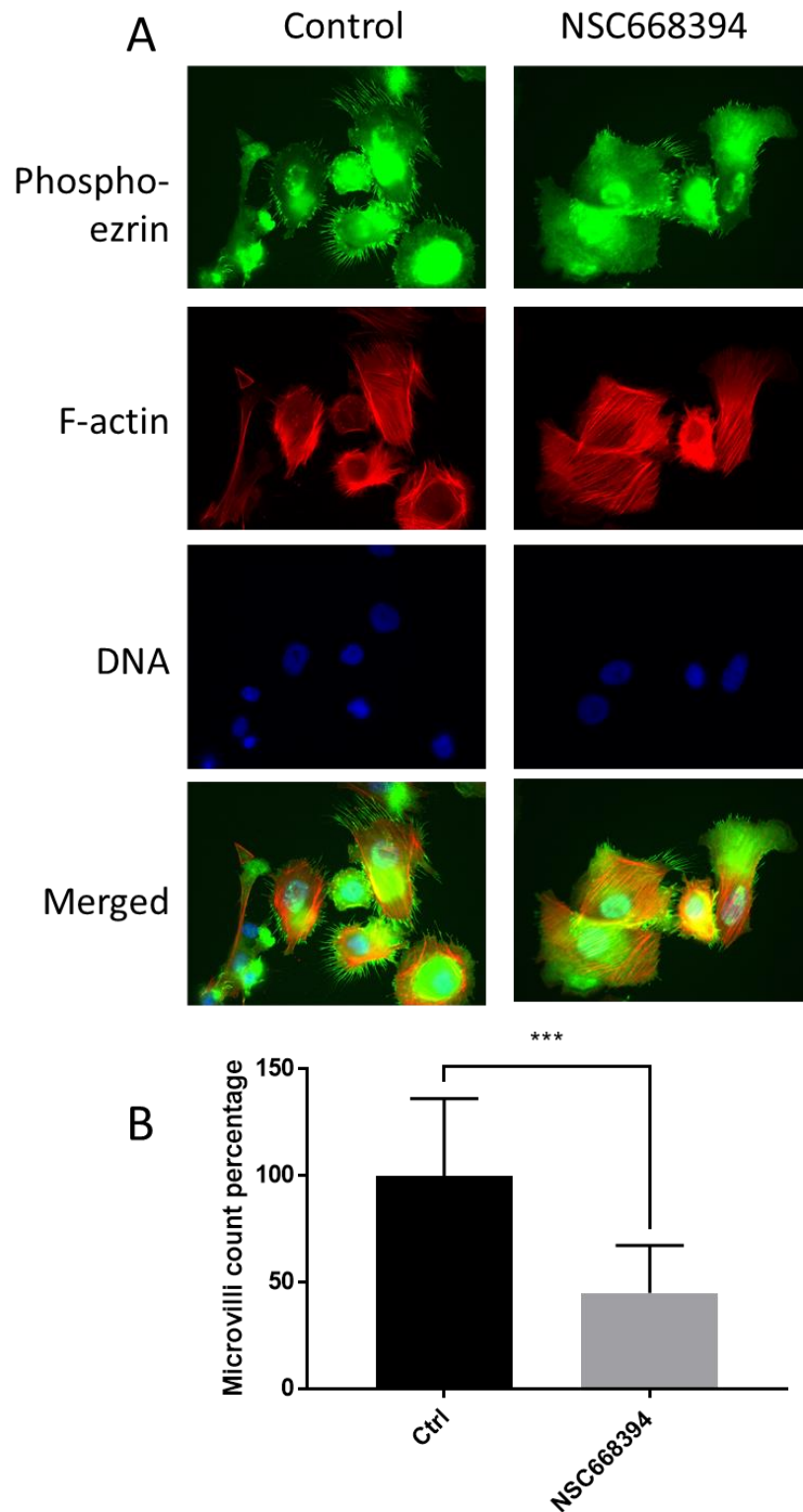


**Figure 4.20 The effect of ezrin inhibition on primary EVT morphology.** The primary EVTs were seeded on fibronectin-coated coverslips while being treated with NSC668394, or with no treatment as control, and incubated for 24 hours. Phospho-ezrin was visualised with FITC, F-

actin with rhodamine phalloidin and DNA with DAPI. The images were taken at 63x magnification. The error bars represent SEM (\*\*\*)  $P < 0.001$ .  $N = 1$ . Sample size for each condition = 12.

#### **4.2.21. The effect of ezrin inhibition on the motility of primary EVTs**

Having shown the effect of ezrin inhibition on the motility of our EVT cell lines, and further demonstrated the effect of NSC668394 on phospho-ezrin localisation in primary EVT<sub>s</sub>, we then looked to determine whether the same inhibition would affect the motility of primary EVT<sub>s</sub>. To do this, primary EVT<sub>s</sub> from first trimester human placenta were seeded in transwells, while being treated with 5  $\mu$ M ezrin inhibitor NSC668394, or with no treatment as control. After 24 hours, the migrated cells were fixed, stained and counted on random fields at 20x magnification and the average number of migrated cells were compared in the treated and the non-treated cells. The inhibition of ezrin in primary EVT<sub>s</sub> significantly ( $P < 0.0001$ ) reduced their migration by 30% (Figure 4.21).

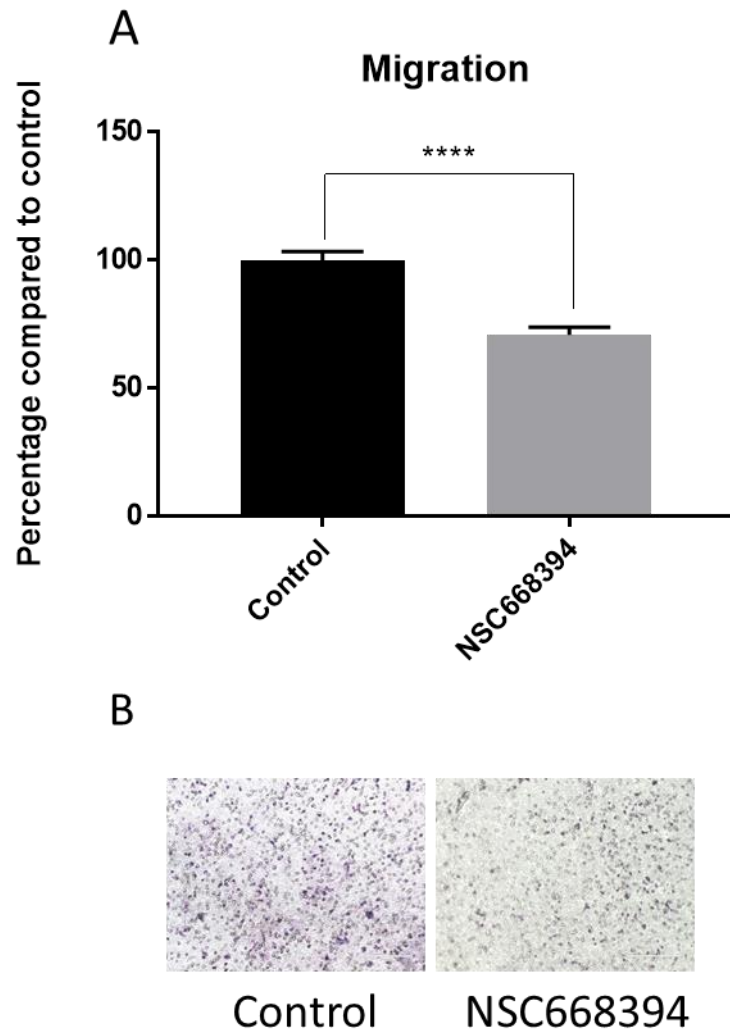


**Figure 4.21 Ezrin inhibition leads to motility reduction in primary EVT.** Primary EVT cells were seeded in transwells without treatment or while being treated with NSC668394. After 24 hours, the transwells were fixed, stained and the stained cells were counted at 20x magnification. The graph (panel A) shows the average cell count percentage compared with control and the error bars represent SEM (\*\*\*\*  $p < 0.0001$ ). Panels B shows representative fields of fixed and stained transwells. N = 3. Sample size = 18 for each condition.

#### **4.2.22. The effect of ezrin inhibition on the invasion of primary EVTs**

We showed that the inhibition of ezrin significantly reduces migration in primate EVT. Here, we aimed to find out if this inhibition also affects EVT invasion. For this purpose, 35,000 primary EVT from first trimester human placenta were seeded on Matrigel-coated transwells, while being treated with 5  $\mu$ M ezrin inhibitor NSC668394, or with no treatment as control. The cells were left to invade for 24 hours, prior to fixation and staining. The cells were counted on random fields at 20x magnification and the average number of migrated cells were compared in the treated and the non-treated cells. The inhibition of ezrin in the primary EVT significantly reduced invasion by 20% ( $P < 0.0001$ ) (Figure 4.22). N = 3.

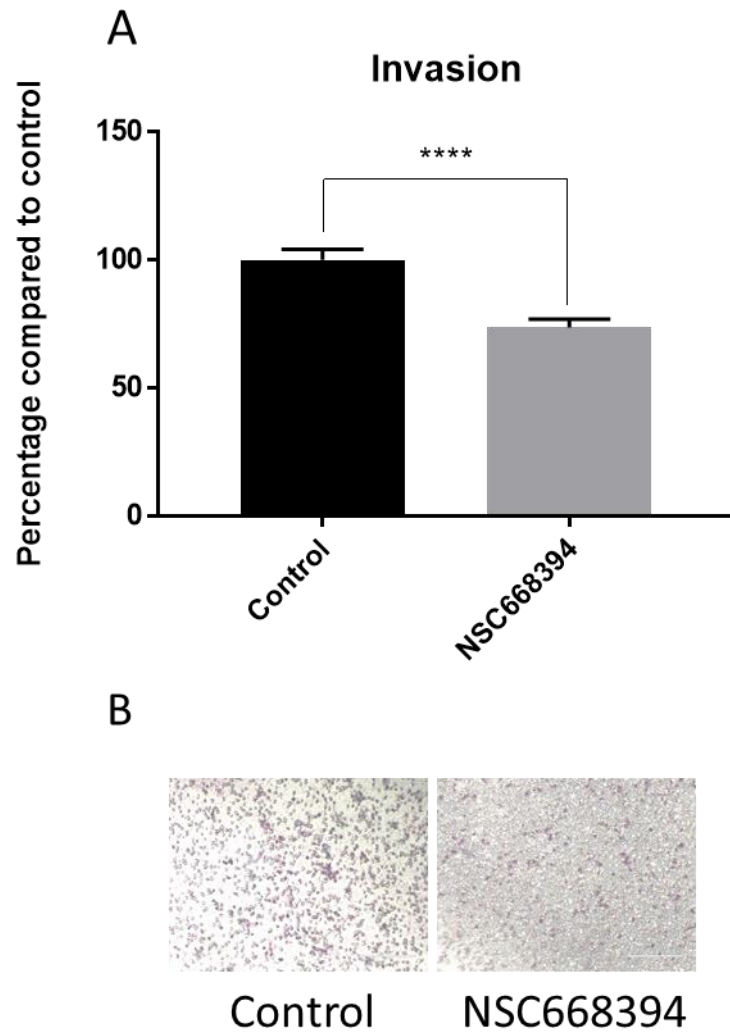


**Figure 4.22 Ezrin inhibition leads to invasion reduction in primary EVT.** Primary EVT cells were seeded in Matrigel-coated transwells without treatment or while being treated with NSC668394. After 24 hours, the transwells were fixed, stained and the stained cells were counted at 20x magnification. The graph (panel A) shows average cell count percentage compared with control and the error bars represent SEM (\*\*\*\*  $p < 0.0001$ ). Panels B shows representative fields of fixed and stained transwells.  $N = 3$ . Sample size = 6 for each condition.

### 4.2.23. Ezrin inhibition does not affect FAs in primary first trimester EVT

Having shown the reduction in in the relative size and the number of FAs in HTR8/SVneo cell line, upon ezrin phosphorylation inhibition (4.2.17), here we aimed to study the effect of ezrin inhibition on FAs in primary first trimester EVT. For this purpose, primary EVT were seeded on fibronectin-coated glass coverslips, while they were treated with 5  $\mu$ M NSC668394, along with non-treated control cells. The cells were left to attach for 24. The coverslips were prepared and incubated with primary anti-paxillin antibody, followed by incubation with secondary FITC-conjugated antibody and rhodamine phalloidin, before mounting and viewing. The cells treated with NSC668394 showed no significant difference in their FA count ( $P = 0.277$ ) (Table 4.5), when compared with the control cells (Figure 4.23).

	Percentage focal adhesions per cell $\pm$ SEM (n=20)	P value (compared with control)
Control	100 $\pm$ 11.44	N/A
NSC668394	120.67 $\pm$ 13.33	0.277

**Table 4.5 Average FA count per cell in primary EVT.** Primary first trimester EVT were seeded on fibronectin-coated coverslips, while being treated with NSC668394 ezrin inhibitor and were left to attach for 24 hours. The cells were then fixed and stained for paxillin. The FAs were counted on all cells in each image.

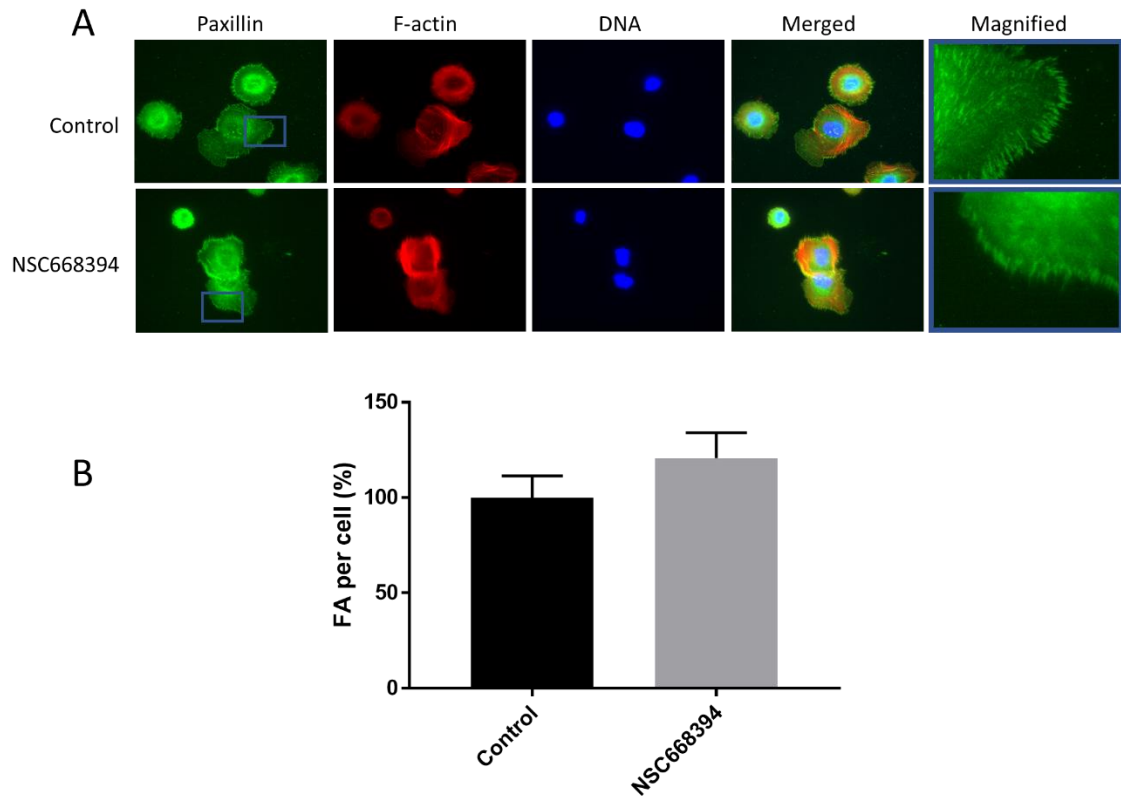


**Figure 4.23 Ezrin inhibition does not affect the FAs in HTR8/SVneo.** Primary EVT<sub>s</sub> were seeded on fibronectin-coated coverslips while being treated with NSC668394 ezrin inhibitor, along with non-treated control and were left to attach for 24 hours. Paxillin was visualised with FITC, F-actin with rhodamine phalloidin and DNA with DAPI. The images were taken at 63x magnification. Panel A shows staining on paxillin, F-actin and DNA. Panel B shows average FA count in NSC668394 treated EVT<sub>s</sub> compared with the non-treated controls. The error bars represent SEM. N = 2. Sample size = 20 for each condition.

### 4.3. Discussion

In this chapter, we have studied how ezrin, a protein that plays a key role in tumour invasion and metastasis (Fehon, McClatchey & Bretscher 2010; McClatchey 2003, 2014), also regulates motility and invasion in trophoblasts cells, using cell lines or primary cells, along with ex vivo work carried out on human placental sections.

By staining the human placental samples available, through specific IHC, we showed that the highest level of ezrin was seen during the first and second trimesters of gestation, while its expression was significantly reduced in third trimester placenta samples (Figure 4.2). Indicating the potential involvement of the protein in earlier stages of gestation. Similarly, placental ezrin expression was shown to decrease in late pregnancy in rats (Higuchi et al. 2010). Moreover, another study showed higher expression levels of ERM proteins in implantation-competent blastocyst compared with dormant blastocyst in mice (Matsumoto et al. 2004). Although IHC did not show a significant difference between ezrin levels in placenta villi sections from first and second trimesters (Figure 4.2), there was a significant difference between the localisation of the active form of ezrin (phospho-ezrin Thr567) in the primary EVT's isolated from these two time-points (Figure 4.19), as phospho-ezrin in the younger EVT's showed more localisation within the nucleus as well as the membrane protrusions, which looked relatively longer as well.

Next, to find out more about the localisation and cell-specific expression of ezrin in human placenta villi, we stained serial sections of first trimester human placenta for ezrin, cytokeratin-7 and HLA-G by IHC. The sections showed ezrin localisation in the cytoplasm of cytotrophoblasts and syncytiotrophoblasts, with the highest levels seen in the apical membrane of the syncytiotrophoblasts (Figure 4.3), similar to what was reported previously (Berryman, Franck & Bretscher 1993; Pidoux et al. 2014). Ezrin has been suggested to play a role in trophoblast fusion and the formation of the syncytium (Pidoux et al. 2014). We also detected ezrin in the invasive trophoblast columns, localised within the cytoplasmic and apical membrane the EVT's (Figure 4.3).

Having shown ezrin expression in placenta sections, we next aimed to find out about its expression in the trophoblast cell lines available to us and have been described in earlier chapters (Jeg-3, BeWo, HTR8/SVneo, SW71, SHGPL4 and -5) as well as primary EVT's isolated from first trimester human placenta. We showed that ezrin is ubiquitously expressed in all of our trophoblast cell lines (Figure 4.4), while Jeg-3 cells expressed the highest amounts relative to the other cells. Ezrin expression was also detected in the primary first trimester EVT's (Figure 4.18).

Having shown that ezrin is expressed in our trophoblast cell lines and primary EVT, we set about to learn about its localisation. Immunofluorescence staining showed that ezrin was localised in the cytoplasm of all cells (Figure 4.5). Ezrin was also detectable in the plasma membrane and the membrane projections of primary first trimester EVT (Figure 4.18) and HTR8/SVneo, SW71, SGHPL-5 and BeWo cells, while the other two cell lines (Jeg-3 and SGHPL-4) showed a different localisation pattern, showing ezrin localisation within their cytoplasm only (Figure 4.5). Different localisation of the proteins might indicate the level of the protein activation, as the active (open) ezrin, similar to other ERM family members, links the cytoskeleton to the plasma membrane via PIP<sub>2</sub>, and therefore is localised within the cell cortex, while the inactive (closed) ezrin is located in the cytoplasm (Fehon, McClatchey & Bretscher 2010).

Unfolding and activation of ezrin happens by the interaction between plasma membrane PIP<sub>2</sub> and the N-terminal side of ezrin, followed by its phosphorylation at a conserved Thr567 residue at the C-terminal side of the protein (Fievet et al. 2004). Here, to find out about the levels of the active form of the protein in our trophoblast cell lines, we probed the cell-lysates for phospho-ezrin (Thr567), by western blot. showed that our trophoblast cell lines expressed different amounts of phospho-ezrin (Figure 4.4). The highest levels of phospho-ezrin were seen in HTR8/SVneo cells. This was in line with the immunofluorescence staining, which showed the HTR8/SVneo cells have the highest levels of cortical ezrin compared with our other trophoblast cell lines (Figure 4.5). In contrast, moderate levels of phospho-ezrin expression in Jeg-3 (measured by western blot) (Figure 4.4) was not in line with ezrin's non-detectable membrane localisation (visualised by immunofluorescence staining) in these cells (Figure 4.5). One possible explanation for this could be that, as explained earlier, for ezrin activation, the phosphorylation of the protein at Thr567, happens after the protein interaction with the membrane-bound PIP<sub>2</sub>, a process that leads to ezrin's conformational change (Fievet et al. 2004). Therefore, high amount of phospho-Thr567 ezrin alone, does not guarantee high ezrin activation, similar to another study, which reported that Thr567 phosphorylation is required for cell spreading, but is not sufficient (Parnell et al. 2015).

Ezrin over-expression has been associated with enhanced cellular motility and invasion, as well as metastasis and poor prognosis for cancer patients (Makitie et al. 2001; Meng et al. 2010; Weng et al. 2005). Here, we aimed to see how this protein regulates motility and invasion in trophoblasts through loss of functions experiments. We used four different sequences of siRNA against ezrin and showed that two of them (siRNA 7 and 9) were the most effective in knocking down ezrin in HTR8/SVneo and SW71 cells (Figure 4.6). None of the ezrin siRNA sequences significantly reduced protein expression, in Jeg-3 (Figure 4.6). We then showed that the reduction in ezrin expression significantly reduced both motility (Figure 4.8) and invasion (Figure 4.9) in

HTR8/SVneo and SW71 cells, while not affecting the Jeg-3 cells. The ineffectiveness of ezrin knockdown in Jeg-3 motility and invasion cells might have been due to the different localisation pattern of the protein, which was shown with immunofluorescence staining, and suggested lower membrane-bound ezrin in these cells (Figure 4.5). However, this also might have been due to the ineffectiveness of our specific siRNA sequences in Jeg-3 cells, since successful ezrin knockdown in these cells has been reported previously with a different sequence of ezrin siRNA, when used at a higher concentration (30 nM) (Viswanatha et al. 2012). In line with our findings, another study showed that ezrin could partially restore invasion in HTR8/SVneo cells with titanium dioxide nanoparticles-induced invasion impairment (Mao et al. 2019). In cancer cells, ezrin knockdown also has been shown to reduce motility and invasion (Fan et al. 2011; Meng et al. 2010; Tang et al. 2019; Zhang et al. 2014). However, despite being a key metastasis regulator (Briggs et al. 2012; Lin & Chen 2013), the over-expression of this protein does not always enhance motility, invasion and metastasis (Elliott et al. 2005).

Through regression analysis, it was shown that there was a positive correlation between the ezrin expression levels, in control, negative control and siRNA 7 and 9 treated HTR8/SVneo and SW71 cells. This correlation was relatively stronger in SW71 cell ( $r = 0.94$  for motility,  $r = 0.96$  for invasion in SW71 compared with  $r = 0.86$  for motility,  $r = 0.86$  for invasion in Jeg-3 cells) and was only significant in SW71 cells (Figure 4.10). The correlation between ezrin expression and motility/invasion has not been previously shown in any cells.

The role of ezrin in trophoblast motility and invasion was validated by showing the ineffectiveness of ezrin knockdown on the viability and the metabolic activity of HTR8/SVneo and SW71 cells (Figure 4.7). This suggests that ezrin does not regulate cell proliferation in trophoblasts, similar to what was shown in some types of tumour cell (Horwitz et al. 2016), where other studies have reported otherwise (Kishore et al. 2005; Quan et al. 2019).

As mentioned in the previous chapter, rapid formation and turnover of the FAs during directional cell movement pulls the cell body forward, while their rapid turnover at the rear end detaches them from the ECM. Here, we aimed to find out if the ezrin-induced cell motility involves observable FA changes, by analysing the localisation pattern of paxillin, an FA component, upon ezrin knockdown. Ezrin has previously been shown to regulate FA dynamics in breast cancer (Hoskin et al. 2015). In our trophoblast cell lines HTR8/SVneo and SW71 however, ezrin knockdown did not result in detectable changes in the overall size or the number of the FAs (Figure 4.11). Although, we cannot rule out the possible changes in the phosphorylation state of the FA components, which have been reported to take place as response to changes in cellular dynamics (Katz et al. 2000; Zamir et al. 2000). Despite the usual association of FA and cell

adhesion dynamics with cell migration (Nagano et al. 2012), not all cells show similar changes in their FAs, due to the difference in their adhesive structures. For example, fast-moving cells seem to have highly dynamic and smaller FAs, while slower-moving cells seem to have larger and more stable FAs (Parsons, Horwitz & Schwartz 2010). This, however, might not necessarily be the case in here, since HTR8/SVneo cells did in fact show a significant reduction in the relative size and the number of FAs, due to S100P expression, in the previous chapter (Figure 3.14). Additionally, cell adhesion does not always correlate with FA size and number. In fact, FA assembly has been shown to contribute to only a small percentage of adhesive strength (Gallant, Michael & García 2005). Furthered more, our FA analysis in fixed cells, is a limited process, which resents only a “snapshot” in a timeframe of a highly dynamic process, and therefore cannot guarantee to provide a holistic view.

Ezrin phosphorylation results in its activation and promotes phenotype changes such as the promotion of apical microvilli formation (Bonilha, Finnemann & Rodriguez-Boulan 1999; Dard et al. 2004) and enhanced migration and invasion (Mak et al. 2012; Zhan et al. 2019). Ezrin phosphorylation at Thr567 by members of the PKC family (Ng et al. 2001; Pietromonaco et al. 1998; Wald et al. 2008), which was shown to be dependent on the p38 MAP-kinase activity (Zhao et al. 2004), has been reported to be crucial for the ezrin-mediated membrane-cytoskeleton anchorage (Zhu et al. 2007) and was suggested to play an important role in metastasis (Jin et al. 2014; Krishnan et al. 2006). Having shown that ezrin knockdown reduces motility (Figure 4.8) and invasion (Figure 4.9) in our EVT cell lines, and that the expression of the phosphorylated form of the protein does not follow a similar pattern as the expression of the total pool of the protein amongst our trophoblast cell lines (Figure 4.4), we were interested to see how the inhibition of ezrin phosphorylation affects our trophoblast cells. For this purpose, HTR8/SVneo and SW71 cells were treated with NSC668394, a compound that prevents ezrin phosphorylation at Thr567, without affecting PKC activity and has been shown to reduce tumour cell motility and causing developmental defects in zebrafish (Bulut et al. 2012) as well as up-regulation of the expression of stress response genes (Celik et al. 2016). Following 24 hours of treatment, through western blot analysis, we showed that the drug has significantly reduced the expression level of the phospho-ezrin in HTR8/SVneo cells, but did not show the same effect in SW71 cells (Figure 4.12). The drug also reduced membrane-bound and nuclear ezrin as well as its active form in HTR8/SVneo cells, without affecting the localisation of either in SW71 cells (Figure 4.13).

Ezrin inhibition reduced both motility (Figure 4.15) and invasion (Figure 4.16) of HTR8/SVneo cells (by 80% and 70% respectively), to a greater extent than the effect seen by protein knockdown (20% for motility and invasion with siRNA 7 and 50% for motility and invasion with

siRNA 9) (Figure 4.8 and Figure 4.9), without affecting the viability of either HTR8/SVneo or SW71 cells (Figure 4.14). Ezrin inhibition also reduced membrane protrusions (Figure 4.19) and significantly decreased both migration (Figure 4.20) and invasion (Figure 4.21) of primary first trimester EVT cells by 30% and 20%, respectively. One possible explanation for the lower effectiveness of ezrin inhibition on the motility and invasion of primary EVT cells compared to HTR8/SVneo cells (30 and 20% compared with 80 and 70%, respectively) might have been due to not using a serum attractant. Serum starving the cells and using a serum attractant has been shown to significantly enhance cell migration in transwell assays (Justus et al. 2014). Additionally, we showed that the changes due to S100P knockdown were more significant in Jeg-3 cells, when they were seeded at higher numbers (Figure 3.7), and this might also, at least partially, explain our relatively lower effect of ezrin inhibition on EVT motility/invasion, compared with the HTR8/SVneo cells, indicating a requirement for EVT cell number optimisation for motility and invasion assays.

Similarly, redistribution of ezrin in membrane and microvilli has been associated with enhanced motility, invasion and proliferation in cancer cells (Curto & McClatchey 2004). Membrane and nuclear localisation of the phosphorylated form of the protein has been linked with metastasis (Di Cristofano et al. 2010), while others have shown the loss of ezrin from the membrane and elevated levels of ezrin in the cytoplasm to be linked with metastasis in different cancers (Arslan et al. 2012; Di Cristofano et al. 2010; Elzagheid et al. 2008; Sarrio et al. 2006; Schlecht et al. 2012).

Interestingly, in contrast to our results with ezrin knockdown, ezrin inhibition also resulted in an increase in both the number and the relative size of FAs in HTR8/SVneo cells (Figure 4.17). This contradictory observation might possibly be due to the greater effect of the inhibition compared with the protein knockdown, although we do not currently have further evidence to support this hypothesis.

Since the effectiveness of ezrin phosphorylation inhibition was more prominent on both motility/invasion (80% and 70% reduction in motility and invasion, respectively, in HTR8/SVneo cells) and FA dynamics, compared with the effect seen with ezrin downregulation (20% by siRNA 7 and 50% by siRNA 9) on both motility and invasion of HTR8/SVneo cells, we suggest the possibility that the availability of active ezrin might play a more crucial role in cytoskeleton regulation in trophoblasts, compared with the total protein availability. In contrast to this, a study has reported the significance of total ezrin levels in the prediction of metastasis and prognosis in osteosarcoma, while the phospho-ezrin levels were not as relevant (Di Cristofano et al. 2010).

Unlike in HTR8/Svneo cells, ezrin inhibition did not affect the number or the relative size of the FAs in primary EVT<sub>s</sub> (Figure 4.23). Other than the earlier possible explanations for our similar observation on the ineffectiveness of ezrin knockdown on the FAs, another explanation for this could be that, although the term “phospho-ezrin”, generally refers to phosphorylated Thr567 residue on the protein, the most well-known region in protein activation, other phosphorylated residues of ezrin, such as tyrosine 477 (Mak et al. 2012; Naba et al. 2008), serine 66 (Zhou et al. 2003), threonine 235 (Yang & Hinds 2003) and tyrosine 145 (Srivastava et al. 2005) also have been associated with its activation. Perhaps studying the role of these less-studied regions, and potentially other unknown regions, would give us a better understanding of how ezrin regulates the cytoskeletal changes in trophoblasts. Moreover, comparing the level and the localisation pattern of the active form of the ezrin in placental villi and the isolated EVT<sub>s</sub> from different gestational ages, as well as its proportional levels compared with total ezrin might give us a better insight about how this protein regulates trophoblasts and implantation. Additionally, we used 24 hours of treatment with the ezrin inhibitor-drug for our western blot, immunofluorescence and motility/invasion assays, while the half-life of active ezrin is in fact rather long (> 1 day) (Grune et al. 2002), and this might have affected our results. Perhaps longer treatment of cells with NSC668394 might have increased the effects we observed in HTR8/SVneo and primary EVT<sub>s</sub>, and even the SW71 cells.

In conclusion, we report that, due to its expression pattern in placental villi throughout the gestation period, and its role in trophoblast motility and invasion, ezrin might potentially play an important role in early placenta development and implantation.

## Chapter 5.

# IQGAP1 regulates trophoblast motility and invasion

## 5.1. Introduction

IQGAP1 is a member of the eukaryotic IQGAP family of scaffold proteins, which have three members in mammals: IQGAP1, IQGAP2, and IQGAP3 (Brown & Sacks 2006). Although IQGAP1 shows ubiquitous expression in all mammals, it is not essential for murine development, as IQGAP1 null mutants were shown to develop normally, except for showing significantly higher late-onset gastric hyperplasia (Li et al. 2000) and heart malfunction compared with wild-type animals (Sbroggiò et al. 2011). IQGAP1 is a regulator of the MAPK (Roy, Li and Sacks, 2004 and 2005) and Wnt signalling pathways (Carmon et al. 2014), F-actin polymerisation (Mateer et al. 2002), cell proliferation (Wang et al. 2009), adhesion (Noritake et al. 2005), motility and invasion (Dong et al. 2008; Hayashi et al. 2010; Mataraza et al. 2003). In physiological conditions, IQGAP1 has been associated with cell adhesion in the kidneys (Rigothier et al. 2012), neuronal proliferation and migration (Li et al. 2005), endothelial cell proliferation and migration in the cardiovascular system (Kohno et al. 2013; Yamaoka-Tojo et al. 2004), smooth muscle cell contraction in the lungs (Bhattacharya et al. 2014) and facilitating insulin secretion through regulating vesicle trafficking (Rittmeyer et al. 2008), while its over-expression and modified localisation within the cells has been associated with carcinogenesis (McDonald et al. 2007; Nabeshima et al. 2002). IQGAP1 expression has been detected in placental microvilli (Berryman & Bretscher 2000; Weissbach et al. 1994) and the syncytiotrophoblast membrane (Paradela et al. 2005), but, to this date, no roles have been reported to be associated with this protein in trophoblasts or the placenta.

### Aim

The role of IQGAP1 is clearly established as a marker of metastasis through its role in promoting cancer cell motility and invasion (White, Brown & Sacks 2009). However, a function for this protein in the context of trophoblast physiology is unknown. We propose to study whether there are changes in trophoblastic IQGAP1 expression levels during gestation and whether its presence regulates trophoblast motility and invasion.

### Objectives

- Establish IQGAP1 expression in placenta
- Establish IQGAP1 expression in trophoblast cell lines
- Test whether modulating IQGAP1 expression affects trophoblast motility and invasion

- Decipher the molecular mechanisms of IQGAP1-promoted motility and invasion in trophoblasts

## **5.2. Results**

### **5.2.1. Immunohistochemical staining optimisation**

Over the course of the study so far, we have aimed to focus our work on determining whether metastasis-associated proteins, namely S100P and ezrin, are expressed during placental development and whether their expression affects trophoblast motility/invasion.

In this chapter, we sought to follow a similar approach in relation to IQGAP1 by looking at its localisation and expression levels in samples of first, second and third trimester human placental villi. First, the optimal concentration of the primary antibody against IQGAP1 was optimised as below.

In order to find the lowest concentration of primary anti-IQGAP1 antibody applicable for the IHC in this part, two dilutions of the antibody (1 and 0.5 µg/ml anti-IQGAP1) were tested for the staining of first trimester samples.

Concentrations of IQGAP antibody at either 1 or 0.5 µg/ml showed efficient staining for IQGAP1, highlighting IQGAP1 localisation within the trophoblasts surrounding placental villi, with weak staining detectable in some parts of the stroma, located in the core of the villi (Figure 5.1).

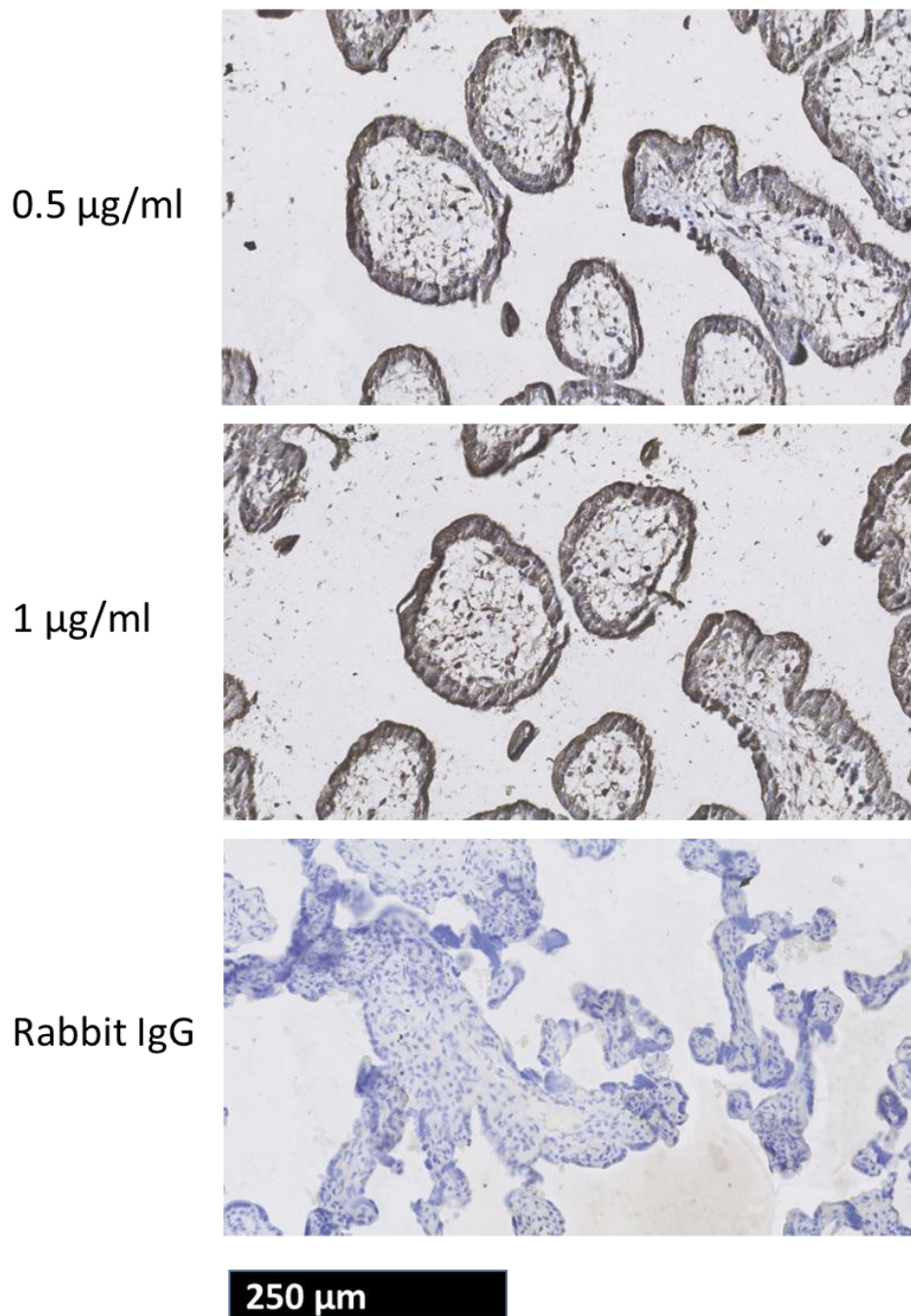


**Figure 5.1 IQGAP1 antibody concentration optimisation for IHC.** Wax-embedded human first trimester placental villi sections were prepared and incubated with two concentrations of primary anti-IQGAP1, along with rabbit IgG as negative control, before being incubated with secondary antibody, and finally were stained using avidin-biotin complex and DAB chromogen and counter-stained using haematoxylin.



### **5.2.2. Placental IQGAP1 expression decreases gradually during gestation**

Having optimised staining for IQGAP1, we now wanted to determine how IQGAP1 levels were affected during gestation as well as its localisation during placental development. To this end, three samples from first trimester, three from second trimester and four third trimester placenta samples were stained for IQGAP1 as detailed earlier. Images were analysed by densitometry using Fiji-ImageJ software. During the first trimester, IQGAP1 expression was detected very strongly in the apical membrane of syncytiotrophoblasts and to a lesser extent in the cytoplasm of syncytiotrophoblasts, as well as in the cytoplasm of cytotrophoblasts (Figure 5.2 5.2 B). The expression of IQGAP1 in the second trimester was reduced by 20% when compared to the first trimester ( $P<0.05$ ), while the third trimester samples expressed very small amounts of IQGAP1 compared with the first trimester (50% lower) ( $P<0.001$ ) and 30% lower compared with the second trimester (Figure 5.2 A and C).

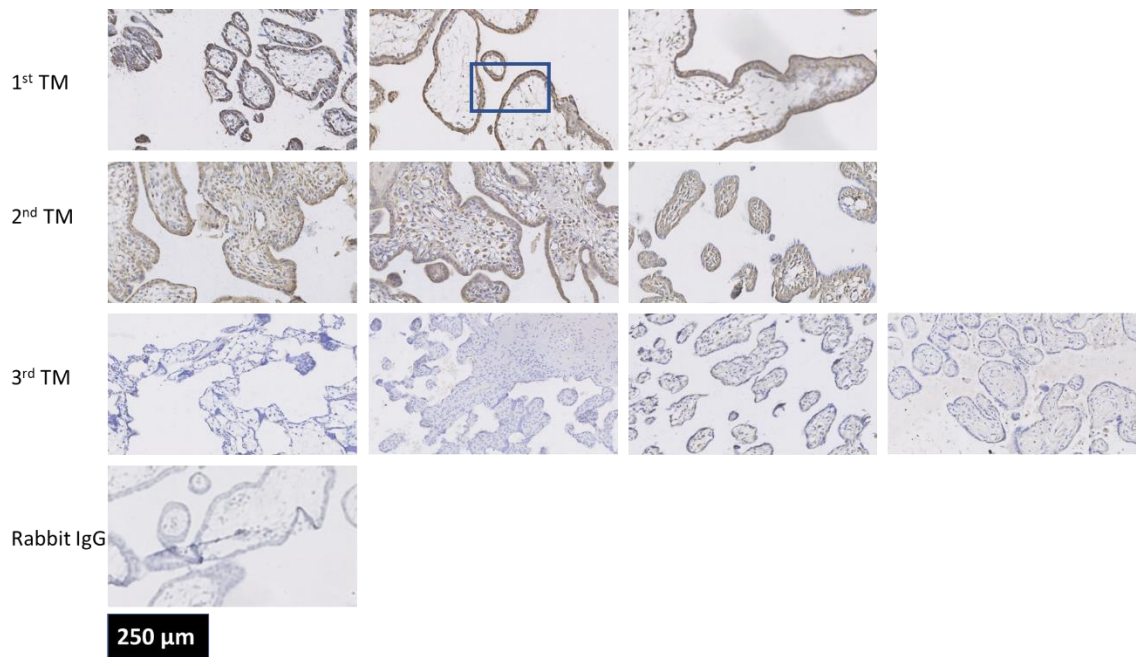


**Figure 5.2 IQGAP1 expression in human placenta is the highest during the first trimester of gestation.** Wax-embedded human first trimester placental villi sections were prepared and incubated with anti-IQGAP1 antibody as well as rabbit IgG as negative control, before being incubated with secondary antibody, and finally staining using avidin-biotin complex and DAB chromogen and counter-staining using haematoxylin. Panel A shows representative images of human placental sections from first, second and third trimesters. Panel B shows a magnified image of one of the first trimester placenta sections, and panel C shows average IQGAP1 expression (calculated by densitometry) in different gestational ages. The error bars represent SD (\*  $P < 0.05$ , \*\*  $P < 0.01$ , \*\*\*  $P < 0.001$ ).  $N = 2$ . Total sample size for each trimester: 6 (1st), 6 (2nd) and 8 (3rd).

### **5.2.3. IQGAP1 is expressed in human trophoblasts and EVT**

Having shown that expression of IQGAP1 in placenta is highest in the early stages of placental development, we now wanted to learn more about its localisation and where it was expressed in first trimester samples using markers for trophoblast (cytokeratin 7) and more specifically EVT (HLA-G). Serial sections of wax-embedded first trimester human placental villi were prepared and incubated anti-IQGAP1, anti-cytokeratin 7, anti-HLA-G, anti-S100P or anti-ezrin as well as mouse and rabbit IgGs (as negative control) overnight, followed by secondary antibody incubation and development using avidin-biotin complex and DAB chromogen. The sections were counter stained with haematoxylin. IQGAP1 was shown to be expressed in the anchoring villi, colocalised with cytokeratin 7 in cyto- and syncytiotrophoblasts, with HLA-G in EVT, and with S100P and ezrin in cyto- and syncytiotrophoblasts as well as the EVT (Figure 5.3).

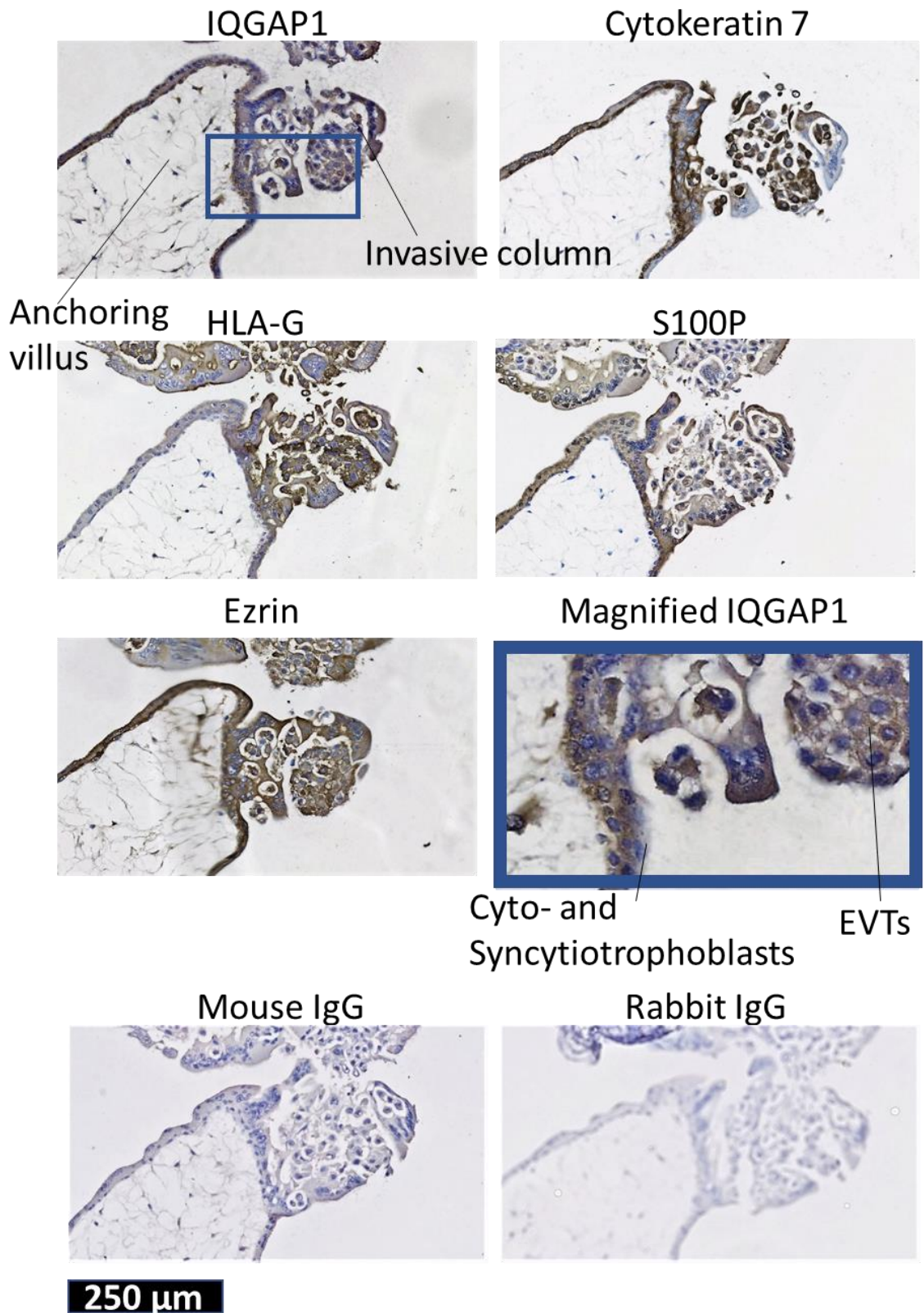


**Figure 5.3 IQGAP1 expression in human trophoblasts and EVT.** Serial sections of wax-embedded human first trimester placental villi were prepared and incubated with primary anti-

IQGAP1, anti-cytokeratin 7, anti-HLA-G, anti-S100P and anti-ezrin as well as mouse and rabbit IgGs as negative control, before being incubated with secondary antibodies, and finally were stained using avidin-biotin complex and DAB chromogen and counter-stained using haematoxylin. The images were taken at 20x magnification.

#### **5.2.4. IQGAP1 is expressed in human trophoblast cell lines**

Having demonstrated IQGAP1 expression in human placenta and more specifically in, trophoblast and EVT, we aimed to investigate whether IQGAP1 could also be detected in trophoblast cell lines. We sought to investigate IQGAP1 expression in the trophoblast cell lines Jeg-3 and BeWo as well as human first trimester EVT cell lines SW71, HTR8/SVneo, SGHPL-4 and SGHPL-5 by western blot.

IQGAP1 was found to be highly expressed in all human trophoblast cell lines used: Jeg-3, BeWo, SW71, HTR8/SVneo, SGHPL-4 and SGHPL-5. Compared with BeWo cells, HTR8/Svneo cells expressed 10% more, Jeg-3 cell expressed 30% more, SW71 expressed 20% less, SGHPL-4 expressed 50% less and SGHPL-5 expressed almost the same level of IQGAP1 protein (Figure 5.4).

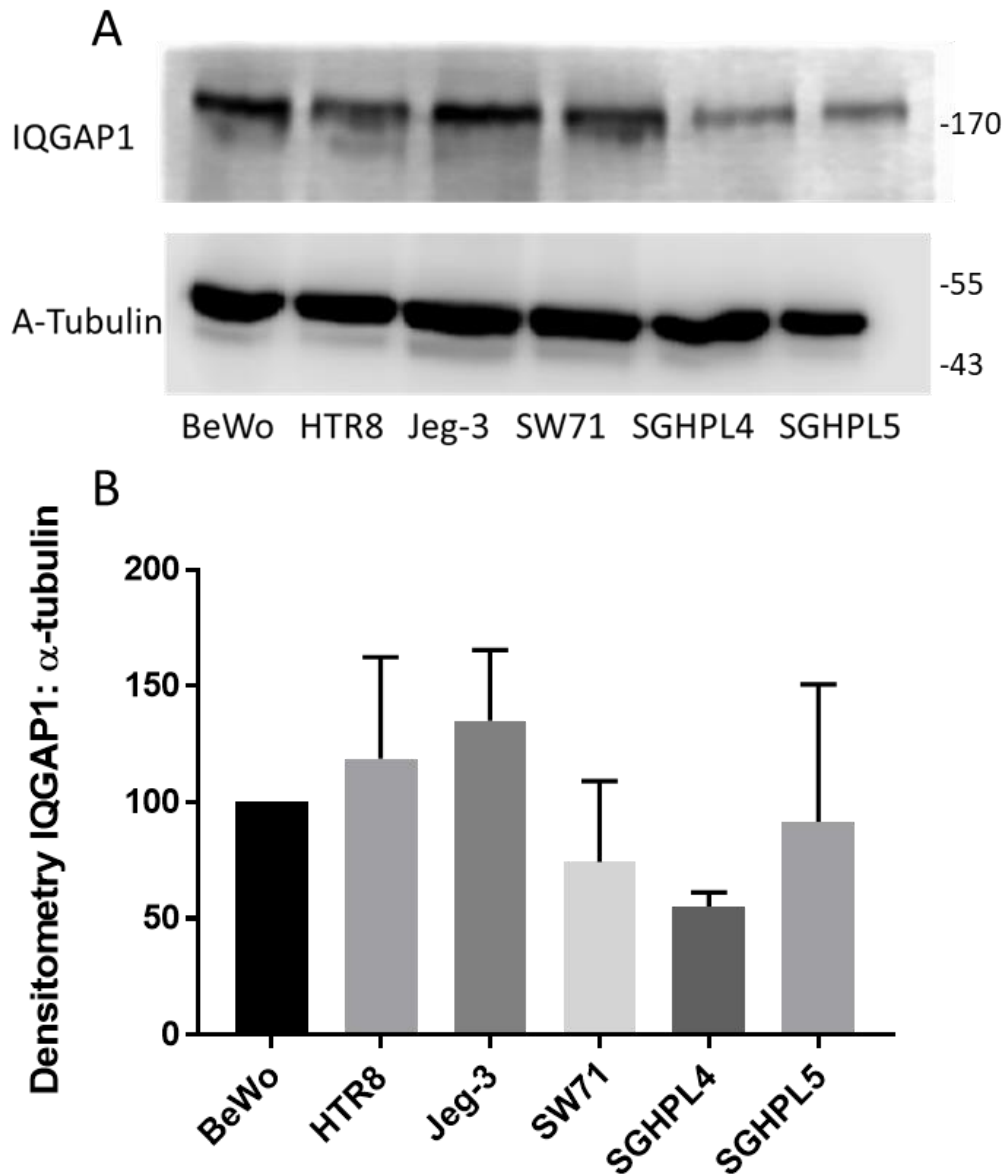


**Figure 5.4 IQGAP1 expression in human trophoblast cell lines.** Human trophoblast cell lines BeWo, HTR8/SVneo, Jeg-3, SW71, SGHPL-4 and SGHPL-5, were collected in protease inhibitor cocktail and sonicated, prior to being separated by 10% SDS-PAGE. The samples were probed for IQGAP1 and  $\alpha$ -tubulin by western blot. Expression levels were quantified by Image Studio Lite software and IQGAP1 expression levels were normalised to the housekeeping gene expression. Panel A shows the western blot bands for IQGAP1 and  $\alpha$ -tubulin, and panel B shows the densitometry. The error bars represent SD. N=3. All differences are non-significant ( $P>0.05$ ). Sample size = 3 for each cell line.

### **5.2.5. IQGAP1 localisation in human trophoblast cell lines**

Having shown that IQGAP1 is expressed in different trophoblast cell lines, we now aimed to study its cellular localisation. To do this, trophoblast cells BeWo, HTR8/SVneo, Jeg-3, SW71, SGHPL-4 and SGHPL-5 were incubated with primary anti-IQGAP1 antibody followed by secondary FITC-conjugated antibody and rhodamine phalloidin, before mounting and viewing. In HTR8/SVneo and SW71, IQGAP1 was localised within the nucleus, cytoplasm, and the membrane, being strongly detectable in the cell protrusions of HTR8/SVneo cells. In the rest of the trophoblasts (SGHPL-4, SGHPL-5, Jeg-3 and BeWo) however, IQGAP1 was detected within the membrane, the cytoplasm and around the nucleus, with the strongest peri-nuclear localisation seen in SGHPL-4 and -5 (Figure 5.5).

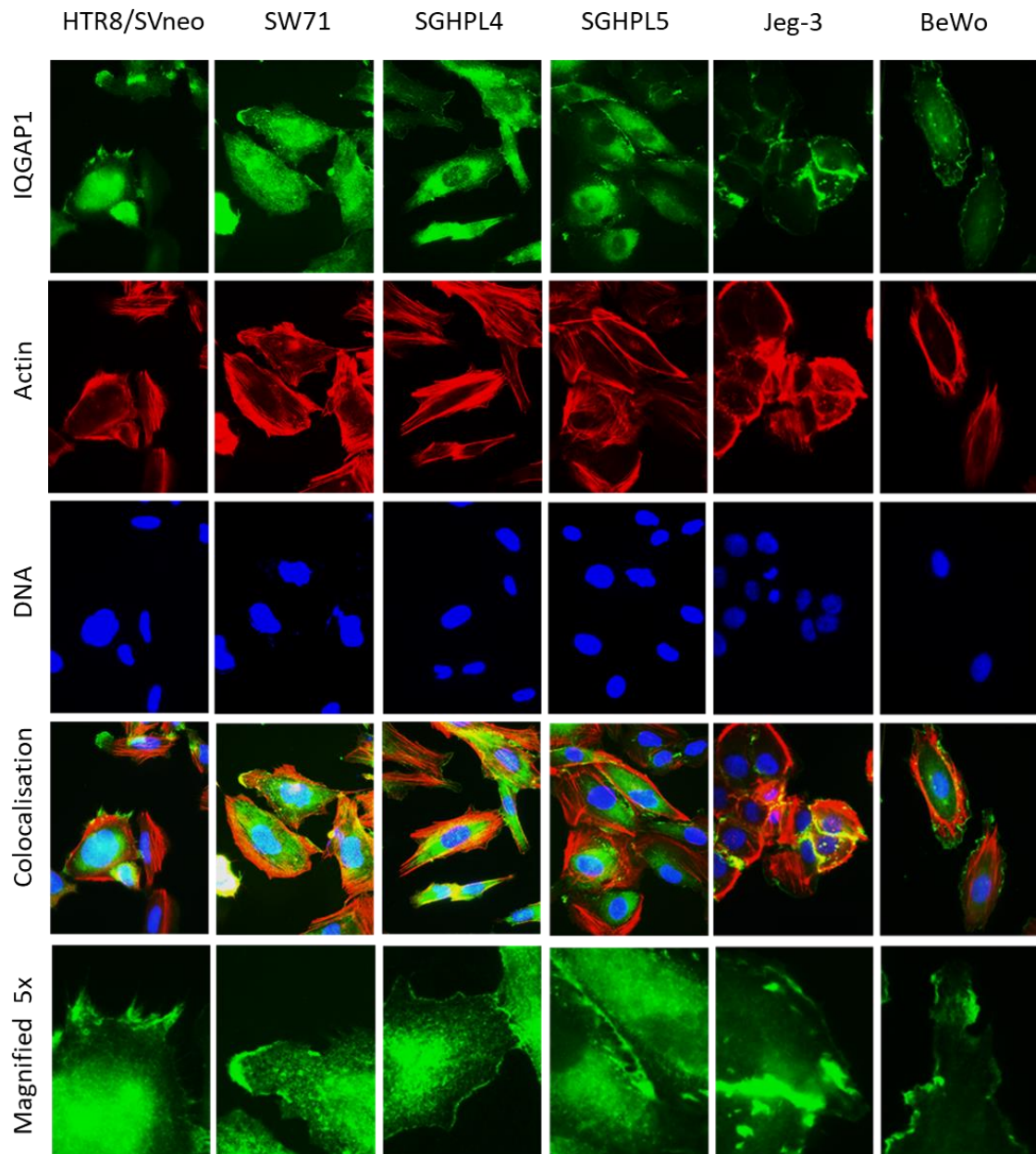


**Figure 5.5 IQGAP1 expression and localisation in trophoblast cell lines.** EVT cell lines HTR8/SVneo, SW71, SGHPL-4 and SGHPL-5 along with choriocarcinoma cell lines Jeg-3 and BeWo were seeded on fibronectin-coated coverslips. The cells were stained for IQGAP1, F-actin and DNA by immunofluorescence. The images were taken at 63x magnification.

### 5.2.6. IQGAP1 expression knockdown

Having confirmed the expression of IQGAP1 in EVT and choriocarcinoma cells-lines, we now wanted to learn more about its potential through loss of function studies, by regulating its expression using siRNA delivery.

For this purpose, HTR8/SVneo and SW71 human EVT cell lines, as well as Jeg-3 choriocarcinoma cell lines were treated with a panel of different siRNA (1, 2, 3 and 5) targeting IQGAP1, along with a non-specific sequence of siRNA as negative control. The treated cells were loaded on 10% SDS-PAGE and were probed for IQGAP1 and  $\alpha$ -tubulin by western blot. IQGAP1 expression was calculated by densitometry normalised to  $\alpha$ -tubulin (housekeeping gene) expression, and the values were compared with each other (Figure 5.6).

IQGAP1 expression was found to be reduced following targeted siRNA delivery in all cell lines used but with different degrees of variation depending on the cells and siRNAs used (Figure 5.6): In HTR8/SVneo, siRNA 2 and 5 were the most effective and reduced IQGAP1 expression significantly by 60% ( $P < 0.01$ ) compared to their control counterparts, while at the same concentration, siRNA 1 and 3 did not significantly affect IQGAP1 expression (Figure 5.6 A1 and 5.6 A2). When the same experiment was conducted in SW71 cells (Figure 5.6 B1 and B2), siRNA 1 and siRNA 3 reduced IQGAP1 expression by 70% and 80% respectively ( $P < 0.001$ ), whilst siRNA 2 and siRNA 5 were the most effective and reduced expression by 90% ( $P < 0.001$  and  $P < 0.0001$ , respectively). Knock-down experiments performed in Jeg-3 resulted in siRNA 1 and siRNA 2 bringing IQGAP1 expression down to 40 and 50%, respectively (although not significantly), while siRNA 3 and 5 did not show any effect on IQGAP1 expression (Figure 5.6 C1 and C2). Therefore, IQGAP1 siRNA 2 and 5 and the cell lines HTR8/SVneo and SW71 were chosen for further experiments on studying the role of IQGAP1 on trophoblast phenotype.

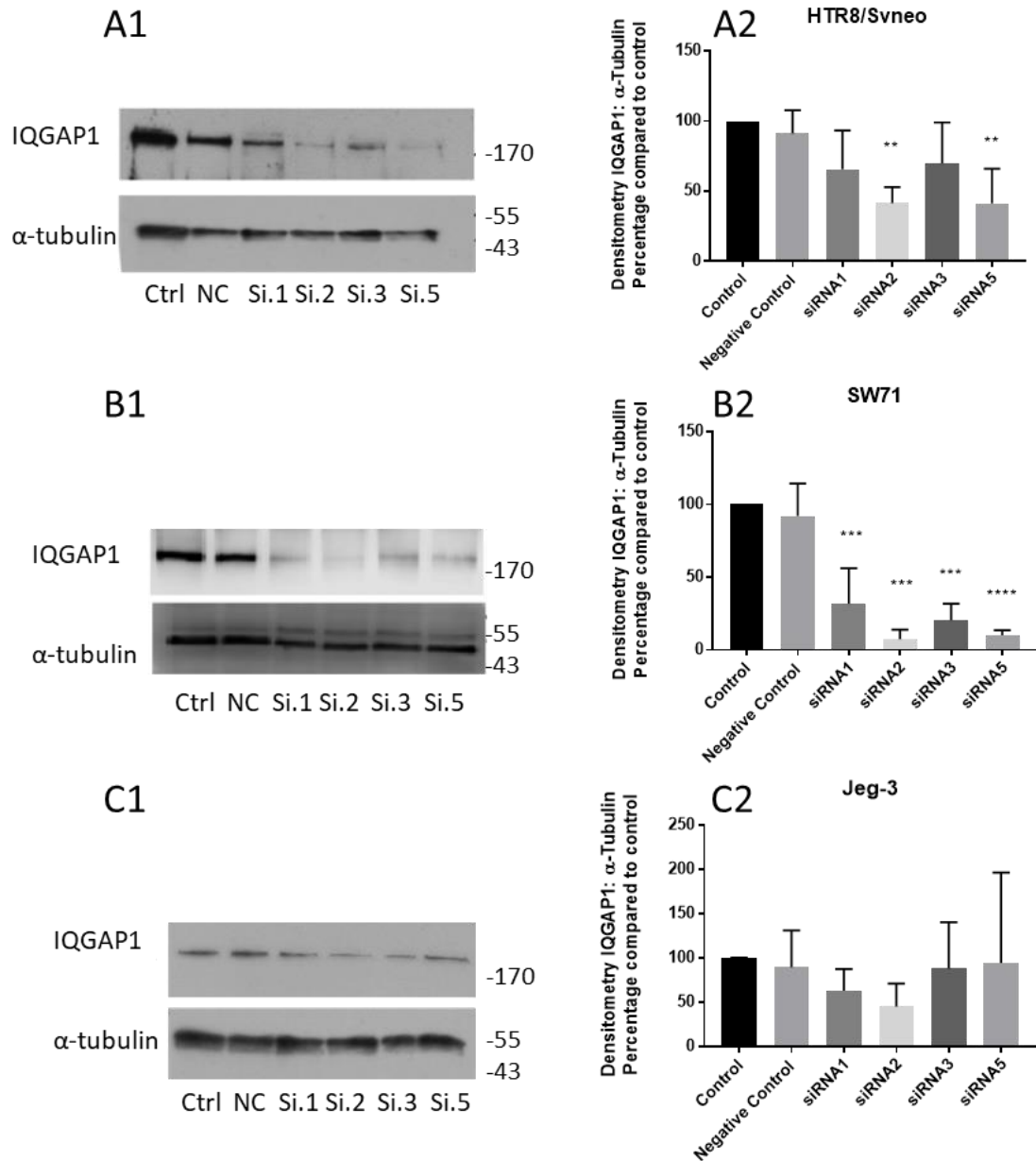


**Figure 5.6** IQGAP1 siRNA treatment knocks down IQGAP1 expression in trophoblast cell lines. HTR8/SVneo, SW71 and Jeg-3 cells, were treated with IQGAP1 siRNA 1, 2, 3 and 5, along with mock treatment. The treated cells along with non-treated control cells were left to grow for 3 days prior to collection, lysing and sonication. The proteins were separated by 10% SDS-PAGE and IQGAP1 and  $\alpha$ -tubulin bands were detected by western blot. Expression levels were quantified by Image Studio Lite software and IQGAP1 expression levels were normalised to the housekeeping gene expression. Panels A1, B1 and C1 show IQGAP1 and  $\alpha$ -tubulin bands in HTR8/SVneo, SW71 and Jeg-3 cells, respectively, while panels A2, B2 and C2 show the densitometry in the mentioned cells in the same order. The error bars represent SD. (\*\* $P < 0.01$ , \*\*\* $P < 0.001$ , \*\*\*\* $P < 0.0001$ ).  $N = 3$  for each cell line. Sample size = 3 for each condition.

### **5.2.7. IQGAP1 knockdown does not affect trophoblast viability**

Having successfully knocked down IQGAP1 expression in trophoblast cell lines, we sought to find out whether this reduction can affect the viability of our EVT cell lines HTR8/SVneo and SW71, as increased levels of IQGAP1 have been associated with enhanced cell growth in cancer cell lines (Wang et al., 2009). To achieve this, cells were treated with IQGAP1 siRNA 2 and 5, which were shown to be the most efficient in reducing IQGAP1 expression in the previous experiment, as well as non-specific siRNA sequence as negative control. Then, the treatment, the viability of the cells as well as their metabolic activity were studied using trypan blue exclusion and MTT assays, respectively, over the course of the next 72 hours.

The untreated HTR8/SVneo cells were increased in number by 50% at 48 hours compared with 24 hours following the seeding and by another 50% at 72 hours compared with 48 hours following the seeding, while SW71 cells increased in cell number by 100% at 48 hours compared with 24 hours following the seeding and 50% at 72 hours compared with 48 hours following the seeding (Figure 5.7). Addition of the IQGAP1 siRNA or the negative control siRNA did not affect the proliferation of HTR8/SVneo cells, while both of the treatments in SW71 cells, at 72 hours, resulted in 20% decrease, with overlapping SDs, compared with the control (Figure 5.7). Metabolic activity of untreated HTR8/SVneo and SW71 cells increased by 60 and 20% respectively, at 48 hours compared with 24 hours following the seeding and then by 100 and 200%, respectively at 72 hours compared with 48 hours following the seeding (Figure 5.7). Addition of IQGAP1 siRNA or the negative control siRNA did not affect the metabolic activity of either HTR8/SVneo or SW71 cells (Figure 5.7).

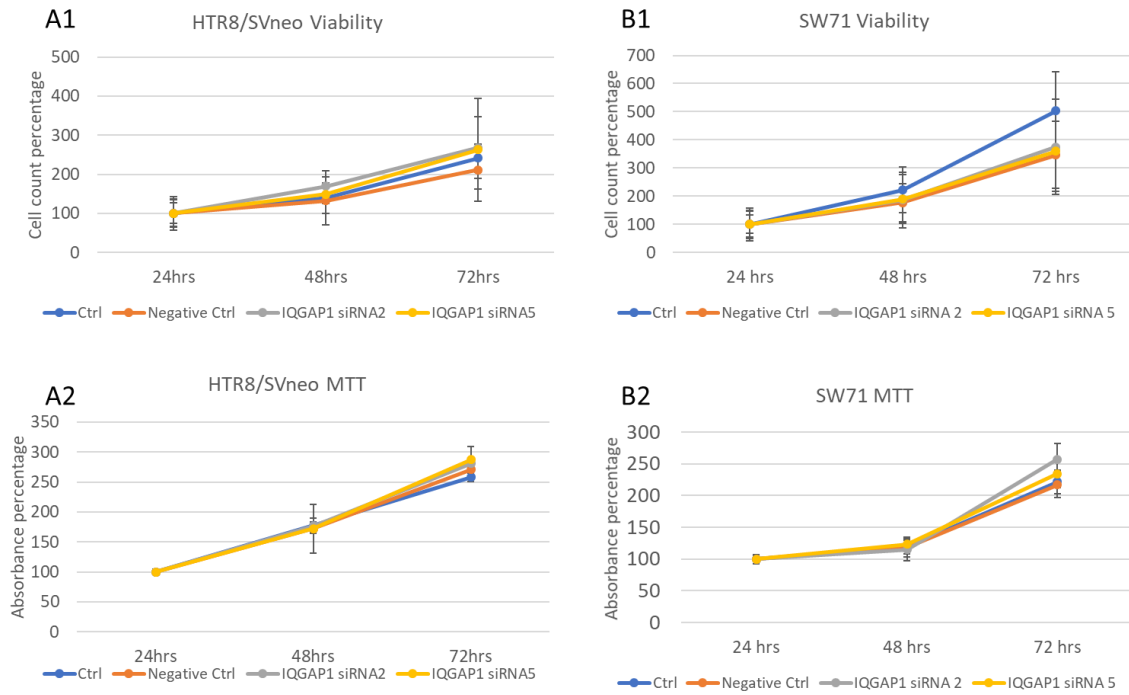


**Figure 5.7 Trophoblast viability with IQGAP1 knockdown.** HTR8/SVneo and SW71 cells were treated with IQGAP1 siRNA 2 and 5, along with a non-specific siRNA sequence, as negative control, for 72 hours. The cells were then collected and reseeded and their viability and metabolic activity (MTT assay) were recorded over the next 72 hours. N = 3 for each condition. Total sample size for each condition: 60 (viability) and 6 (for MTT).

### **5.2.8. IQGAP1 knockdown reduces trophoblast motility**

IQGAP1 has been suggested to be a key regulator of cell motility (Brown & Sacks 2006; Noritake et al. 2005; Watanabe et al. 2004). However, it is not clear whether it plays a similar role in trophoblast cells. Having shown that IQGAP levels can be specifically and significantly reduced in HTR8/SVneo and SW71 EVT cells, the cell lines were treated with IQGAP1 siRNA 2 and 5 and then were seeded in transwells to assess their migration. The cells were counted on random fields at 20x magnification and the average number of migrated treated cells were compared with non-treated cells. Knocking down IQGAP1 significantly reduced migration in HTR8/SVneo EVT cell lines by 50% (siRNA 2,  $P < 0.0001$ ) and 40% (siRNA 5,  $P < 0.001$ ) compared with control. The effect on migration in SW71 was slightly higher, reducing it by 70% (siRNA 2,  $P < 0.0001$ ) and 50% (siRNA 5,  $P < 0.0001$ ) compared with control (Figure 5.8).

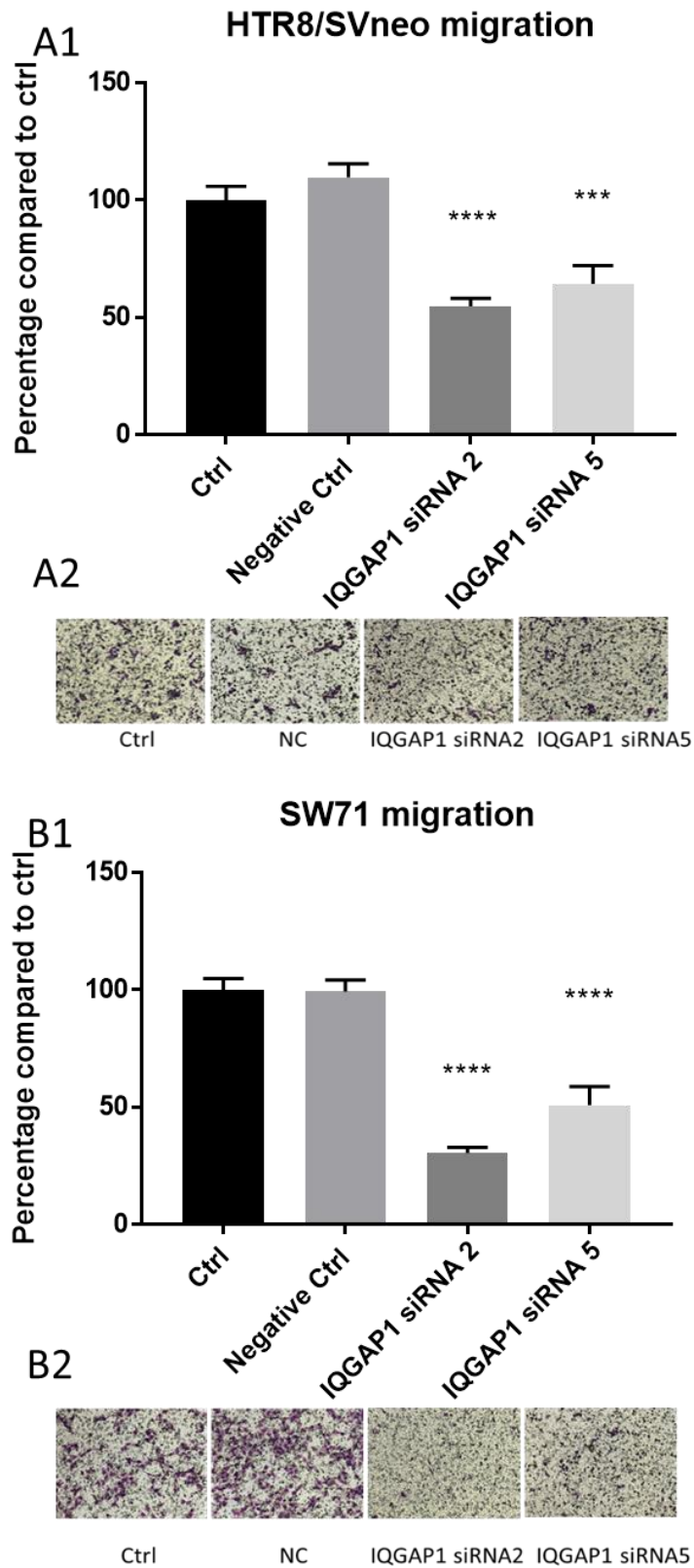


**Figure 5.8 The effect of IQGAP1 knockdown on trophoblast motility.** HTR8/SVneo and SW71 cells were seeded in 24-well plates and were treated with IQGAP1 siRNA 1, 2, 3 and 5,

along with mock treatment and non-treated control. They were left to grow for 48 hours before the medium was replaced with serum starvation medium. After another 24 hours of incubation, the cells were collected and were seeded in transwells, while the lower wells contained complete medium. After 24 hours of incubation, the transwells were fixed and stained. The cells were counted in fields with 20x magnification. Panels A1 and B1 show average cell count percentage compared with control in HTR8/SVneo and SW71 cells, respectively and the bars represent SEM (\*\*\*)  $P < 0.001$ , \*\*\*\*  $p < 0.0001$ ). Panels A2 and B2 show representative fields of fixed and stained transwells for HTR8/SVneo and SW71 cells, respectively.  $N = 3$  for each cell line. Total sample size = 18 for each condition.

### **5.2.9. IQGAP1 knockdown reduces trophoblast invasion**

IQGAP1 has been linked with enhanced cellular invasion (Chellini et al. 2019; Sakurai-Yageta et al. 2008). Having shown the role of IQGAP1 in trophoblast motility, here we aimed to test the possible role of the protein in trophoblast invasion.

HTR8/SVneo and SW71 EVT cell lines were treated with IQGAP1 siRNA 2 and 5 along with a non-specific sequence of siRNA as negative control for 72 hours prior to being seeded in Matrigel-coated transwells. The invaded cells fixed, stained and counted on random fields at 20x magnification. Knocking down IQGAP1 significantly reduced invasion in HTR8/SVneo EVT cell lines by 40% (siRNA 2,  $P < 0.0001$ ) and 50% (siRNA 5,  $P < 0.001$ ), and in SW71, by 80% (siRNA 7,  $P < 0.0001$ ) and 70% (siRNA 9,  $P < 0.0001$ ) (Figure 5.9) compared with their control counterparts.

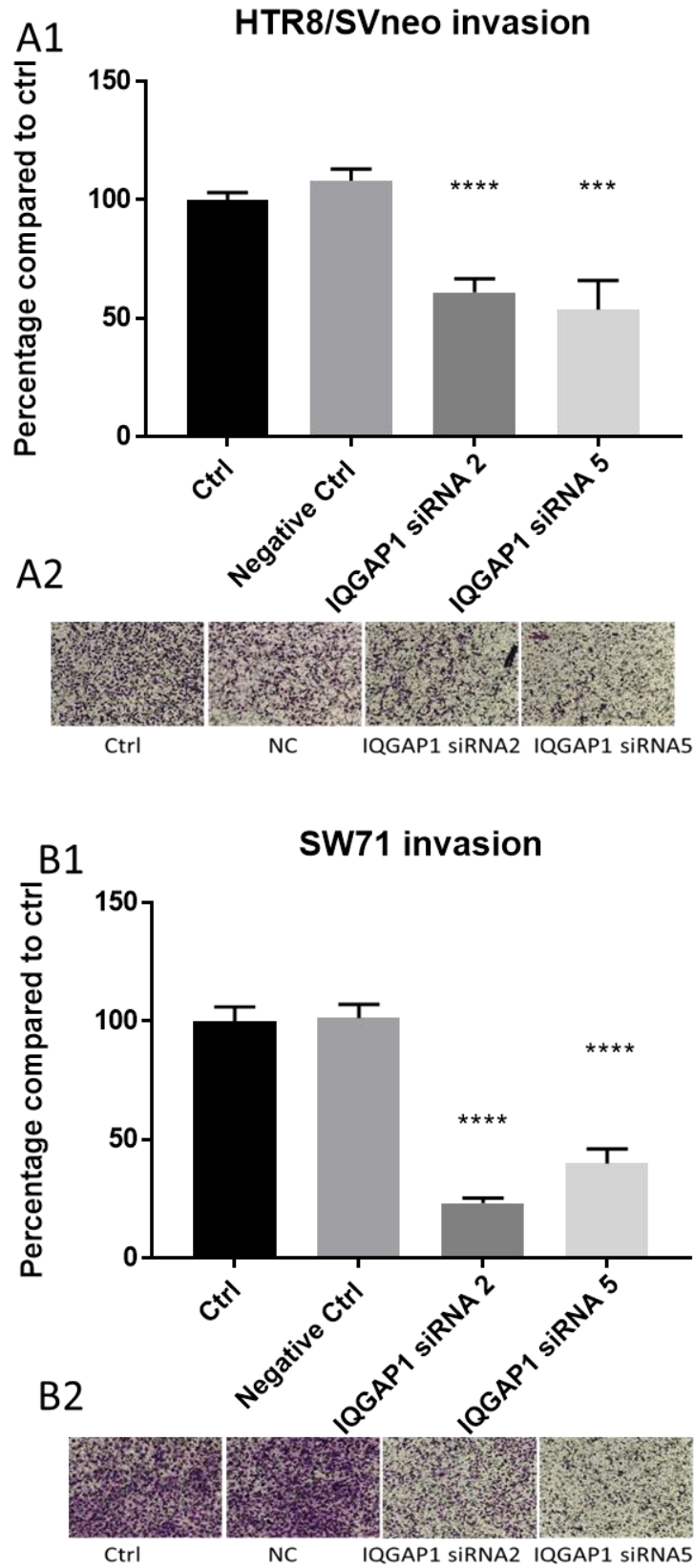


**Figure 5.9** The effect of IQGAP1 knockdown on trophoblast invasion. HTR8/SVneo and SW71 cells were seeded in 24-well plates and were treated with IQGAP1 siRNA 1, 2, 3 and 5,

along with mock treatment and non-treated control. They were left to grow for 48 hours before the medium was replaced with serum starvation medium. After another 24 hours of incubation, the cells were collected and were seeded on Matrigel-coated transwells, while the lower wells contained complete medium. After 24 hours of incubation, the transwells were fixed and stained. The cells were counted in fields at 20x magnification. Panels A1 and B1 show average cell count percentage compared with control in HTR8/SVneo and SW71 cells, respectively and the bars represent SEM (\*\* $P < 0.001$ , \*\*\*\* $p < 0.0001$ ). Panels A2 and B2 show representative fields of fixed and stained transwells for HTR8/SVneo and SW71 cells, respectively.  $N = 3$  for each cell line. Total sample size = 6 for each condition.

### 5.2.10. Regression analysis

Having shown the effect of IQGAP1 down regulation on trophoblast cell line migration and invasion, we next aimed to see whether there is a meaningful correlation between IQGAP1 expression and migration/invasion in these cells, by regression analysis. To do this, IQGAP1 expression levels in trophoblast cells HTR8/SVneo and SW71, with two sequences of IQGAP1 siRNA (2 and 5), mock negative control, along with non-treated control (Figure 5.6) were correlated with their migration (Figure 5.8) and invasion (Figure 5.9). The Pearson correlation coefficient,  $r$  was calculated, and Student's  $t$ -distribution was used to test the significance of the correlation. Regression analysis showed a significant positive correlation ( $r > 0$ ) between IQGAP1 expression and cell migration/invasion for both trophoblast cells (Figure 5.10): IQGAP1 expression and HTR8/SVneo migration  $r = 0.95$  ( $P < 0.05$ ) and invasion  $r = 0.96$  ( $P < 0.01$ ), IQGAP1 expression and SW71 motility  $r = 0.98$  ( $P < 0.01$ ) and invasion  $r = 0.99$  ( $P < 0.01$ ).

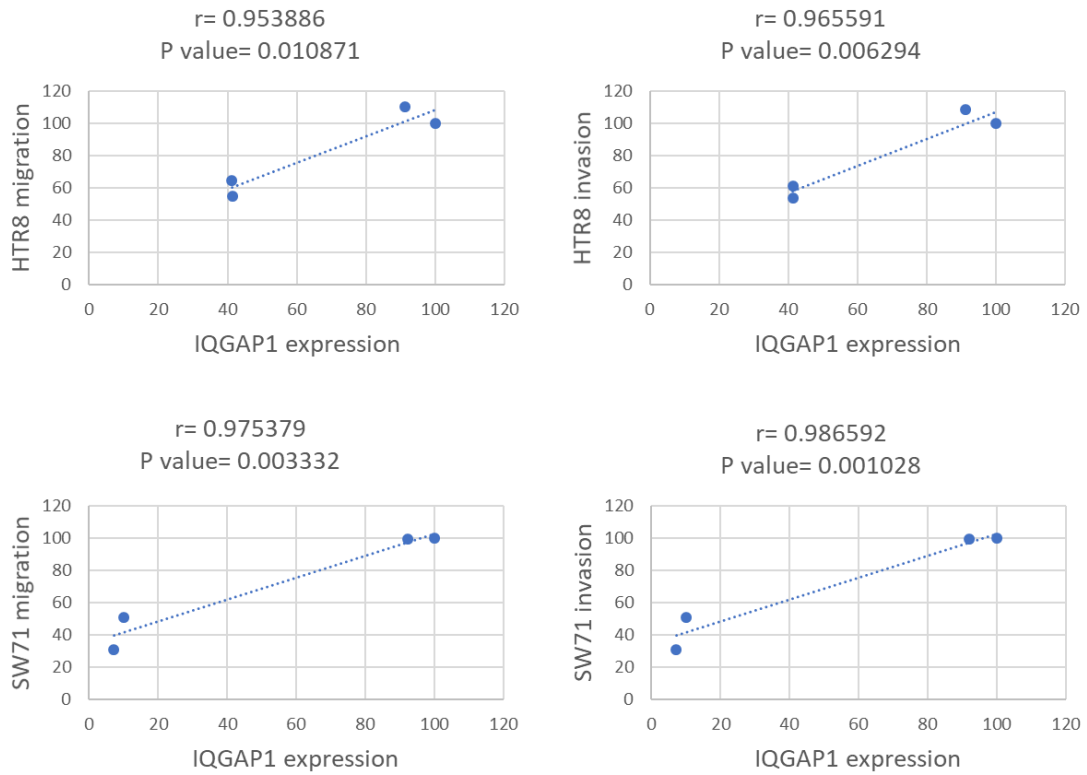


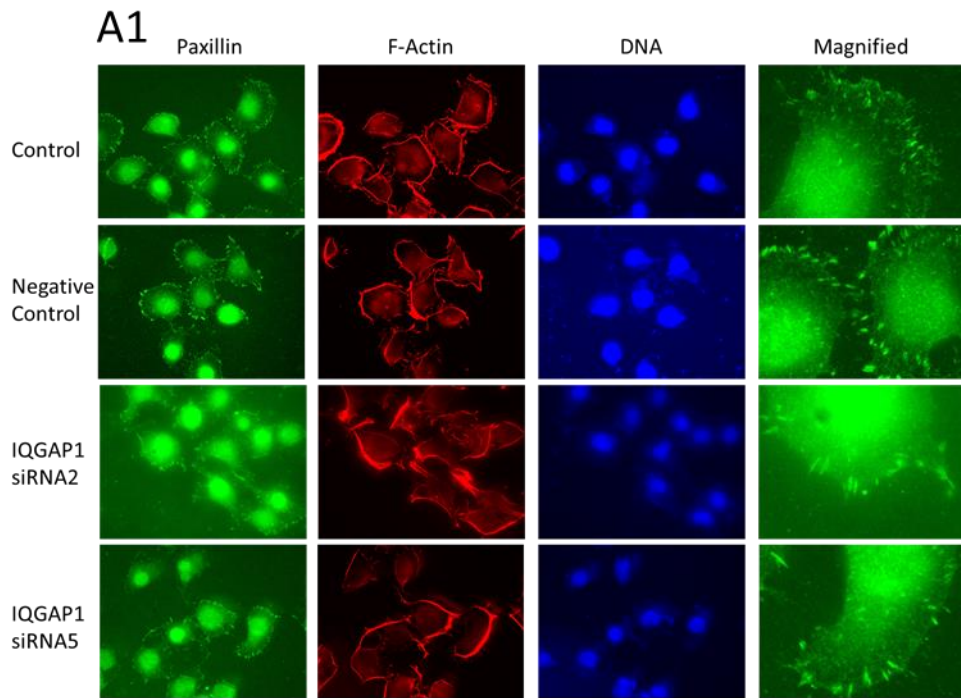
**Figure 5.10 Positive correlation between trophoblast migration/invasion and IQGAP1 expression.** Average IQGAP1 expression levels in trophoblast cell lines HTR8/SVneo and SW71 were correlated with their migration and invasion and Pearson correlation coefficient,  $r$ , was calculated. Student's t-distribution was used to measure the P-values.

### 5.2.11. The effect of IQGAP1 knockdown on trophoblast FAs

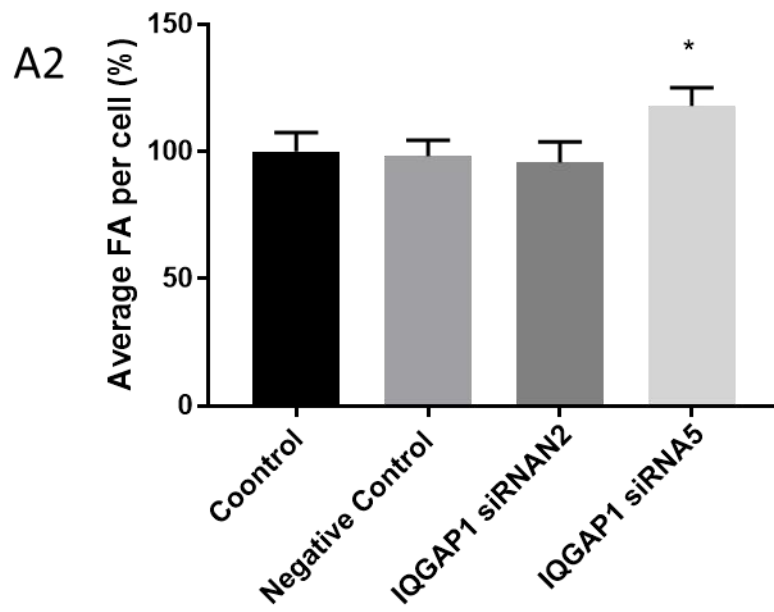
IQGAP1 knockdown in endothelial cells has been shown to reduce the turnover of FAs at the leading edge of the cells as well as their migration (Kohno et al. 2013). Here, we hypothesised that the motility and invasion of trophoblast cells might also be regulated by IQGAP1 through a similar mechanism. For this purpose, IQGAP1 was knocked down in HTR8/SVneo and SW71 cells, through treatment with IQGAP1 siRNA 2 and 5. The cells were seeded on fibronectin-coated coverslips. The coverslips were fixed and incubated with primary anti-paxillin antibody followed by secondary FITC-conjugated antibody and rhodamine phalloidin, before mounting and viewing. Treating HTR8/SVneo cells with IQGAP1 siRNA5 significantly increased FA count by 20% ( $P<0.05$ ) compared with control cells, while siRNA 2 did not affect FA count (Table 5.1). In SW71 cells, IQGAP1 knockdown resulted in an increase in the relative size (Figure 5.11) of the FAs as well as a significant 30% (siRNA 2) and 60% (siRNA 5) increase in their number (Table 5.1) compared with control cells ( $P<0.05$  and  $P<0.0001$ , respectively) (Figure 5.11).

	Percentage focal adhesions per cell $\pm$ SEM (n=20)	P value (compared with control)
HTR8/SVneo Control	100 $\pm$ 7.39	N/A
HTR8/SVneo Negative Control	98.23 $\pm$ 6.26	0.9963
HTR8/SVneo IQGAP1 siRNA 2	95.68 $\pm$ 8.14	0.9525
HTR8/SVneo IQGAP1 siRNA 5	117.88 $\pm$ 7.17	0.0234
SW71 Control	100 $\pm$ 9.99	N/A
SW71 Negative Control	99.63 $\pm$ 5.96	0.1654
SW71 IQGAP1 siRNA 2	132.90 $\pm$ 7.35	0.0228
SW71 IQGAP1 siRNA 5	160.51 $\pm$ 10.14	<0.0001

**Table 5.1 Average FA count per cell in HTR8/SVneo and SW71 cells.** HTR8/SVneo cells and SW71 trophoblast cell lines were treated with IQGAP1 siRNA 2 and 5 for 48 hours before collection. The cells were then seeded on fibronectin-coated coverslips, were left to attach for 24 hours, and stained for paxillin. The FAs were counted on all cells in each image.



HTR8/SVneo



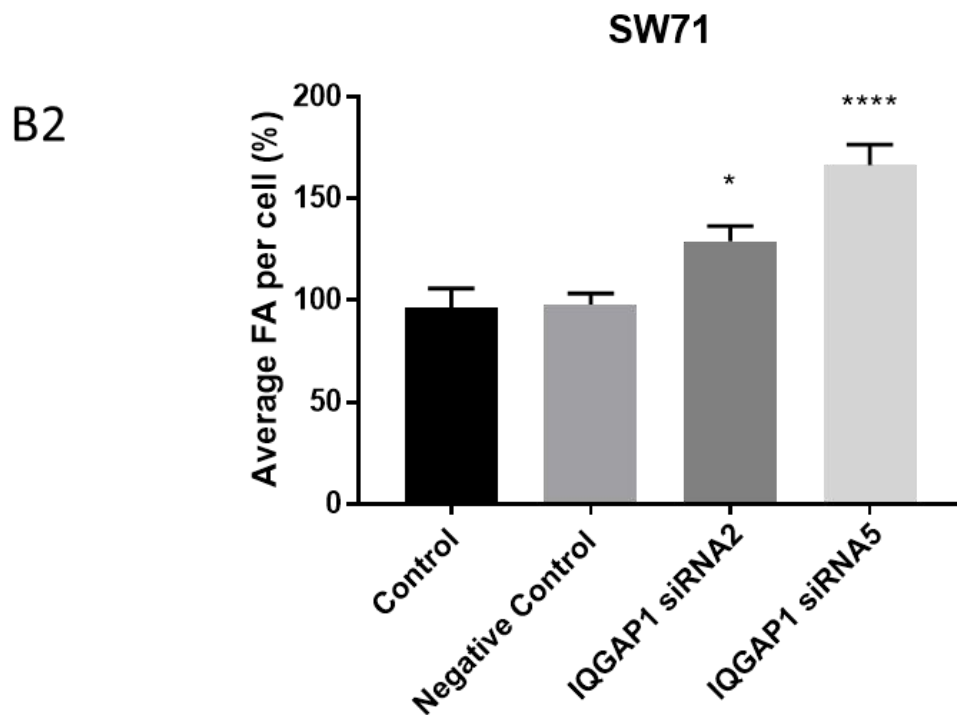
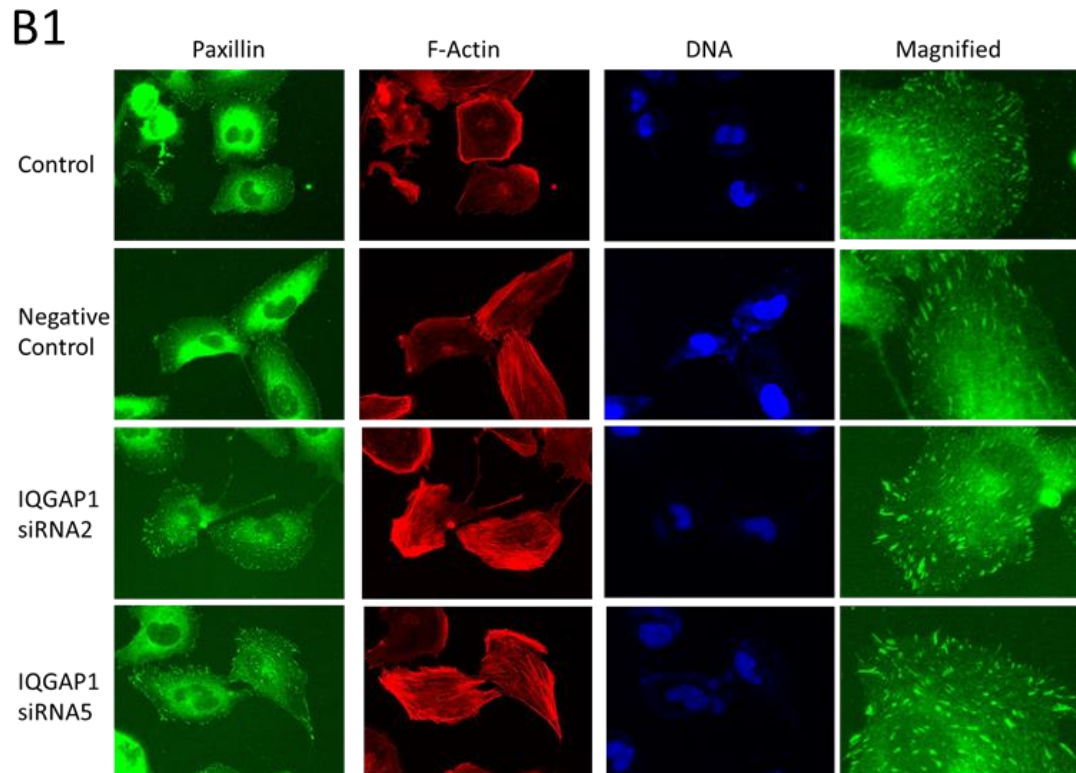


**Figure 5.11** The effect of IQGAP1 knockdown on FAs. HTR8/SVneo cells and SW71 trophoblast cell lines were treated with IQGAP1 siRNA 2 and 5 as well as non-specific siRNA (negative control) for 48 hours before collection and being seeded on fibronectin-coated coverslips. They were left attach for 24 hours. The cells were then stained for paxillin, F-actin

and DNA by immunofluorescence. The images were taken at 63x magnification. Panels A1 and B1 show the staining on HTR8/SVneo and SW71 cells, respectively. Panels B1 and B2 show the average FA count (in percentage) in treated cells compared with the non-treated controls in HTR8/SVneo and SW71, respectively. The error bars represent SEM (\* $<0.05$ , \*\* $<0.001$ ). N = 1 for each cell line. Total sample size = 20 for each condition.

### **5.2.12. IQGAP1 is expressed in primary EVT**

Having shown IQGAP1 expression in all trophoblast cell lines, here we aimed to look for the expression of the protein in primary EVT cells, which were isolated from first trimester human placenta by western blot. IQGAP1 signal was obtained (Figure 5.12A).

To find out more about the localisation of the protein in primary EVTs, the same cells were fixed and stained with primary anti-IQGAP1 antibody followed by incubation with secondary FITC-conjugated antibody, as well as rhodamine phalloidin, before mounting and viewing. The immunofluorescence staining showed strong localisation of the protein in the EVT membrane and nucleus as well as lower levels of localisation in their cytoplasm (Figure 5.12B).

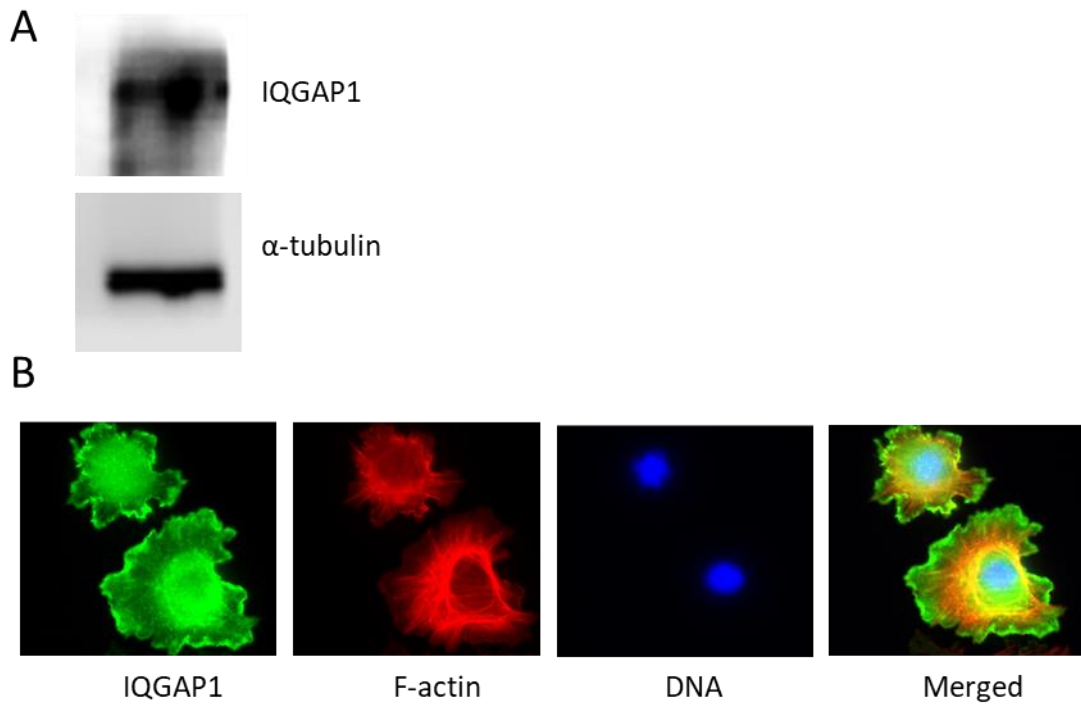


**Figure 5.12 IQGAP1 expression and localisation in primary EVTs.** For expression analysis (panel A) EVT cells were collected, lysed and separated by 10% SDS-PAGE, and probed for IQGAP1 and  $\alpha$ -tubulin by western blotting. For the localisation experiment, (panel B) the EVTs were seeded on fibronectin-coated coverslips and were incubated for 24 hours. IQGAP1 was visualised by immunofluorescence with FITC and counterstained, F-actin with rhodamine phalloidin and DNA with DAPI. The images were taken at 63x magnification.

### 5.3. Discussion

Having shown the role of two metastasis-associated proteins in trophoblast motility and invasion in previous chapters, in this chapter we aimed to find out about the role of IQGAP1, another metastasis-associated protein, in these cells.

IQGAP1 is ubiquitously expressed and has been shown to regulate cell morphology, motility, invasion and cell cycle by interacting with cytoskeletal components and signalling molecules (Johnson, Sharma & Henderson 2009; White, Brown & Sacks 2009). The over-expression of the protein has been associated with metastasis and poor prognosis in cancers of different origins (Hu et al. 2019; Jin et al. 2015; Li et al. 2017; C.-C. Wu et al. 2018; Zeng et al. 2018). Moreover, around 10% of all metastasis-associated proteins have been reported to be binding partners of IQGAP1 (White, Brown, and Sacks 2009).

IQGAP1 expression has previously been reported to be present in placental microvilli (Berryman & Bretscher 2000) and the syncytiotrophoblast microvillous membrane (Paradela et al. 2005). Here, through staining human placental sections by IHC, we also showed IQGAP1 expression in the placental villi. The highest expression level of the protein was detected in first trimester placenta with a gradual reduction in IQGAP expression throughout gestation. (Figure 5.2). IHC showed IQGAP expression in the trophoblasts forming the anchoring villi, and in the invasive trophoblast columns. The protein was localised within the cytoplasm of all trophoblasts, but its highest expression levels were seen in the apical membrane of syncytiotrophoblasts and EVT's (Figure 5.2 and Figure 5.3). IQGAP1 was shown to colocalise with cytokeratin 7, ezrin and S100P in trophoblasts (Figure 5.3). This colocalisation is in line with other studies, which have reported the interaction of these three proteins (S100P, ezrin and IQGAP1) with one another (Heil et al. 2011; Koltzschner et al. 2003; Nammalwar, Heil & Gerke 2015). This pattern of expression in the early stages of implantation is suggestive of a potential role of the protein in trophoblast invasion and implantation, due to the highest invasive capabilities of the EVT's during the first trimester, peaking at around weeks 10-12 of gestation (Caniggia et al. 2000), and in line with our observation regarding the other metastasis-associated proteins in this study.

Western blot analysis confirmed IQGAP1 expression in all our trophoblast cell lines: BeWo, HTR8/SVneo, Jeg-3, SW71, SGHPL-4 and SGHPL-5 (Figure 5.4) as well as first trimester EVT's (Figure 5.12), with Jeg-3 expressing the highest and SGHPL-4 expressing the lowest amount of the protein amongst all cell lines. Furthermore, immunofluorescence staining showed IQGAP1 localisation in the membrane, the cytoplasm as well as the nuclear envelope in all trophoblast cell lines (Figure 5.5) and primary EVT's (Figure 5.12). IQGAP1 has been reported to show strong

localisation within the membrane at the invasive front of metastatic cancer cells (McDonald et al. 2007; Nabeshima et al. 2002). In the HTR8/SVneo and SW71 cell lines and primary EVT, the protein also seemed to be localised within the nucleus (Figure 5.5 and Figure 5.11). Nuclear IQGAP1 has been reported to make up only a very small portion of the total pool of IQGAP1 and is involved in DNA replication (Bielak-Zmijewska et al. 2008; Johnson et al. 2011). This again is the first evidence of IQGAP1 expression in trophoblast cell lines and suggest that all our model systems are suitable for further studies to decipher the role of the protein in cell behaviours.

To further study the role of IQGAP1 in trophoblast cell lines, we sought to modulate its expression levels. HTR8/SVneo and SW71 EVT cell lines and Jeg-3 choriocarcinoma cell lines were treated with four sequences of siRNA targeting IQGAP1. We showed that two of our siRNA sequences (siRNA 2 and 5) successfully knocked down IQGAP1 expression in HTR8/SVneo and SW71 cells, while none of the sequences showed a significant effect on Jeg-3 cells (Figure 5.6). Through transwell assays, it was shown that downregulation of IQGAP1 reduced the migration (Figure 5.8) and invasion (Figure 5.9) of EVT cell lines HTR8/SVneo and SW71. Regression analysis revealed that the expression level of the protein positively and significantly correlated with both migration and invasion in HTR8/SVneo and SW71 cells (Figure 5.10). IQGAP1 downregulation was not shown to affect the viability of neither of our two trophoblast cells (Figure 5.7), and this ruled out the possibility of a difference in cell viability affecting our transwell results. In cancer cells, IQGAP1 downregulation has been shown to reduce migration and invasion as well as proliferation (Diao et al. 2017; Hu et al. 2019), or, similar to our results, invasion and migration only, without affecting their proliferation (Dong et al. 2008).

FA formation and turnover have been shown to regulate directional cell motility by modulating the linkage between the intracellular cytoskeleton and the ECM (Nagano et al. 2012). Here, in order to find out about the mechanisms involved in IQGAP1-induced motility, HTR8/SVneo and SW71 cells with reduced IQGAP1 expression were stained for paxillin, one of the components of the FA complex. We showed that IQGAP1 downregulation using both siRNAs 2 and 5 significantly increased the number as well as the relative size of FAs in SW71 cells (Figure 5.11). In HTR8/SVneo cells however, only IQGAP1 siRNA5 significantly increased the number of FAs (Figure 5.11). In line with this, the regression analysis also had revealed a slightly stronger correlation between IQGAP expression with both migration and invasion in SW71 ( $r = 0.98$  for migration,  $r = 0.99$  for invasion), compared with HTR8/SVneo ( $r = 0.95$  for migration and  $r = 0.96$ ), which was also more significant in SW71 (P-value = 0.003 for migration, P-value = 0.001 for invasion) compared with HTR8/SVneo (P-value = 0.011 for migration and P-value = 0.006) (Figure 5.10). One explanation for this observation could be the higher IQGAP1 expression levels

of IQGAP1 in HTR8/SVneo cells compared with SW71 (Figure 5.4), which might have resulted in a relatively lower efficiency of siRNA treatment in reducing protein levels in HTR8/SVneo. IQGAP1 was previously shown to colocalise with FAs (Kuo et al. 2011; Schiller et al. 2011) to and to directly interact with FA components (Schiefermeier et al. 2014). The down regulation of the protein was shown to result in the elongation of FAs, without affecting cell migration in fibroblasts (Schiefermeier et al. 2014). While the upregulation of the protein was shown to impair FA formation, as well as the migration of fibroblasts (Shen et al. 2017). Moreover, paxillin is only one of the many adapter proteins involved in multiprotein FA structures, and therefore might not always show a true representation of the changes in FA dynamics, while being studied alone. Likewise, different FA proteins show different levels of stability and are recruited to the FA at different timepoints. For example, a study reported that paxillin and vinculin are more stably associated with FAs, while zyxin and vasodilator-stimulated phosphoprotein (VASP) are associated them in a more transient manner. Moreover, paxillin, zyxin and VASP were more dynamic than vinculin in FAs closer to the edge of the cell membrane (Legerstee et al. 2019). Zyxin and VASP have been reported to be more closely linked with actin compared with paxillin and vinculin, while being recruited to FAs at a later stage compared with paxillin and vinculin (Choi et al. 2008). Therefore, studying FA dynamics using other makers, might perhaps give a better view of how IQGAP1 regulates their dynamics. In line with this, other FA markers such as vinculin and VASP have already been suggested to play a role in trophoblast migration and invasion (Kayisli et al. 2002; Lang et al. 2004). Additionally, VASP was shown to be a binding partner for IQGAP1 (Routray et al. 2011), while IQGAP-rich areas in the adhesion sites of cells were shown to have reduced vinculin expression (Foroutannejad et al. 2014),

To conclude, IQGAP1 expression was shown in cyto- and syncytiotrophoblasts as well as EVT, and there was a gradual reduction in its expression throughout gestation. IQGAP1 was shown to regulate trophoblast migration as well as invasion. Based on these findings, we propose a potential role for IQGAP1 in early placenta development and implantation.

# Chapter 6.

## Conclusions

## 6.1. General discussion

Miscarriage and preeclampsia are the most common pregnancy-related issues in humans (Jauniaux, Poston & Burton 2006). As much as 30% of all pregnancy cases have been estimated to end with spontaneous abortion or miscarriage before 20 weeks of gestation, with about 80% of these cases happen during the first trimester (Wilcox et al. 1988; Zinaman et al. 1996). Preeclampsia, which also occurs in about 10% of otherwise normal pregnancies (Roberts & Lain 2002) can also be detected during the first trimester (Roberts & Hubel 2009). Preeclampsia, miscarriage and foetal growth restriction have been associated with inadequate trophoblast invasion, which results in impaired transformation of the spiral arteries in the placenta (Ball et al. 2006; Brosens, Robertson & Dixon 1972; Khong et al. 1986; Reister et al. 2006). In an attempt to address this issue, we aimed to study trophoblast invasion as well as motility.

Our hypothesis was that three well-known metastasis-associated proteins (S100P, ezrin and IQGAP1) can equally play important roles in the migration and invasion of trophoblast cells. For this purpose, we chose three different, yet interacting (Heil et al. 2011; Koltzschner et al. 2003; Nammalwar, Heil & Gerke 2015), metastasis-associated proteins from three different families i.e. S100P, ezrin and IQGAP1, all of which are well-known effectors of tumour cell motility and invasion and metastasis (Chen et al. 2014; Clucas & Valderrama 2014; Johnson, Sharma & Henderson 2009), and studied their role in the motility and invasion of trophoblast cell lines.

By comparing DAB signals, though IHC, we showed high expression of S100P, ezrin and IQGAP1 in human placenta sections from early gestational age (Figure 3.2, Figure 4.2 and Figure 5.2). It was shown that expression level of these proteins gradually declines throughout gestation (Figure 3.2, Figure 4.2 and Figure 5.2). High expression levels of these three proteins during the first trimester suggests their role in early placenta development, during which most of trophoblast motility and invasion takes place (Caniggia et al. 2000).

All three proteins were shown to be expressed in the cytoplasm of cyto- and syncytiotrophoblasts, colocalising with the trophoblast marker cytokeratin 7 (Figure 3.3, Figure 4.3 and Figure 5.3). Through colocalisation with the marker HLA-G, the expression of these three proteins was also confirmed in an invasive subpopulation of trophoblasts, located at the tip of trophoblastic columns, known as EVT's (Figure 3.3, Figure 4.3 and Figure 5.3). Interestingly, the highest levels of these proteins were detected in the apical membrane of syncytiotrophoblasts as well as EVT's (Figure 3.3, Figure 4.3 and Figure 5.3). Unlike ezrin and IQGAP1, staining by IHC showed occasional nuclear localisation of S100P in syncytiotrophoblasts and EVT's (Figure 3.3).

Through western blot analysis, we detected IQGAP1 and ezrin in all of our trophoblast cell lines, Jeg-3, BeWo, HTR8/SVneo, SW71, SGHPL-4 and SGHPL-5, while S100P was only detectable in the choriocarcinoma cell lines Jeg-3 and BeWo, and not in the first trimester EVT cell lines: HTR8/SVneo, SW71, SGHPL-4 and SGHPL-5 (Figure 3.4, Figure 4.4 and Figure 5.4). Primary EVTs isolated from first trimester placenta did express our three proteins (Figure 3.26, Figure 4.18 and Figure 5.12). We also showed S100P expression modifications, when Jeg-3 cells were grown in “physiological-like” microenvironments i.e. on fibronectin, Matrigel and 2% gelatine, while none of these conditions induced S100P expression in our EVT cell lines (Figure 3.5).

We then attempted to look at the localisation of these three metastasis-associated proteins in our trophoblast cell lines through immunofluorescence staining. S100P immunofluorescence staining did not provide a clear view but showed cytoplasmic and nuclear localisation of the protein (data not shown). Ezrin (Figure 4.5) and IQGAP1 (Figure 5.5) were localised within the cytoplasm as well as the plasma membrane in all trophoblast cell lines, except for Jeg-3 and SGHPL-4, which showed cytoplasmic ezrin expression only (Figure 4.5). IQGAP1 also showed peri-nuclear localisation in the trophoblast cell lines and was detected within the nucleus in HTR8/SVneo and SW71 (Figure 5.5). Active ezrin localised within the cortex via interaction with PIP<sub>2</sub> in the membrane, while the closed inactive ezrin is mainly located within the cytoplasm (Fehon, McClatchey & Bretscher 2010). Changes in the localisation of ezrin in the membrane and microvilli (either decrease or increase) have been associated with enhanced motility, invasion and proliferation in cancer cells (Arslan et al. 2012; Di Cristofano et al. 2010; Curto & McClatchey 2004; Elzagheid et al. 2008; Sarrío et al. 2006; Schlecht et al. 2012). The phosphorylated (active) form of ezrin has been shown to localise within long spike projections from the plasma membrane of gastric cells (Zhou et al. 2005). Here, phospho-ezrin (at Thr567) was shown to be localised within the membrane as well as long membrane projections in primary EVTs, and these projections were more abundant and longer in EVTs isolated from first trimester placenta compared with second trimester (Figure 4.19). Membrane IQGAP1 at the invasive front of cells has been associated with metastasis (McDonald et al. 2007; Nabeshima et al. 2002), while nuclear IQGAP1, which was reported to involve only a small proportion of total IQGAP1, has been reported to be involved in DNA replication (Bielak-Zmijewska et al. 2008; Johnson et al. 2011). Moreover, both ezrin, and IQGAP1 have been shown to be present in placental microvilli (Berryman & Bretscher 2000).

We then aimed to find out about the role of these three metastasis-associated proteins in trophoblast cell lines. For this purpose, we knocked down the expression of these three proteins through siRNA delivery (Figure 3.6, Figure 4.6 and Figure 5.6), and found out, through transwell

assays, that reduction in the expression of either of these proteins resulted in significant reduction in cell motility (Figure 3.9, Figure 4.8 and Figure 5.8) and invasion (Figure 3.10, Figure 4.9 and Figure 5.9). S100P expression in HTR8/SVneo cells (which do not endogenously express S100P), at similar levels to Jeg-3, significantly enhanced their motility (Figure 3.12) and invasion (Figure 3.13). While these three metastasis-associated proteins, i.e. S100P (Arumugam et al. 2005; Jiang et al. 2011; Liu et al. 2017), ezrin (Fan et al. 2011; Meng et al. 2010; Tang et al. 2019; Zhang et al. 2014) and IQGAP1 (Diao et al. 2017; Dong et al. 2008; Hu et al. 2019) have previously been shown to enhance cancer cell motility and invasion, here we report their involvement in trophoblast motility and invasion for the first time, and as the main discovery in this piece of work. Knocking down or expression induction of S100P (Figure 3.15 and Figure 3.17 and Tabrizi et al. 2018), and down regulation of ezrin (Figure 4.7) or IQGAP1 (Figure 5.7) did not affect the viability of our trophoblast cell lines, similar to what was shown in some types of tumour cells (Barry et al. 2013; Dong et al. 2008; Du et al. 2012; Horwitz et al. 2016; Hsu et al. 2015). Additionally, we also suggested that S100P can regulate trophoblast motility (Figure 3.21) and invasion (Figure 3.22) from a pathway that involves a pool of S100P that is extracellular membrane-bound and/or soluble in the stroma. Furthermore, we showed that ezrin inhibition affects primary EVT morphology (Figure 4.20) and downregulates motility and invasion in these cells (Figure 4.21 and Figure 4.22, respectively) as well as HTR8/SVneo cells (Figure 4.15 and Figure 4.16 respectively).

Trophoblasts have been shown to bind to fibronectin through integrins  $\alpha_5\beta_1$  and  $\alpha_v\beta_3$  (Burrows et al. 1995). The assembly of FAs, which bind to the cytoplasmic part of clustered integrins, have been shown to be regulated, at least partially, through insulin-like growth factor-I signalling in trophoblasts (Kabir-Salmani et al. 2002). Moreover, alterations in FAs have been reported to play an important role in trophoblast fusion (Ishikawa et al. 2014). Here, in an attempt to learn about the possible mechanisms involved in trophoblast motility and invasion, we looked at how FA dynamics are regulated by our three proteins. We showed that the expression of S100P in HTR8/SVneo cells reduced the relative size and the number of FAs (Figure 3.14), while knocking down S100P in Jeg-3 and BeWo (Tabrizi et al. 2018) and IQGAP1 in SW71 cells (Figure 5.11) increased their relative size and number. More mature FAs are a sign of a higher ratio of FA formation relative to its turnover, which are mostly seen in stationary cells (Nagano et al. 2012). The FAs were not affected in Jeg-3 cells when extracellular S100P was inhibited and in HTR8/SVneo and SW71 when ezrin was knocked down. This lack of an effect on FAs might have been due to the fact that only a small percentage of cell adhesion strength is linked with FA assembly (Gallant, Michael & García 2005), and because we did a limited FA analysis on fixed cells, which might have represented only a “snapshot” of a highly

dynamic process, which cannot guarantee to provide a holistic view. Interestingly, unlike ezrin knockdown, the inhibition of ezrin significantly increased the number and the relative size of FAs in HTR8/SVneo (Figure 4.17), but not in primary EVT<sub>s</sub> (Figure 4.23). This was in line with the greater effectiveness of the ezrin inhibitor on the motility and invasion of HTR8/SVneo (Figure 4.15 and Figure 4.16 80% and 70%, respectively) compared with the primary EVT<sub>s</sub> (Figure 4.21 and Figure 4.22 30% and 20%, respectively).

EGF is one of the main regulators of the placental development and trophoblast migration and invasion during early gestation (Bass et al. 1994; Han et al. 2010; Maruo et al. 1995). Upon EGF stimulation, and subsequent  $Ca^{2+}$  elevation, ezrin and S100P colocalise in microvillar cell protrusions. The hydrophobic residues in the C-terminal hand of S100P have been shown to compete (at least partially) with  $PIP_2$  in binding to the F2 lobe of ezrin N-ERMAD (in a  $Ca^{2+}$ -dependent manner), resulting in ezrin activation by unmasking its F-actin binding site (Austermann et al. 2008; Koltzsch et al. 2003). EGF also stimulates the interaction between the other (non-canonical) EF hands of S100P and the IQ domain of IQGAP1 (also in a  $Ca^{2+}$ -dependent manner), resulting in the inhibition of IQGAP1 and therefore interfering with the downstream MAPK pathway (Heil et al. 2011). On the other hand, following the conformational change in ezrin upon binding to the membrane  $PIP_2$ , the N-ERMAD domain of the protein has been shown to interact with the IQ domain in IQGAP1 in a  $Ca^{2+}$ -independent manner (and without a requirement for ezrin phosphorylation), resulting in IQGAP1 recruitment to the cell cortex (Nammalwar, Heil & Gerke 2015). In line with this, we also detected reduced cortical IQGAP1 in HTR8/SVneo, following ezrin inhibition (data not shown). Moreover, an elevation in intracellular  $Ca^{2+}$  was shown to recruit S100P to the ezrin-IQGAP1 complex (Nammalwar, Heil & Gerke 2015). Furthermore, ezrin plays an important role in EGF-induced tumour cell motility and invasion (Y. Wang et al. 2014) and IQGAP1 mediates EGF-induced MAPK activation through binding to B-Raf, MEK, ERK and EGFR and the phosphorylation of EGFR (McNulty et al. 2011). Additionally, the transcription factor SP1, a member of SP/KLF family, also might link these three proteins at the transcriptional level as it has been shown to promote ezrin (Gao et al. 2009) and IQGAP1 expression (Jin et al. 2019), while S100P has been shown to include a SP/KLF-binding site in its promoter region (Gibadulinova et al. 2008). Interestingly, trophoblastic SP1 was shown to be more frequent in placental villi sections from early gestation compared with term samples (Knofler et al. 2004).

Based on our observation of a high degree of expression of these three proteins in trophoblasts during the first trimester, we suggest that the S100P, ezrin and IQGAP1 might form a complex and link the trophoblast membrane with F-actin and regulate cytoskeleton dynamics upon EGF

stimulation, similar to what was shown in other cell types (Nammalwar, Heil & Gerke 2015). These proteins are also suggested to further regulate actin dynamics by the potential recruitment of other IQGAP1-binding proteins such as Cdc42 and Rac1 to the complex (Nammalwar, Heil & Gerke 2015).

To conclude, we showed that three different metastasis-associated proteins i.e. S100P, ezrin and IQGAP1, colocalise in cytotrophoblasts, syncytiotrophoblasts and EVT<sub>s</sub> from first trimester placenta sections. We also showed that these three proteins play important roles in trophoblast migration and invasion and are involved in placenta development. However, we have yet to determine the mechanisms involved in these two pathways in trophoblasts and we still do not know whether these three proteins work together in trophoblasts to make motility and invasion possible.

## **6.2. Future work**

To have a better view of some of the processes carried out in this study, further investigation can be carried out as follows:

- We showed the colocalisation of our three proteins: S100P, ezrin and IQGAP1 in trophoblasts though IHC; therefore it would be useful to have a closer look at how these three proteins colocalise within primary trophoblasts by immunofluorescence staining.
- Having shown that the localisation of phospho-ezrin is significantly different between the first trimester and second trimester primary EVT<sub>s</sub>, it is equally important to find out whether there are differences in the localisation patterns of the total pool of ezrin, S100P and IQGAP1 in first, second and third trimester EVT<sub>s</sub>, though both epifluorescence and confocal microscopy.
- Motility changes in this study were studied though transwell assays. It would perhaps be useful to confirm our results using other methods such as scratch assay or using the Dunn chemotaxis chamber.
- It would be interesting to investigate trophoblast invasion in more details by investigating the effect of knocking down our three proteins on the activity of ECM-degrading enzymes.
- We studied how our three proteins affect the FA dynamics in trophoblasts, by targeting paxillin, one of the many components of the multi-protein FA complex. Studying the other components such as vinculin, zyxin and VASP separately or at the same time might give us a better view of the process.

- Ezrin inhibition did not show the same level of effect on the motility and invasion of primary EVT<sub>s</sub> or their FAs, as we saw in HTR8/SVneo cells; therefore, it would be interesting to see whether the application of our ezrin inhibitor, NSC668394, on EVT<sub>s</sub> at higher concentrations and for longer periods would further reduce their motility and invasion and affect FA dynamics.
- Boyden chamber assays with primary EVT might show more prominent results if they were optimised accordingly.
- Having shown the importance of ezrin phosphorylation on Thr567 in trophoblast motility and invasion, it would be interesting to see how other phosphorylation sites such as tyrosine 477, serine 66, threonine 235, and tyrosine 145 might regulate the mentioned pathways as well as the morphology of trophoblasts.
- Having shown the expression pattern of ezrin in placenta, at different stages of gestation, though IHC, it would be useful to find out about the expression pattern of the phosphorylated form of the protein in the same organ.
- In this study we used HTR8/SVneo, SW71 and Jeg-3 to study the role of ezrin and IQGAP1 in their motility and invasion, but it would be equally informative to see how these two proteins regulate the mentioned pathways in our other trophoblast cell lines, since all of them expressed these two proteins.
- IQGAP1-null mice are viable (Li et al. 2000; Sbroggio et al. 2011); therefore, they could be used to compare placenta and/or foetus development in the absence and presence of IQGAP1.

# References

- Abdou, A.G., Maraee, A.H., El-Sayed, E.M.M. & Elnaidany, N.F. 2011, 'Immunohistochemical expression of ezrin in cutaneous basal and squamous cell carcinomas.', *Annals of Diagnostic Pathology*, vol. 15, no. 6, pp. 394–401.
- Abel, A.M., Schuldt, K.M., Rajasekaran, K., Hwang, D., Riese, M.M.J., Rao, S., Thakar, M.S. & Malarkannan, S. 2016, 'IQGAP1 : Insights into the function of a molecular puppeteer', *Molecular Immunology*, vol. 65, no. 2, pp. 336–49.
- Achache, H. & Revel, A. 2006, 'Endometrial receptivity markers, the journey to successful embryo implantation.', *Human reproduction update*, vol. 12, no. 6, pp. 731–46.
- Adachi, H., Takahashi, Y., Hasebe, T., Shirouzu, M., Yokoyama, S. & Sutoh, K. 1997, 'Dictyostelium IQGAP-related protein specifically involved in the completion of cytokinesis', *The Journal of Cell Biology*, vol. 137, no. 4, pp. 891–8.
- Ahmed, A., Rezai, H. & Broadway-Stringer, S. 2017, 'Evidence-based revised view of the pathophysiology of preeclampsia.', *Advances in Experimental Medicine and Biology*, vol. 956, pp. 355–74.
- Akisawa, N., Nishimori, I., Iwamura, T., Onishi, S. & Hollingsworth, M.A. 1999, 'High levels of ezrin expressed by human pancreatic adenocarcinoma cell lines with high metastatic potential.', *Biochemical and Biophysical Research Communications*, vol. 258, no. 2, pp. 395–400.
- Alberts, B., Johnson, A., Lewis, J., Morgan, D., Raff, M., Roberts, K. & Walter, P. 2014, *Molecular Biology of the Cell*, 6th edn, Garland Science, New York and Abingdon.
- Albuquerque, T.A.F., Drummond do Val, L., Doherty, A. & de Magalhaes, J.P. 2018, 'From humans to hydra: patterns of cancer across the tree of life.', *Biological Reviews of the Cambridge Philosophical Society*, vol. 93, no. 3, pp. 1715–34.
- Allen, R.D. & Allen, N.S. 1978, 'Cytoplasmic streaming in amoeboid movement.', *Annual Review of Biophysics and Bioengineering*, vol. 7, pp. 469–95.
- Andersson, G., Wennersten, C., Gaber, A., Boman, K., Nodin, B., Uhlén, M., Segersten, U., Malmström, P.-U. & Jirström, K. 2014, 'Reduced expression of ezrin in urothelial bladder cancer signifies more advanced tumours and an impaired survival: validity study of two independent patient cohorts', *BMC Urology*, vol. 14, p. 36.
- Antelmi, E., Cardone, R.A., Greco, M.R., Rubino, R., Di Sole, F., Martino, N.A., Casavola, V., Carcangiu, M., Moro, L. & Reshkin, S.J. 2013, 'β1 integrin binding phosphorylates ezrin at T567 to activate a lipid raft signalsome driving invadopodia activity and invasion', *PloS One*, vol. 8, no. 9, pp. e75113–e75113.
- Aplin, J.D. 1991, 'Implantation, trophoblast differentiation and haemochorial placentation: mechanistic evidence in vivo and in vitro.', *Journal of Cell Science*, vol. 99 ( Pt 4), pp. 681–92.
- Arcondeguy, T., Lacazette, E., Millevoi, S., Prats, H. & Touriol, C. 2013, 'VEGF-A mRNA processing, stability and translation: a paradigm for intricate regulation of gene expression at the post-transcriptional level.', *Nucleic Acids Research*, vol. 41, no. 17, pp. 7997–8010.
- Arjonen, A., Kaukonen, R. & Ivaska, J. 2011, 'Filopodia and adhesion in cancer cell motility', *Cell Adhesion & Migration*, vol. 5, no. 5, pp. 421–30.
- Arpin, M., Chirivino, D., Naba, A. & Zwaenepoel, I. 2011, 'Emerging role for ERM proteins in cell adhesion and migration', *Cell Adhesion & Migration*, vol. 5, no. 2, pp. 199–206.
- Arslan, A.A., Silvera, D., Arju, R., Giashuddin, S., Belitskaya-Levy, I., Formenti, S.C. & Schneider, R.J. 2012, 'Atypical ezrin localization as a marker of locally advanced breast cancer.', *Breast Cancer Research and Treatment*, vol. 134, no. 3, pp. 981–8.
- Arumugam, T., Ramachandran, V. & Logsdon, C.D. 2006, 'Effect of cromolyn on S100P interactions with RAGE and pancreatic cancer growth and invasion in mouse models.', *Journal of the National Cancer Institute*, vol. 98, no. 24, pp. 1806–18.
- Arumugam, T., Simeone, D.M., Van Golen, K. & Logsdon, C.D. 2005, 'S100P promotes pancreatic cancer growth, survival, and invasion.', *Clinical Cancer Research : an Official Journal of the American Association for Cancer Research*, vol. 11, no. 15, pp. 5356–64.
- Arumugam, T., Simeone, D.M., Schmidt, A.M. & Logsdon, C.D. 2004, 'S100P stimulates cell proliferation and survival via receptor for activated glycation end products (RAGE).', *The Journal of Biological Chemistry*, vol. 279, no. 7, pp. 5059–65.
- Austermann, J., Nazmi, A.R., Muller-Tidow, C. & Gerke, V. 2008, 'Characterization of the Ca<sup>2+</sup> - regulated ezrin-S100P interaction and its role in tumor cell migration.', *The Journal of Biological*

- Chemistry*, vol. 283, no. 43, pp. 29331–40.
- Averboukh, L., Liang, P., Kantoff, P.W. & Pardee, A.B. 1996, 'Regulation of S100P expression by androgen.', *The Prostate*, vol. 29, no. 6, pp. 350–5.
- Baker, J.R., Jeffery, R., May, R.D., Mathies, M., Spencer-Dene, B., Poulson, R. & Hogg, N. 2011, 'Distinct roles for S100a8 in early embryo development and in the maternal deciduum.', *Developmental Dynamics : an Official Publication of the American Association of Anatomists*, vol. 240, no. 9, pp. 2194–203.
- Balenci, L., Saoudi, Y., Grunwald, D., Deloulme, J.C., Bouron, A., Bernards, A. & Baudier, J. 2007, 'IQGAP1 regulates adult neural progenitors in vivo and vascular endothelial growth factor-triggered neural progenitor migration in vitro.', *The Journal of Neuroscience : the Official Journal of the Society for Neuroscience*, vol. 27, no. 17, pp. 4716–24.
- Ball, E., Bulmer, J.N., Ayis, S., Lyall, F. & Robson, S.C. 2006, 'Late sporadic miscarriage is associated with abnormalities in spiral artery transformation and trophoblast invasion.', *The Journal of Pathology*, vol. 208, no. 4, pp. 535–42.
- Bamidele, A.O., Kremer, K.N., Hirsova, P., Clift, I.C., Gores, G.J., Billadeau, D.D. & Hedin, K.E. 2015, 'IQGAP1 promotes CXCR4 chemokine receptor function and trafficking via EEA-1+ endosomes.', *The Journal of Cell Biology*, vol. 210, no. 2, pp. 257–72.
- Bardwell, A.J., Lagunes, L., Zebajedi, R. & Bardwell, L. 2017, 'The WW domain of the scaffolding protein IQGAP1 is neither necessary nor sufficient for binding to the MAPKs ERK1 and ERK2.', *The Journal of Biological Chemistry*, vol. 292, no. 21, pp. 8750–61.
- Barreiro, O., Yanez-Mo, M., Serrador, J.M., Montoya, M.C., Vicente-Manzanares, M., Tejedor, R., Furthmayr, H. & Sanchez-Madrid, F. 2002, 'Dynamic interaction of VCAM-1 and ICAM-1 with moesin and ezrin in a novel endothelial docking structure for adherent leukocytes', *The Journal of Cell Biology*, vol. 157, no. 7, pp. 1233–45.
- Barry, S., Chelala, C., Lines, K., Sunamura, M., Wang, A., Marelli-Berg, F.M., Brennan, C., Lemoine, N.R. & Crnogorac-Jurcevic, T. 2013, 'S100P is a metastasis-associated gene that facilitates transendothelial migration of pancreatic cancer cells.', *Clinical & Experimental Metastasis*, vol. 30, no. 3, pp. 251–64.
- Bashour, A.M., Fullerton, A.T., Hart, M.J. & Bloom, G.S. 1997, 'IQGAP1, a Rac- and Cdc42-binding protein, directly binds and cross-links microfilaments.', *The Journal of Cell Biology*, vol. 137, no. 7, pp. 1555–66.
- Bass, K.E., Morrish, D., Roth, I., Bhardwaj, D., Taylor, R., Zhou, Y. & Fisher, S.J. 1994, 'Human cytotrophoblast invasion is up-regulated by epidermal growth factor: evidence that paracrine factors modify this process.', *Developmental Biology*, vol. 164, no. 2, pp. 550–61.
- Basu, G.D., Azorsa, D.O., Kiefer, J.A., Rojas, A.M., Tuzmen, S., Barrett, M.T., Trent, J.M., Kallioniemi, O. & Mousses, S. 2008, 'Functional evidence implicating S100P in prostate cancer progression.', *International Journal of Cancer*, vol. 123, no. 2, pp. 330–9.
- Batchelor, C.L., Woodward, A.M. & Crouch, D.H. 2004, 'Nuclear ERM (ezrin, radixin, moesin) proteins: regulation by cell density and nuclear import', *Experimental Cell Research*, vol. 296, no. 2, pp. 208–22.
- Baumgartner, M., Sillman, A.L., Blackwood, E.M., Srivastava, J., Madson, N., Schilling, J.W., Wright, J.H. & Barber, D.L. 2006, 'The Nck-interacting kinase phosphorylates ERM proteins for formation of lamellipodium by growth factors', *Proceedings of the National Academy of Sciences of the United States of America*, vol. 103, no. 36, pp. 13391–6.
- Beard, J. 1905, 'The cancer problem', *The Lancet*, vol. 165, no. 4249, pp. 281–3.
- Becker, T., Gerke, V., Kube, E. & Weber, K. 1992, 'S100P, a novel Ca(2+)-binding protein from human placenta. cDNA cloning, recombinant protein expression and Ca<sup>2+</sup> binding properties.', *European Journal of Biochemistry*, vol. 207, no. 2, pp. 541–7.
- Belkina, N. V., Liu, Y., Hao, J.-J., Karasuyama, H. & Shaw, S. 2009, 'LOK is a major ERM kinase in resting lymphocytes and regulates cytoskeletal rearrangement through ERM phosphorylation', *Proceedings of the National Academy of Sciences of the United States of America*, vol. 106, no. 12, pp. 4707–12.
- Bellahcene, A., Castronovo, V., Ogbureke, K.U.E., Fisher, L.W. & Fedarko, N.S. 2008, 'Small integrin-binding ligand N-linked glycoproteins (SIBLINGs): multifunctional proteins in cancer.', *Nature Reviews. Cancer*, vol. 8, no. 3, pp. 212–26.
- Bensenor, L.B., Kan, H.-M., Wang, N., Wallrabe, H., Davidson, L.A., Cai, Y., Schafer, D.A. & Bloom, G.S. 2007, 'IQGAP1 regulates cell motility by linking growth factor signaling to actin assembly.', *Journal of Cell Science*, vol. 120, no. Pt 4, pp. 658–69.
- Berryman, M. & Bretscher, A. 2000, 'Identification of a novel member of the chloride intracellular

- channel gene family (CLIC5) that associates with the actin cytoskeleton of placental microvilli', *Molecular Biology of the Cell*, vol. 11, no. 5, pp. 1509–21.
- Berryman, M., Franck, Z. & Bretscher, A. 1993, 'Ezrin is concentrated in the apical microvilli of a wide variety of epithelial cells whereas moesin is found primarily in endothelial cells.', *Journal of Cell Science*, vol. 105 ( Pt 4), pp. 1025–43.
- Berryman, M., Gary, R. & Bretscher, A. 1995, 'Ezrin oligomers are major cytoskeletal components of placental microvilli: a proposal for their involvement in cortical morphogenesis.', *The Journal of Cell Biology*, vol. 131, no. 5, pp. 1231–42.
- Bessède, E., Molina, S., Acuña-Amador, L., Dubus, P., Staedel, C., Chambonnier, L., Buissonnière, A., Sifré, E., Giese, A., Bénéjat, L., Rousseau, B., Costet, P., Sacks, D.B., Mégraud, F. & Varon, C. 2016, 'Deletion of IQGAP1 promotes *Helicobacter pylori*-induced gastric dysplasia in mice and acquisition of cancer stem cell properties in vitro', *Oncotarget*, vol. 7, no. 49, pp. 80688–99.
- Bethesda (MD): National Library of Medicine (US) 2019, 'Gene', *National Center for Biotechnology Information*, viewed 17 December 2019, <<https://www.ncbi.nlm.nih.gov/gene?Db=gene&Cmd=DetailsSearch&Term=7430>>.
- Bhattacharya, M., Sundaram, A., Kudo, M., Farmer, J., Ganesan, P., Khalifeh-Soltani, A., Arjomandi, M., Atabai, K., Huang, X. & Sheppard, D. 2014, 'IQGAP1-dependent scaffold suppresses RhoA and inhibits airway smooth muscle contraction.', *The Journal of Clinical Investigation*, vol. 124, no. 11, pp. 4895–8.
- Bielak-Zmijewska, A., Kolano, A., Szczepanska, K., Maleszewski, M. & Borsuk, E. 2008, 'Cdc42 protein acts upstream of IQGAP1 and regulates cytokinesis in mouse oocytes and embryos.', *Developmental Biology*, vol. 322, no. 1, pp. 21–32.
- Bissonnette, L., Drissenek, L., Antoine, Y., Tiers, L., Hirtz, C., Lehmann, S., Perrochia, H., Bissonnette, F., Kadoch, I.-J., Haouzi, D. & Hamamah, S. 2016, 'Human S100A10 plays a crucial role in the acquisition of the endometrial receptivity phenotype.', *Cell Adhesion & Migration*, vol. 10, no. 3, pp. 282–98.
- Boden, S.D. & Kaplan, F.S. 1990, 'Calcium homeostasis.', *The Orthopedic Clinics of North America*, vol. 21, no. 1, pp. 31–42.
- Bonilha, V.L., Finnemann, S.C. & Rodriguez-Boulan, E. 1999, 'Ezrin promotes morphogenesis of apical microvilli and basal infoldings in retinal pigment epithelium', *The Journal of Cell Biology*, vol. 147, no. 7, pp. 1533–48.
- Bosk, S., Braunger, J.A., Gerke, V. & Steinem, C. 2011, 'Activation of F-actin binding capacity of ezrin: synergism of PIP<sub>2</sub> interaction and phosphorylation', *Biophysical Journal*, vol. 100, no. 7, pp. 1708–17.
- Boureaux, A., Vignal, E., Faure, S. & Fort, P. 2007, 'Evolution of the Rho family of ras-like GTPases in eukaryotes', *Molecular Biology and Evolution*, vol. 24, no. 1, pp. 203–16.
- Bourguignon, L.Y.W., Gilad, E., Rothman, K. & Peyrollier, K. 2005, 'Hyaluronan-CD44 interaction with IQGAP1 promotes Cdc42 and ERK signaling, leading to actin binding, Elk-1/estrogen receptor transcriptional activation, and ovarian cancer progression.', *The Journal of Biological Chemistry*, vol. 280, no. 12, pp. 11961–72.
- Bowen, R. 2011, 'Placental structure and classification', *Colorado State University*, viewed 2 November 2019, <<http://www.vivo.colostate.edu/hbooks/pathphys/reprod/placenta/structure.html>>.
- Bowers, R.R., Manevich, Y., Townsend, D.M. & Tew, K.D. 2012, 'Sulfiredoxin redox-sensitive interaction with S100A4 and non-muscle myosin IIA regulates cancer cell motility.', *Biochemistry*, vol. 51, no. 39, pp. 7740–54.
- Bradshaw, A.D. 2012, 'Diverse biological functions of the SPARC family of proteins.', *The International Journal of Biochemistry & Cell Biology*, vol. 44, no. 3, pp. 480–8.
- Brandt, D.T. & Grosse, R. 2007, 'Get to grips: steering local actin dynamics with IQGAPs', *EMBO Reports*, vol. 8, no. 11, pp. 1019–23.
- Breitsprecher, D. & Goode, B.L. 2013, 'Formins at a glance.', *Journal of Cell Science*, vol. 126, no. Pt 1, pp. 1–7.
- Bretscher, A. 1983, 'Purification of an 80000-dalton protein that is a component of the isolated microvillus cytoskeleton, and its localization in nonmuscle cells', *J Cell Biol*, vol. 97, no. 2, pp. 425–32.
- Bretscher, A. 1989, 'Rapid phosphorylation and reorganization of ezrin and spectrin accompany morphological changes induced in A-431 cells by epidermal growth factor', *The Journal of Cell Biology*, vol. 108, no. 3, pp. 921–30.
- Bretscher, A., Edwards, K. & Fehon, R.G. 2002, 'ERM proteins and merlin: integrators at the cell cortex', *Nature Reviews. Molecular Cell Biology*, vol. 3, no. 8, pp. 586–99.

- Bretscher, A., Gary, R. & Berryman, M. 1995, 'Soluble ezrin purified from placenta exists as stable monomers and elongated dimers with masked C-terminal ezrin-radixin-moesin association domains.', *Biochemistry*, vol. 34, no. 51, pp. 16830–7.
- Briggs, J.W., Ren, L., Nguyen, R., Chakrabarti, K., Cassavaugh, J., Rahim, S., Bulut, G., Zhou, M., Veenstra, T.D., Chen, Q., Wei, J.S., Khan, J., Uren, A. & Khanna, C. 2012, 'The ezrin metastatic phenotype is associated with the initiation of protein translation.', *Neoplasia (New York, N.Y.)*, vol. 14, no. 4, pp. 297–310.
- Briggs, M.W., Li, Z. & Sacks, D.B. 2002, 'IQGAP1-mediated stimulation of transcriptional co-activation by beta-catenin is modulated by calmodulin.', *The Journal of Biological Chemistry*, vol. 277, no. 9, pp. 7453–65.
- Briggs, M.W. & Sacks, D.B. 2003, 'IQGAP proteins are integral components of cytoskeletal regulation', *EMBO Reports*, vol. 4, no. 6, pp. 571–4.
- Brosens, I.A., Robertson, W.B. & Dixon, H.G. 1972, 'The role of the spiral arteries in the pathogenesis of preeclampsia.', *Obstetrics and Gynecology Annual*, vol. 1, pp. 177–91.
- Brown, M.D., Bry, L., Li, Z. & Sacks, D.B. 2008, 'Actin pedestal formation by enteropathogenic *Escherichia coli* is regulated by IQGAP1, calcium, and calmodulin', *The Journal of Biological Chemistry*, vol. 283, no. 50, 2008/09/22., pp. 35212–22.
- Brown, M.D. & Sacks, D.B. 2006, 'IQGAP1 in cellular signaling: bridging the GAP.', *Trends in Cell Biology*, vol. 16, no. 5, pp. 242–9.
- Bruce, B., Khanna, G., Ren, L., Landberg, G., Jirstrom, K., Powell, C., Borczuk, A., Keller, E.T., Wojno, K.J., Meltzer, P., Baird, K., McClatchey, A., Bretscher, A., Hewitt, S.M. & Khanna, C. 2007, 'Expression of the cytoskeleton linker protein ezrin in human cancers.', *Clinical & Experimental Metastasis*, vol. 24, no. 2, pp. 69–78.
- Brukner, I. & Tremblay, G.A. 2000, 'Cellular proteins prevent antisense phosphorothioate oligonucleotide (SdT18) to target sense RNA (rA18): development of a new in vitro assay.', *Biochemistry*, vol. 39, no. 37, pp. 11463–6.
- Bulut, G., Hong, S.-H., Chen, K., Beauchamp, E.M., Rahim, S., Kosturko, G.W., Glasgow, E., Dakshanamurthy, S., Lee, H.-S., Daar, I., Toretsky, J.A., Khanna, C. & Uren, A. 2012, 'Small molecule inhibitors of ezrin inhibit the invasive phenotype of osteosarcoma cells.', *Oncogene*, vol. 31, no. 3, pp. 269–81.
- Burrows, T.D., King, A., Smith, S.K. & Loke, Y.W. 1995, 'Human trophoblast adhesion to matrix proteins: inhibition and signal transduction.', *Molecular Human Reproduction*, vol. 10, no. 9, pp. 2489–500.
- Bustelo, X.R., Sauzeau, V. & Berenjeno, I.M. 2007, 'GTP-binding proteins of the Rho/Rac family: regulation, effectors and functions in vivo', *BioEssays : News and Reviews in Molecular, Cellular and Developmental Biology*, vol. 29, no. 4, pp. 356–70.
- Cancer Australia 2019, 'Invasion and metastasis', *EdCaN*, viewed 10 November 2019, <<http://edcan.org.au/edcan-learning-resources/supporting-resources/biology-of-cancer/defining-cancer/invasion-metastasis>>.
- Caniggia, I., Winter, J., Lye, S.J. & Post, M. 2000, 'Oxygen and placental development during the first trimester: implications for the pathophysiology of pre-eclampsia.', *Placenta*, vol. 21 Suppl A, pp. S25-30.
- Carmon, K.S., Gong, X., Yi, J., Thomas, A. & Liu, Q. 2014, 'RSPO-LGR4 functions via IQGAP1 to potentiate Wnt signaling.', *Proceedings of the National Academy of Sciences of the United States of America*, vol. 111, no. 13, pp. E1221-9.
- Carmona-Fontaine, C., Matthews, H. & Mayor, R. 2008, 'Directional cell migration in vivo: wnt at the crest', *Cell Adhesion & Migration*, vol. 2, no. 4, 2008/10/05., pp. 240–2.
- Carneiro, A., Bendahl, P.-O., Akerman, M., Domanski, H.A., Rydholm, A., Engellau, J. & Nilbert, M. 2011, 'Ezrin expression predicts local recurrence and development of metastases in soft tissue sarcomas', *Journal of Clinical Pathology*, vol. 64, no. 8, pp. 689 LP – 694.
- Carter, G.W., Prinz, S., Neou, C., Shelby, J.P., Marzolf, B., Thorsson, V. & Galitski, T. 2007, 'Prediction of phenotype and gene expression for combinations of mutations.', *Molecular Systems Biology*, vol. 3, p. 96.
- Casaleto, J.B., Saotome, I., Curto, M. & McClatchey, A.I. 2011, 'Ezrin-mediated apical integrity is required for intestinal homeostasis', *Proceedings of the National Academy of Sciences of the United States of America*, vol. 108, no. 29, 2011/07/05., pp. 11924–9.
- Cavallaro, U. & Christofori, G. 2004, 'Cell adhesion and signalling by cadherins and Ig-CAMs in cancer.', *Nature Reviews. Cancer*, vol. 4, no. 2, pp. 118–32.
- Celik, H., Bulut, G., Han, J., Graham, G.T., Minas, T.Z., Conn, E.J., Hong, S.-H., Pauly, G.T., Hayran,

- M., Li, X., Ozdemirli, M., Ayhan, A., Rudek, M.A., Toretsky, J.A. & Uren, A. 2016, 'Ezrin inhibition up-regulates stress response gene expression.', *The Journal of Biological Chemistry*, vol. 291, no. 25, pp. 13257–70.
- Chandramouli, A., Mercado-Pimentel, M.E., Hutchinson, A., Gibadulinová, A., Olson, E.R., Dickinson, S., Shañas, R., Davenport, J., Owens, J., Bhattacharyya, A.K., Regan, J.W., Pastorekova, S., Arumugam, T., Logsdon, C.D. & Nelson, M.A. 2010, 'The induction of S100p expression by the Prostaglandin E<sub>2</sub> (PGE<sub>2</sub>)/EP4 receptor signaling pathway in colon cancer cells', *Cancer Biology & Therapy*, vol. 10, no. 10, 2010/11/15., pp. 1056–66.
- Chang, F., Woollard, A. & Nurse, P. 1996, 'Isolation and characterization of fission yeast mutants defective in the assembly and placement of the contractile actin ring.', *Journal of Cell Science*, vol. 109 ( Pt 1, pp. 131–42.
- Chellini, L., Caprara, V., Spadaro, F., Sestito, R., Bagnato, A. & Rosano, L. 2019, 'Regulation of extracellular matrix degradation and metastatic spread by IQGAP1 through endothelin-1 receptor signalling in ovarian cancer.', *Matrix Biology : Journal of the International Society for Matrix Biology*, vol. 81, pp. 17–33.
- Chen, H., Xu, C., Jin, Q. & Liu, Z. 2014, 'S100 protein family in human cancer', *American Journal of Cancer Research*, vol. 4, no. 2, pp. 89–115.
- Chen, H., Yuan, Y., Zhang, C., Luo, A., Ding, F., Ma, J., Yang, S., Tian, Y., Tong, T., Zhan, Q. & Liu, Z. 2012, 'Involvement of S100A14 protein in cell invasion by affecting expression and function of matrix metalloproteinase (MMP)-2 via p53-dependent transcriptional regulation.', *The Journal of Biological Chemistry*, vol. 287, no. 21, pp. 17109–19.
- Chen, Q., Zhang, X.H.-F. & Massague, J. 2011, 'Macrophage binding to receptor VCAM-1 transmits survival signals in breast cancer cells that invade the lungs.', *Cancer Cell*, vol. 20, no. 4, pp. 538–49.
- Cheung, A.N.Y., Zhang, H.J., Xue, W.C. & Siu, M.K.Y. 2009, 'Pathogenesis of choriocarcinoma: clinical, genetic and stem cell perspectives.', *Future Oncology*, vol. 5, no. 2, pp. 217–31.
- Choi, C.K., Vicente-Manzanares, M., Zareno, J., Whitmore, L.A., Mogilner, A. & Horwitz, A.R. 2008, 'Actin and alpha-actinin orchestrate the assembly and maturation of nascent adhesions in a myosin II motor-independent manner.', *Nature Cell Biology*, vol. 10, no. 9, pp. 1039–50.
- Choi, S. & Anderson, R.A. 2016, 'IQGAP1 is a phosphoinositide effector and kinase scaffold', *Advances in Biological Regulation*, vol. 60, 2015/10/28., pp. 29–35.
- Choi, S., Thapa, N., Hedman, A.C., Li, Z., Sacks, D.B. & Anderson, R.A. 2013, 'IQGAP1 is a novel phosphatidylinositol 4,5 bisphosphate effector in regulation of directional cell migration.', *The EMBO Journal*, vol. 32, no. 19, pp. 2617–30.
- Choy, M.Y., St Whitley, G. & Manyonda, I.T. 2000, 'Efficient, rapid and reliable establishment of human trophoblast cell lines using poly-L-ornithine.', *Early Pregnancy (Online)*, vol. 4, no. 2, pp. 124–43.
- Le Clainche, C., Schlaepfer, D., Ferrari, A., Klingauf, M., Grohmanova, K., Veligodskiy, A., Didry, D., Le, D., Egile, C., Carlier, M.-F. & Kroschewski, R. 2007, 'IQGAP1 stimulates actin assembly through the N-WASP-Arp2/3 pathway.', *The Journal of Biological Chemistry*, vol. 282, no. 1, pp. 426–35.
- Clarke, C.J., Gross, S.R., Ismail, T.M., Rudland, P.S., Al-Medhtiy, M., Santangeli, M. & Barraclough, R. 2017, 'Activation of tissue plasminogen activator by metastasis-inducing S100P protein', *The Biochemical Journal*, vol. 474, no. 19, pp. 3227–40.
- Clucas, J. & Valderrama, F. 2014, 'ERM proteins in cancer progression', *Journal of Cell Science*, vol. 127, no. Pt 2, pp. 267–75.
- Cooper, G.M.C. 2000, *The Cell: A Molecular Approach*, 2nd edn, Sinauer Associates, Sunderland (MA).
- Di Cristofano, C., Leopizzi, M., Miraglia, A., Sardella, B., Moretti, V., Ferrara, A., Petrozza, V. & Della Rocca, C. 2010, 'Phosphorylated ezrin is located in the nucleus of the osteosarcoma cell.', *Modern Pathology : an Official Journal of the United States and Canadian Academy of Pathology, Inc*, vol. 23, no. 7, pp. 1012–20.
- Cupit, L.D., Schmidt, V.A., Miller, F. & Bahou, W.F. 2004, 'Distinct PAR/IQGAP expression patterns during murine development: implications for thrombin-associated cytoskeletal reorganization.', *Mammalian Genome : Official Journal of the International Mammalian Genome Society*, vol. 15, no. 8, pp. 618–29.
- Curto, M. & McClatchey, A.I. 2004, 'Ezrin...a metastatic detERMinant?', *Cancer Cell*, vol. 5, no. 2, pp. 113–4.
- Cybulsky, A. V., Guillemette, J., Papillon, J. & Abouelazm, N.T. 2017, 'Regulation of Ste20-like kinase, SLK, activity: Dimerization and activation segment phosphorylation', *PloS One*, vol. 12, no. 5, p.

e0177226.

- Dard, N., Louvet-Vallee, S., Santa-Maria, A. & Maro, B. 2004, 'Phosphorylation of ezrin on threonine T567 plays a crucial role during compaction in the mouse early embryo.', *Developmental Biology*, vol. 271, no. 1, pp. 87–97.
- Dard, N., Louvet, S., Santa-Maria, A., Aghion, J., Martin, M., Mangeat, P. & Maro, B. 2001, 'In vivo functional analysis of ezrin during mouse blastocyst formation', *Developmental Biology*, vol. 233, no. 1, pp. 161–73.
- DaSilva-Arnold, S.C., Zamudio, S., Al-Khan, A., Alvarez-Perez, J., Mannion, C., Koenig, C., Luke, D., Perez, A.M., Petroff, M., Alvarez, M. & Illsley, N.P. 2018, 'Human trophoblast epithelial-mesenchymal transition in abnormally invasive placenta', *Biology of Reproduction*, vol. 99, no. 2, pp. 409–21.
- Davies, B.R., Davies, M.P., Gibbs, F.E., Barraclough, R. & Rudland, P.S. 1993, 'Induction of the metastatic phenotype by transfection of a benign rat mammary epithelial cell line with the gene for p9Ka, a rat calcium-binding protein, but not with the oncogene EJ-ras-1.', *Oncogene*, vol. 8, no. 4, pp. 999–1008.
- Dekel, N., Gnainsky, Y., Granot, I. & Mor, G. 2010, 'Inflammation and implantation', *American Journal of Reproductive Immunology*, vol. 63, no. 1, pp. 17–21.
- Desgrosellier, J.S. & Cheresh, D.A. 2010, 'Integrins in cancer: biological implications and therapeutic opportunities.', *Nature Reviews. Cancer*, vol. 10, no. 1, pp. 9–22.
- Dey, S.K., Lim, H., Das, S.K., Reese, J., Paria, B.C., Daikoku, T. & Wang, H. 2004, 'Molecular cues to implantation.', *Endocrine Reviews*, vol. 25, no. 3, pp. 341–73.
- Diao, B., Liu, Y., Zhang, Y., Yu, J., Xie, J. & Xu, G.-Z. 2017, 'IQGAP1-siRNA inhibits proliferation and metastasis of U251 and U373 glioma cell lines', *Molecular Medicine Reports*, vol. 15, no. 4, 2017/02/28., pp. 2074–82.
- Diederichs, S., Bulk, E., Steffen, B., Ji, P., Tickenbrock, L., Lang, K., Zanker, K.S., Metzger, R., Schneider, P.M., Gerke, V., Thomas, M., Berdel, W.E., Serve, H. & Muller-Tidow, C. 2004, 'S100 family members and trypsinogens are predictors of distant metastasis and survival in early-stage non-small cell lung cancer.', *Cancer Research*, vol. 64, no. 16, pp. 5564–9.
- Donato, R. 1986, 'S-100 proteins', *Cell Calcium*, vol. 7, no. 3, pp. 123–45.
- Donato, R. 2001, 'S100: a multigenic family of calcium-modulated proteins of the EF-hand type with intracellular and extracellular functional roles.', *The International Journal of Biochemistry & Cell Biology*, vol. 33, no. 7, pp. 637–68.
- Donato, R., Cannon, B.R., Sorci, G., Riuzzi, F., Hsu, K., Weber, D.J. & Geczy, C.L. 2013, 'Functions of S100 proteins.', *Current Molecular Medicine*, vol. 13, no. 1, pp. 24–57.
- Dong, L., Gao, T., Yue, W. & Yu, W. 2016, 'Mechanism underlying the regulation of trophoblast-like cell invasion by miR-183 screened from the peripheral blood of pregnant women with preeclampsia', *Int J Clin Exp Pathol*, vol. 9, no. 6, pp. 6154–62.
- Dong, P., Ihira, K., Xiong, Y., Watari, H., Hanley, S.J.B., Yamada, T., Hosaka, M., Kudo, M., Yue, J. & Sakuragi, N. 2016, 'Reactivation of epigenetically silenced miR-124 reverses the epithelial-to-mesenchymal transition and inhibits invasion in endometrial cancer cells via the direct repression of IQGAP1 expression.', *Oncotarget*, vol. 7, no. 15, pp. 20260–70.
- Dong, P., Nabeshima, K., Nishimura, N., Kawakami, T., Hachisuga, T., Kawarabayashi, T. & Iwasaki, H. 2006, 'Overexpression and diffuse expression pattern of IQGAP1 at invasion fronts are independent prognostic parameters in ovarian carcinomas.', *Cancer Letters*, vol. 243, no. 1, pp. 120–7.
- Dong, P.X., Jia, N., Xu, Z.J., Liu, Y.T., Li, D.J. & Feng, Y.J. 2008, 'Silencing of IQGAP1 by shRNA inhibits the invasion of ovarian carcinoma HO-8910PM cells in vitro', *Journal of Experimental and Clinical Cancer Research*.
- Dormann, D. & Weijer, C.J. 2006, 'Chemotactic cell movement during Dictyostelium development and gastrulation.', *Current Opinion in Genetics & Development*, vol. 16, no. 4, pp. 367–73.
- Dowen, S.E., Crnogorac-Jurcevic, T., Gangeswaran, R., Hansen, M., Eloranta, J.J., Bhakta, V., Brentnall, T.A., Luttges, J., Kloppel, G. & Lemoine, N.R. 2005, 'Expression of S100P and its novel binding partner S100PBPR in early pancreatic cancer.', *The American Journal of Pathology*, vol. 166, no. 1, pp. 81–92.
- Drohat, A.C., Baldisseri, D.M., Rustandi, R.R. & Weber, D.J. 1998, 'Solution structure of calcium-bound rat S100B(beta-beta) as determined by nuclear magnetic resonance spectroscopy', *Biochemistry*, vol. 37, no. 9, pp. 2729–40.
- Du, M., Wang, G., Ismail, T.M., Gross, S., Fernig, D.G., Barraclough, R. & Rudland, P.S. 2012, 'S100P dissociates myosin IIA filaments and focal adhesion sites to reduce cell adhesion and enhance cell

- migration.’, *The Journal of Biological Chemistry*, vol. 287, no. 19, pp. 15330–44.
- Dunn, C.L., Kelly, R.W. & Critchley, H.O.D. 2003, ‘Decidualization of the human endometrial stromal cell: an enigmatic transformation.’, *Reproductive Biomedicine Online*, vol. 7, no. 2, pp. 151–61.
- Eaton, B.E., Gold, L. & Zichi, D.A. 1995, ‘Let’s get specific: the relationship between specificity and affinity’, *Chemistry & Biology*, vol. 2, no. 10, pp. 633–8.
- Edwards, R.G. 2007, ‘Human implantation: the last barrier in assisted reproduction technologies?’, *Reproductive Biomedicine Online*, vol. 14 Spec No, pp. 5–22.
- Elliott, B.E., Meens, J.A., SenGupta, S.K., Louvard, D. & Arpin, M. 2005, ‘The membrane cytoskeletal crosslinker ezrin is required for metastasis of breast carcinoma cells’, *Breast Cancer Research : BCR*, vol. 7, no. 3, 2005/03/21., pp. R365–73.
- Elzagheid, A., Korkeila, E., Bendardaf, R., Buhmeida, A., Heikkila, S., Vaheri, A., Syrjanen, K., Pyrhonen, S. & Carpen, O. 2008, ‘Intense cytoplasmic ezrin immunoreactivity predicts poor survival in colorectal cancer.’, *Human Pathology*, vol. 39, no. 12, pp. 1737–43.
- Emoto, Y., Kobayashi, R., Akatsuka, H. & Hidaka, H. 1992, ‘Purification and characterization of a new member of the S-100 protein family from human placenta’, *Biochemical and Biophysical Research Communications*, vol. 182, no. 3, pp. 1246–53.
- Eng, K., Naqvi, N.I., Wong, K.C. & Balasubramanian, M.K. 1998, ‘Rng2p, a protein required for cytokinesis in fission yeast, is a component of the actomyosin ring and the spindle pole body.’, *Current Biology : CB*, vol. 8, no. 11, pp. 611–21.
- Epp, J.A. & Chant, J. 1997, ‘An IQGAP-related protein controls actin-ring formation and cytokinesis in yeast.’, *Current Biology : CB*, vol. 7, no. 12, pp. 921–9.
- Erickson, J.W., Cerione, R.A. & Hart, M.J. 1997, ‘Identification of an actin cytoskeletal complex that includes IQGAP and the Cdc42 GTPase.’, *The Journal of Biological Chemistry*, vol. 272, no. 39, pp. 24443–7.
- Errasfa, M. & Stern, A. 1994, ‘Inhibition of epidermal growth factor-dependent protein tyrosine phosphorylation by phorbol myristate acetate is mediated by protein tyrosine phosphatase activity’, *FEBS Letters*, vol. 339, no. 1–2, pp. 7–10.
- Esterman, A., Greco, M.A., Mitani, Y., Finlay, T.H., Ismail-Beigi, F. & Dancis, J. 1997, ‘The effect of hypoxia on human trophoblast in culture: Morphology, glucose transport and metabolism’, *Placenta*, vol. 18, no. 2, pp. 129–36.
- Fais, S., De Milito, A. & Lozupone, F. 2005, ‘The role of FAS to ezrin association in FAS-mediated apoptosis.’, *Apoptosis : an International Journal on Programmed Cell Death*, vol. 10, no. 5, pp. 941–7.
- Faix, J. & Dittrich, W. 1996, ‘DGAP1, a homologue of rasGTPase activating proteins that controls growth, cytokinesis, and development in Dictyostelium discoideum.’, *FEBS Letters*, vol. 394, no. 3, pp. 251–7.
- Fan, L.-L., Chen, D.-F., Lan, C.-H., Liu, K.-Y. & Fang, D.-C. 2011, ‘Knockdown of ezrin via RNA interference suppresses Helicobacter pylori-enhanced invasion of gastric cancer cells.’, *Cancer Biology & Therapy*, vol. 11, no. 8, pp. 746–52.
- Fehon, R.G., McClatchey, A.I. & Bretscher, A. 2010, ‘Organizing the cell cortex: the role of ERM proteins.’, *Nature Reviews. Molecular Cell Biology*, vol. 11, no. 4, pp. 276–87.
- Fidalgo, M., Guerrero, A., Fraile, M., Iglesias, C., Pombo, C.M. & Zalvide, J. 2012, ‘Adaptor protein cerebral cavernous malformation 3 (CCM3) mediates phosphorylation of the cytoskeletal proteins ezrin/radixin/moesin by mammalian Ste20-4 to protect cells from oxidative stress’, *The Journal of Biological Chemistry*, vol. 287, no. 14, pp. 11556–65.
- Fievet, B.T., Gautreau, A., Roy, C., Del Maestro, L., Mangeat, P., Louvard, D. & Arpin, M. 2004, ‘Phosphoinositide binding and phosphorylation act sequentially in the activation mechanism of ezrin.’, *The Journal of Cell Biology*, vol. 164, no. 5, pp. 653–9.
- Filipek, A., Jastrzebska, B., Nowotny, M. & Kuznicki, J. 2002, ‘CacyBP/SIP, a calcyclin and Siah-1-interacting protein, binds EF-hand proteins of the S100 family.’, *The Journal of Biological Chemistry*, vol. 277, no. 32, pp. 28848–52.
- Firth, J.A., Farr, A. & Bauman, K. 1980, ‘The role of gap junctions in trophoblastic cell fusion in the guinea-pig placenta.’, *Cell and Tissue Research*, vol. 205, no. 2, pp. 311–8.
- Ford, H.L. & Zain, S.B. 1995, ‘Interaction of metastasis associated Mts1 protein with nonmuscle myosin.’, *Oncogene*, vol. 10, no. 8, pp. 1597–605.
- Foroutannejad, S., Rohner, N., Reimer, M., Kwon, G. & Schober, J.M. 2014, ‘A novel role for IQGAP1 protein in cell motility through cell retraction.’, *Biochemical and Biophysical Research Communications*, vol. 448, no. 1, pp. 39–44.
- Fouassier, L., Duan, C.Y., Feranchak, A.P., Yun, C.H., Sutherland, E., Simon, F., Fitz, J.G. & Doctor,

- R.B. 2001, 'Ezrin-radixin-moesin-binding phosphoprotein 50 is expressed at the apical membrane of rat liver epithelia', *Hepatology (Baltimore, Md.)*, vol. 33, no. 1, pp. 166–76.
- Frantz, C., Stewart, K.M. & Weaver, V.M. 2010, 'The extracellular matrix at a glance.', *Journal of Cell Science*, vol. 123, no. Pt 24, pp. 4195–200.
- Friedl, P. & Alexander, S. 2011, 'Cancer invasion and the microenvironment: plasticity and reciprocity', *Cell*, vol. 147, no. 5, pp. 992–1009.
- Friedl, P., Zanker, K.S. & Brocker, E.B. 1998, 'Cell migration strategies in 3-D extracellular matrix: differences in morphology, cell matrix interactions, and integrin function.', *Microscopy Research and Technique*, vol. 43, no. 5, pp. 369–78.
- Fu, G., Brkic, J., Hayder, H. & Peng, C. 2013, 'MicroRNAs in human placental development and pregnancy complications', *International Journal of Molecular Sciences*, vol. 14, no. 3, pp. 5519–44.
- Fuentes, M.K., Nigavekar, S.S., Arumugam, T., Logsdon, C.D., Schmidt, A.M., Park, J.C. & Huang, E.H. 2007, 'RAGE activation by S100P in colon cancer stimulates growth, migration, and cell signaling pathways.', *Diseases of the Colon and Rectum*, vol. 50, no. 8, pp. 1230–40.
- Fukata, M., Kuroda, S., Nakagawa, M., Kawajiri, A., Itoh, N., Shoji, I., Matsuura, Y., Yonehara, S., Fujisawa, H., Kikuchi, A. & Kaibuchi, K. 1999, 'Cdc42 and Rac1 regulate the interaction of IQGAP1 with beta-catenin.', *The Journal of Biological Chemistry*, vol. 274, no. 37, pp. 26044–50.
- Fukata, M., Watanabe, T., Noritake, J., Nakagawa, M., Yamaga, M., Kuroda, S., Matsuura, Y., Iwamatsu, A., Perez, F. & Kaibuchi, K. 2002, 'Rac1 and Cdc42 capture microtubules through IQGAP1 and CLIP-170.', *Cell*, vol. 109, no. 7, pp. 873–85.
- Van Furden, D., Johnson, K., Segbert, C. & Bossinger, O. 2004, 'The *C. elegans* ezrin-radixin-moesin protein ERM-1 is necessary for apical junction remodelling and tubulogenesis in the intestine', *Developmental Biology*, vol. 272, no. 1, pp. 262–76.
- Furukawa, S., Kuroda, Y. & Sugiyama, A. 2014, 'A comparison of the histological structure of the placenta in experimental animals', *Journal of Toxicologic Pathology*, vol. 27, no. 1, 2014/04/30., pp. 11–8.
- Gallant, N.D., Michael, K.E. & García, A.J. 2005, 'Cell adhesion strengthening: contributions of adhesive area, integrin binding, and focal adhesion assembly', *Molecular Biology of the Cell*, vol. 16, no. 9, 2005/07/06., pp. 4329–40.
- Gao, S.-Y., Li, E.-M., Cui, L., Lu, X.-F., Meng, L.-Y., Yuan, H.-M., Xie, J.-J., Du, Z.-P., Pang, J.-X. & Xu, L.-Y. 2009, 'Sp1 and AP-1 regulate expression of the human gene VIL2 in esophageal carcinoma cells.', *The Journal of Biological Chemistry*, vol. 284, no. 12, pp. 7995–8004.
- Gary, R. & Bretscher, A. 1993, 'Heterotypic and homotypic associations between ezrin and moesin, two putative membrane-cytoskeletal linking proteins', *Proceedings of the National Academy of Sciences of the United States of America*, vol. 90, no. 22, pp. 10846–50.
- Gautreau, A., Poulet, P., Louvard, D. & Arpin, M. 1999, 'Ezrin, a plasma membrane-microfilament linker, signals cell survival through the phosphatidylinositol 3-kinase/Akt pathway.', *Proceedings of the National Academy of Sciences of the United States of America*, vol. 96, no. 13, pp. 7300–5.
- Geiger, K.D., Stoldt, P., Schlote, W. & Derouiche, A. 2000, 'Ezrin immunoreactivity is associated with increasing malignancy of astrocytic tumors but is absent in oligodendrogliomas', *The American Journal of Pathology*, vol. 157, no. 6, pp. 1785–93.
- Ghaffari, A., Hoskin, V., Turashvili, G., Varma, S., Mewburn, J., Mullins, G., Greer, P.A., Kiefer, F., Day, A.G., Madarnas, Y., SenGupta, S. & Elliott, B.E. 2019, 'Intravital imaging reveals systemic ezrin inhibition impedes cancer cell migration and lymph node metastasis in breast cancer', *Breast Cancer Research : BCR*, vol. 21, no. 1, p. 12.
- Giampieri, S., Manning, C., Hooper, S., Jones, L., Hill, C.S. & Sahai, E. 2009, 'Localized and reversible TGFbeta signalling switches breast cancer cells from cohesive to single cell motility.', *Nature Cell Biology*, vol. 11, no. 11, pp. 1287–96.
- Gibadulinova, A., Oveckova, I., Parkkila, S., Pastorekova, S. & Pastorek, J. 2008, 'Key promoter elements involved in transcriptional activation of the cancer-related gene coding for S100P calcium-binding protein.', *Oncology Reports*, vol. 20, no. 2, pp. 391–6.
- Goh Then Sin, C., Hersch, N., Rudland, P.S., Barraclough, R., Hoffmann, B. & Gross, S.R. 2011, 'S100A4 downregulates filopodia formation through increased dynamic instability.', *Cell Adhesion & Migration*, vol. 5, no. 5, pp. 439–47.
- Gong, L., Zhu, L., Wang, S. & Zhang, Z. 2017, 'Transthyretin regulates the migration and invasion of JEG-3 cells', *Oncology Letters*, vol. 13, no. 3, 2016/12/28., pp. 1242–6.
- Gonzalez-Amaro, R. & Sanchez-Madrid, F. 1999, 'Cell adhesion molecules: selectins and integrins.',

- Critical Reviews in Immunology*, vol. 19, no. 5–6, pp. 389–429.
- Goslin, K., Birgbauer, E., Banker, G. & Solomon, F. 1989, 'The role of cytoskeleton in organizing growth cones: a microfilament-associated growth cone component depends upon microtubules for its localization', *The Journal of Cell Biology*, vol. 109, no. 4 Pt 1, pp. 1621–31.
- Gould, K.L., Cooper, J.A., Bretscher, A. & Hunter, T. 1986, 'The protein-tyrosine kinase substrate, p81, is homologous to a chicken microvillar core protein', *The Journal of Cell Biology*, vol. 102, no. 2, pp. 660–9.
- Graham, C.H., Hawley, T.S., Hawley, R.G., MacDougall, J.R., Kerbel, R.S., Khoo, N. & Lala, P.K. 1993, 'Establishment and characterization of first trimester human trophoblast cells with extended lifespan.', *Experimental Cell Research*, vol. 206, no. 2, pp. 204–11.
- Grahammer, F., Schell, C. & Huber, T.B. 2013, 'The podocyte slit diaphragm--from a thin grey line to a complex signalling hub.', *Nature Reviews. Nephrology*, vol. 9, no. 10, pp. 587–98.
- Grohmanova, K., Schlaepfer, D., Hess, D., Gutierrez, P., Beck, M. & Kroschewski, R. 2004, 'Phosphorylation of IQGAP1 modulates its binding to Cdc42, revealing a new type of rho-GTPase regulator.', *The Journal of Biological Chemistry*, vol. 279, no. 47, pp. 48495–504.
- Gross, S.R., Sin, C.G.T., Barraclough, R. & Rudland, P.S. 2014, 'Joining S100 proteins and migration: for better or for worse, in sickness and in health.', *Cellular and Molecular Life Sciences: CMLS*, vol. 71, no. 9, pp. 1551–79.
- Grune, T., Reinheckel, T., North, J.A., Li, R., Bescos, P.B., Shringarpure, R. & Davies, K.J.A. 2002, 'Ezrin turnover and cell shape changes catalyzed by proteasome in oxidatively stressed cells', *FASEB Journal*, vol. 16, no. 12, pp. 1602–10.
- Gude, N.M., Roberts, C.T., Kalionis, B. & King, R.G. 2004, 'Growth and function of the normal human placenta', *Thrombosis Research*, vol. 114, no. 5–6, pp. 397–407.
- Guerreiro Da Silva, I.D., Hu, Y.F., Russo, I.H., Ao, X., Salicioni, A.M., Yang, X. & Russo, J. 2000, 'S100P calcium-binding protein overexpression is associated with immortalization of human breast epithelial cells in vitro and early stages of breast cancer development in vivo.', *International Journal of Oncology*, vol. 16, no. 2, pp. 231–40.
- Guo, L., Chen, S., Jiang, H., Huang, J., Jin, W. & Yao, S. 2014, 'The expression of S100P increases and promotes cellular proliferation by increasing nuclear translocation of beta-catenin in endometrial cancer.', *International Journal of Clinical and Experimental Pathology*, vol. 7, no. 5, pp. 2102–12.
- Haeger, J., Hambruch, N., Dantzer, V., Hoelker, M., Schellander, K., Klisch, K. & Pfarrer, C. 2015, 'Changes in endometrial ezrin and cytokeratin 18 expression during bovine implantation and in caruncular endometrial spheroids in vitro', *Placenta*, vol. 36, no. 8, pp. 821–31.
- Hago, A.M., Gamallat, Y., Mahmoud, S.A., Huang, Y., Zhang, J., Mahmoud, Y.K., Wang, J., Wei, Y., Wang, L., Zhou, S., Awsh, M.A., Yabasin, I.B. & Tang, J. 2017, 'Ezrin expression is altered in mice lymphatic metastatic hepatocellular carcinoma and subcellular fractions upon Annexin 7 modulation in-vitro.', *Biomedicine & Pharmacotherapy*, vol. 85, pp. 209–17.
- Hajjar, K.A. & Krishnan, S. 1999, 'Annexin II: a mediator of the plasmin/plasminogen activator system', *Trends in Cardiovascular Medicine*, vol. 9, no. 5, pp. 128–38.
- Halon, A., Donizy, P., Surowiak, P. & Matkowski, R. 2013, 'ERM/Rho protein expression in ductal breast cancer: a 15 year follow-up.', *Cellular Oncology (Dordrecht)*, vol. 36, no. 3, pp. 181–90.
- Han, J., Li, L., Hu, J., Yu, L., Zheng, Y., Guo, J., Zheng, X., Yi, P. & Zhou, Y. 2010, 'Epidermal growth factor stimulates human trophoblast cell migration through Rho A and Rho C activation.', *Endocrinology*, vol. 151, no. 4, pp. 1732–42.
- Hanahan, D. & Weinberg, R.A. 2011, 'Hallmarks of cancer: the next generation.', *Cell*, vol. 144, no. 5, pp. 646–74.
- Hantak, A.M., Bagchi, I.C. & Bagchi, M.K. 2014, 'Role of uterine stromal-epithelial crosstalk in embryo implantation', *International Journal of Developmental Biology*, vol. 58, no. 2–4, pp. 139–46.
- Hanzel, D., Reggio, H., Bretscher, A., Forte, J.G. & Mangeat, P. 1991, 'The secretion-stimulated 80K phosphoprotein of parietal cells is ezrin, and has properties of a membrane cytoskeletal linker in the induced apical microvilli.', *The EMBO Journal*, vol. 10, no. 9, pp. 2363–73.
- Hao, D., Li, C., Zhang, S., Lu, J., Jiang, Y., Wang, S. & Zhou, M. 2014, 'Network-based analysis of genotype-phenotype correlations between different inheritance modes.', *Bioinformatics (Oxford, England)*, vol. 30, no. 22, pp. 3223–31.
- Haram, K., Mortensen, J.H. & Nagy, B. 2014, 'Genetic aspects of preeclampsia and the HELLP syndrome.', *Journal of Pregnancy*, vol. 2014, p. 910751.
- Hart, M.J., Callow, M.G., Souza, B. & Polakis, P. 1996, 'IQGAP1, a calmodulin-binding protein with a rasGAP-related domain, is a potential effector for cdc42Hs.', *The EMBO Journal*, vol. 15, no. 12, pp. 2997–3005.

- Hayashi, H., Nabeshima, K., Aoki, M., Hamasaki, M., Enatsu, S., Yamauchi, Y., Yamashita, Y. & Iwasaki, H. 2010, 'Overexpression of IQGAP1 in advanced colorectal cancer correlates with poor prognosis-critical role in tumor invasion.', *International Journal of Cancer*, vol. 126, no. 11, pp. 2563–74.
- Heasman, S.J. & Ridley, A.J. 2008, 'Mammalian Rho GTPases: new insights into their functions from in vivo studies', *Nature Reviews. Molecular Cell Biology*, vol. 9, no. 9, pp. 690–701.
- Hebert, A.M., DuBoff, B., Casaletto, J.B., Gladden, A.B. & McClatchey, A.I. 2012, 'Merlin/ERM proteins establish cortical asymmetry and centrosome position.', *Genes & development*, vol. 26, no. 24, pp. 2709–23.
- Hedman, A.C., Smith, J.M. & Sacks, D.B. 2015, 'The biology of IQGAP proteins: beyond the cytoskeleton.', *EMBO Reports*, vol. 16, no. 4, pp. 427–46.
- Heil, A., Nazmi, A.R., Koltzsch, M., Poeter, M., Austermann, J., Assard, N., Baudier, J., Kaibuchi, K. & Gerke, V. 2011, 'S100P is a novel interaction partner and regulator of IQGAP1.', *The Journal of Biological Chemistry*, vol. 286, no. 9, pp. 7227–38.
- Heiska, L., Alftan, K., Gronholm, M., Vilja, P., Vaheri, A. & Carpen, O. 1998, 'Association of ezrin with intercellular adhesion molecule-1 and -2 (ICAM-1 and ICAM-2). Regulation by phosphatidylinositol 4, 5-bisphosphate', *The Journal of Biological Chemistry*, vol. 273, no. 34, pp. 21893–900.
- Heiska, L. & Carpen, O. 2005, 'Src phosphorylates ezrin at tyrosine 477 and induces a phosphospecific association between ezrin and a kelch-repeat protein family member.', *The Journal of Biological Chemistry*, vol. 280, no. 11, pp. 10244–52.
- Hidden, U., Ghaffari-Tabrizi, N., Gauster, M., Tam-Amersdorfer, C., Cetin, I., Dieber-Rotheneder, M., Lang, U. & Desoye, G. 2013, 'Membrane-type matrix metalloproteinase 1 regulates trophoblast functions and is reduced in fetal growth restriction', *The American Journal of Pathology*, vol. 182, no. 5, pp. 1563–71.
- Higuchi, K., Iizasa, H., Sai, Y., Horieya, S., Lee, K.-E., Wada, M., Deguchi, M., Nishimura, T., Wakayama, T., Tamura, A., Tsukita, S., Kose, N., Kang, Y.-S. & Nakashima, E. 2010, 'Differential expression of ezrin and CLP36 in the two layers of syncytiotrophoblast in rats.', *Biological & Pharmaceutical Bulletin*, vol. 33, no. 8, pp. 1400–6.
- Hill, M. 2019, 'Embryology Week 1', *UNSW Embryology*, viewed 4 November 2019, <[https://embryology.med.unsw.edu.au/embryology/index.php/Week\\_1](https://embryology.med.unsw.edu.au/embryology/index.php/Week_1)>.
- Hilliard, T.S., Miklossy, G., Chock, C., Yue, P., Williams, P. & Turkson, J. 2017, '15 $\alpha$ -methoxypuuphenol induces antitumor effects in vitro and in vivo against human glioblastoma and breast cancer models', *Molecular Cancer Therapeutics*, vol. 16, no. 4, 2017/01/09., pp. 601–13.
- Hipfner, D.R., Keller, N. & Cohen, S.M. 2004, 'Slik sterile-20 kinase regulates moesin activity to promote epithelial integrity during tissue growth', *Genes & Development*, vol. 18, no. 18, pp. 2243–8.
- Ho, J., Kong, J.-W.-F., Choong, L.-Y., Loh, M.-C.-S., Toy, W., Chong, P.-K., Wong, C.-H., Wong, C.-Y., Shah, N. & Lim, Y.-P. 2009, 'Novel breast cancer metastasis-associated proteins.', *Journal of Proteome Research*, vol. 8, no. 2, pp. 583–94.
- Ho, Y.D., Joyal, J.L., Li, Z. & Sacks, D.B. 1999, 'IQGAP1 integrates Ca<sup>2+</sup>/calmodulin and Cdc42 signaling.', *The Journal of Biological Chemistry*, vol. 274, no. 1, pp. 464–70.
- Hofmann Bowman, M., Wilk, J., Heydemann, A., Kim, G., Rehman, J., Lodato, J.A., Raman, J. & McNally, E.M. 2010, 'S100A12 mediates aortic wall remodeling and aortic aneurysm.', *Circulation Research*, vol. 106, no. 1, pp. 145–54.
- Holst-Hansen, C., Johannessen, B., Hoyer-Hansen, G., Romer, J., Ellis, V. & Brunner, N. 1996, 'Urokinase-type plasminogen activation in three human breast cancer cell lines correlates with their in vitro invasiveness.', *Clinical & Experimental Metastasis*, vol. 14, no. 3, pp. 297–307.
- Holtan, S.G., Creedon, D.J., Haluska, P. & Markovic, S.N. 2009, 'Cancer and pregnancy: parallels in growth, invasion, and immune modulation and implications for cancer therapeutic agents.', *Mayo Clinic Proceedings*, vol. 84, no. 11, pp. 985–1000.
- Horwitz, V., Davidson, B., Stern, D., Trope, C.G., Tavor Re'em, T. & Reich, R. 2016, 'Ezrin is associated with disease progression in ovarian carcinoma.', *PloS One*, vol. 11, no. 9, p. e0162502.
- Hoskin, V., Szeto, A., Ghaffari, A., Greer, P.A., Cote, G.P. & Elliott, B.E. 2015, 'Ezrin regulates focal adhesion and invadopodia dynamics by altering calpain activity to promote breast cancer cell invasion.', *Molecular Biology of the Cell*, vol. 26, no. 19, pp. 3464–79.
- Hotulainen, P. & Lappalainen, P. 2006, 'Stress fibers are generated by two distinct actin assembly mechanisms in motile cells', *The Journal of Cell Biology*, vol. 173, no. 3, pp. 383–94.
- Hsu, Y.-L., Hung, J.-Y., Liang, Y.-Y., Lin, Y.-S., Tsai, M.-J., Chou, S.-H., Lu, C.-Y. & Kuo, P.-L. 2015,

- 'S100P interacts with integrin alpha7 and increases cancer cell migration and invasion in lung cancer.', *Oncotarget*, vol. 6, no. 30, pp. 29585–98.
- Hu, B., Shi, B., Jarzynka, M.J., Yiin, J.-J., D'Souza-Schorey, C. & Cheng, S.-Y. 2009, 'ADP-ribosylation factor 6 regulates glioma cell invasion through the IQ-domain GTPase-activating protein 1-Rac1-mediated pathway.', *Cancer Research*, vol. 69, no. 3, pp. 794–801.
- Hu, H., Zhang, Q., Huang, C., Shen, Y., Chen, X., Shi, X. & Tang, W. 2014, 'Diagnostic value of S100P for pancreatic cancer: a meta-analysis.', *Tumour Biology: the Journal of the International Society for Oncodevelopmental Biology and Medicine*, vol. 35, no. 10, pp. 9479–85.
- Hu, W., Wang, Zhongxia, Zhang, S., Lu, X., Wu, Junyi, Yu, K., Ji, A., Lu, W., Wang, Zhong, Wu, Junhua & Jiang, C. 2019, 'IQGAP1 promotes pancreatic cancer progression and epithelial-mesenchymal transition (EMT) through Wnt/ $\beta$ -catenin signaling', *Scientific Reports*, vol. 9, no. 1, p. 7539.
- Huang, H.-Y., Li, C.-F., Fang, F.-M., Tsai, J.-W., Li, S.-H., Lee, Y.-T. & Wei, H.-M. 2010, 'Prognostic implication of ezrin overexpression in myxofibrosarcomas.', *Annals of Surgical Oncology*, vol. 17, no. 12, pp. 3212–9.
- Huang, H., Xiao, Y., Lin, H., Fu, D., Zhan, Z., Liang, L., Yang, X., Fan, J., Ye, Y., Sun, L. & Xu, H. 2011, 'Increased phosphorylation of ezrin/radixin/moesin proteins contributes to proliferation of rheumatoid fibroblast-like synoviocytes', *Rheumatology*, vol. 50, no. 6, pp. 1045–53.
- Hunter, K.W. 2004, 'Ezrin, a key component in tumor metastasis.', *Trends in Molecular Medicine*, vol. 10, no. 5, pp. 201–4.
- Ikura, M. & Ames, J.B. 2006, 'Genetic polymorphism and protein conformational plasticity in the calmodulin superfamily: two ways to promote multifunctionality.', *Proceedings of the National Academy of Sciences of the United States of America*, vol. 103, no. 5, pp. 1159–64.
- Ilmonen, S., Vaheri, A., Asko-Seljavaara, S. & Carpen, O. 2005, 'Ezrin in primary cutaneous melanoma.', *Modern Pathology: an Official Journal of the United States and Canadian Academy of Pathology, Inc*, vol. 18, no. 4, pp. 503–10.
- Isaka, K., Usuda, S., Ito, H., Sagawa, Y., Nakamura, H., Nishi, H., Suzuki, Y., Li, Y.F. & Takayama, M. 2003, 'Expression and activity of matrix metalloproteinase 2 and 9 in human trophoblasts', *Placenta*, vol. 24, no. 1, pp. 53–64.
- Ishijima, S., Oshio, S. & Mohri, H. 1986, 'Flagellar movement of human spermatozoa', *Gamete Research*, vol. 3, no. 3, pp. 185–97.
- Ishikawa, A., Omata, W., Ackerman, W.E. 4th, Takeshita, T., Vandre, D.D. & Robinson, J.M. 2014, 'Cell fusion mediates dramatic alterations in the actin cytoskeleton, focal adhesions, and E-cadherin in trophoblastic cells.', *Cytoskeleton (Hoboken, N.J.)*, vol. 71, no. 4, pp. 241–56.
- Izumi, D., Toden, S., Ureta, E., Ishimoto, T., Baba, H. & Goel, A. 2019, 'TIAM1 promotes chemoresistance and tumor invasiveness in colorectal cancer', *Cell Death & Disease*, vol. 10, no. 4, p. 267.
- Jadeski, L., Mataraza, J.M., Jeong, H.-W., Li, Z. & Sacks, D.B. 2008, 'IQGAP1 stimulates proliferation and enhances tumorigenesis of human breast epithelial cells.', *The Journal of Biological Chemistry*, vol. 283, no. 2, pp. 1008–17.
- Jameson, K.L., Mazur, P.K., Zehnder, A.M., Zhang, J., Zarnegar, B., Sage, J. & Khavari, P.A. 2013, 'IQGAP1 scaffold-kinase interaction blockade selectively targets RAS-MAP kinase-driven tumors.', *Nature Medicine*, vol. 19, no. 5, pp. 626–30.
- Jarvela, I.Y., Ruokonen, A. & Tekay, A. 2008, 'Effect of rising hCG levels on the human corpus luteum during early pregnancy', *Human Reproduction*, vol. 23, no. 12, pp. 2775–81.
- Jauniaux, E., Poston, L. & Burton, G.J. 2006, 'Placental-related diseases of pregnancy: Involvement of oxidative stress and implications in human evolution', *Human Reproduction Update*, vol. 12, no. 6, 2006/05/08., pp. 747–55.
- Jeong, H.-W., Li, Z., Brown, M.D. & Sacks, D.B. 2007, 'IQGAP1 binds Rap1 and modulates its activity.', *The Journal of Biological Chemistry*, vol. 282, no. 28, pp. 20752–62.
- Jeong, J., Choi, J., Kim, W., Dann, P., Takyar, F., Gefter, J. V, Friedman, X.P.A., Wysolmerski, J.J., Friedman, P.A. & Wysolmerski, J.J. 2019, 'Inhibition of ezrin causes PKC $\alpha$ -mediated internalization of erbb2/HER2 tyrosine kinase in breast cancer cells', *The Journal of Biological Chemistry*, vol. 294, no. 3, pp. 887–901.
- Jiang, L., Lai, Y.-K., Zhang, J., Wang, H., Lin, M.C., He, M.-L. & Kung, H.-F. 2011, 'Targeting S100P inhibits colon cancer growth and metastasis by Lentivirus-mediated RNA interference and proteomic analysis.', *Molecular Medicine*, vol. 17, no. 7–8, pp. 709–16.
- Jiang, Q.-H., Wang, A.-X. & Chen, Y. 2014, 'Radixin enhances colon cancer cell invasion by increasing MMP-7 production via Rac1-ERK pathway', *The Scientific World Journal*, vol. 2014, p. 340271.

- Jin, G., Wang, S., Hu, X., Jing, Z., Chen, J., Ying, K., Xie, Y. & Mao, Y. 2003, 'Characterization of the tissue-specific expression of the s100P gene which encodes an EF-hand Ca<sup>2+</sup>-binding protein.', *Molecular Biology Reports*, vol. 30, no. 4, pp. 243–8.
- Jin, J., Lee, J.W., Rha, K.-S., Kim, D.W. & Kim, Y.M. 2012, 'Expression pattern of IQGAP1 in sinonasal inverted papillomas and squamous cell carcinomas.', *The Laryngoscope*, vol. 122, no. 12, pp. 2640–6.
- Jin, T., Jin, J., Li, X., Zhang, S., Choi, Y.H., Piao, Y., Shen, X. & Lin, Z. 2014, 'Prognostic implications of ezrin and phosphorylated ezrin expression in non-small cell lung cancer', *BMC Cancer*, vol. 14, p. 191.
- Jin, X., Liu, Y., Liu, J., Lu, W., Liang, Z., Zhang, D., Liu, G., Zhu, H., Xu, N. & Liang, S. 2015, 'The overexpression of IQGAP1 and beta-catenin is associated with tumor progression in hepatocellular carcinoma in vitro and in vivo.', *PloS One*, vol. 10, no. 8, p. e0133770.
- Jin, Z., Zhou, S., Ye, H., Jiang, S., Yu, K. & Ma, Y. 2019, 'The mechanism of SP1/p300 complex promotes proliferation of multiple myeloma cells through regulating IQGAP1 transcription.', *Biomedicine & Pharmacotherapy*, vol. 119, p. 109434.
- Johnson, M., Sharma, M., Brocardo, M.G. & Henderson, B.R. 2011, 'IQGAP1 translocates to the nucleus in early S-phase and contributes to cell cycle progression after DNA replication arrest.', *The International Journal of Biochemistry & Cell Biology*, vol. 43, no. 1, pp. 65–73.
- Johnson, M., Sharma, M. & Henderson, B.R. 2009, 'IQGAP1 regulation and roles in cancer.', *Cellular Signalling*, vol. 21, no. 10, pp. 1471–8.
- Joseph-Silverstein, J. & Silverstein, R.L. 1998, 'Cell adhesion molecules: an overview.', *Cancer Investigation*, vol. 16, no. 3, pp. 176–82.
- Joyal, J.L., Annan, R.S., Ho, Y.D., Huddleston, M.E., Carr, S.A., Hart, M.J. & Sacks, D.B. 1997, 'Calmodulin modulates the interaction between IQGAP1 and Cdc42. Identification of IQGAP1 by nano-electrospray tandem mass spectrometry.', *The Journal of Biological Chemistry*, vol. 272, no. 24, pp. 15419–25.
- Justus, C.R., Leffler, N., Ruiz-Echevarria, M. & Yang, L. V 2014, 'In vitro cell migration and invasion assays', *Journal of Visualized Experiments : JoVE*, no. 88, p. 51046.
- Kabir-Salmani, M., Shiokawa, S., Akimoto, Y., Hasan-Nejad, H., Sakai, Keiji, Nagamatsu, S., Sakai, Ken, Nakamura, Y., Hosseini, A. & Iwashita, M. 2002, 'Characterization of morphological and cytoskeletal changes in trophoblast cells induced by insulin growth factor-I.', *The Journal of Clinical Endocrinology and Metabolism*, vol. 87, no. 12, pp. 5751–9.
- Kahsai, A.W., Zhu, S. & Fenteany, G. 2010, 'G protein-coupled receptor kinase 2 activates radixin, regulating membrane protrusion and motility in epithelial cells', *Biochimica et Biophysica Acta*, vol. 1803, no. 2, pp. 300–10.
- Kaksonen, M., Toret, C.P. & Drubin, D.G. 2006, 'Harnessing actin dynamics for clathrin-mediated endocytosis.', *Nature Reviews. Molecular Cell Biology*, vol. 7, no. 6, pp. 404–14.
- Kang, Y.K., Hong, S.W., Lee, H. & Kim, W.H. 2010, 'Prognostic implications of ezrin expression in human hepatocellular carcinoma.', *Molecular Carcinogenesis*, vol. 49, no. 9, pp. 798–804.
- Karlsson, T., Turkina, M. V, Yakymenko, O., Magnusson, K.-E. & Vikstrom, E. 2012, 'The Pseudomonas aeruginosa N-acylhomoserine lactone quorum sensing molecules target IQGAP1 and modulate epithelial cell migration.', *PloS Pathogens*, vol. 8, no. 10, p. e1002953.
- Kataoka, K., Ono, T., Murata, H., Morishita, M., Yamamoto, K.-I., Sakaguchi, M. & Huh, N.-H. 2012, 'S100A7 promotes the migration and invasion of osteosarcoma cells via the receptor for advanced glycation end products.', *Oncology Letters*, vol. 3, no. 5, pp. 1149–53.
- Katz, B.Z., Zamir, E., Bershadsky, A., Kam, Z., Yamada, K.M. & Geiger, B. 2000, 'Physical state of the extracellular matrix regulates the structure and molecular composition of cell-matrix adhesions', *Molecular Biology of the Cell*, vol. 11, no. 3, pp. 1047–60.
- Kawasaki, H., Nakayama, S. & Kretsinger, R.H. 1998, 'Classification and evolution of EF-hand proteins.', *Biometals : an International Journal on the Role of Metal Ions in Biology, Biochemistry, and Medicine*, vol. 11, no. 4, pp. 277–95.
- Kayisli, U.A., Selam, B., Demir, R. & Arici, A. 2002, 'Expression of vasodilator-stimulated phosphoprotein in human placenta: possible implications in trophoblast invasion', *Molecular Human Reproduction*, vol. 8, no. 1, pp. 88–94.
- Khanna, C., Wan, X., Bose, S., Cassaday, R., Olomu, O., Mendoza, A., Yeung, C., Gorlick, R., Hewitt, S.M. & Helman, L.J. 2004, 'The membrane-cytoskeleton linker ezrin is necessary for osteosarcoma metastasis.', *Nature Medicine*, vol. 10, no. 2, pp. 182–6.
- Kholmanskikh, S.S., Koeller, H.B., Wynshaw-Boris, A., Gomez, T., Letourneau, P.C. & Ross, M.E. 2006, 'Calcium-dependent interaction of Lis1 with IQGAP1 and Cdc42 promotes neuronal

- motility.’, *Nature Neuroscience*, vol. 9, no. 1, pp. 50–7.
- Khong, T.Y., De Wolf, F., Robertson, W.B. & Brosens, I. 1986, ‘Inadequate maternal vascular response to placentation in pregnancies complicated by pre-eclampsia and by small-for-gestational age infants.’, *British Journal of Obstetrics and Gynaecology*, vol. 93, no. 10, pp. 1049–59.
- Kikuchi, K., McNamara, K.M., Miki, Y., Iwabuchi, E., Kanai, A., Miyashita, M., Ishida, T. & Sasano, H. 2019, ‘S100P and Ezrin promote trans-endothelial migration of triple negative breast cancer cells.’, *Cellular Oncology (Dordrecht)*, vol. 42, no. 1, pp. 67–80.
- Kiley, S.C., Clark, K.J., Goodnough, M., Welch, D.R. & Jaken, S. 1999, ‘Protein kinase C delta involvement in mammary tumor cell metastasis’, *Cancer Research*, vol. 59, no. 13, pp. 3230–8.
- Kim, J., Gee, H.Y. & Lee, M.G. 2018, ‘Unconventional protein secretion - new insights into the pathogenesis and therapeutic targets of human diseases.’, *Journal of Cell Science*, vol. 131, no. 12.
- Kim, J.K., Jung, K.H., Noh, J.H., Eun, J.W., Bae, H.J., Xie, H.J., Ahn, Y.M., Ryu, J.C., Park, W.S., Lee, J.Y. & Nam, S.W. 2009, ‘Targeted disruption of S100P suppresses tumor cell growth by down-regulation of cyclin D1 and CDK2 in human hepatocellular carcinoma.’, *International Journal of Oncology*, vol. 35, no. 6, pp. 1257–64.
- Kimura, T., Yamaoka, M., Taniguchi, S., Okamoto, M., Takei, M., Ando, T., Iwamatsu, A., Watanabe, T., Kaibuchi, K., Ishizaki, T. & Niki, I. 2013, ‘Activated Cdc42-bound IQGAP1 determines the cellular endocytic site.’, *Molecular and Cellular Biology*, vol. 33, no. 24, pp. 4834–43.
- Kishore, R., Qin, G., Luedemann, C., Bord, E., Hanley, A., Silver, M., Gavin, M., Yoon, Y., Goukassian, D. & Losordo, D.W. 2005, ‘The cytoskeletal protein ezrin regulates EC proliferation and angiogenesis via TNF-alpha-induced transcriptional repression of cyclin A’, *The Journal of Clinical Investigation*, vol. 115, no. 7, 2005/06/16., pp. 1785–96.
- Kizawa, K., Tsuchimoto, S., Hashimoto, K. & Uchiwa, H. 1998, ‘Gene expression of mouse S100A3, a cysteine-rich calcium-binding protein, in developing hair follicle’, *Journal of Investigative Dermatology*, vol. 111, no. 5, pp. 879–86.
- ten Klooster, J.P., Jansen, M., Yuan, J., Oorschot, V., Begthel, H., Di Giacomo, V., Colland, F., de Koning, J., Maurice, M.M., Hornbeck, P. & Clevers, H. 2009, ‘Mst4 and ezrin induce brush borders downstream of the Lkb1/Strad/Mo25 polarization complex’, *Developmental Cell*, vol. 16, no. 4, pp. 551–62.
- Knofler, M., Saleh, L., Bauer, S., Galos, B., Rotheneder, H., Husslein, P. & Helmer, H. 2004, ‘Transcriptional regulation of the human chorionic gonadotropin beta gene during villous trophoblast differentiation.’, *Endocrinology*, vol. 145, no. 4, pp. 1685–94.
- Kobel, M., Langhammer, T., Huttelmaier, S., Schmitt, W.D., Kriese, K., Dittmer, J., Strauss, H.-G., Thomssen, C. & Hauptmann, S. 2006, ‘Ezrin expression is related to poor prognosis in FIGO stage I endometrioid carcinomas.’, *Modern Pathology : an Official Journal of the United States and Canadian Academy of Pathology, Inc*, vol. 19, no. 4, pp. 581–7.
- Kohno, T., Urao, N., Ashino, T., Sudhakar, V., Inomata, H., Yamaoka-Tojo, M., McKinney, R.D., Fukai, T. & Ushio-Fukai, M. 2013, ‘IQGAP1 links PDGF receptor-beta signal to focal adhesions involved in vascular smooth muscle cell migration: role in neointimal formation after vascular injury.’, *American Journal of Physiology. Cell Physiology*, vol. 305, no. 6, pp. C591-600.
- Koltzscher, M., Neumann, C., Konig, S. & Gerke, V. 2003, ‘Ca<sup>2+</sup>-dependent binding and activation of dormant ezrin by dimeric S100P.’, *Molecular Biology of the Cell*, vol. 14, no. 6, pp. 2372–84.
- Kong, J., Di, C., Piao, J., Sun, J., Han, L., Chen, L., Yan, G. & Lin, Z. 2016, ‘Ezrin contributes to cervical cancer progression through induction of epithelial-mesenchymal transition’, *Oncotarget*, vol. 7, no. 15, pp. 19631–42.
- Kong, J., Li, Yan, Liu, S., Jin, H., Shang, Y., Quan, C., Li, Yulin & Lin, Z. 2013, ‘High expression of ezrin predicts poor prognosis in uterine cervical cancer’, *BMC Cancer*, vol. 13, p. 520.
- Korkeila, E.A., Syrjanen, K., Bendardaf, R., Laulajainen, M., Carpen, O., Pyrhonen, S. & Sundstrom, J. 2011, ‘Preoperative radiotherapy modulates ezrin expression and its value as a predictive marker in patients with rectal cancer.’, *Human Pathology*, vol. 42, no. 3, pp. 384–92.
- Krakhmal, N. V., Zavyalova, M. V., Denisov, E. V., Vtorushin, S. V & Perelmuter, V.M. 2015, ‘Cancer invasion: patterns and mechanisms’, *Acta Naturae*, vol. 7, no. 2, pp. 17–28.
- Krause, M. & Gautreau, A. 2014, ‘Steering cell migration: lamellipodium dynamics and the regulation of directional persistence’, *Nature Reviews. Molecular Cell Biology*, vol. 15, no. 9, pp. 577–90.
- Krishnan, K., Bruce, B., Hewitt, S., Thomas, D., Khanna, C. & Helman, L.J. 2006, ‘Ezrin mediates growth and survival in Ewing’s sarcoma through the AKT/mTOR, but not the MAPK, signaling pathway.’, *Clinical & Experimental Metastasis*, vol. 23, no. 3–4, pp. 227–36.
- Kumar, S., Maxwell, I.Z., Heisterkamp, A., Polte, T.R., Lele, T.P., Salanga, M., Mazur, E. & Ingber, D.E. 2006, ‘Viscoelastic retraction of single living stress fibers and its impact on cell shape,

- cytoskeletal organization, and extracellular matrix mechanics', *Biophysical Journal*, vol. 90, no. 10, 2006/02/24., pp. 3762–73.
- Kunda, P., Pelling, A.E., Liu, T. & Baum, B. 2008, 'Moesin controls cortical rigidity, cell rounding, and spindle morphogenesis during mitosis', *Current Biology : CB*, vol. 18, no. 2, pp. 91–101.
- Kuo, J.-C., Han, X., Hsiao, C.-T., Yates, J.R. 3rd & Waterman, C.M. 2011, 'Analysis of the myosin-II-responsive focal adhesion proteome reveals a role for beta-Pix in negative regulation of focal adhesion maturation.', *Nature Cell Biology*, vol. 13, no. 4, pp. 383–93.
- Kurella, V.B., Richard, J.M., Parke, C.L., Lecour, L.F.J., Bellamy, H.D. & Worthylake, D.K. 2009, 'Crystal structure of the GTPase-activating protein-related domain from IQGAP1.', *The Journal of Biological Chemistry*, vol. 284, no. 22, pp. 14857–65.
- Kuroda, S., Fukata, M., Kobayashi, K., Nakafuku, M., Nomura, N., Iwamatsu, A. & Kaibuchi, K. 1996, 'Identification of IQGAP as a putative target for the small GTPases, Cdc42 and Rac1.', *The Journal of Biological Chemistry*, vol. 271, no. 38, pp. 23363–7.
- Kuroda, S., Fukata, M., Nakagawa, M., Fujii, K., Nakamura, T., Ookubo, T., Izawa, I., Nagase, T., Nomura, N., Tani, H., Shoji, I., Matsuura, Y., Yonehara, S. & Kaibuchi, K. 1998, 'Role of IQGAP1, a target of the small GTPases Cdc42 and Rac1, in regulation of E-cadherin-mediated cell-cell adhesion.', *Science*, vol. 281, no. 5378, pp. 832–5.
- Kuwayama, A., Kuruto, R., Horie, N., Takeishi, K. & Nozawa, R. 1993, 'Appearance of nuclear factors that interact with genes for myeloid calcium binding proteins (MRP-8 and MRP-14) in differentiated HL-60 cells.', *Blood*, vol. 81, no. 11, pp. 3116–21.
- Kwon, M., MacLeod, T.J., Zhang, Y. & Waisman, D.M. 2005, 'S100A10, annexin A2, and annexin a2 heterotetramer as candidate plasminogen receptors.', *Frontiers in Bioscience : a Journal and Virtual Library*, vol. 10, pp. 300–25.
- Lamouille, S., Xu, J. & Derynck, R. 2014, 'Molecular mechanisms of epithelial–mesenchymal transition', *Nature Reviews Molecular Cell Biology*, vol. 15, no. 3, pp. 178–96.
- Lang, C.Y., Hallack, S., Leiser, R. & Pfarrer, C. 2004, 'Cytoskeletal filaments and associated proteins during restricted trophoblast invasion in bovine placentomes: light and transmission electron microscopy and RT-PCR', *Cell and Tissue Research*, vol. 315, no. 3, pp. 339–48.
- Langley, R.R. & Fidler, I.J. 2011, 'The seed and soil hypothesis revisited--the role of tumor-stroma interactions in metastasis to different organs', *International Journal of Cancer*, vol. 128, no. 11, 2011/03/25., pp. 2527–35.
- Lawler, P.R. & Lawler, J. 2012, 'Molecular basis for the regulation of angiogenesis by thrombospondin-1 and -2', *Cold Spring Harbor perspectives in medicine*, vol. 2, no. 5, pp. a006627–a006627.
- Lawrie, A., Spiekerkoetter, E., Martinez, E.C., Ambartsumian, N., Sheward, W.J., MacLean, M.R., Harmar, A.J., Schmidt, A.-M., Lukanidin, E. & Rabinovitch, M. 2005, 'Interdependent serotonin transporter and receptor pathways regulate S100A4/Mts1, a gene associated with pulmonary vascular disease.', *Circulation Research*, vol. 97, no. 3, pp. 227–35.
- Le, Q.-T., Denko, N.C. & Giaccia, A.J. 2004, 'Hypoxic gene expression and metastasis.', *Cancer Metastasis Reviews*, vol. 23, no. 3–4, pp. 293–310.
- Legerstee, K., Geverts, B., Slotman, J.A. & Houtsmuller, A.B. 2019, 'Dynamics and distribution of paxillin, vinculin, zyxin and VASP depend on focal adhesion location and orientation.', *Scientific Reports*, vol. 9, no. 1, p. 10460.
- Legg, J.W., Lewis, C.A., Parsons, M., Ng, T. & Isacke, C.M. 2002, 'A novel PKC-regulated mechanism controls CD44 ezrin association and directional cell motility', *Nature Cell Biology*, vol. 4, no. 6, pp. 399–407.
- Lehtonen, S., Ryan, J.J., Kudlicka, K., Iino, N., Zhou, H. & Farquhar, M.G. 2005, 'Cell junction-associated proteins IQGAP1, MAGI-2, CASK, spectrins, and alpha-actinin are components of the nephrin multiprotein complex.', *Proceedings of the National Academy of Sciences of the United States of America*, vol. 102, no. 28, pp. 9814–9.
- Li, C.-R., Wang, Y.-M. & Wang, Y. 2008, 'The IQGAP Iqg1 is a regulatory target of CDK for cytokinesis in *Candida albicans*', *The EMBO Journal*, vol. 27, no. 22, 2008/10/16., pp. 2998–3010.
- Li, C., Chen, H., Ding, F., Zhang, Y., Luo, A., Wang, M. & Liu, Z. 2009, 'A novel p53 target gene, S100A9, induces p53-dependent cellular apoptosis and mediates the p53 apoptosis pathway.', *The Biochemical Journal*, vol. 422, no. 2, pp. 363–72.
- Li, C., Wen, T.-F., Zhang, X.-Y., Chen, X. & Shen, J.-Y. 2017, 'IQGAP1 expression in hepatocellular carcinoma predicts poor prognosis by inducing epithelial-mesenchymal transition', *Translational Cancer Research*, vol. 6, no. 3, pp. 530–40.
- Li, Q., Gao, H., Xu, H., Wang, X., Pan, Y., Hao, F., Qiu, X., Stoecker, M., Wang, Endi & Wang, Enhua 2012, 'Expression of ezrin correlates with malignant phenotype of lung cancer, and in vitro

- knockdown of ezrin reverses the aggressive biological behavior of lung cancer cells.’, *Tumour Biology: the Journal of the International Society for Oncodevelopmental Biology and Medicine*, vol. 33, no. 5, pp. 1493–504.
- Li, S., Wang, Q., Chakladar, A., Bronson, R.T. & Bernards, A. 2000, ‘Gastric hyperplasia in mice lacking the putative Cdc42 effector IQGAP1.’, *Molecular and Cellular Biology*, vol. 20, no. 2, pp. 697–701.
- Li, Z., McNulty, D.E., Marler, K.J.M., Lim, L., Hall, C., Annan, R.S. & Sacks, D.B. 2005, ‘IQGAP1 promotes neurite outgrowth in a phosphorylation-dependent manner.’, *The Journal of Biological Chemistry*, vol. 280, no. 14, pp. 13871–8.
- Liang, F., Wang, Y., Shi, L. & Zhang, J. 2017, ‘Association of Ezrin expression with the progression and prognosis of gastrointestinal cancer: a meta-analysis.’, *Oncotarget*, vol. 8, no. 54, pp. 93186–95.
- Lijnen, H.R., Van Hoef, B., Lupu, F., Moons, L., Carmeliet, P. & Collen, D. 1998, ‘Function of the plasminogen/plasmin and matrix metalloproteinase systems after vascular injury in mice with targeted inactivation of fibrinolytic system genes’, *Arteriosclerosis, Thrombosis, and Vascular Biology*, vol. 18, no. 7, pp. 1035–45.
- Lin, L.-J. & Chen, L.-T. 2013, ‘Association between ezrin protein expression and the prognosis of colorectal adenocarcinoma’, *Molecular Medicine Reports*, vol. 8, no. 1, pp. 61–6.
- Lippincott, J. & Li, R. 1998, ‘Sequential assembly of myosin II, an IQGAP-like protein, and filamentous actin to a ring structure involved in budding yeast cytokinesis’, *The Journal of Cell Biology*, vol. 140, no. 2, pp. 355–66.
- Liu, A.-X., Jin, F., Zhang, W.-W., Zhou, T.-H., Zhou, C.-Y., Yao, W.-M., Qian, Y.-L. & Huang, H.-F. 2006, ‘Proteomic analysis on the alteration of protein expression in the placental villous tissue of early pregnancy loss.’, *Biology of Reproduction*, vol. 75, no. 3, pp. 414–20.
- Liu, D., Rudland, P.S., Sibson, D.R., Platt-Higgins, A. & Barraclough, R. 2005, ‘Human homologue of cement gland protein, a novel metastasis inducer associated with breast carcinomas.’, *Cancer Research*, vol. 65, no. 9, pp. 3796–805.
- Liu, J., Guidry, J.J. & Worthylake, D.K. 2014, ‘Conserved sequence repeats of IQGAP1 mediate binding to Ezrin.’, *Journal of Proteome Research*, vol. 13, no. 2, pp. 1156–66.
- Liu, J., Kurella, V.B., LeCour, L.J., Vanagunas, T. & Worthylake, D.K. 2016, ‘The IQGAP1 N-terminus forms dimers, and the dimer interface is required for binding F-actin and calcium-bound calmodulin’, *Biochemistry*, vol. 55, no. 46, pp. 6433–44.
- Liu, Q., Yan, X., Li, Y., Zhang, Y., Zhao, X. & Shen, Y. 2004, ‘Pre-eclampsia is associated with the failure of melanoma cell adhesion molecule (MCAM/CD146) expression by intermediate trophoblast’, *Laboratory Investigation; a Journal of Technical Methods and Pathology*, vol. 84, no. 2, pp. 221–8.
- Liu, S., Zheng, Q., Cui, X.-Y., Dai, K.-X., Yang, X.-S., Li, F.-S. & Yan, Q. 2015, ‘Expression of uPAR in human trophoblast and its role in trophoblast invasion’, *International Journal of Clinical and Experimental Pathology*, vol. 8, no. 11, pp. 14325–34.
- Liu, Y., Belkina, N. V., Park, C., Nambiar, R., Loughhead, S.M., Patino-Lopez, G., Ben-Aissa, K., Hao, J.-J., Kruhlik, M.J., Qi, H., von Andrian, U.H., Kehrl, J.H., Tyska, M.J. & Shaw, S. 2012, ‘Constitutively active ezrin increases membrane tension, slows migration, and impedes endothelial transmigration of lymphocytes in vivo in mice’, *Blood*, vol. 119, no. 2, pp. 445–53.
- Liu, Y., Myrvang, H.K. & Dekker, L. V. 2015, ‘Annexin A2 complexes with S100 proteins: Structure, function and pharmacological manipulation’, *British Journal of Pharmacology*, vol. 172, no. 7, 2014/12/15., pp. 1664–76.
- Liu, Y., Wang, C., Shan, X., Wu, J., Liu, Huanhai, Liu, Haibin, Zhang, J., Xu, W., Sha, Z., He, J. & Fan, J. 2017, ‘S100P is associated with proliferation and migration in nasopharyngeal carcinoma.’, *Oncology Letters*, vol. 14, no. 1, pp. 525–32.
- Liu, Y., Zhang, R., Xin, J., Sun, Y., Li, J., Wei, D. & Zhao, A.Z. 2011, ‘Identification of S100A16 as a novel adipogenesis promoting factor in 3T3-L1 cells’, *Endocrinology*, vol. 152, no. 3, pp. 903–11.
- Liu, Z., Liu, D., Bojdani, E., El-Naggar, A.K., Vasko, V. & Xing, M. 2010, ‘IQGAP1 plays an important role in the invasiveness of thyroid cancer’, *Clinical Cancer Research: an Official Journal of the American Association for Cancer Research*, vol. 16, no. 24, 2010/10/19., pp. 6009–18.
- Lu, P., Weaver, V.M. & Werb, Z. 2012, ‘The extracellular matrix: a dynamic niche in cancer progression’, *The Journal of Cell Biology*, vol. 196, no. 4, pp. 395–406.
- Macias, M.J., Wiesner, S. & Sudol, M. 2002, ‘WW and SH3 domains, two different scaffolds to recognize proline-rich ligands.’, *FEBS Letters*, vol. 513, no. 1, pp. 30–7.
- Mackay, D.J., Esch, F., Furthmayr, H. & Hall, A. 1997, ‘Rho- and rac-dependent assembly of focal adhesion complexes and actin filaments in permeabilized fibroblasts: an essential role for

- ezrin/radixin/moesin proteins.’, *The Journal of Cell Biology*, vol. 138, no. 4, pp. 927–38.
- Madan, R., Brandwein-Gensler, M., Schlecht, N.F., Elias, K., Gorbovitsky, E., Belbin, T.J., Mahmood, R., Breining, D., Qian, H., Childs, G., Locker, J., Smith, R., Haigentz, M.J., Gunn-Moore, F. & Prystowsky, M.B. 2006, ‘Differential tissue and subcellular expression of ERM proteins in normal and malignant tissues: cytoplasmic ezrin expression has prognostic significance for head and neck squamous cell carcinoma.’, *Head & Neck*, vol. 28, no. 11, pp. 1018–27.
- Mak, H., Naba, A., Varma, S., Schick, C., Day, A., SenGupta, S.K., Arpin, M. & Elliott, B.E. 2012, ‘Ezrin phosphorylation on tyrosine 477 regulates invasion and metastasis of breast cancer cells.’, *BMC Cancer*, vol. 12, p. 82.
- Makitie, T., Carpen, O., Vaheri, A. & Kivela, T. 2001, ‘Ezrin as a prognostic indicator and its relationship to tumor characteristics in uveal malignant melanoma.’, *Investigative Ophthalmology & Visual Science*, vol. 42, no. 11, pp. 2442–9.
- Maldonado-Estrada, J., Menu, E., Roques, P., Barre-Sinoussi, F. & Chaouat, G. 2004, ‘Evaluation of cytokeratin 7 as an accurate intracellular marker with which to assess the purity of human placental villous trophoblast cells by flow cytometry.’, *Journal of Immunological Methods*, vol. 286, no. 1–2, pp. 21–34.
- Manahan, C.L., Iglesias, P.A., Long, Y. & Devreotes, P.N. 2004, ‘Chemoattractant signaling in Dictyostelium discoideum’, *Annual Review of Cell and Developmental Biology*, vol. 20, no. 1, pp. 223–53.
- Mao, Z., Guan, Y., Li, T., Zhang, L., Liu, M., Xing, B., Yao, M. & Chen, M. 2019, ‘Up regulation of miR-96-5p is responsible for TiO<sub>2</sub> NPs induced invasion dysfunction of human trophoblastic cells via disturbing Ezrin mediated cytoskeletons arrangement.’, *Biomedicine & Pharmacotherapy*, vol. 117, p. 109125.
- Marenholz, I., Heizmann, C.W. & Fritz, G. 2004, ‘S100 proteins in mouse and man: from evolution to function and pathology (including an update of the nomenclature).’, *Biochemical and Biophysical Research Communications*, vol. 322, no. 4, pp. 1111–22.
- Maresso, A.W., Baldwin, M.R. & Barbieri, J.T. 2004, ‘Ezrin/radixin/moesin proteins are high affinity targets for ADP-ribosylation by Pseudomonas aeruginosa ExoS’, *The Journal of Biological Chemistry*, vol. 279, no. 37, pp. 38402–8.
- Marianayagam, N.J., Sunde, M. & Matthews, J.M. 2004, ‘The power of two: protein dimerization in biology.’, *Trends in Biochemical Sciences*, vol. 29, no. 11, pp. 618–25.
- Maruo, T., Matsuo, H., Otani, T. & Mochizuki, M. 1995, ‘Role of epidermal growth factor (EGF) and its receptor in the development of the human placenta.’, *Reproduction, Fertility, and Development*, vol. 7, no. 6, pp. 1465–70.
- Mataraza, J.M., Briggs, M.W., Li, Z., Entwistle, A., Ridley, A.J. & Sacks, D.B. 2003, ‘IQGAP1 promotes cell motility and invasion’, *The Journal of Biological Chemistry*, vol. 278, no. 42, pp. 41237–45.
- Mateer, S.C., McDaniel, A.E., Nicolas, V., Habermacher, G.M., Lin, M.-J.S., Cromer, D.A., King, M.E. & Bloom, G.S. 2002, ‘The mechanism for regulation of the F-actin binding activity of IQGAP1 by calcium/calmodulin.’, *The Journal of Biological Chemistry*, vol. 277, no. 14, pp. 12324–33.
- Mateer, S.C., Morris, L.E., Cromer, D.A., Bensenor, L.B. & Bloom, G.S. 2004, ‘Actin filament binding by a monomeric IQGAP1 fragment with a single calponin homology domain.’, *Cell Motility and the Cytoskeleton*, vol. 58, no. 4, pp. 231–41.
- Matsui, T., Maeda, M., Doi, Y., Yonemura, S., Amano, M., Kaibuchi, K., Tsukita, S. & Tsukita, S. 1998, ‘Rho-kinase phosphorylates COOH-terminal threonines of ezrin/radixin/moesin (ERM) proteins and regulates their head-to-tail association’, *The Journal of Cell Biology*, vol. 140, no. 3, pp. 647–57.
- Matsumoto, H., Daikoku, T., Wang, H., Sato, E. & Dey, S.K. 2004, ‘Differential expression of ezrin/radixin/moesin (ERM) and ERM-associated adhesion molecules in the blastocyst and uterus suggests their functions during implantation.’, *Biology of Reproduction*, vol. 70, no. 3, pp. 729–36.
- Mattila, P.K. & Lappalainen, P. 2008, ‘Filopodia: molecular architecture and cellular functions.’, *Nature Reviews. Molecular Cell Biology*, vol. 9, no. 6, pp. 446–54.
- Mbele, G.O., Deloulme, J.C., Gentil, B.J., Delphin, C., Ferro, M., Garin, J., Takahashi, M. & Baudier, J. 2002, ‘The zinc- and calcium-binding S100B interacts and co-localizes with IQGAP1 during dynamic rearrangement of cell membranes.’, *The Journal of Biological Chemistry*, vol. 277, no. 51, pp. 49998–50007.
- McClatchey, A.I. 2003, ‘Merlin and ERM proteins: unappreciated roles in cancer development?’, *Nature Reviews. Cancer*, England, pp. 877–83.
- McClatchey, A.I. 2014, ‘ERM proteins at a glance.’, *Journal of Cell Science*, vol. 127, no. Pt 15, pp. 3199–204.

- McClatchey, A.I. & Fehon, R.G. 2009, 'Merlin and the ERM proteins--regulators of receptor distribution and signaling at the cell cortex', *Trends in Cell Biology*, vol. 19, no. 5, 2009/04/01., pp. 198–206.
- McDonald, K.L., O'Sullivan, M.G., Parkinson, J.F., Shaw, J.M., Payne, C.A., Brewer, J.M., Young, L., Reader, D.J., Wheeler, H.T., Cook, R.J., Biggs, M.T., Little, N.S., Teo, C., Stone, G. & Robinson, B.G. 2007, 'IQGAP1 and IGFBP2: valuable biomarkers for determining prognosis in glioma patients.', *Journal of Neuropathology and Experimental Neurology*, vol. 66, no. 5, pp. 405–17.
- McNulty, D.E., Li, Z., White, C.D., Sacks, D.B. & Annan, R.S. 2011, 'MAPK scaffold IQGAP1 binds the EGF receptor and modulates its activation.', *The Journal of Biological Chemistry*, vol. 286, no. 17, pp. 15010–21.
- Meng, Y., Lu, Z., Yu, S., Zhang, Q., Ma, Y. & Chen, J. 2010, 'Ezrin promotes invasion and metastasis of pancreatic cancer cells', *Journal of Translational Medicine*, vol. 8, p. 61.
- Mercado-Pimentel, M.E., Onyeagucha, B.C., Li, Q., Pimentel, A.C., Jandova, J. & Nelson, M.A. 2015, 'The S100P/RAGE signaling pathway regulates expression of microRNA-21 in colon cancer cells', *FEBS Letters*, vol. 589, no. 18, 2015/07/17., pp. 2388–93.
- Meyer, R.D., Sacks, D.B. & Rahimi, N. 2008, 'IQGAP1-dependent signaling pathway regulates endothelial cell proliferation and angiogenesis.', *PLoS One*, vol. 3, no. 12, p. e3848.
- Mohanraj, R., Ramani, P., Premkumar, P., Natesan, A., Sherlin, H.J. & Sukumaran, G. 2017, 'Immunohistochemical expression of ezrin in oral potentially malignant disorders-A descriptive study', *Journal of Pharmacy & Bioallied Sciences*, vol. 9, no. Suppl 1, pp. S205–10.
- Moilanen, J., Lassus, H., Leminen, A., Vaheri, A., Butzow, R. & Carpen, O. 2003, 'Ezrin immunoreactivity in relation to survival in serous ovarian carcinoma patients.', *Gynecologic Oncology*, vol. 90, no. 2, pp. 273–81.
- Monk, M. & Holding, C. 2001, 'Human embryonic genes re-expressed in cancer cells.', *Oncogene*, vol. 20, no. 56, pp. 8085–91.
- Monteleon, C.L., McNeal, A., Duperret, E.K., Oh, S.J., Schapira, E. & Ridky, T.W. 2015, 'IQGAP1 and IQGAP3 serve individually essential roles in normal epidermal homeostasis and tumor progression', *The Journal of Investigative Dermatology*, vol. 135, no. 9, pp. 2258–65.
- Moore, B.W. 1965, 'A soluble protein characteristic of the nervous system.', *Biochemical and Biophysical Research Communications*, vol. 19, no. 6, pp. 739–44.
- Morales, F.C., Takahashi, Y., Kreimann, E.L. & Georgescu, M.-M. 2004, 'Ezrin-radixin-moesin (ERM)-binding phosphoprotein 50 organizes ERM proteins at the apical membrane of polarized epithelia.', *Proceedings of the National Academy of Sciences of the United States of America*, vol. 101, no. 51, pp. 17705–10.
- Morita, E., Sandrin, V., Chung, H.-Y., Morham, S.G., Gygi, S.P., Rodesch, C.K. & Sundquist, W.I. 2007, 'Human ESCRT and ALIX proteins interact with proteins of the midbody and function in cytokinesis', *The EMBO Journal*, vol. 26, no. 19, 2007/09/13., pp. 4215–27.
- Moser, G., Orendi, K., Gauster, M., Siwetz, M., Helige, C. & Huppertz, B. 2011, 'The art of identification of extravillous trophoblast.', *Placenta*, vol. 32, no. 2, pp. 197–9.
- Mousses, S., Bubendorf, L., Wagner, U., Hostetter, G., Kononen, J., Cornelison, R., Goldberger, N., Elkahoul, A.G., Willi, N., Koivisto, P., Ferhle, W., Raffeld, M., Sauter, G. & Kallioniemi, O.-P. 2002, 'Clinical validation of candidate genes associated with prostate cancer progression in the CWR22 model system using tissue microarrays.', *Cancer Research*, vol. 62, no. 5, pp. 1256–60.
- Mueller, A., Schafer, B.W., Ferrari, S., Weibel, M., Makek, M., Hochli, M. & Heizmann, C.W. 2005, 'The calcium-binding protein S100A2 interacts with p53 and modulates its transcriptional activity.', *The Journal of Biological Chemistry*, vol. 280, no. 32, pp. 29186–93.
- Naba, A., Reverdy, C., Louvard, D. & Arpin, M. 2008, 'Spatial recruitment and activation of the Fes kinase by ezrin promotes HGF-induced cell scattering', *The EMBO Journal*, vol. 27, no. 1, 2007/11/29., pp. 38–50.
- Nabeshima, K., Shimao, Y., Inoue, T. & Koono, M. 2002, 'Immunohistochemical analysis of IQGAP1 expression in human colorectal carcinomas: its overexpression in carcinomas and association with invasion fronts.', *Cancer Letters*, vol. 176, no. 1, pp. 101–9.
- Nagano, M., Hoshino, D., Koshikawa, N., Akizawa, T. & Seiki, M. 2012, 'Turnover of focal adhesions and cancer cell migration.', *International Journal of Cell Biology*, vol. 2012, p. 310616.
- Nagy, N., Brenner, C., Markadieu, N., Chaboteaux, C., Camby, I., Schafer, B.W., Pochet, R., Heizmann, C.W., Salmon, I., Kiss, R. & Decaestecker, C. 2001, 'S100A2, a putative tumor suppressor gene, regulates in vitro squamous cell carcinoma migration.', *Laboratory Investigation; a Journal of Technical Methods and Pathology*, vol. 81, no. 4, pp. 599–612.
- Namba, T., Homan, T., Nishimura, T., Mima, S., Hoshino, T. & Mizushima, T. 2009, 'Up-regulation of S100P expression by non-steroidal anti-inflammatory drugs and its role in anti-tumorigenic

- effects.’, *The Journal of Biological Chemistry*, vol. 284, no. 7, pp. 4158–67.
- Nammalwar, R.C., Heil, A. & Gerke, V. 2015, ‘Ezrin interacts with the scaffold protein IQGAP1 and affects its cortical localization.’, *Biochimica et Biophysica Acta*, vol. 1853, no. 9, pp. 2086–94.
- Neel, N.F., Sai, J., Ham, A.-J.L.J.L., Sobolik-Delmaire, T., Mernaugh, R.L. & Richmond, A. 2011, ‘IQGAP1 is a novel CXCR2-interacting protein and essential component of the “chemosynapse”’, *PloS One*, vol. 6, no. 8, 2011/08/18., pp. e23813–e23813.
- Neisch, A.L. & Fehon, R.G. 2011, ‘Ezrin, Radixin and Moesin: key regulators of membrane-cortex interactions and signaling’, *Current Opinion in Cell Biology*, vol. 23, no. 4, pp. 377–82.
- Nemeth, J., Stein, I., Haag, D., Riehl, A., Longerich, T., Horwitz, E., Breuhahn, K., Gebhardt, C., Schirmacher, P., Hahn, M., Ben-Neriah, Y., Pikarsky, E., Angel, P. & Hess, J. 2009, ‘S100A8 and S100A9 are novel nuclear factor kappa B target genes during malignant progression of murine and human liver carcinogenesis.’, *Hepatology (Baltimore, Md.)*, vol. 50, no. 4, pp. 1251–62.
- Neudauer, C.L., Joberty, G., Tatsis, N. & Macara, I.G. 1998, ‘Distinct cellular effects and interactions of the Rho-family GTPase TC10.’, *Current Biology : CB*, vol. 8, no. 21, pp. 1151–60.
- Ng, T., Parsons, M., Hughes, W.E., Monypenny, J., Zicha, D., Gautreau, A., Arpin, M., Gschmeissner, S., Verwee, P.J., Bastiaens, P.I. & Parker, P.J. 2001, ‘Ezrin is a downstream effector of trafficking PKC-integrin complexes involved in the control of cell motility.’, *The EMBO Journal*, vol. 20, no. 11, pp. 2723–41.
- Nishikawa, T., Lee, I.S., Shiraishi, N., Ishikawa, T., Ohta, Y. & Nishikimi, M. 1997, ‘Identification of S100b protein as copper-binding protein and its suppression of copper-induced cell damage.’, *The Journal of Biological Chemistry*, vol. 272, no. 37, pp. 23037–41.
- Noritake, J., Fukata, M., Sato, K., Nakagawa, M., Watanabe, T., Izumi, N., Wang, S., Fukata, Y. & Kaibuchi, K. 2004, ‘Positive role of IQGAP1, an effector of Rac1, in actin-meshwork formation at sites of cell-cell contact’, *Molecular Biology of the Cell*, vol. 15, no. 3, 2003/12/29., pp. 1065–76.
- Noritake, J., Watanabe, T., Sato, K., Wang, S. & Kaibuchi, K. 2005, ‘IQGAP1: a key regulator of adhesion and migration.’, *Journal of Cell Science*, vol. 118, no. Pt 10, pp. 2085–92.
- Novoa-Herran, S., Umana-Perez, A., Canals, F. & Sanchez-Gomez, M. 2016, ‘Serum depletion induces changes in protein expression in the trophoblast-derived cell line HTR-8/SVneo.’, *Cellular & Molecular Biology Letters*, vol. 21, p. 22.
- Nuriya, M., Oh, S. & Haganir, R.L. 2005, ‘Phosphorylation-dependent interactions of alpha-Actinin-1/IQGAP1 with the AMPA receptor subunit GluR4.’, *Journal of Neurochemistry*, vol. 95, no. 2, pp. 544–52.
- Ohtani, K., Sakamoto, H., Rutherford, T., Chen, Z., Kikuchi, A., Yamamoto, T., Satoh, K. & Naftolin, F. 2002, ‘Ezrin, a membrane-cytoskeletal linking protein, is highly expressed in atypical endometrial hyperplasia and uterine endometrioid adenocarcinoma.’, *Cancer Letters*, vol. 179, no. 1, pp. 79–86.
- Ohuchida, K., Mizumoto, K., Egami, T., Yamaguchi, H., Fujii, K., Konomi, H., Nagai, E., Yamaguchi, K., Tsuneyoshi, M. & Tanaka, M. 2006, ‘S100P is an early developmental marker of pancreatic carcinogenesis.’, *Clinical Cancer Research : an Official Journal of the American Association for Cancer Research*, vol. 12, no. 18, pp. 5411–6.
- Omelchenko, T., Vasiliev, J.M., Gelfand, I.M., Feder, H.H. & Bonder, E.M. 2002, ‘Mechanisms of polarization of the shape of fibroblasts and epitheliocytes: Separation of the roles of microtubules and Rho-dependent actin-myosin contractility’, *Proceedings of the National Academy of Sciences of the United States of America*, vol. 99, no. 16, 2002/07/29., pp. 10452–7.
- Orre, L.M., Panizza, E., Kaminsky, V.O., Vernet, E., Graslund, T., Zhivotovsky, B. & Lehtio, J. 2013, ‘S100A4 interacts with p53 in the nucleus and promotes p53 degradation.’, *Oncogene*, vol. 32, no. 49, pp. 5531–40.
- Oslejskova, L., Grigorian, M., Hulejova, H., Vencovsky, J., Pavelka, K., Klingelhofer, J., Gay, S., Neidhart, M., Brabcova, H., Suchy, D. & Senolt, L. 2009, ‘Metastasis-inducing S100A4 protein is associated with the disease activity of rheumatoid arthritis.’, *Rheumatology*, vol. 48, no. 12, pp. 1590–4.
- Osman, M.A. & Cerione, R.A. 1998, ‘Iqg1p, a yeast homologue of the mammalian IQGAPs, mediates cdc42p effects on the actin cytoskeleton’, *The Journal of Cell Biology*, vol. 142, no. 2, pp. 443–55.
- Ostendorp, T., Leclerc, E., Galichet, A., Koch, M., Demling, N., Weigle, B., Heizmann, C.W., Kroneck, P.M.H. & Fritz, G. 2007, ‘Structural and functional insights into RAGE activation by multimeric S100B’, *The EMBO Journal*, vol. 26, no. 16, 2007/07/26., pp. 3868–78.
- Ou-Yang, M., Liu, H.-R., Zhang, Y., Zhu, X. & Yang, Q. 2011, ‘ERM stable knockdown by siRNA reduced in vitro migration and invasion of human SGC-7901 cells’, *Biochimie*, vol. 93, no. 5, pp. 954–61.
- Palecek, S.P., Loftus, J.C., Ginsberg, M.H., Lauffenburger, D.A. & Horwitz, A.F. 1997, ‘Integrin-ligand

- binding properties govern cell migration speed through cell-substratum adhesiveness.’, *Nature*, vol. 385, no. 6616, pp. 537–40.
- Pan, C.Q., Sudol, M., Sheetz, M. & Low, B.C. 2012, ‘Modularity and functional plasticity of scaffold proteins as p(l)acemakers in cell signaling.’, *Cellular Signalling*, vol. 24, no. 11, pp. 2143–65.
- Pan, S.-C., Li, C.-Y., Kuo, C.-Y., Kuo, Y.-Z., Fang, W.-Y., Huang, Y.-H., Hsieh, T.-C., Kao, H.-Y., Kuo, Y., Kang, Y.-R., Tsai, W.-C., Tsai, S.-T. & Wu, L.-W. 2018, ‘The p53-S100A2 positive feedback loop negatively regulates epithelialization in cutaneous wound healing’, *Scientific Reports*, vol. 8, no. 1, p. 5458.
- Pankova, K., Rosel, D., Novotny, M. & Brabek, J. 2010, ‘The molecular mechanisms of transition between mesenchymal and amoeboid invasiveness in tumor cells.’, *Cellular and Molecular Life Sciences : CMLS*, vol. 67, no. 1, pp. 63–71.
- Paradela, A., Bravo, S.B., Henriquez, M., Riquelme, G., Gavilanes, F., Gonzalez-Ros, J.M. & Albar, J.P. 2005, ‘Proteomic analysis of apical microvillous membranes of syncytiotrophoblast cells reveals a high degree of similarity with lipid rafts.’, *Journal of Proteome Research*, vol. 4, no. 6, pp. 2435–41.
- Park, J.-M., Han, Y.-M., Jeong, M., Chung, M.H., Kwon, C. Il, Ko, K.H. & Hahm, K.B. 2017, ‘Synthetic 8-hydroxydeoxyguanosine inhibited metastasis of pancreatic cancer through concerted inhibitions of ERM and Rho-GTPase’, *Free Radical Biology & Medicine*, vol. 110, pp. 151–61.
- Parkkila, S., Pan, P.-W., Ward, A., Gibadulinova, A., Oveckova, I., Pastorekova, S., Pastorek, J., Martinez, A.R., Helin, H.O. & Isola, J. 2008, ‘The calcium-binding protein S100P in normal and malignant human tissues.’, *BMC Clinical Pathology*, vol. 8, p. 2.
- Parlato, S., Giammarioli, A.M., Logozzi, M., Lozupone, F., Matarrese, P., Luciani, F., Falchi, M., Malorni, W. & Fais, S. 2000, ‘CD95 (APO-1/Fas) linkage to the actin cytoskeleton through ezrin in human T lymphocytes: a novel regulatory mechanism of the CD95 apoptotic pathway’, *The EMBO Journal*, vol. 19, no. 19, pp. 5123–34.
- Parnell, E., Koschinski, A., Zaccolo, M., Cameron, R.T., Baillie, G.L.G.S., Baillie, G.L.G.S., Porter, A., McElroy, S.P. & Yarwood, S.J. 2015, ‘Phosphorylation of ezrin on Thr567 is required for the synergistic activation of cell spreading by EPAC1 and protein kinase A in HEK293T cells’, *Biochimica et Biophysica Acta*, vol. 1853, no. 7, 2015/04/23., pp. 1749–58.
- Parsons, J.T., Horwitz, A.R. & Schwartz, M.A. 2010, ‘Cell adhesion: integrating cytoskeletal dynamics and cellular tension’, *Nature Reviews. Molecular Cell Biology*, vol. 11, no. 9, pp. 633–43.
- Patara, M., Santos, E.M.M., Coudry, R. de A., Soares, F.A., Ferreira, F.O. & Rossi, B.M. 2011, ‘Ezrin expression as a prognostic marker in colorectal adenocarcinoma.’, *Pathology Oncology Research : POR*, vol. 17, no. 4, pp. 827–33.
- Pearson, M.A., Reczek, D., Bretscher, A. & Karplus, P.A. 2000, ‘Structure of the ERM protein moesin reveals the FERM domain fold masked by an extended actin binding tail domain’, *Cell*, vol. 101, no. 3, pp. 259–70.
- Penela, P., Ribas, C., Aymerich, I., Eijkelkamp, N., Barreiro, O., Heijnen, C.J., Kavelaars, A., Sanchez-Madrid, F. & Mayor, F.J. 2008, ‘G protein-coupled receptor kinase 2 positively regulates epithelial cell migration.’, *The EMBO Journal*, vol. 27, no. 8, pp. 1206–18.
- Peng, C., Chen, H., Wallwiener, M., Modugno, C., Cuk, K., Madhavan, D., Trumpp, A., Heil, J., Marme, F., Nees, J., Riethdorf, S., Schott, S., Sohn, C., Pantel, K., Schneeweiss, A., Yang, R. & Burwinkel, B. 2016, ‘Plasma S100P level as a novel prognostic marker of metastatic breast cancer.’, *Breast Cancer Research and Treatment*, vol. 157, no. 2, pp. 329–38.
- Petit, V. & Thiery, J.P. 2000, ‘Focal adhesions: structure and dynamics.’, *Biology of the Cell*, vol. 92, no. 7, pp. 477–94.
- Petrie, R.J., Doyle, A.D. & Yamada, K.M. 2009, ‘Random versus directionally persistent cell migration.’, *Nature Reviews. Molecular Cell Biology*, vol. 10, no. 8, pp. 538–49.
- Pidoux, G., Gerbaud, P., Dompierre, J., Lygren, B., Solstad, T., Evain-Brion, D. & Tasken, K. 2014, ‘A PKA-ezrin-Cx43 signaling complex controls gap junction communication and thereby trophoblast cell fusion.’, *Journal of Cell Science*, vol. 127, no. Pt 19, pp. 4172–85.
- Pierce, G.B. 1983, ‘The cancer cell and its control by the embryo. Rous-Whipple Award lecture.’, *The American Journal of Pathology*, vol. 113, no. 1, pp. 117–24.
- Pietromonaco, S.F., Simons, P.C., Altman, A. & Elias, L. 1998, ‘Protein kinase C- $\theta$  phosphorylation of moesin in the actin-binding sequence’, *Journal of Biological Chemistry*, vol. 273, no. 13, pp. 7594–603.
- Pilot, F., Philippe, J.-M., Lemmers, C. & Lecuit, T. 2006, ‘Spatial control of actin organization at adherens junctions by a synaptotagmin-like protein Btsz’, *Nature*, vol. 442, no. 7102, pp. 580–4.
- Pollard, T.D. & Borisy, G.G. 2003, ‘Cellular motility driven by assembly and disassembly of actin

- filaments.’, *Cell*, vol. 112, no. 4, pp. 453–65.
- Pollheimer, J., Vondra, S., Baltayeva, J., Beristain, A.G. & Knöfler, M. 2018, ‘Regulation of Placental Extravillous trophoblasts by the maternal uterine environment’, *Frontiers in Immunology*, vol. 9, p. 2597.
- Ponuwei, G.A. 2016, ‘A glimpse of the ERM proteins’, *Journal of Biomedical Science*, vol. 23, p. 35.
- Popovici, R.M., Betzler, N.K., Krause, M.S., Luo, M., Jauckus, J., Germeyer, A., Bloethner, S., Schlotterer, A., Kumar, R., Strowitzki, T. & von Wolff, M. 2006, ‘Gene expression profiling of human endometrial-trophoblast interaction in a coculture model.’, *Endocrinology*, vol. 147, no. 12, pp. 5662–75.
- Pore, D. & Gupta, N. 2015, ‘The ezrin-radixin-moesin family of proteins in the regulation of B-cell immune response’, *Critical Reviews in Immunology*, vol. 35, no. 1, pp. 15–31.
- Prica, F., Radon, T., Cheng, Y. & Crnogorac-Jurcevic, T. 2016, ‘The life and works of S100P - from conception to cancer.’, *American Journal of Cancer Research*, vol. 6, no. 2, pp. 562–76.
- Prosser, B.L., Wright, N.T., Hernandez-Ochoa, E.O., Varney, K.M., Liu, Y., Olojo, R.O., Zimmer, D.B., Weber, D.J. & Schneider, M.F. 2008, ‘S100A1 binds to the calmodulin-binding site of ryanodine receptor and modulates skeletal muscle excitation-contraction coupling.’, *The Journal of Biological Chemistry*, vol. 283, no. 8, pp. 5046–57.
- Purwin, M., Bruzgo, I., Markowska, A. & Midura-Nowaczek, K. 2009, ‘Short peptides containing L-lysine and epsilon-aminocaproic acid as potential plasmin inhibitors.’, *Die Pharmazie*, vol. 64, no. 11, pp. 765–7.
- Quan, C., Sun, J., Lin, Z., Jin, T., Dong, B., Meng, Z. & Piao, J. 2019, ‘Ezrin promotes pancreatic cancer cell proliferation and invasion through activating the Akt/mTOR pathway and inducing YAP translocation’, *Cancer Management and Research*, vol. 11, pp. 6553–66.
- Rafelski, S.M. & Theriot, J.A. 2004, ‘Crawling toward a unified model of cell mobility: spatial and temporal regulation of actin dynamics.’, *Annual Review of Biochemistry*, vol. 73, pp. 209–39.
- Raffat, M.A., Hadi, N.I., Hosein, M., Mirza, S., Ikram, S. & Akram, Z. 2018, ‘S100 proteins in oral squamous cell carcinoma.’, *Clinica Chimica Acta; International Journal of Clinical Chemistry*, vol. 480, pp. 143–9.
- Rambotti, M.G., Giambanco, I., Spreca, A. & Donato, R. 1999, ‘S100B and S100A1 proteins in bovine retina: their calcium-dependent stimulation of a membrane-bound guanylate cyclase activity as investigated by ultracytochemistry.’, *Neuroscience*, vol. 92, no. 3, pp. 1089–101.
- Red-Horse, K., Zhou, Y., Genbacev, O., Prakobphol, A., Foulk, R., McMaster, M. & Fisher, S.J. 2004, ‘Trophoblast differentiation during embryo implantation and formation of the maternal-fetal interface’, *The Journal of Clinical Investigation*, vol. 114, no. 6, pp. 744–54.
- Reister, F., Kingdom, J.C.P., Ruck, P., Marzusch, K., Heyl, W., Pauer, U., Kaufmann, P., Rath, W. & Huppertz, B. 2006, ‘Altered protease expression by periarterial trophoblast cells in severe early-onset preeclampsia with IUGR.’, *Journal of Perinatal Medicine*, vol. 34, no. 4, pp. 272–9.
- Ren, J.-G., Li, Z., Crimmins, D.L. & Sacks, D.B. 2005, ‘Self-association of IQGAP1: characterization and functional sequelae.’, *The Journal of Biological Chemistry*, vol. 280, no. 41, pp. 34548–57.
- Ren, J.-G., Li, Z. & Sacks, D.B. 2007, ‘IQGAP1 modulates activation of B-Raf.’, *Proceedings of the National Academy of Sciences of the United States of America*, vol. 104, no. 25, pp. 10465–9.
- Rety, S., Sopkova, J., Renouard, M., Osterloh, D., Gerke, V., Tabaries, S., Russo-Marie, F. & Lewit-Bentley, A. 1999, ‘The crystal structure of a complex of p11 with the annexin II N-terminal peptide.’, *Nature Structural Biology*, vol. 6, no. 1, pp. 89–95.
- Ridley, A.J., Schwartz, M.A., Burridge, K., Firtel, R.A., Ginsberg, M.H., Borisy, G., Parsons, J.T. & Horwitz, A.R. 2003, ‘Cell migration: integrating signals from front to back’, *Science*, vol. 302, no. 5651, pp. 1704–9.
- Rigothier, C., Auguste, P., Welsh, G.I., Lepreux, S., Deminiere, C., Mathieson, P.W., Saleem, M.A., Ripoche, J. & Combe, C. 2012, ‘IQGAP1 interacts with components of the slit diaphragm complex in podocytes and is involved in podocyte migration and permeability in vitro.’, *PloS One*, vol. 7, no. 5, p. e37695.
- Rittmeyer, E.N., Daniel, S., Hsu, S.-C. & Osman, M.A. 2008, ‘A dual role for IQGAP1 in regulating exocytosis.’, *Journal of Cell Science*, vol. 121, no. Pt 3, pp. 391–403.
- Roberts, J.M. & Hubel, C.A. 2009, ‘The two stage model of preeclampsia: variations on the theme.’, *Placenta*, vol. 30 Suppl A, pp. S32–7.
- Roberts, J.M. & Lain, K.Y. 2002, ‘Recent insights into the pathogenesis of pre-eclampsia’, *Placenta*, vol. 23, no. 5, pp. 359–72.
- Rohde, D., Ritterhoff, J., Voelkers, M., Katus, H.A., Parker, T.G. & Most, P. 2010, ‘S100A1: a multifaceted therapeutic target in cardiovascular disease.’, *Journal of Cardiovascular Translational*

- Research*, vol. 3, no. 5, pp. 525–37.
- Rosario, G.X., Konno, T. & Soares, M.J. 2008, 'Maternal hypoxia activates endovascular trophoblast cell invasion', *Developmental Biology*, vol. 314, no. 2, 2007/12/15., pp. 362–75.
- Rotoli, D., Morales, M., Maeso, M.D.C., Garcia, M.D.P., Gutierrez, R., Valladares, F., Avila, J., Diaz-Flores, L., Mobasheri, A. & Martin-Vasallo, P. 2017, 'Alterations in IQGAP1 expression and localization in colorectal carcinoma and liver metastases following oxaliplatin-based chemotherapy.', *Oncology Letters*, vol. 14, no. 3, pp. 2621–8.
- Rousseaux, S., Debernardi, A., Jacquiau, B., Vitte, A.-L., Vesin, A., Nagy-Mignotte, H., Moro-Sibilot, D., Brichon, P.-Y., Lantuejoul, S., Hainaut, P., Laffaire, J., de Reynies, A., Beer, D.G., Timsit, J.-F., Brambilla, C., Brambilla, E. & Khochbin, S. 2013, 'Ectopic activation of germline and placental genes identifies aggressive metastasis-prone lung cancers', *Science Translational Medicine*, vol. 5, no. 186, p. 186ra66.
- Routray, C., Liu, C., Yaqoob, U., Billadeau, D.D., Bloch, K.D., Kaibuchi, K., Shah, V.H. & Kang, N. 2011, 'Protein kinase G signaling disrupts Rac1-dependent focal adhesion assembly in liver specific pericytes', *American Journal of Physiology. Cell Physiology*, vol. 301, no. 1, 2011/03/30., pp. C66–74.
- Roy, M., Li, Z. & Sacks, D.B. 2005, 'IQGAP1 is a scaffold for mitogen-activated protein kinase signaling.', *Molecular and Cellular Biology*, vol. 25, no. 18, pp. 7940–52.
- Ruiz-Saenz, A., Kremer, L., Alonso, M.A., Millan, J. & Correas, I. 2011, 'Protein 4.1R regulates cell migration and IQGAP1 recruitment to the leading edge.', *Journal of Cell Science*, vol. 124, no. Pt 15, pp. 2529–38.
- Ruiz-Velasco, R., Lanning, C.C. & Williams, C.L. 2002, 'The activation of Rac1 by M3 muscarinic acetylcholine receptors involves the translocation of Rac1 and IQGAP1 to cell junctions and changes in the composition of protein complexes containing Rac1, IQGAP1, and actin.', *The Journal of Biological Chemistry*, vol. 277, no. 36, pp. 33081–91.
- Ruppelt, A., Mosenden, R., Gronholm, M., Aandahl, E.M., Tobin, D., Carlson, C.R., Abrahamsen, H., Herberg, F.W., Carpen, O. & Tasken, K. 2007, 'Inhibition of T cell activation by cyclic adenosine 5'-monophosphate requires lipid raft targeting of protein kinase A type I by the A-kinase anchoring protein ezrin.', *Journal of Immunology*, vol. 179, no. 8, pp. 5159–68.
- Sahai, E. & Marshall, C.J. 2003, 'Differing modes of tumour cell invasion have distinct requirements for Rho/ROCK signalling and extracellular proteolysis.', *Nature Cell Biology*, vol. 5, no. 8, pp. 711–9.
- Sakurai-Yageta, M., Recchi, C., Le Dez, G., Sibarita, J.-B., Daviet, L., Camonis, J., D'Souza-Schorey, C. & Chavrier, P. 2008, 'The interaction of IQGAP1 with the exocyst complex is required for tumor cell invasion downstream of Cdc42 and RhoA.', *The Journal of Cell Biology*, vol. 181, no. 6, pp. 985–98.
- Salas, S., Bartoli, C., Deville, J.-L., Gaudart, J., Fina, F., Calisti, A., Bollini, G., Curvale, G., Gentet, J.-C., Duffaud, F., Figarella-Branger, D. & Bouvier, C. 2007, 'Ezrin and alpha-smooth muscle actin are immunohistochemical prognostic markers in conventional osteosarcomas.', *Virchows Archiv: an International Journal of Pathology*, vol. 451, no. 6, pp. 999–1007.
- Saotome, I., Curto, M. & McClatchey, A.I. 2004, 'Ezrin is essential for epithelial organization and villus morphogenesis in the developing intestine', *Developmental Cell*, vol. 6, no. 6, pp. 855–64.
- Sapkota, D., Bruland, O., Costea, D.E., Haugen, H., Vasstrand, E.N. & Ibrahim, S.O. 2011, 'S100A14 regulates the invasive potential of oral squamous cell carcinoma derived cell-lines in vitro by modulating expression of matrix metalloproteinases, MMP1 and MMP9.', *European Journal of Cancer*, vol. 47, no. 4, pp. 600–10.
- Sarrio, D., Rodriguez-Pinilla, S.M., Dotor, A., Calero, F., Hardisson, D. & Palacios, J. 2006, 'Abnormal ezrin localization is associated with clinicopathological features in invasive breast carcinomas.', *Breast Cancer Research and Treatment*, vol. 98, no. 1, pp. 71–9.
- Sastry, M., Ketchum, R.R., Crescenzi, O., Weber, C., Lubienski, M.J., Hidaka, H. & Chazin, W.J. 1998, 'The three-dimensional structure of Ca<sup>2+</sup>-bound calyculin: implications for Ca<sup>2+</sup>-signal transduction by S100 proteins', *Structure*, vol. 6, no. 2, pp. 223–31.
- Sato, N., Fukushima, N., Matsubayashi, H. & Goggins, M. 2004, 'Identification of maspin and S100P as novel hypomethylation targets in pancreatic cancer using global gene expression profiling.', *Oncogene*, vol. 23, no. 8, pp. 1531–8.
- Sato, Y., Fujiwara, H. & Konishi, I. 2011, 'Mechanism of maternal vascular remodeling during human pregnancy', *Reproductive Medicine and Biology*, vol. 11, no. 1, pp. 27–36.
- Sbroggiò, M., Bertero, A., Velasco, S., Fusella, F., De Blasio, E., Bahou, W.F., Silengo, L., Turco, E., Brancaccio, M. & Tarone, G. 2011, 'ERK1/2 activation in heart is controlled by melusin, focal adhesion kinase and the scaffold protein IQGAP1', *Journal of Cell Science*, vol. 124, no. Pt 20, pp.

- 3515–24.
- Sbroglio, M., Carnevale, D., Bertero, A., Cifelli, G., De Blasio, E., Mascio, G., Hirsch, E., Bahou, W.F., Turco, E., Silengo, L., Brancaccio, M., Lembo, G. & Tarone, G. 2011, 'IQGAP1 regulates ERK1/2 and AKT signalling in the heart and sustains functional remodelling upon pressure overload.', *Cardiovascular Research*, vol. 91, no. 3, pp. 456–64.
- Schafer, B.W., Fritschy, J.M., Murmann, P., Troxler, H., Durussel, I., Heizmann, C.W. & Cox, J.A. 2000, 'Brain S100A5 is a novel calcium-, zinc-, and copper ion-binding protein of the EF-hand superfamily.', *The Journal of Biological Chemistry*, vol. 275, no. 39, pp. 30623–30.
- Schafer, B.W. & Heizmann, C.W. 1996, 'The S100 family of EF-hand calcium-binding proteins: functions and pathology.', *Trends in Biochemical Sciences*, vol. 21, no. 4, pp. 134–40.
- Schiefermeier, N., Scheffler, J.M., de Araujo, M.E.G., Stasyk, T., Yordanov, T., Ebner, H.L., Offterdinger, M., Munck, S., Hess, M.W., Wickström, S.A., Lange, A., Wunderlich, W., Fässler, R., Teis, D. & Huber, L.A. 2014, 'The late endosomal p14-MP1 (LAMTOR2/3) complex regulates focal adhesion dynamics during cell migration', *The Journal of Cell Biology*, vol. 205, no. 4, 2014/05/19., pp. 525–40.
- Schiller, H.B., Friedel, C.C., Boulegue, C. & Fassler, R. 2011, 'Quantitative proteomics of the integrin adhesome show a myosin II-dependent recruitment of LIM domain proteins.', *EMBO Reports*, vol. 12, no. 3, pp. 259–66.
- Schindelin, J., Arganda-Carreras, I., Frise, E., Kaynig, V., Longair, M., Pietzsch, T., Preibisch, S., Rueden, C., Saalfeld, S., Schmid, B., Tinevez, J.-Y., White, D.J., Hartenstein, V., Eliceiri, K., Tomancak, P. & Cardona, A. 2012, 'Fiji: an open-source platform for biological-image analysis', *Nature Methods*, vol. 9, no. 7, pp. 676–82.
- Schlecht, N.F., Brandwein-Gensler, M., Smith, R. V., Kawachi, N., Broughel, D., Lin, J., Keller, C.E., Reynolds, P.A., Gunn-Moore, F.J., Harris, T., Childs, G., Belbin, T.J. & Prystowsky, M.B. 2012, 'Cytoplasmic ezrin and moesin correlate with poor survival in head and neck squamous cell carcinoma.', *Head and Neck Pathology*, vol. 6, no. 2, pp. 232–43.
- Schor, A.P.T., Carvalho, F.M., Kemp, C., Silva, I.D.C.G. & Russo, J. 2006, 'S100P calcium-binding protein expression is associated with high-risk proliferative lesions of the breast.', *Oncology Reports*, vol. 15, no. 1, pp. 3–6.
- Schwanhausser, B., Busse, D., Li, N., Dittmar, G., Schuchhardt, J., Wolf, J., Chen, W. & Selbach, M. 2011, 'Global quantification of mammalian gene expression control.', *Nature*, vol. 473, no. 7347, pp. 337–42.
- Semizarov, D., Frost, L., Sarthy, A., Kroeger, P., Halbert, D.N. & Fesik, S.W. 2003, 'Specificity of short interfering RNA determined through gene expression signatures', *Proceedings of the National Academy of Sciences of the United States of America*, vol. 100, no. 11, 2003/05/13., pp. 6347–52.
- Semov, A., Moreno, M.J., Onichtchenko, A., Abulrob, A., Ball, M., Ekiel, I., Pietrzynski, G., Stanimirovic, D. & Alakhov, V. 2005, 'Metastasis-associated protein S100A4 induces angiogenesis through interaction with Annexin II and accelerated plasmin formation.', *The Journal of Biological Chemistry*, vol. 280, no. 21, pp. 20833–41.
- Sen, N., Gui, B. & Kumar, R. 2014, 'Physiological functions of MTA family of proteins', *Cancer Metastasis Reviews*, vol. 33, no. 4, pp. 869–77.
- Serrador, J.M., Nieto, M., Alonso-Lebrero, J.L., del Pozo, M.A., Calvo, J., Furthmayr, H., Schwartz-Albiez, R., Lozano, F., Gonzalez-Amaro, R., Sanchez-Mateos, P. & Sanchez-Madrid, F. 1998, 'CD43 interacts with moesin and ezrin and regulates its redistribution to the uropods of T lymphocytes at the cell-cell contacts.', *Blood*, vol. 91, no. 12, pp. 4632–44.
- Shang, X., Cheng, H. & Zhou, R. 2008, 'Chromosomal mapping, differential origin and evolution of the S100 gene family', *Genetics, Selection, Evolution : GSE*, vol. 40, no. 4, 2008/06/17., pp. 449–64.
- Shannon, K.B. & Li, R. 1999, 'The multiple roles of Cyk1p in the assembly and function of the actomyosin ring in budding yeast.', *Molecular Biology of the Cell*, vol. 10, no. 2, pp. 283–96.
- Shen, X., Jia, Z., D'Alonzo, D., Wang, X., Bruder, E., Emch, F.H., De Geyter, C. & Zhang, H. 2017, 'HECTD1 controls the protein level of IQGAP1 to regulate the dynamics of adhesive structures', *Cell Communication and Signaling*, vol. 15, no. 1, p. 2.
- Shiue, H., Musch, M.W., Wang, Y., Chang, E.B. & Turner, J.R. 2005, 'Akt2 phosphorylates ezrin to trigger NHE3 translocation and activation.', *The Journal of Biological Chemistry*, vol. 280, no. 2, pp. 1688–95.
- Sikorska, J., Gawel, D., Domek, H., Rudzinska, M. & Czarnocka, B. 2019, 'Podoplanin (PDPN) affects the invasiveness of thyroid carcinoma cells by inducing ezrin, radixin and moesin (E/R/M) phosphorylation in association with matrix metalloproteinases.', *BMC Cancer*, vol. 19, no. 1, p. 85.
- Skop, A.R., Liu, H., Yates, J. 3rd, Meyer, B.J. & Heald, R. 2004, 'Dissection of the mammalian midbody

- proteome reveals conserved cytokinesis mechanisms.’, *Science*, vol. 305, no. 5680, pp. 61–6.
- Smith, S.P. & Shaw, G.S. 1998, ‘A novel calcium-sensitive switch revealed by the structure of human S100B in the calcium-bound form.’, *Structure*, vol. 6, no. 2, pp. 211–22.
- Song, J., Fadiel, A., Edusa, V., Chen, Z., So, J., Sakamoto, H., Fishman, D.A. & Naftolin, F. 2005, ‘Estradiol-induced ezrin overexpression in ovarian cancer: a new signaling domain for estrogen.’, *Cancer Letters*, vol. 220, no. 1, pp. 57–65.
- Sorci, G., Agneletti, A.L., Bianchi, R. & Donato, R. 1998, ‘Association of S100B with intermediate filaments and microtubules in glial cells.’, *Biochimica et Biophysica Acta*, vol. 1448, no. 2, pp. 277–89.
- Sorci, G., Agneletti, A.L. & Donato, R. 2000, ‘Effects of S100A1 and S100B on microtubule stability. An in vitro study using triton-cytoskeletons from astrocyte and myoblast cell lines.’, *Neuroscience*, vol. 99, no. 4, pp. 773–83.
- Speck, O., Hughes, S.C., Noren, N.K., Kulikauskas, R.M. & Fehon, R.G. 2003, ‘Moesin functions antagonistically to the Rho pathway to maintain epithelial integrity’, *Nature*, vol. 421, no. 6918, pp. 83–7.
- Spratt, D.E., Barber, K.R., Marlatt, N.M., Ngo, V., Macklin, J.A., Xiao, Y., Konermann, L., Duennwald, M.L. & Shaw, G.S. 2019, ‘A subset of calcium-binding S100 proteins show preferential heterodimerization.’, *The FEBS Journal*, vol. 286, no. 10, pp. 1859–76.
- Srivastava, J., Elliott, B.E., Louvard, D. & Arpin, M. 2005, ‘Src-dependent ezrin phosphorylation in adhesion-mediated signaling’, *Molecular Biology of the Cell*, vol. 16, no. 3, 2005/01/12., pp. 1481–90.
- Staun-Ram, E. & Shalev, E. 2005, ‘Human trophoblast function during the implantation process’, *Reproductive Biology and Endocrinology: RB&E*, vol. 3, p. 56.
- Straszewski-Chavez, S.L., Abrahams, V.M., Alvero, A.B., Aldo, P.B., Ma, Y., Guller, S., Romero, R. & Mor, G. 2009, ‘The isolation and characterization of a novel telomerase immortalized first trimester trophoblast cell line, Swan 71.’, *Placenta*, vol. 30, no. 11, pp. 939–48.
- Su, D., Liu, Y. & Song, T. 2017, ‘Knockdown of IQGAP1 inhibits proliferation and epithelial-mesenchymal transition by Wnt/beta-catenin pathway in thyroid cancer.’, *OncoTargets and Therapy*, vol. 10, pp. 1549–59.
- Summy, J.M. & Gallick, G.E. 2003, ‘Src family kinases in tumor progression and metastasis.’, *Cancer Metastasis Reviews*, vol. 22, no. 4, pp. 337–58.
- Sun, B., Zhang, S., Zhang, D., Li, Y., Zhao, X., Luo, Y. & Guo, Y. 2008, ‘Identification of metastasis-related proteins and their clinical relevance to triple-negative human breast cancer.’, *Clinical Cancer Research: an Official Journal of the American Association for Cancer Research*, vol. 14, no. 21, pp. 7050–9.
- Suzuki, S., Ishii, G., Matsuwaki, R., Neri, S., Hashimoto, H., Yamauchi, C., Aokage, K., Hishida, T., Yoshida, J., Kohno, M., Nagai, K. & Ochiai, A. 2015, ‘Ezrin-expressing lung adenocarcinoma cells and podoplanin-positive fibroblasts form a malignant microenvironment.’, *Journal of Cancer Research and Clinical Oncology*, vol. 141, no. 3, pp. 475–84.
- Swiech, L., Blazejczyk, M., Urbanska, M., Pietruszka, P., Dortland, B.R., Malik, A.R., Wulf, P.S., Hoogenraad, C.C. & Jaworski, J. 2011, ‘CLIP-170 and IQGAP1 cooperatively regulate dendrite morphology.’, *The Journal of Neuroscience: the Official Journal of the Society for Neuroscience*, vol. 31, no. 12, pp. 4555–68.
- Tabrizi, M.E.A. 2014, ‘B and H-NMR evaluation of chemical interactions between two Polyphenols; epigallocatechingallate and quercetin with bortezomib’, *Biosciences, Biotechnology Research Asia*, vol. 11, no. 2, pp. 577–86.
- Tabrizi, M.E.A., Lancaster, T.L., Ismail, T.M., Georgiadou, A., Ganguly, A., Mistry, J.J., Wang, K., Rudland, P.S., Ahmad, S. & Gross, S.R. 2018, ‘S100P enhances the motility and invasion of human trophoblast cell lines.’, *Scientific Reports*, vol. 8, no. 1, p. 11488.
- Takeuchi, K., Sato, N., Kasahara, H., Funayama, N., Nagafuchi, A., Yonemura, S., Tsukita, S. & Tsukita, S. 1994, ‘Perturbation of cell adhesion and microvilli formation by antisense oligonucleotides to ERM family members’, *The Journal of Cell Biology*, vol. 125, no. 6, pp. 1371–84.
- Tan, O., Ornek, T., Fadiel, A., Carrick, K.S., Arici, A., Doody, K., Carr, B.R. & Naftolin, F. 2012, ‘Expression and activation of the membrane-cytoskeleton protein ezrin during the normal endometrial cycle.’, *Fertility and Sterility*, vol. 97, no. 1, pp. 192-9.e2.
- Tang, C.-H., Hill, M.L., Brumwell, A.N., Chapman, H.A. & Wei, Y. 2008, ‘Signaling through urokinase and urokinase receptor in lung cancer cells requires interactions with beta1 integrins’, *Journal of Cell Science*, vol. 121, no. Pt 22, pp. 3747–56.
- Tang, Y., Sun, X., Yu, S., Bie, X., Wang, J. & Ren, L. 2019, ‘Inhibition of Ezrin suppresses cell

- migration and invasion in human nasopharyngeal carcinoma', *Oncology Letters*, vol. 18, no. 1, pp. 553–60.
- Tarrade, A., Goffin, F., Munaut, C., Lai-Kuen, R., Tricottet, V., Foidart, J.-M., Vidaud, M., Frankenre, F. & Evain-Brion, D. 2002, 'Effect of matrigel on human extravillous Trophoblasts differentiation: modulation of protease pattern gene expression1', *Biology of Reproduction*, vol. 67, no. 5, pp. 1628–37.
- Tarui, T., Majumdar, M., Miles, L.A., Ruf, W. & Takada, Y. 2002, 'Plasmin-induced migration of endothelial cells. A potential target for the anti-angiogenic action of angiostatin.', *The Journal of Biological Chemistry*, vol. 277, no. 37, pp. 33564–70.
- Titus, M.A. & Goodson, H. V 2017, 'An evolutionary perspective on cell migration: Digging for the roots of amoeboid motility', *The Journal of Cell biology*, vol. 216, no. 6, pp. 1509–11.
- Tojkander, S., Gateva, G. & Lappalainen, P. 2012, 'Actin stress fibers-assembly, dynamics and biological roles', *Journal of Cell Science*, vol. 125, no. Pt 8, pp. 1855–64.
- Tong, X.-M., Lin, X.-N., Song, T., Liu, L. & Zhang, S. 2010, 'Calcium-binding protein S100P is highly expressed during the implantation window in human endometrium.', *Fertility and Sterility*, vol. 94, no. 4, pp. 1510–8.
- Toro, A.R., Maymo, J.L., Ibarbalz, F.M., Perez-Perez, A., Maskin, B., Faletti, A.G., Sanchez-Margalet, V. & Varone, C.L. 2014, 'Leptin is an anti-apoptotic effector in placental cells involving p53 downregulation.', *PloS One*, vol. 9, no. 6, p. e99187.
- Tsukita, S., Oishi, K., Sato, N., Sagara, J., Kawai, A. & Tsukita, S. 1994, 'ERM family members as molecular linkers between the cell surface glycoprotein CD44 and actin-based cytoskeletons', *The Journal of Cell Biology*, vol. 126, no. 2, pp. 391–401.
- Tsukita, S. & Yonemura, S. 1999, 'Cortical actin organization: lessons from ERM (ezrin/radixin/moesin) proteins', *The Journal of Biological Chemistry*, vol. 274, no. 49, pp. 34507–10.
- Tsukita, S., Yonemura, S. & Tsukita, S. 1997, 'ERM proteins: head-to-tail regulation of actin-plasma membrane interaction.', *Trends in Biochemical Sciences*, vol. 22, no. 2, pp. 53–8.
- Turunen, O., Wahlstrom, T. & Vaheri, A. 1994, 'Ezrin has a COOH-terminal actin-binding site that is conserved in the ezrin protein family.', *The Journal of Cell Biology*, vol. 126, no. 6, pp. 1445–53.
- Urushidani, T., Hanzel, D.K. & Forte, J.G. 1989, 'Characterization of an 80-kDa phosphoprotein involved in parietal cell stimulation.', *The American Journal of Physiology*, vol. 256, no. 6 Pt 1, pp. G1070-81.
- Vergara, D., Simeone, P., Franck, J., Trerotola, M., Giudetti, A., Capobianco, L., Tinelli, A., Bellomo, C., Fournier, I., Gaballo, A., Alberti, S., Salzet, M. & Maffia, M. 2016, 'Translating epithelial mesenchymal transition markers into the clinic: Novel insights from proteomics', *EuPA Open Proteomics*, vol. 10, pp. 31–41.
- Vicente-Manzanares, M., Webb, D.J. & Horwitz, A.R. 2005, 'Cell migration at a glance.', *Journal of Cell Science*, vol. 118, no. Pt 21, pp. 4917–9.
- Viswanatha, R., Ohouo, P.Y., Smolka, M.B. & Bretscher, A. 2012, 'Local phosphocycling mediated by LOK/SLK restricts ezrin function to the apical aspect of epithelial cells', *The Journal of Cell Biology*, vol. 199, no. 6, 2012/12/03., pp. 969–84.
- Vlahou, G. & Rivero, F. 2006, 'Rho GTPase signaling in Dictyostelium discoideum: insights from the genome.', *European Journal of Cell Biology*, vol. 85, no. 9–10, pp. 947–59.
- Voss, A., Bode, G., Sopalla, C., Benedyk, M., Varga, G., Bohm, M., Nacken, W. & Kerckhoff, C. 2011, 'Expression of S100A8/A9 in HaCaT keratinocytes alters the rate of cell proliferation and differentiation.', *FEBS Letters*, vol. 585, no. 2, pp. 440–6.
- Wakayama, T., Nakata, H., Kurobo, M., Sai, Y. & Iseki, S. 2009, 'Expression, localization, and binding activity of the ezrin/radixin/moesin proteins in the mouse testis', *The Journal of Histochemistry and Cytochemistry*, vol. 57, no. 4, 2008/12/08., pp. 351–62.
- Wakeland, A.K., Soncin, F., Moretto-Zita, M., Chang, C.-W., Horii, M., Pizzo, D., Nelson, K.K., Laurent, L.C. & Parast, M.M. 2017, 'Hypoxia directs human extravillous trophoblast differentiation in a hypoxia-inducible factor-dependent manner', *The American Journal of Pathology*, vol. 187, no. 4, 2017/02/04., pp. 767–80.
- Walch, A., Seidl, S., Hermannstadter, C., Rauser, S., Deplazes, J., Langer, R., von Weyhern, C.H., Sarbia, M., Busch, R., Feith, M., Gillen, S., Hofler, H. & Luber, B. 2008, 'Combined analysis of Rac1, IQGAP1, Tiam1 and E-cadherin expression in gastric cancer.', *Modern Pathology : an Official Journal of the United States and Canadian Academy of Pathology, Inc.*, vol. 21, no. 5, pp. 544–52.
- Wald, F.A., Oriolo, A.S., Mashukova, A., Fregien, N.L., Langshaw, A.H. & Salas, P.J.I. 2008, 'Atypical protein kinase C (iota) activates ezrin in the apical domain of intestinal epithelial cells.', *Journal of*

- Cell Science*, vol. 121, no. Pt 5, pp. 644–54.
- Wang, G., Platt-Higgins, A., Carroll, J., de Silva Rudland, S., Winstanley, J., Barraclough, R. & Rudland, P.S. 2006, 'Induction of metastasis by S100P in a rat mammary model and its association with poor survival of breast cancer patients.', *Cancer Research*, vol. 66, no. 2, pp. 1199–207.
- Wang, G., Zhang, S., Fernig, D.G., Spiller, D., Martin-Fernandez, M., Zhang, H., Ding, Y., Rao, Z., Rudland, P.S. & Barraclough, R. 2004, 'Heterodimeric interaction and interfaces of S100A1 and S100P', *The Biochemical Journal*, vol. 382, no. Pt 1, pp. 375–83.
- Wang, H., Cheng, H., Shao, Q., Dong, Z., Xie, Q., Zhao, L., Wang, Q., Kong, B. & Qu, X. 2014, 'Leptin-promoted human extravillous trophoblast invasion is MMP14 dependent and requires the cross talk between Notch1 and PI3K/Akt signaling', *Biology of Reproduction*, vol. 90, no. 4, p. 78.
- Wang, J.-B., Sonn, R., Tekletsadik, Y.K., Samorodnitsky, D. & Osman, M.A. 2009, 'IQGAP1 regulates cell proliferation through a novel CDC42-mTOR pathway.', *Journal of Cell Science*, vol. 122, no. Pt 12, pp. 2024–33.
- Wang, L., Lin, G.-N., Jiang, X.-L. & Lu, Y. 2011, 'Expression of ezrin correlates with poor prognosis of nasopharyngeal carcinoma.', *Tumour Biology: the Journal of the International Society for Oncodevelopmental Biology and Medicine*, vol. 32, no. 4, pp. 707–12.
- Wang, L., Wang, X., Liang, Y., Diao, X. & Chen, Q. 2012, 'S100A4 promotes invasion and angiogenesis in breast cancer MDA-MB-231 cells by upregulating matrix metalloproteinase-13.', *Acta Biochimica Polonica*, vol. 59, no. 4, pp. 593–8.
- Wang, Q., Zhang, Y.-N., Lin, G.-L., Qiu, H.-Z., Wu, B., Wu, H.-Y., Zhao, Y., Chen, Y.-J. & Lu, C.-M. 2012, 'S100P, a potential novel prognostic marker in colorectal cancer', *Oncology Reports*, vol. 28, no. 1, pp. 303–10.
- Wang, S., Watanabe, T., Noritake, J., Fukata, M., Yoshimura, T., Itoh, N., Harada, T., Nakagawa, M., Matsuura, Y., Arimura, N. & Kaibuchi, K. 2007, 'IQGAP3, a novel effector of Rac1 and Cdc42, regulates neurite outgrowth.', *Journal of Cell Science*, vol. 120, no. Pt 4, pp. 567–77.
- Wang, X.-X., Li, X.-Z., Zhai, L.-Q., Liu, Z.-R., Chen, X.-J. & Pei, Y. 2013, 'Overexpression of IQGAP1 in human pancreatic cancer.', *Hepatobiliary & Pancreatic Diseases International: HBPD INT*, vol. 12, no. 5, pp. 540–5.
- Wang, X.-X., Wang, K., Li, X.-Z., Zhai, L.-Q., Qu, C.-X., Zhao, Y., Liu, Z.-R., Wang, H.-Z., An, Q.-J., Jing, L.-W. & Wang, X.-H. 2014, 'Targeted knockdown of IQGAP1 inhibits the progression of esophageal squamous cell carcinoma in vitro and in vivo.', *PLoS One*, vol. 9, no. 5, p. e96501.
- Wang, X., He, C., Li, C., Ren, B., Deng, Q., Gao, W. & Wang, B. 2018, 'IQGAP1 silencing suppresses the malignant characteristics of laryngeal squamous cell carcinoma cells.', *The International Journal of Biological Markers*, vol. 33, no. 1, pp. 73–8.
- Wang, X., Liu, M. & Zhao, C.Y. 2014, 'Expression of ezrin and moesin related to invasion, metastasis and prognosis of laryngeal squamous cell carcinoma.', *Genetics and Molecular Research: GMR*, vol. 13, no. 3, pp. 8002–13.
- Wang, X., Tian, T., Li, X., Zhao, M., Lou, Y., Qian, J., Liu, Z., Chen, H. & Cui, Z. 2015, 'High expression of S100P is associated with unfavorable prognosis and tumor progression in patients with epithelial ovarian cancer', *American Journal of Cancer Research*, vol. 5, no. 8, pp. 2409–21.
- Wang, Y., Lin, Z., Sun, L., Fan, S., Huang, Z., Zhang, D., Yang, Z., Li, J. & Chen, W. 2014, 'Akt/ezrin Tyr353/NF- $\kappa$ B pathway regulates EGF-induced EMT and metastasis in tongue squamous cell carcinoma', *British Journal of Cancer*, vol. 110, no. 3, 2013/12/17., pp. 695–705.
- Wang, Y. & Zhao, S. 2010, *Vascular Biology of the Placenta*, Morgan & Claypool Life Sciences, San Rafael, CA.
- Watanabe, T., Noritake, J. & Kaibuchi, K. 2005, 'Regulation of microtubules in cell migration', *Trends in Cell Biology*, vol. 15, no. 2, pp. 76–83.
- Watanabe, T., Wang, S. & Kaibuchi, K. 2015, 'IQGAPs as key regulators of actin-cytoskeleton dynamics', *Cell Structure and Function*, vol. 40, no. 2, pp. 69–77.
- Watanabe, T., Wang, S., Noritake, J., Sato, K., Fukata, M., Takefuji, M., Nakagawa, M., Izumi, N., Akiyama, T. & Kaibuchi, K. 2004, 'Interaction with IQGAP1 links APC to Rac1, Cdc42, and actin filaments during cell polarization and migration.', *Developmental Cell*, vol. 7, no. 6, pp. 871–83.
- Wei, Y.-C., Li, C.-F., Yu, S.-C., Chou, F.-F., Fang, F.-M., Eng, H.-L., Uen, Y.-H., Tian, Y.-F., Wu, J.-M., Li, S.-H., Huang, W.-W., Li, W.-M. & Huang, H.-Y. 2009, 'Ezrin overexpression in gastrointestinal stromal tumors: an independent adverse prognosticator associated with the non-gastric location.', *Modern Pathology: an Official Journal of the United States and Canadian Academy of Pathology, Inc*, vol. 22, no. 10, pp. 1351–60.
- Weissbach, L., Bernards, A. & Herion, D.W. 1998, 'Binding of myosin essential light chain to the cytoskeleton-associated protein IQGAP1.', *Biochemical and Biophysical Research*

- Communications*, vol. 251, no. 1, pp. 269–76.
- Weissbach, L., Settleman, J., Kalady, M.F., Snijders, A.J., Murthy, A.E., Yan, Y.X. & Bernards, A. 1994, 'Identification of a human rasGAP-related protein containing calmodulin-binding motifs.', *The Journal of Biological Chemistry*, vol. 269, no. 32, pp. 20517–21.
- Welsh, A.O. & Enders, A.C. 1987, 'Trophoblast-decidual cell interactions and establishment of maternal blood circulation in the parietal yolk sac placenta of the rat.', *The Anatomical Record*, vol. 217, no. 2, pp. 203–19.
- Weng, W.-H., Ahlen, J., Astrom, K., Lui, W.-O. & Larsson, C. 2005, 'Prognostic impact of immunohistochemical expression of ezrin in highly malignant soft tissue sarcomas.', *Clinical Cancer Research : an Official Journal of the American Association for Cancer Research*, vol. 11, no. 17, pp. 6198–204.
- White, C.D., Brown, M.D. & Sacks, D.B. 2009, 'IQGAPs in cancer: a family of scaffold proteins underlying tumorigenesis.', *FEBS Letters*, vol. 583, no. 12, pp. 1817–24.
- White, C.D., Li, Z., Dillon, D.A. & Sacks, D.B. 2011, 'IQGAP1 protein binds human epidermal growth factor receptor 2 (HER2) and modulates trastuzumab resistance.', *The Journal of Biological Chemistry*, vol. 286, no. 34, pp. 29734–47.
- Whiteman, H.J., Weeks, M.E., Downen, S.E., Barry, S., Timms, J.F., Lemoine, N.R. & Crnogorac-Jurcevic, T. 2007, 'The role of S100P in the invasion of pancreatic cancer cells is mediated through cytoskeletal changes and regulation of cathepsin D.', *Cancer Research*, vol. 67, no. 18, pp. 8633–42.
- Wilcox, A.J., Weinberg, C.R., O'Connor, J.F., Baird, D.D., Schlatterer, J.P., Canfield, R.E., Armstrong, E.G. & Nisula, B.C. 1988, 'Incidence of early loss of pregnancy.', *The New England Journal of Medicine*, vol. 319, no. 4, pp. 189–94.
- Woods, L., Perez-Garcia, V. & Hemberger, M. 2018, 'Regulation of placental development and its impact on fetal growth-new insights from mouse models', *Frontiers in Endocrinology*, vol. 9, p. 570.
- Wu, C.-C., Li, H., Xiao, Y., Yang, L.-L., Chen, L., Deng, W.-W., Wu, L., Zhang, W.-F. & Sun, Z.-J. 2018, 'Over-expression of IQGAP1 indicates poor prognosis in head and neck squamous cell carcinoma.', *Journal of Molecular Histology*, vol. 49, no. 4, pp. 389–98.
- Wu, L., Song, W.Y., Xie, Y., Hu, L.L., Hou, X.M., Wang, R., Gao, Y., Zhang, J.N., Zhang, L., Li, W.W., Zhu, C., Gao, Z.Y. & Sun, Y.P. 2018, 'MiR-181a-5p suppresses invasion and migration of HTR-8/SVneo cells by directly targeting IGF2BP2 article', *Cell Death and Disease*, vol. 9, no. 2, p. 16.
- Xiao, Y., Sun, M., Zhan, Z., Ye, Y., Huang, M., Zou, Y., Liang, L., Yang, X. & Xu, H. 2014, 'Increased phosphorylation of ezrin is associated with the migration and invasion of fibroblast-like synoviocytes from patients with rheumatoid arthritis', *Rheumatology*, vol. 53, no. 7, pp. 1291–300.
- Xie, J.-J., Xu, L.-Y., Wu, Z.-Y., Zhao, Q., Xu, X.-E., Wu, J.-Y., Huang, Q. & Li, E.-M. 2011, 'Prognostic implication of ezrin expression in esophageal squamous cell carcinoma.', *Journal of Surgical Oncology*, vol. 104, no. 5, pp. 538–43.
- Yamaoka-Tojo, M., Ushio-Fukai, M., Hilenski, L., Dikalov, S.I., Chen, Y.E., Tojo, T., Fukai, T., Fujimoto, M., Patrushev, N.A., Wang, N., Kontos, C.D., Bloom, G.S. & Alexander, R.W. 2004, 'IQGAP1, a novel vascular endothelial growth factor receptor binding protein, is involved in reactive oxygen species--dependent endothelial migration and proliferation.', *Circulation Research*, vol. 95, no. 3, pp. 276–83.
- Yang, H.-S. & Hinds, P.W. 2003, 'Increased ezrin expression and activation by CDK5 coincident with acquisition of the senescent phenotype', *Molecular Cell*, vol. 11, no. 5, pp. 1163–76.
- Yang, Z., Tao, T., Raftery, M.J., Youssef, P., Di Girolamo, N. & Geczy, C.L. 2001, 'Proinflammatory properties of the human S100 protein S100A12.', *Journal of Leukocyte Biology*, vol. 69, no. 6, pp. 986–94.
- Yao, X., Thibodeau, A. & Forte, J.G. 1993, 'Ezrin-calpain I interactions in gastric parietal cells', *The American Journal of Physiology*, vol. 265, no. 1 Pt 1, pp. C36-46.
- Yu, Y., Khan, J., Khanna, C., Helman, L., Meltzer, P.S. & Merlino, G. 2004, 'Expression profiling identifies the cytoskeletal organizer ezrin and the developmental homeoprotein Six-1 as key metastatic regulators.', *Nature Medicine*, vol. 10, no. 2, pp. 175–81.
- Yuan, R.-H., Chang, K.-T., Chen, Y.-L., Hsu, H.-C., Lee, P.-H., Lai, P.-L. & Jeng, Y.-M. 2013, 'S100P expression is a novel prognostic factor in hepatocellular carcinoma and predicts survival in patients with high tumor stage or early recurrent tumors.', *PLoS One*, vol. 8, no. 6, p. e65501.
- Zamir, E., Katz, M., Posen, Y., Erez, N., Yamada, K.M., Katz, B.Z., Lin, S., Lin, D.C., Bershadsky, A., Kam, Z. & Geiger, B. 2000, 'Dynamics and segregation of cell-matrix adhesions in cultured fibroblasts.', *Nature Cell Biology*, vol. 2, no. 4, pp. 191–6.

- Zeng, B.-X., Fujiwara, H., Sato, Y., Nishioka, Y., Yamada, S., Yoshioka, S., Ueda, M., Higuchi, T. & Fujii, S. 2007, 'Integrin alpha5 is involved in fibronectin-induced human extravillous trophoblast invasion.', *Journal of Reproductive Immunology*, vol. 73, no. 1, pp. 1–10.
- Zeng, F., Jiang, W., Zhao, W., Fan, Y., Zhu, Y. & Zhang, H. 2018, 'Ras GTPase-activating-like protein IQGAP1 (IQGAP1) promotes breast cancer proliferation and invasion and correlates with poor clinical outcomes', *Medical Science Monitor : International Medical Journal of Experimental and Clinical Research*, vol. 24, pp. 3315–23.
- Zhan, X.-H., Jiao, J.-W., Zhang, H.-F., Xu, X.-E., He, J.-Z., Li, R.-L., Zou, H.-Y., Wu, Z.-Y., Wang, S.-H., Wu, J.-Y., Liao, L.-D., Wang, J.-J., Cheng, Y.-W., Zhang, K., Neufeld, G., Xu, L.-Y. & Li, E.-M. 2019, 'LOXL2 upregulates phosphorylation of ezrin to promote cytoskeletal reorganization and tumor cell invasion', *Cancer Research*, p. canres.0860.2019.
- Zhang, D., Ma, C., Sun, X., Xia, H. & Zhang, W. 2012, 'S100P expression in response to sex steroids during the implantation window in human endometrium', *Reproductive biology and endocrinology : RB&E*, vol. 10, p. 106.
- Zhang, J., Zuo, J., Lei, M., Wu, S., Zang, X. & Zhang, C. 2014, 'Ezrin promotes invasion and migration of the MG63 osteosarcoma cell', *Chinese Medical Journal*, vol. 127, no. 10, pp. 1954–9.
- Zhang, L., Fogg, D.K. & Waisman, D.M. 2004, 'RNA interference-mediated silencing of the S100A10 gene attenuates plasmin generation and invasiveness of Colo 222 colorectal cancer cells.', *The Journal of Biological Chemistry*, vol. 279, no. 3, pp. 2053–62.
- Zhang, Y. & Wang, G. 2019, 'MicroRNA-183 inhibits A375 human melanoma cell migration and invasion by targeting Ezrin and MMP-9', *Oncology Letters*, vol. 17, no. 1, pp. 548–54.
- Zhao, H., Shiue, H., Palkon, S., Wang, Y., Cullinan, P., Burkhardt, J.K., Musch, M.W., Chang, E.B. & Turner, J.R. 2004, 'Ezrin regulates NHE3 translocation and activation after Na<sup>+</sup>-glucose cotransport.', *Proceedings of the National Academy of Sciences of the United States of America*, vol. 101, no. 25, pp. 9485–90.
- Zhao, J., Zhang, X. & Xin, Y. 2011, 'Up-regulated expression of Ezrin and c-Met proteins are related to the metastasis and prognosis of gastric carcinomas.', *Histology and Histopathology*, vol. 26, no. 9, pp. 1111–20.
- Zhou, J., Feng, Y., Tao, K., Su, Z., Yu, X., Zheng, J., Zhang, L. & Yang, D. 2014, 'The expression and phosphorylation of ezrin and merlin in human pancreatic cancer.', *International Journal of Oncology*, vol. 44, no. 6, pp. 2059–67.
- Zhou, R., Cao, X., Watson, C., Miao, Y., Guo, Z., Forte, J.G. & Yao, X. 2003, 'Characterization of protein kinase A-mediated phosphorylation of ezrin in gastric parietal cell activation.', *The Journal of Biological Chemistry*, vol. 278, no. 37, pp. 35651–9.
- Zhou, R., Zhu, L., Kodani, A., Hauser, P., Yao, X. & Forte, J.G. 2005, 'Phosphorylation of ezrin on threonine 567 produces a change in secretory phenotype and repolarizes the gastric parietal cell.', *Journal of Cell Science*, vol. 118, no. Pt 19, pp. 4381–91.
- Zhu, H.-Y., Tong, X.-M., Lin, X.-N., Jiang, L.-Y., Wang, J.-X. & Zhang, S.-Y. 2015, 'Expression and distribution of calcium-binding protein S100P in human placenta during pregnancy', *International Journal of Fertility & Sterility*, vol. 8, no. 4, 2015/02/07., pp. 445–52.
- Zhu, L., Liu, Y. & Forte, J. 2005, 'Ezrin oligomers are the membrane-bound dormant form in gastric parietal cells', *Am J Physiol Cell Physiol*, vol. 228, no. 6, pp. 1242–54.
- Zhu, L., Zhou, R., Mettler, S., Wu, T., Abbas, A., Delaney, J. & Forte, J.G. 2007, 'High turnover of ezrin T567 phosphorylation: conformation, activity, and cellular function.', *American Journal of Physiology. Cell Physiology*, vol. 293, no. 3, pp. C874-84.
- Zigmond, S.H. 2000, 'How WASP regulates actin polymerization.', *The Journal of Cell Biology*, vol. 150, no. 6, pp. F117-20.
- van Zijl, F., Krupitza, G. & Mikulits, W. 2011, 'Initial steps of metastasis: cell invasion and endothelial transmigration.', *Mutation Research*, vol. 728, no. 1–2, pp. 23–34.
- Zimmer, D.B., Cornwall, E.H., Landar, A. & Song, W. 1995, 'The S100 protein family: history, function, and expression.', *Brain Research Bulletin*, vol. 37, no. 4, pp. 417–29.
- Zimmer, D.B., Eubanks, J.O., Ramakrishnan, D. & Criscitiello, M.F. 2013, 'Evolution of the S100 family of calcium sensor proteins.', *Cell Calcium*, vol. 53, no. 3, pp. 170–9.
- Zinaman, M.J., Clegg, E.D., Brown, C.C., O'Connor, J. & Selevan, S.G. 1996, 'Estimates of human fertility and pregnancy loss.', *Fertility and Sterility*, vol. 65, no. 3, pp. 503–9.

# Appendix



## Health Research Authority

West Midlands - Edgbaston Research Ethics Committee

The Old Chapel  
Royal Standard Place  
Nottingham  
NG1 6FS

Telephone: 0207 104 8069

29 February 2016

Professor [REDACTED]  
Pro-Vice-Chancellor for Health  
Aston University  
Aston Triangle  
Birmingham  
B4 7ET

Dear Professor [REDACTED]

Study title:	Research into Pregnancy Complications
REC reference:	15/WM/0284
Protocol number:	RGP001
IRAS project ID:	171356

Thank you for your letter of 23 February 2016, responding to the Committee's request for further information on the above research and submitting revised documentation.

The further information has been considered on behalf of the Committee by the Chair.

We plan to publish your research summary wording for the above study on the HRA website, together with your contact details. Publication will be no earlier than three months from [REDACTED]. Should you wish to provide a substitute contact point, require further information, or wish to make a request to postpone publication, please contact the REC Manager, [REDACTED].

### Confirmation of ethical opinion

On behalf of the Committee, I am pleased to confirm a favourable ethical opinion for the above research on the basis described in the application form, protocol and supporting documentation as revised, subject to the conditions specified below.

### Conditions of the favourable opinion

The REC favourable opinion is subject to the following conditions being met prior to the start of the study.

Management permission must be obtained from each host organisation prior to the start of the study at the site concerned.

*Management permission should be sought from all NHS organisations involved in the study in accordance with NHS research governance arrangements. Each NHS organisation must confirm through the signing of agreements and/or other documents that it has given permission for the research to proceed (except where explicitly specified otherwise).*

*Guidance on applying for NHS permission for research is available in the Integrated Research Application System, [www.hra.nhs.uk](http://www.hra.nhs.uk) or at <http://www.rdforum.nhs.uk>.*

*Where a NHS organisation's role in the study is limited to identifying and referring potential participants to research sites ("participant identification centre"), guidance should be sought from the R&D office on the information it requires to give permission for this activity.*

*For non-NHS sites, site management permission should be obtained in accordance with the procedures of the relevant host organisation.*

*Sponsors are not required to notify the Committee of management permissions from host organisations*

### Registration of Clinical Trials

All clinical trials (defined as the first four categories on the IRAS filter page) must be registered on a publically accessible database within 6 weeks of recruitment of the first participant (for medical device studies, within the timeline determined by the current registration and publication trees).

There is no requirement to separately notify the REC but you should do so at the earliest opportunity e.g. when submitting an amendment. We will audit the registration details as part of the annual progress reporting process.

To ensure transparency in research, we strongly recommend that all research is registered but for non-clinical trials this is not currently mandatory.

If a sponsor wishes to contest the need for registration they should contact [REDACTED] the HRA does not, however, expect exceptions to be made. Guidance on where to register is provided within IRAS.

**It is the responsibility of the sponsor to ensure that all the conditions are complied with before the start of the study or its initiation at a particular site (as applicable).**

### **Ethical review of research sites**

#### NHS sites

The favourable opinion applies to all NHS sites taking part in the study, subject to management permission being obtained from the NHS/HSC R&D office prior to the start of the study (see "Conditions of the favourable opinion" below).

## Approved documents

The final list of documents reviewed and approved by the Committee is as follows:

<i>Document</i>	<i>Version</i>	<i>Date</i>
Covering letter on headed paper [Covering letter]		10 July 2015
Covering letter on headed paper [Covering Letter Placenta Ethics]		
Evidence of Sponsor insurance or indemnity (non NHS Sponsors only) [Aston Insurance]		
GP/consultant information sheets or letters [AstonGovernceCVtemplate 2015 JKG]	01	19 November 2015
IRAS Checklist XML [Checklist_23022016]		23 February 2016
Letter from sponsor [Letter from Sponsor]		03 July 2015
Letter from statistician [Letter from Statistician]	01	19 November 2015
Letters of invitation to participant [Letters of invitation to participant SRG]	V1	10 July 2015
Other [Sumary CV for Lead investigator]		04 June 2015
Other [Standard Operating Procedure]	5.0	31 October 2013
Other [CV - ██████████]		04 June 2015
Other [Response to NHS Research Ethics Committee]		
Other [Email re Response to PO Queries ]		09 December 2015
Other [Participant information sheet v2 08.02.16 with track changes]	V2	08 February 2016
Other [Second response to NHS Research Ethics Committee review]	1	09 February 2016
Other [Second covering letter Placenta ethics to REC]		09 February 2016
Participant consent form [Consent Form]	1.0	03 June 2015
Participant information sheet (PIS) [Participant information sheet v2 final]	V2	08 February 2016
REC Application Form [REC_Form_20072015]		20 July 2015
Research protocol or project proposal [Protocol template RPG001]	03	12 November 2015
Summary CV for Chief Investigator (CI)		19 June 2015
Summary CV for supervisor (student research) [AstonGovernceCV SRG]		04 June 2015

## Statement of compliance

The Committee is constituted in accordance with the Governance Arrangements for Research Ethics Committees and complies fully with the Standard Operating Procedures for Research Ethics Committees in the UK.

## After ethical review

### Reporting requirements

The attached document “*After ethical review – guidance for researchers*” gives detailed guidance on reporting requirements for studies with a favourable opinion, including:

- Notifying substantial amendments

- Adding new sites and investigators
- Notification of serious breaches of the protocol
- Progress and safety reports
- Notifying the end of the study

The HRA website also provides guidance on these topics, which is updated in the light of changes in reporting requirements or procedures.

### User Feedback

The Health Research Authority is continually striving to provide a high quality service to all applicants and sponsors. You are invited to give your view of the service you have received and the application procedure. If you wish to make your views known please use the feedback form available on the HRA website:

<http://www.hra.nhs.uk/about-the-hra/governance/quality-assurance/>

### HRA Training

We are pleased to welcome researchers and R&D staff at our training days – see details at

<http://www.hra.nhs.uk/hra-training/>

**15/WM/0284**

**Please quote this number on all correspondence**

With the Committee's best wishes for the success of this project.

Yours sincerely

[Redacted Signature]

Professor [Redacted]  
Vice Chair

[Redacted Line]

Enclosures: "After ethical review – guidance for researchers"

Copy to:

[Redacted]  
[Redacted] Birmingham Women's Hospital R&D department